Characterization of the Metalloprotease ADAMTS16 and its Role in Fibronectin Assembly

INAUGURALDISSERTATION

zur

Erlangung der Würde eines Doktors der Philosophie vorgelegt

der

Philosophisch-Naturwissenschaftlichen Fakultät

der Universität Basel

von

Rahel Schnellmann

aus der Schweiz, Schüblebach, Schwyz

Basel, 2018

Genehmigt von der Philosophisch-Naturwissenschaftlichen Fakultät

auf Antrag von:

Prof. Dr. Nancy E. Hynes

Prof. Dr. Kurt Ballmer- Hofer

Basel den 12.12.2017

Prof. Dr. Martin Spiess
Dekan

ACKNOWLEDGMENTS

First of all I would like to thank my thesis advisor Ruth Chiquet- Ehrismann for giving me the opportunity to work in her lab. She was always open minded towards new ideas and techniques and always gave me the freedom in developing and pursuing my own ideas, therefore helping me in growing as a scientist. She was always available for discussions and ready to help with every problem. She was a great person and mentor and she will be missed dearly.

I am very thankful to Dr. Suneel Apte for his help and supervision and for allowing me in finishing my project in his lab.

Additionally I would like to thank my thesis committee members, Prof. Nancy E. Hynes, Prof. Kurt Ballmer-Hofer and Dr. Jörg Betschinger for their valuable contributions and scientific inputs during committee meetings. I especially want to thank Dr. Jörg Betschinger for hosting me in his lab and letting me participate in the lab meetings of his group. A special thank also goes to Prof. Nancy Hynes for her big moral and scientific support during my last year as PhD student.

Additionally I would like to thank Prof. Susan Gasser for her great support and help during my PhD time.

I would like to thank all former members of the Chiquet lab for the really nice and cooperative working atmosphere. I am grateful that I got the chance to work in such a great lab, which became like a second family to me. I especially want to thank Anina, Ismail, Jonas and Keith for being friends and being such a big moral support during hard times.

Additionally I want to thank the Betschinger and the Apte lab for welcoming me into their labs. Especially Sumeda and Tim who both were a big help and support when I had scientific questions.

I also would like to thank the FMI facilities especially Ragna Sack and Daniel Hess for helping me with my mass spectrometry experiments. Additionally I would like to thank Steve and Jan from the FMI imaging facility for their help with various experiments. I also would like to thank the imaging core at the LRI for their help with various experiments.

In addition I would like to thank Aicha and Courtney for being my friends and making my stay in the US a great experience.

Last but definitely not least, I am extremely grateful to my parents, Andreas and Gabriela Schnellmann for their never ending support during all those years. Additionally I am also extremely grateful to my brother Ives and the rest of my family for their great support.

Table of Contents

1. Summary **1**

2. Introduction **3**

2.1 The Extracellular Matrix 3

2.2 The Basement Membrane 8

2.3 Fibronectin 11

2.4 Fibronectin Fibrillogenesis 13

2.5 Extracellular Metalloproteinases and their function in ECM degradation and remodeling 18

2.5.1 The MMP-family 18

2.5.2 The ADAMs-family 22

2.6 The ADAMTS superfamily 26

2.6.1 Structure and Proteolytic Mechanisms 26

2.6.2 ADAMTSs in Development and Disease 29

2.6.3 ADAMTS-like proteins 35

2.6.4 ADAMTS16 37

3. Aim of the Thesis **39**

4. Results **40**

4.1 Manuscript 40

4.2 Supplementary Information ..... **Error! Bookmark not defined.**

5. Unpublished Results **54**

5.1 Materials and Methods 75

5.2 Results 81

5.2.1 ADAMTS16 is C-terminally processed and forms high order oligomers 81

5.2.3 ADAMTS16 potentially processes MMP14 and MMP3 88

5.2.4 ADAMTS16 is expressed in various cancer cell lines and during development 92

5.2.5 ADAMTS16 affects cell migration and proliferation 95

6. Discussion and Future Directions **97**

7. References **106**

8. Appendix **119**

8.1 Supplementary Figures 119

8.2 Abbreviations 124

8.3 CV 126

1. Summary

The A Disintegrin And Metalloproteinase with Thrombospondin Motif (ADAMTS) family is a family of extracellular metalloproteinases involved in the degradation and reorganization of the extracellular matrix (ECM). These proteinases play important roles during embryogenesis, wound healing and cancer progression. During cancer progression the degradation of the ECM by proteinases is a key step allowing cancer cells to leave the primary tumor site and invade the surrounding tissue.

ADAMTS16 is a poorly characterized family member but although nothing is known about its substrates or its mechanism of action, several studies showed that ADAMTS16 plays a role during renal and gonadal development. In addition to its role during embryogenesis, ADAMTS16 has been implicated in blood pressure regulation. Moreover, several studies linked *ADAMTS16* expression to cancer progression and metastasis. Thus, ADAMTS16 is well-connected to morphogenesis and human diseases, but without knowledge of its characteristics, substrates, and the molecular pathways in which it participates.

We developed an assay using a decellularized ECM and liquid chromatography–mass spectrometry (LC-MS/MS) to identify substrates of ADAMTS16 and to gain further insights into its mechanism of action. Using this approach we identified fibronectin (FN) as a substrate of ADAMTS16.

FN is one of the most abundant proteins within the ECM. FN fibers allow binding and fibrillogenesis of other ECM proteins such as fibrillins, collagens, tenascin-C and TGFβ-binding proteins and are therefore important components for the formation of an intact ECM. We showed that cleavage of FN near its N-terminus by ADAMTS16, leads to inhibition of FN fibril maturation, thereby having a strong impact on ECM assembly.

Furthermore, we observed that ectopic ADAMTS16 expression in the epithelial cell line MDCKI strongly altered morphology when cultured in 3D collagen gels. MDCKI spheroids lacked FN in their matrix, resulting in smaller size and the formation of multiple lumina.

FN is, however, not only important for ECM formation, but has a crucial role in cell adhesion, migration and cell signaling via binding to cell surface integrins. We could show that ADAMTS16

expression and the resulting cleavage of FN upregulates *MMP3* expression in MDCKI cells, therefore creating an intriguing dual protease feed-forward loop that may serve to limit and fine-tune FN assembly and control tubular morphogenesis.

2. Introduction

2.1 The Extracellular Matrix

The extracellular matrix (ECM) is a non-cellular structure that is present in all tissues and organs (Fig.2.1). It acts as a scaffold giving physical support and structure to tissues, organs and single cells. Additionally, the ECM actively modulates cellular responses such as cell migration, proliferation, differentiation and cell survival through complex biochemical and biomechanical cues [1]. The ECM is composed of proteoglycans (e.g., decorin, perlecan and aggrecan) and glycoproteins (e.g., collagens, fibronectin, laminin and tenascin). A variety of ECM proteins share common structural motifs such as an Arg-Gly-Asp (RGD) motif, which allows their binding to the surface receptors of the integrin family [2, 3].

Proteoglycans and glycoproteins form a tight network that allows binding and storage of various growth factors. Therefore the ECM controls their localization, function and presentation to the cells and provides binding sites for cell-surface receptors such as integrins and syndecans [2]. Similar to soluble growth factors, the molecular composition and the physical properties of the matrix (e.g., stiffness, elasticity) can influence cell behavior and cell fate [3]. The ECM thus has an important function in regulating the development, function and homeostasis of all eukaryotic cells. It not only regulates cell adhesion, but also actively influences cell signaling, not only by controlled release of growth factors, but also by changes in ECM stiffness and mechanical properties.

The most abundant proteins within the ECM are members of the collagen family. Collagen makes up 30% of the total protein mass of a multicellular animal [1, 3]. There are 28 known collagens and these are the products of 49 distinct collagen α-chain gene products [4]. Collagens assemble into tight right-handed triple helical pro-collagens with loose ends at their carboxy-terminus and their amino-terminus. Some collagen molecules are known to be homotrimers, whereas others assemble as heterotrimers that are comprised of two or three distinguishable α-chain types [3-6]. After secretion the loose ends at the N- and C-terminus of pro-collagen molecules are cut off by specific proteinases, which leads to the formation of mature tropocollagen [7]. Most collagens are so-called fibrillar collagens. After secretion several tropocollagen molecules bind to each other forming collagen fibrils, which in turn interact with each other, forming collagen bundles also called collagen fibers with a radius of several micrometers [8] (Fig.2.2).

Other fibrous glycoproteins within the ECM are fibronectin (FN) and tenascin (TN). Their structures can be described as 'beads-on-a-string', since both consist of many small domains in a row, connected by short linker regions. In addition, both are glycoproteins, and both consist to a large part of fibronectin type III

domains [9]. Opposite to FN, which is strongly adhesive, tenascins are generally anti-adhesive and strongly influence the adhesion of cells to other ECM proteins [10]. There are four tenascins described thus far: tenascin-C, tenascin-W, tenascin-R, and tenascin-X [9, 11]. The heptad domain at the N-terminus of each molecule is responsible for tenascin assembly into homo-trimers, which in the case of tenascin-C and tenascin-W can dimerize by disulfide bonds through their N-termini to homo-hexamers (Figure 2.3).

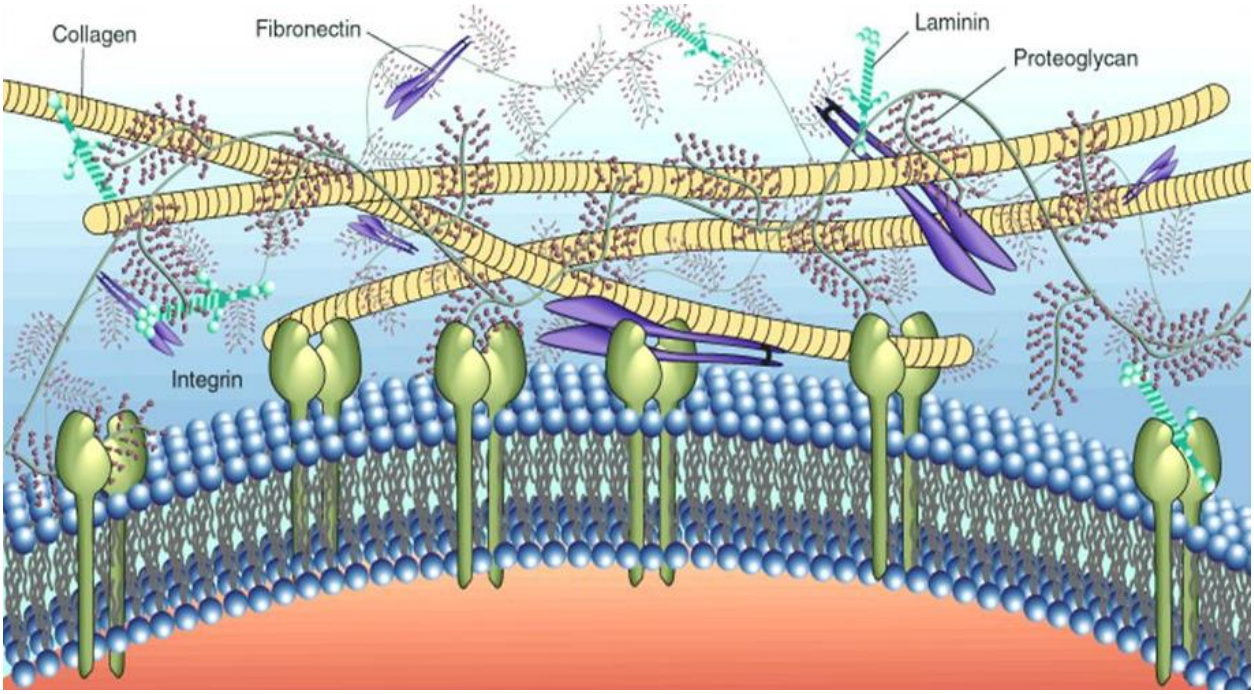

Figure 2.1: Overview of the extracellular matrix (adapted from [12])
The proteins, fibronectin, collagen, and laminin contain binding sites for one another, as well as binding sites for cell surface receptors such as integrins. The proteoglycans are huge protein polysaccharide complexes that occupy much of the volume of the extracellular space.

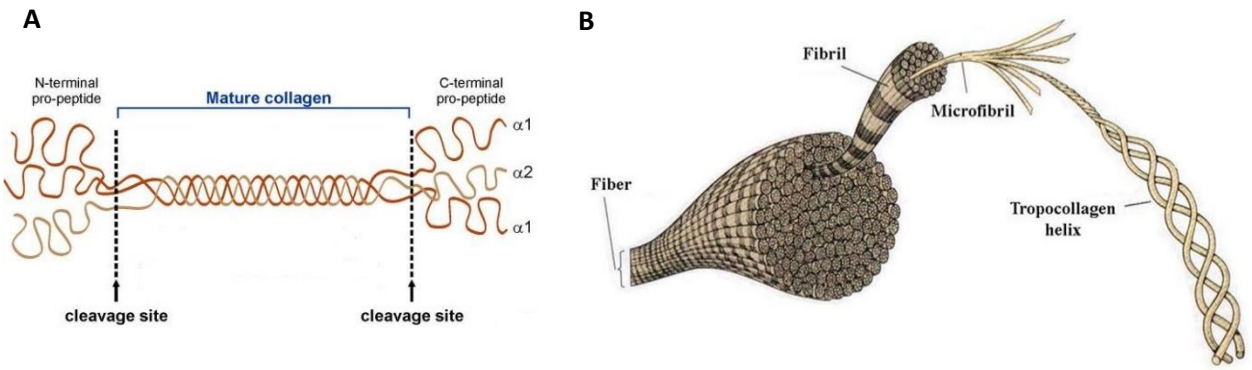

Figure 2.2: Overview of collagen assembly
A.Three single α-chains form a triple helical pro-collagen molecule. After secretion the pro-peptide domains at the C-terminals and N-terminals are cleaved, resulting in formation of mature collagen, also called tropocollagen [7]. **B.** The tropocollagen molecules than assemble into oligomeric collagen fibrils, which assemble into thick collagen fibers [13].

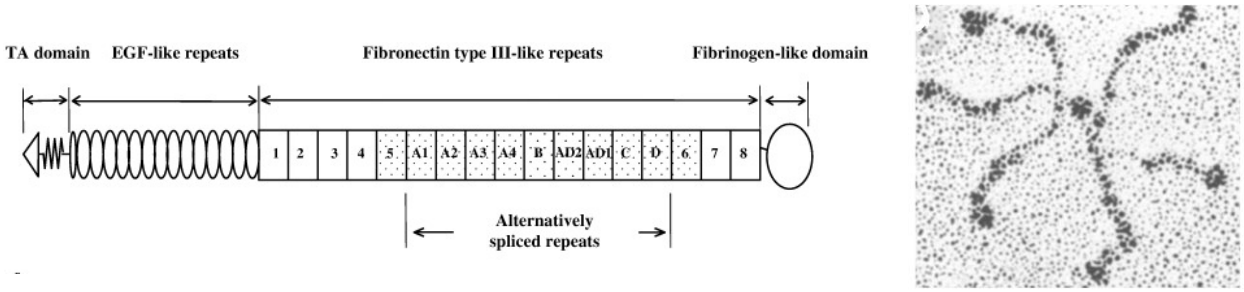

Figure 2.3: Tenascin-C
Overview of the domain organization of tenascine C [14]. The electron micrograph of purified tenascin-C reveals its oligomerization into a hexamer [15].

Proteoglycans, another important family of ECM proteins, consist of a core protein that is covalently bound to glycosaminoglycans (GAGs). The only exception within the proteoglycan family is hyaluronan (HA), which is made up entirely of GAGs therefore lacking the core protein. GAGs are long, unbranched sulfated polysaccharides with a highly negative charge. GAG chains consist of disaccharide repeating regions containing acetylated amino sugar moieties (N-acetyl-galactosamine or N-acetyl-glucosamine) and uronic acids (D-glucoronic acid or L-iduronic acid) [8, 16].

The core proteins of proteoglycans can be divided into several subgroups depending on their location and binding: small leucine-rich proteoglycans (SLRP), modular proteoglycans (hyalectins and non-HA binding PGs), and cell-surface proteoglycans [16] (Fig. 2.4). The GAG chains tend to be very hydrophilic and stiff,

which is helpful in forming hydrogels that can withstand very high compressive forces. These properties are very important in the knee joint, where they act as natural lubricant [17].

However, proteoglycans also contribute to other processes like cell adhesion, migration, and proliferation. One of the hyalectins, neurocan, is involved in the inhibition of neuronal attachment and neurite outgrowth [16]. Another example is the SLRP decorin, which functions in signaling, as it can bind to multiple receptors. Moreover, decorin has been shown to inhibit transforming growth factor-β (TGF-β) receptor signaling. Several possible mechanisms have been postulated for the inhibitory effect of decorin on TGF-β signalling, such as direct binding of decorin to TGF-β leading to inactivation and sequestration into the ECM [18]. Another possible mechanism for decorin-mediated interference with TGF-β signalling, is either through phosphorylation of Smad2 [19], or low-density lipoprotein-related protein-1 (LRP-1), a known cell-surface receptor for decorin [20]. Additionally decorin can regulate the synthesis of other ECM proteins such as fibrillin-1, via binding and phosphorylation of insulin-like growth factor-I (IGF-I) receptor [16, 21, 22]. Thus proteoglycans have a variety of different functions and are therefore important components of the ECM.

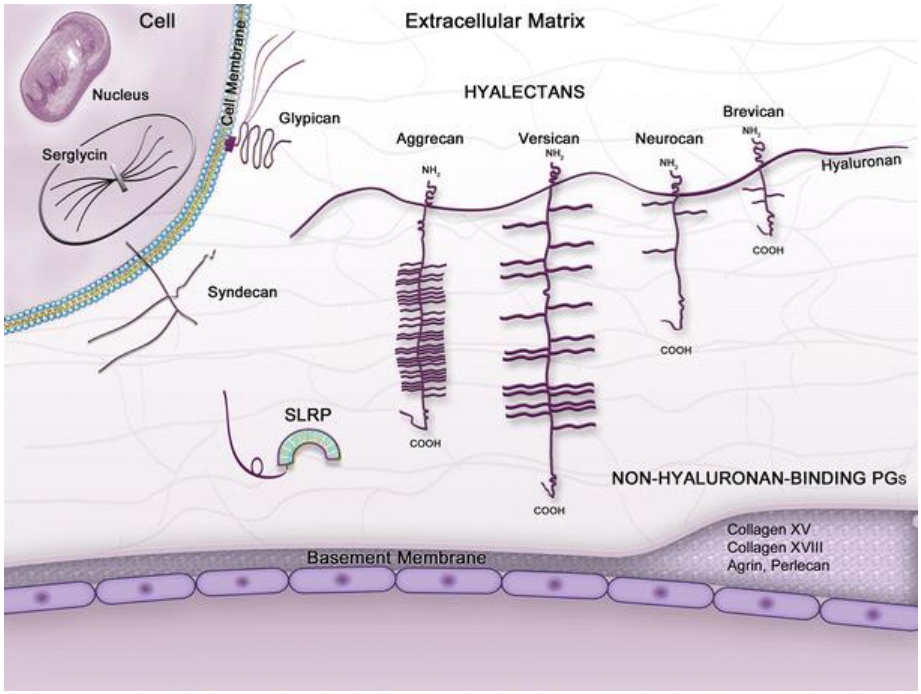

Figure 2.4: Overview of the proteoglycan family (adapted from [16])

Classification of proteoglycans based on their location and binding. The heterogeneous group of proteoglycans include small leucine-rich (*SLRP*; e.g., decorin) and modular proteoglycans. Modular proteoglycans are divided into hyalectans (hyaluronan- and lectin-binding proteoglycans) and the non-hyaluronan-binding proteoglycans (perlecan and agrin) of the basement membrane. The third group of cell-surface proteoglycans are the membrane-spanning syndecans and the glycosylphosphatidylinositol-anchored glypicans.

There are many other known ECM components which, together with the above mentioned proteins, make up the matrisome [23]. The mammalian core matrisome includes all common ECM proteins and consists of approximately 300 proteins. There is also a large number of ECM-affiliated and ECM-modifying proteins that are not included in the core matrisome [23].

As discussed above the ECM, is not just a simple scaffold for cell attachment, but plays a crucial role in cell signaling, adhesion and survival. Therefore the ECM has a highly dynamic structure that is consistently remodeled and its molecular components are subjected to a variety of post-translational modifications [1, 5]. Alterations in ECM turnover can lead to severe defects during embryogenesis and promote the development of various diseases such as the formation of solid tumors and cancer metastasis, osteoarthritis, atherosclerosis and fibrosis [3, 24-26].

2.2 The Basement Membrane

The basement membrane (BM) is a specific type of ECM (Figure 2.5), which is always associated with cells and separates the epithelium from the stroma of any tissue. The BM provides structural support, divides tissues into compartments and regulates cellular behavior [27, 28]. The BM constitutes of large insoluble molecules that form sheet-like structures via self-assembly, which is driven by cell-surface anchors and receptors [29-31]. The main components of the BM are laminin, type IV collagen, heparan-sulfate proteoglycans (HSPGs) and nidogen [27].

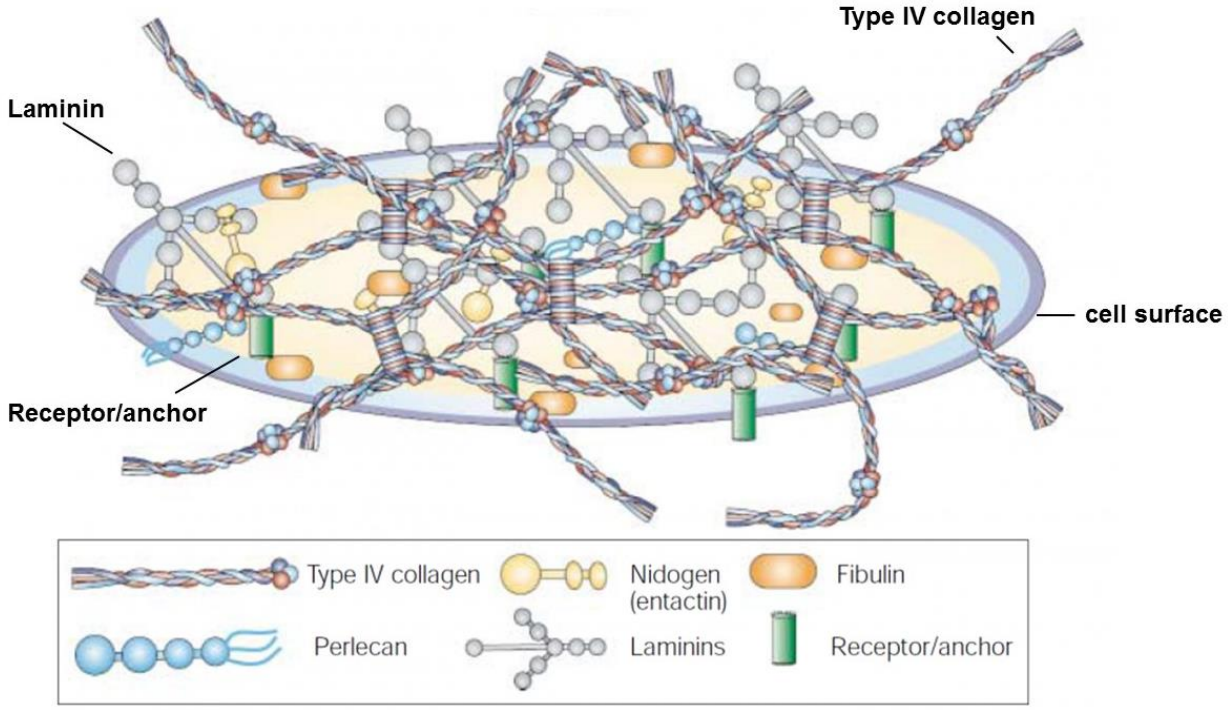

Figure 2.5: Schematic drawing of the basement membrane (adapted from [27])
The basement membrane consists of several ECM proteins and is anchored to the receptors of neighboring cells. Laminin and collagen IV form independent networks that interact with each other and other ECM components.

The most abundant proteins in the BM are laminin and collagen IV. The laminin structure is unique since the chains form a cross-like structure. Laminins consist of an α, β, and γ chain, making them heterotrimeric and quite diverse. At least 16 isoforms have been described so far (Fig. 2.6) [32]. As already mentioned above laminins are one of the main components of the BM and are involved in cell-specific processes such as

proliferation and adhesion. Via ligand binding to cell membrane receptors, laminins can alter transcriptional levels of genes and even influence chromatin remodeling of the gene promoters. Moreover, polarization of cells upon interaction with laminins can affect their response to signaling from the extracellular space [32, 33].

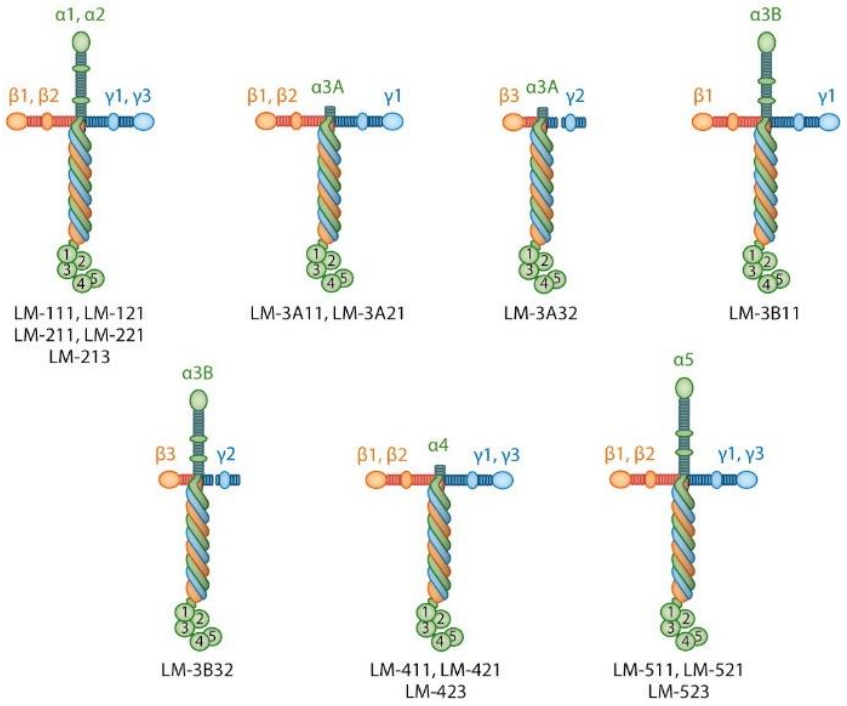

Figure 2.6: Structure of laminins (adapted from [27])
Overview of the structures of the laminin family of proteins, and the types of α, β, and γ chains that these ECM proteins consist of.

Another main component of the BM is collagen IV. Along with laminin it plays an important role in cell adhesion, migration, differentiation and growth [28, 34]. Type IV collagen is ubiquitously present in all BMs independent of the tissue. It is also called the 'network-forming collagen', due to its capacity to self-assemble into organized networks (Fig. 2.7). This property makes it different from the fibrillar collagens (types I, II and III collagen), which need an already formed network, mainly fibronectin, to assembly into fibrils [27]. Each type IV collagen α-chain consists of three domains: an N-terminal 7S domain, a middle triple-helical domain, and a C-terminal globular non-collagenous (NC1) domain. It is assumed that the six α-chains of type IV collagen self-assemble to form predominantly three sets of triple-helical molecules that

self-associate via their NC1 domains and their middle triple-helical regions to form spider web-like scaffolds which interact with the laminin network and form a basic BM scaffold [35, 36].

Various studies have shown that type IV collagen network formation is crucial for BM stability and assembly [37, 38]. Mutations in the type IV collagen α3-chain and α5-chain have been associated with Goodpasture syndrome and Alport syndrome [27, 39-42].

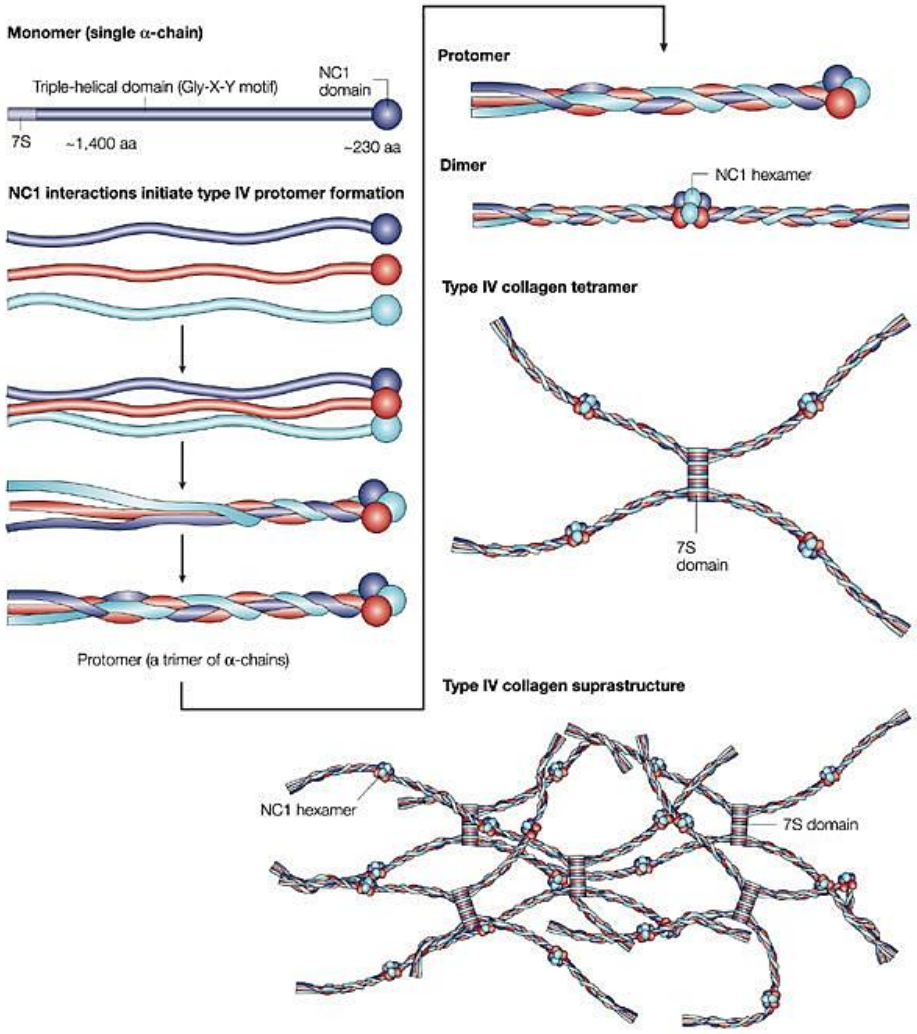

Figure 2.7: Type IV collagen network formation (adapted from [27])

All of the type IV collagen in mammals is derived from six genetically distinct α-chain polypeptides. The α -chains can be separated into three domains: an N-terminal 7S domain, a middle triple-helical domain, and a C-terminal globular non-collagenous (NC1) domain. The assembly of a particular trimer begins when the three NC1 domains initiate a molecular interaction. The next step in the assembly is the type IV collagen dimer formation. Two type IV collagen protomers associate via their NC1 trimers to form an NC1 hexamer. Next, four protomers interact at the glycosylated amino-terminal 7S region to form tetramers. These interactions form the nucleus for a type IV collagen scaffold.

2.3 Fibronectin

Fibronectin (FN) is a multidomain glycoprotein, which connects the cells to the surrounding ECM and BM via integrin binding [43]. Furthermore FN is an important binding partner for other ECM proteins such as collagens, tenascins, fibrillins and latent-transforming growth factor beta-binding proteins (LTBPs), which need an intact FN network that serves as a template for their own fibril formation [44-47]. Therefore FN plays an important role for the development of an intact mature ECM.

In addition to its structural importance, FN mediates a variety of cellular interactions with the ECM and plays important roles in cell adhesion, migration, growth and differentiation [48]. FN is widely expressed by multiple cell types. Consistent with its observed impact on ECM ontogeny, cell adhesion and migration, inactivation of the *Fn1* gene in mice leads to embryonic lethality by 8.5 days of gestation, with embryos showing impaired cardiovascular development and other morphogenetic defects [49].

FN is usually secreted as a dimeric glycoprotein composed of two nearly identical subunits that range in size from 230 kDa to 270 kDa. The two subunits are covalently linked near their C-terminus by a pair of disulfide bonds. Variation in subunit size are primarily the results of alternative splicing [50, 51]. Although FN molecules are the product of a single gene, alternative splicing of a single pre-mRNA can generate as many as 20 variants in human FN [48].

FN is composed of three different types of modules namely type I, II, and III repeats. Type I repeats are about 40 amino-acid residues in length and contain two disulfide bonds; type II repeats comprise a stretch of approximately 60 amino acids and two intrachain disulfide bonds; type III repeats have a 7-stranded β-barrel structure without any disulfide bonds and can therefore undergo conformational changes [52, 53]. These modules contain functional domains that mediate interactions with other ECM proteins, cell surface receptors and FN itself [54].

FN can be subdivided into two major forms, based on its solubility. The soluble plasma FN and the less soluble cellular FN. Plasma FN is synthesized predominantly in the liver by hepatocytes and shows a relatively simple splicing pattern where the extra type III repeats EIIIA and EIIIB are missing (Fig. 2.8). The V region (also called IIICS in human FN) is included in the majority of cellular FN subunits, but is only present in one subunit of each plasma FN dimer [48, 54]. EIIIA and the V region are both known to have an effect on cell adhesion. In fact, both the EIIIA and the V region have a direct role in cell adhesion by binding to α_4 and α_9 integrins [55 56]. In addition to integrin binding the V region is essential for FN dimer secretion [57]. The function of the EIIIB is not yet properly understood although it may have an effect in cell adhesion as well [43, 54]. Cellular FN consists of a much larger and more heterogeneous group of FN isoforms that

result from cell-type-specific and species-specific splicing patterns. Thus, alternative splicing of precursor mRNA from the single *FN* gene has the capacity to produce a large number of variants, generating FNs with different cell-adhesive and ligand-binding properties, which allows cells to precisely alter the composition of the ECM in a developmental and tissue-specific manner [48]. Figure 2.8 provides an overview of the different FN variants, their integrin and ligand binding sites, their major proteolytic digestion sites and sites involved in fibronectin fibrillogenesis.

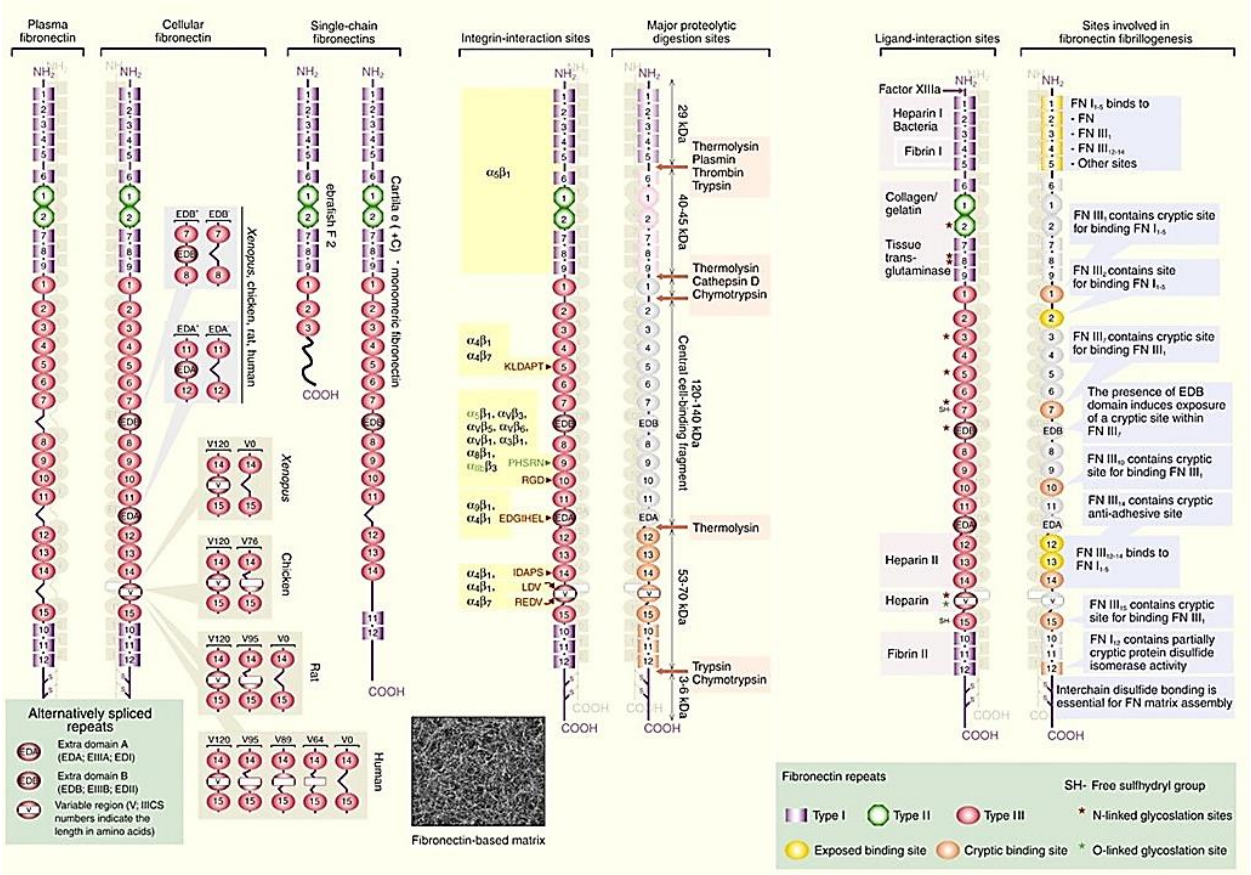

Figure 2.8: Overview of the structure and different splice variants of FN (adapted from [48])
Overview of the domain structure of plasma, cellular and single chain FN. Integrin and ligand (collagen, heparin etc.) interactions sites are marked in yellow or purple respectively. Red arrows indicate sites accessible for proteolytic cleavage by a variety of extracellular proteinases. All domains involved in fibronectin self-assembly and fibrillogenesis are marked in blue.

2.4 Fibronectin Fibrillogenesis

FN fibrillogenesis and matrix assembly is a complex process involving binding domains and repeating modules from all regions of FN. FN fibrillogenesis requires the interaction of FN molecules with cell surface integrins as well as with other FN molecules [54]. Upon secretion FN dimers bind to transmembrane integrin receptors. The primary receptor mediating FN assembly is integrin $\alpha_5\beta_1$ [58], although other integrins can have a similar function under appropriate circumstances [59]. Integrins link FN to the actin cytoskeleton through interactions between their cytoplasmic domains and cytoskeletal-associated proteins, such as focal adhesion kinase (FAK), talin and vinculin [60]. The association of cytoplasmic domains of integrins with the actin cytoskeletal network is essential for FN matrix assembly. FN-integrin interactions activate the RhoA GTPase pathway followed by RhoA-Rock mediated actin–myosin interactions which leads to the contractility of the cytoskeleton, resulting in FN fibril formation (Fig. 2.9) [51, 61, 62]. Treatments that enhance contractility stimulate matrix assembly whereas inhibition of myosin light chain kinase or RhoA GTPase reduces assembly [61, 63]. This linkage is not only important for FN fibrillogeneses, but also allows the ECM to influence cell signaling via mechanotransduction. The actin-talin-integrin-FN clutch is transmitting mechanical forces caused by tissue rigidity into biochemical signals. Strong FN accumulation and increased tissue stiffness, lead to conformational changes in talin, which influences the organization of the actin cytoskeleton, followed by the translocation of the transcription factor YAP into the nucleus (Fig. 2.9) [64].

On the outside of the cell, interactions between FN and integrins promote FN–FN association and fibril formation, most likely by inducing conformational changes in bound FN. During the assembly process FN-fibrils are converted into a detergent deoxycholate (DOC)-insoluble fibrillar network [54, 65]. The thickness of FN fibrils varies substantially from 10 to 1000 nm in diameter indicating that fibrils probably range from a few to several hundred FN molecules across [54, 66].

A major site for FN self-association is within the N-terminal assembly domain spanning the first five type I repeats ($I_{1\text{-}5}$) (Fig. 2.8) [67-69]. The N-terminal domain has several other binding partners in addition to FN such as fibrin, heparin, thrombospondin-1, and tenascin-C [51, 70] and is therefore a key mediator for proper FN fibrillognesis and ECM maturation. Recombinant FN lacking the first five type I repeats is unable to assemble into fibrils, while addition of recombinant N-terminal 70 kDa FN fragment containing the first five type I repeats blocks FN matrix assembly [67, 68]. In addition to these non-covalent interactions involving the N-terminal FN domains, dimerization of FN also depends on covalent associations within the C-terminal disulfide bonds. Indeed monomeric FN lacking the C-terminal region is not able to assemble into fibrils [68, 71].

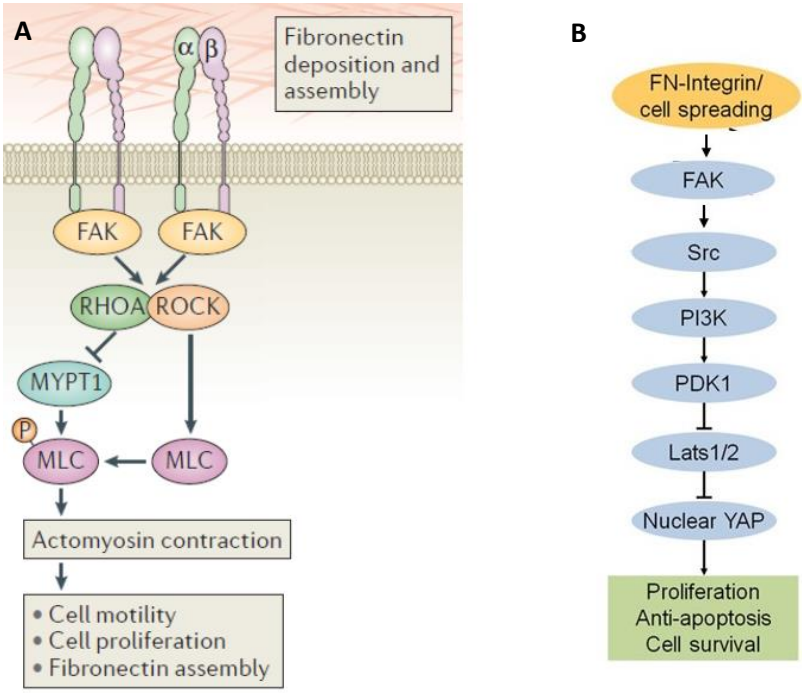

Figure 2.9: Integrin signaling mediates FN assembly and activation of YAP
A. FN assembly requires focal adhesion kinase (FAK) activation and RHOA–ROCK-mediated actomyosin contraction [62] **B.** Integrin receptors bind to FN. The mechanical stimulus leads to conformational changes in talin which triggers the activation of YAP via FAK-Src signaling in a PI3K–PDK1-dependent manner [72].

Although the N-terminal repeats $I_{1\text{-}5}$ are the most important ones for fibronectin fibril assembly, other FN domains participate and regulate FN-FN interactions, fibril assembly and the formation of a DOC insoluble matrix as well. Deletion of the entire $III_{1–2}$ domain for example, significantly reduces matrix assembly. This small domain contains at least two FN binding sites and binds in addition to various proteoglycans. Where deletions of the FN domain III_1 alone had no significant influence on FN fibril assembly, deletion of the domains $III_{1\text{-}2}$ significantly reduced ECM assembly with a primary effect on the ECM maturation into a DOC-insoluble matrix [73]. This observation indicates that, other than the N-terminal assembly domain ($I_{1\text{-}5}$) which is an important mediator for the initiation of FN assembly and fibrillognesis, the FN binding site in III_2 or $III_{1–2}$ together mainly participate in the maturation of the FN matrix rather than in in the initiation of FN fibrillogenesis.

FN–FN interactions are not only important for fibril formation but they can also participate in intramolecular interactions that keep soluble FN in a compact form, unable to form fibrils in solution. FN fragments containing the domains $III_{2–3}$ and/or $III_{12–14}$ were shown to inhibit FN assembly, possibly through dual blockade of FN–FN and FN–cell interactions [74, 75].

As mentioned above, FN fibril assembly starts with the binding of FN to cell surface integrins. This step is required for subsequent FN-FN interactions, fibril maturation and the formation of multimeric structures [54]. Incorporation of FN requires interactions with integrins [58], but FN is also recruited from solution into existing fibrils through homophilic interactions that are independent of the RGD integrin binding site [76]. FN in solution has a very compact globular structure, where many binding sites required for assembly are not properly accessible. FN is transformed from a compact conformation to an extended conformation as it goes from solution to fibrils. Thus the extension of FN and the exposure of FN binding sites play important roles in the initiation of FN fibrillogenesis. Such conformational changes are also dependent on the actin cytoskeleton. Stress fibers, which are contractile actin-myosin filaments, generate tension at sites of contact between integrins and FN. Integrin engagement with the cytoskeleton allows these receptors to translocate away from the contact sites along actin filaments and, in the process, to pull on bound FN molecules, which leads to the extension of the FN molecule needed for FN-FN interactions and fibrillogenesis [77] [61]. FN–FN interactions, where FN dimers associate end-to-end [78], initially give rise to short fibrils around the cell periphery. As assembly proceeds, longer and thicker fibrils are formed. As the fibrils grow, they are converted from a detergent DOC-soluble form into DOC-insoluble material, a process that is irreversible [65]. The exact mechanism by which FN fibrils become DOC-insoluble is not well understood. However, fibril insolubility appears to depend on strong noncovalent, protein–protein interactions [79]. Extension of FN during assembly requires disruption of interdomain interactions. It could be shown that partial unfolding of the β-sheet structure of the III_9 module promoted self-polymerization through β-strand exchange [80]. Domain swapping and the formation of intermolecular β-sheets might be the primary mechanism that underlies DOC-insolubility [81]. Figure 2.10 provides an overview of FN assembly and fibrillogenesis.

The FN matrix is not a static structure. Fibrils within a matrix are under significant tension and relax to as little as one-quarter of their original length when tension is removed, for example, when one end of a fibril is released from its attachment site. Thus, cell contractility and tension are needed to initiate fibrillogenesis and to maintain fibril architecture in established matrices [82].

Proper FN matrix assembly is an important step for the development of an intact mature ECM. Remodeling of the FN network can have severe effects on the overall composition of the ECM and influence processes such as cell signaling, adhesion and proliferation. How ECM is assembled at cell and tissue surfaces has become an important question, because of the growing realization that the three-dimensional (3D) organization of the ECM can have distinct instructive properties in terms of cellular responses. FN, along with other ECM glycoproteins, collagens, and proteoglycans, are assembled into complex 3D

microenvironments that provide structural support to cells and tissues, and restrict the diffusion of growth factors and other soluble signaling molecules to direct or influence cell behavior, proliferation and growth, gene expression, and cell fate specification [3]. Therefore FN network formation has a crucial role during organ development. For example, FN is an important regulator of cleft formation during epithelial branching morphogenesis. Inhibition of FN assembly or knock-down of *FN1* blocks cleft formation and branching, whereas the addition of exogenous FN promotes these processes. Interestingly, the assembly of FN at sites of cleft formation was associated with a reduction in cadherin-dependent cell–cell adhesions, suggesting a possible mechanistic link or adhesive "crosstalk" critical for branching morphogenesis. Btbd7 was recently discovered as one of the key players during FN induced cleft formation. It is expressed by cells in the emerging clefts in response to local FN accumulation. Btbd7 induces Snail2 and suppresses E-cadherin expression thereby promoting morphogenetic changes required for cleft formation (Fig. 2.11) [83, 84].

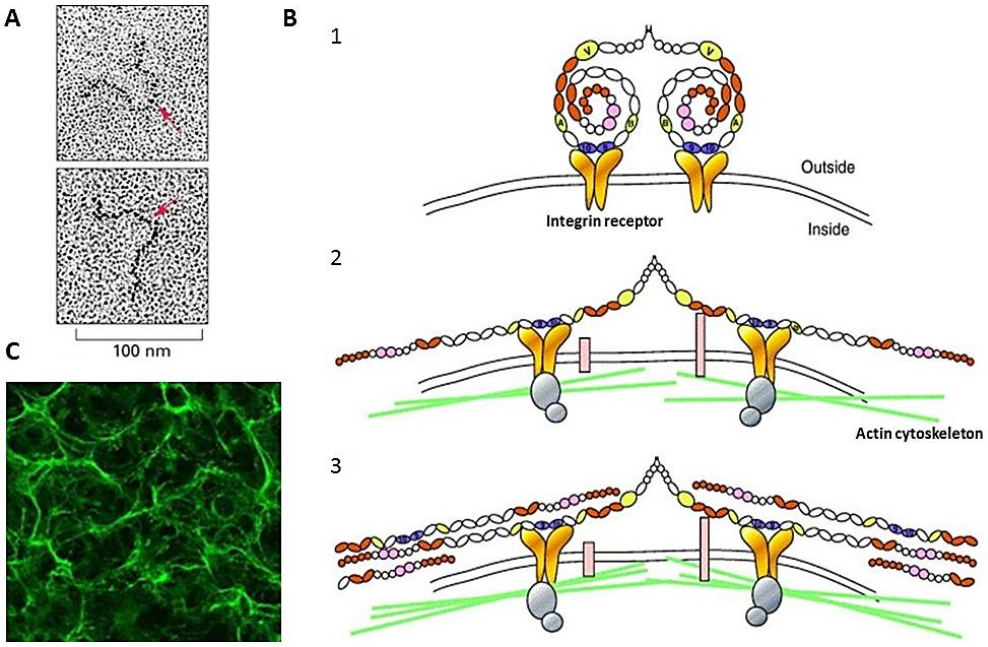

Figure 2.10: Major steps of FN fibril assembly
A. Electron microscopy image of a FN dimer. The red arrows indicate the C-terminal disulfide bonds [8]. **B.** (1) Compact soluble FN binds to integrin $\alpha_5\beta_1$ (gold) via its cell binding domain (blue). The exact organization of FN subunits in the compact form of soluble FN is not known but appears to depend on intramolecular interactions between $III_{2–3}$ and $III_{12–14}$ and other FN binding sites (red modules). (2) FN binding to integrins and other receptors (pink bars) induces reorganization of the actin cytoskeleton (green lines) and activates intracellular signaling complexes (silver circles). Cell contractility aids in FN conformational changes thus exposing sequestered FN binding domains in the extended molecule. (3) Fibrils form through FN–FN interactions. Alignment of FN molecules within fibrils might vary depending on which domains interact, such as $I_{1–5}$ binding to $III_{1–2}$ versus with $III_{12–14}$ **[54]. C.** FN matrix of wild type mouse embryonal fibroblasts (MEF) after 3 days in culture [85].

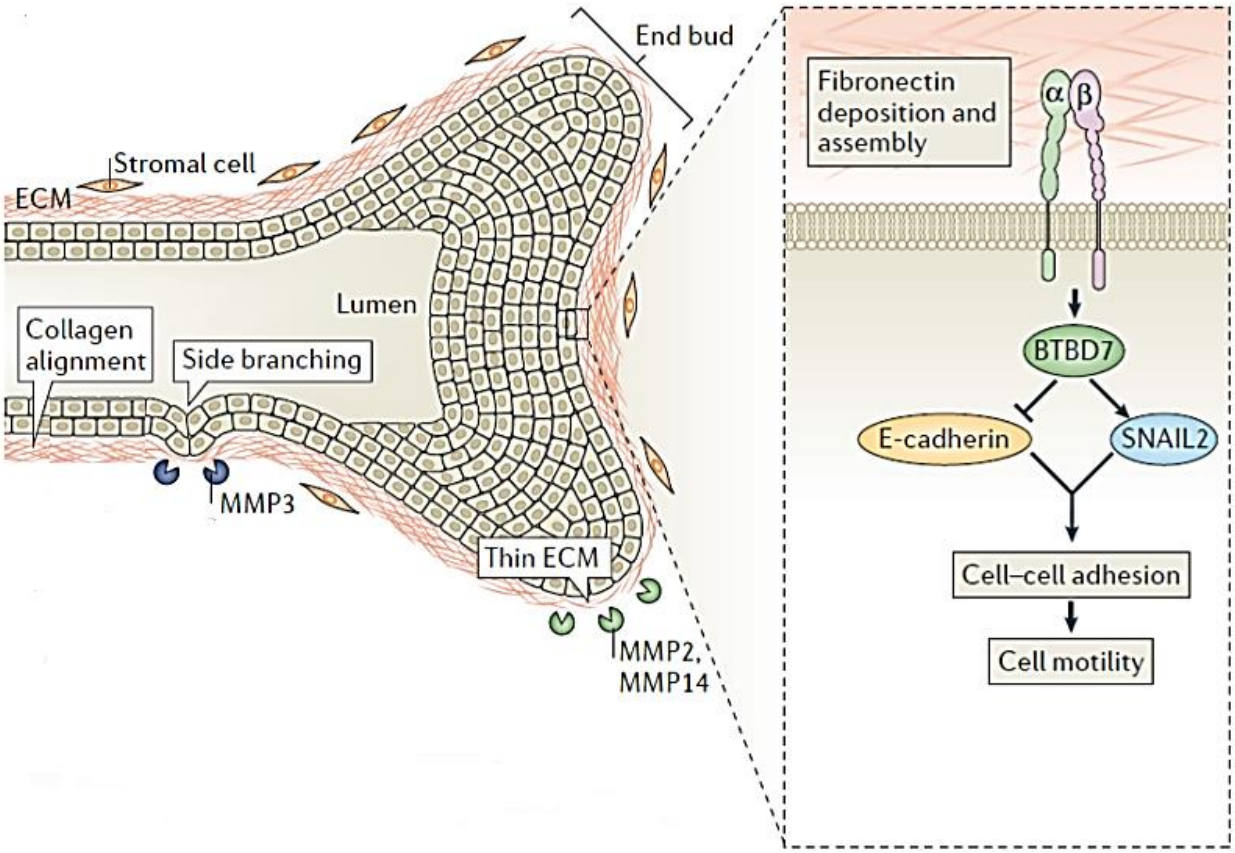

Figure 2.11: ECM remodeling during cleft formation and branching morphogenesis (adapted from [62])
Cleft formation and deepening during branching morphogenesis. Fibronectin is locally assembled in the basement membrane and induces BTBD7 at the base of forming clefts. BTBD7 expression leads to the upregulation of the transcription factor SNAIL2 and the downregulation of the adhesion molecule E-cadherin. These molecular events promote alterations in cell shape, decrease cell–cell adhesion and promote a motile phenotype.

2.5 Extracellular Metalloproteinases and their function in ECM degradation and remodeling

2.5.1 The MMP-family

A number of extracellular proteinases, which are classified as either exopeptidases or endopeptidases based on whether they cleave terminal or internal peptide bonds, respectively, are involved in the degradation and remodeling of the ECM. Most endopeptidases are classified as serine, cysteine, aspartic or metalloproteinases based on their catalytic mechanism and inhibitor sensitivities. Based on sequence considerations, metalloproteinases are further separated into five superfamilies. The MMP-, ADAMTS- and the ADAM-family are all part of the metzincin superfamily. The metzincin superfamily is distinguished by a highly conserved motif containing three histidine residues that bind zinc at the catalytic site and a conserved methionine turn located beneath the active site zinc [86]. The most prominent family within the metzincin superfamily is the Matrix Metalloproteinase (MMP) family. MMPs are endopeptidases that are either fully secreted or membrane bound (MT-MMP). MMPs show a broad spectrum of substrates within the ECM and are grouped into eight distinct structural classes (Fig. 2.12) [87]. Many of the extracellular signaling events that regulate cell behavior happen in close proximity of the cell membrane and are regulated by pericellular proteolysis [87]. Therefore close proximity of MMPs to the cell membrane is needed to achieve a proper cell response upon ECM proteolysis. Whereas the MT-MMPs are covalently linked to the cell membrane, secreted MMPs either localize to the cell surface by binding to cell surface receptors such as integrins [88] and CD44 [89, 90] or through interactions with cell-surface-associated heparan sulphate proteoglycans, collagen type IV and extracellular matrix metalloproteinase inducer (EMMPRIN) [91].

MMPs are secreted as inactive zymogens (pro-MMPs). Interactions of the propeptide with the catalytic domain keep the enzyme in its inactive state. To activate pro-MMPs the proteolytic removal of the propeptide is required [92]. Most MMPs are activated outside of the cell by other MMPs or serine proteinases. However MT-MMPs, MMP11 and MMP28 can also be activated within the secretory pathway by the proprotein convertase furin [93, 94]. MMP activity is tightly controlled by endogenous inhibitors. The best studied inhibitors of MMPs are TIMPs (Tissue Inhibitors of Metalloproteinases). The TIMPs represent a family of at least four secreted proteins (TIMPs 1–4) that reversibly inhibit MMPs. Individual TIMPs differ in their ability to inhibit various MMPs [91]. The inhibitory effect of TIMPs is not just restricted to MMPs. TIMP3 was shown to inhibit ADAMs-10 and -17, ADAMTS4, and ADAMTS5 [95], where TIMP1 can inhibit ADAMTS-1 [91, 96]. TIMPs are not the only endogenous MMP inhibitors. Indeed, α2-macroglobulin is a major endogenous inhibitor of MMPs, but also inhibits a broad variety of other proteinases such as ADAMs and

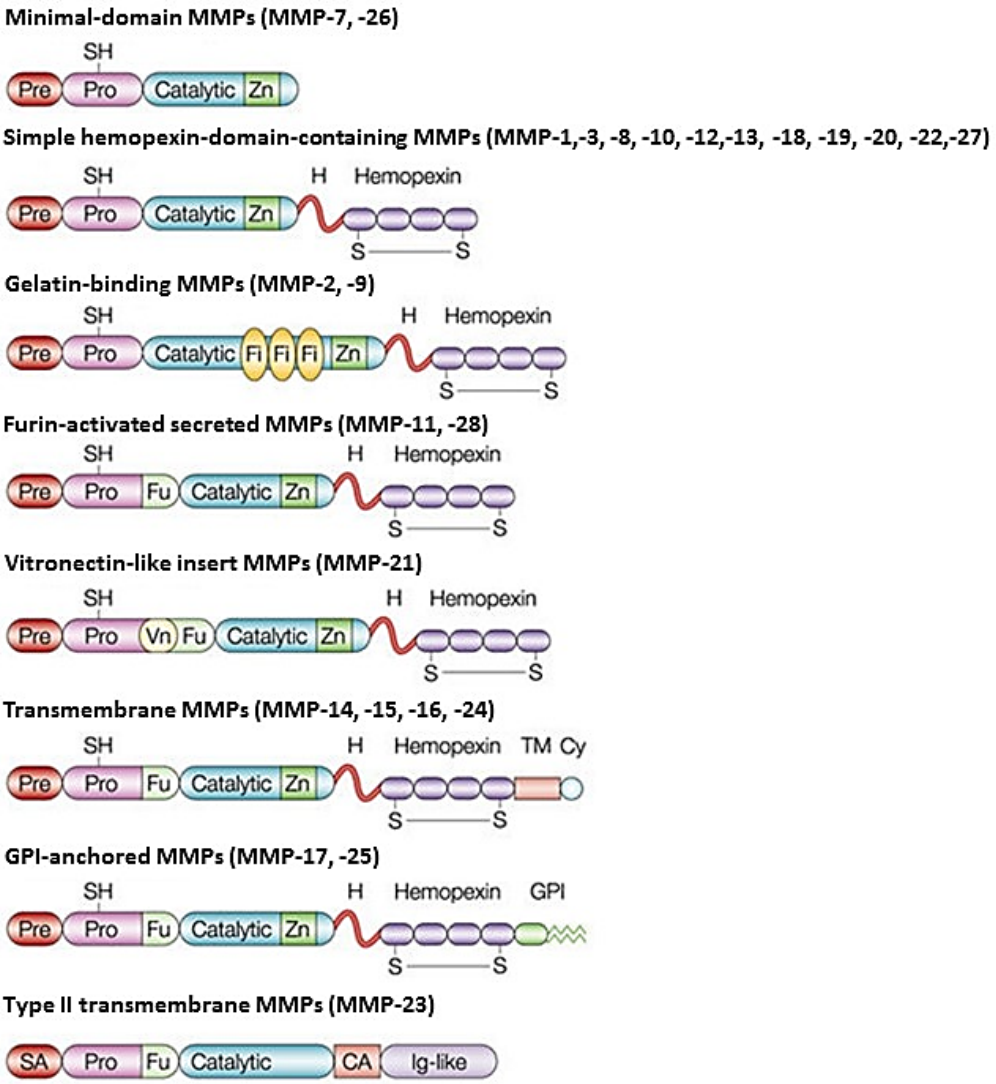

Figure 2.12: Overview of the eight structural classes of MMPs (adapted from [87])

Matrix metalloproteinases (MMPs) can be divided into eight distinct structural groups, five of which are secreted and three of which are membrane-type MMPs (MT-MMPs). All secreted MMPs share the same N-terminal structural organization. Every secreted MMP has an amino-terminal signal sequence (Pre), a propeptide (Pro) containing a zinc-interacting thiol (SH) group, which maintains them as inactive zymogens, and a catalytic domain with a zinc-binding site (Zn). Whereas the minimal-domain MMPs are comprised of these domains, other secreted MMPs contain an additional hemopexin domain at their C-terminus. The gelatin-binding MMPs contain additional inserts that resemble collagen-binding type II repeats of fibronectin (Fi), where the furin-activated secreted MMPs contain a recognition motif for the proprotein convertase furin (Fu) that allows intracellular removal of the propetide. This motif is also found in the vitronectin-like insert (Vn) MMPs and the membrane-type MMPs (MT-MMPs). MT-MMPs include transmembrane MMPs that have a C-terminal, single-span transmembrane domain (TM) and a very short cytoplasmic domain (Cy). Some MMPs contain a glycosylphosphatidylinositol (GPI)-anchor. MMP-23 is characterized by its unique cysteine array (CA) and immunoglobulin (Ig)-like domains. It has an N-terminal signal anchor (SA) that targets it to the cell membrane, which makes it the only type II transmembrane MMP.

ADAMTSs. Inhibition of MMPs by α2-macroglobulin is an irreversible process. α2-macroglobulin contains a 35 amino acid "bait" region, which is especially susceptible to proteolytic cleavage. MMP binding and cleavage of α2-macroglobulin, leads to conformational change within α2-macroglobulin such that the α2-macroglobulin collapses about the proteinase. In the resulting α2-macroglobulin-MMP complex, the active site of the proteinase is sterically shielded, thus substantially decreasing access to protein substrates [97]. The α2-macroglobulin-MMP complexes are further removed by scavenger receptor-mediated endocytosis. Therefore α2-macroglobulin plays an important role in the irreversible clearance of MMPs [98]. Because α2-macroglobulin is an abundant plasma protein, it represents the major inhibitor of MMPs in tissue fluids, whereas TIMPs may act locally [91].

MMPs have a broad variety of substrates within the ECM, such as collagens, fibronectin and laminin [99-101]. Cleavage of the ECM components by MMPs not only facilitates cell migration, but also leads to the release of biologically active ECM cleavage products. Cleavage of plasminogen and Col-XVIII, for example, results in the generation of the anti-angiogenic factors angiostatin and endostatin [102, 103]. Moreover, ECM degradation by MMPs leads to the release of bound growth factors, such as insulin-like growth factors (IGFs) and fibroblast growth factors (FGFs) and therefore directly affects cell signaling [104, 105]. In addition to causing the activation and release of cytokines and growth factors, MMPs can also cleave their cell surface receptors. MMP2, for example, cleaves FGF receptor 1 at a specific extracellular juxtamembrane site, thereby releasing a soluble receptor fragment that retains its ability to bind FGF. Soluble FGF receptor type 1 has been found in the circulation and in vascular basement membranes and may indirectly influence FGF availability [106]. Moreover MMP9 was shown to cleave interleukin 2 receptor α (IL2Rα) on T cells and therefore significantly downregulate their proliferative response to interleukin 2 (IL2) [107]. The substrate specificity of MMPs is not just limited to secreted ECM molecules and receptors. MMPs also preoteolyticaly act on cell-adhesion molecules such as E-cadherin and CD44 [108, 109]. Proteolytic processing of those molecules strongly increases cell invasion. Further leads the processing of α_v integrin precursor by MMP14 to an increase in cancer cell invasion [110]. Finally as already mentioned above MMPs can activate their own zymogens [24]. Figure 2.13 summarizes the different pathways and molecules that MMPs act on. MMPs are involved in all processes that require ECM remodeling. Changes in expression levels of MMPs can therefore have severe consequences during organ development and play a significant role in the development of diseases, such as osteoarthritis or inflammatory processes. However, the biggest interest has been in the contribution of MMPs to cancer progression and metastasis. Because of their strong contribution to tumor growth and metastasis MMPs have been intensively studied over the last decade [111, 112]. MMPs are generally present in greater amounts and activated more often in and around malignant

cancers, with the highest expression taking place in areas of active invasion at the tumor-stroma interface [91]. Significant positive correlations have been found between the expression of multiple MMPs and various indicators of a poor prognosis in virtually all types of cancer. In some instances, increased MMP levels represent an independent predictor of shortened disease-free and overall survival [87, 91].

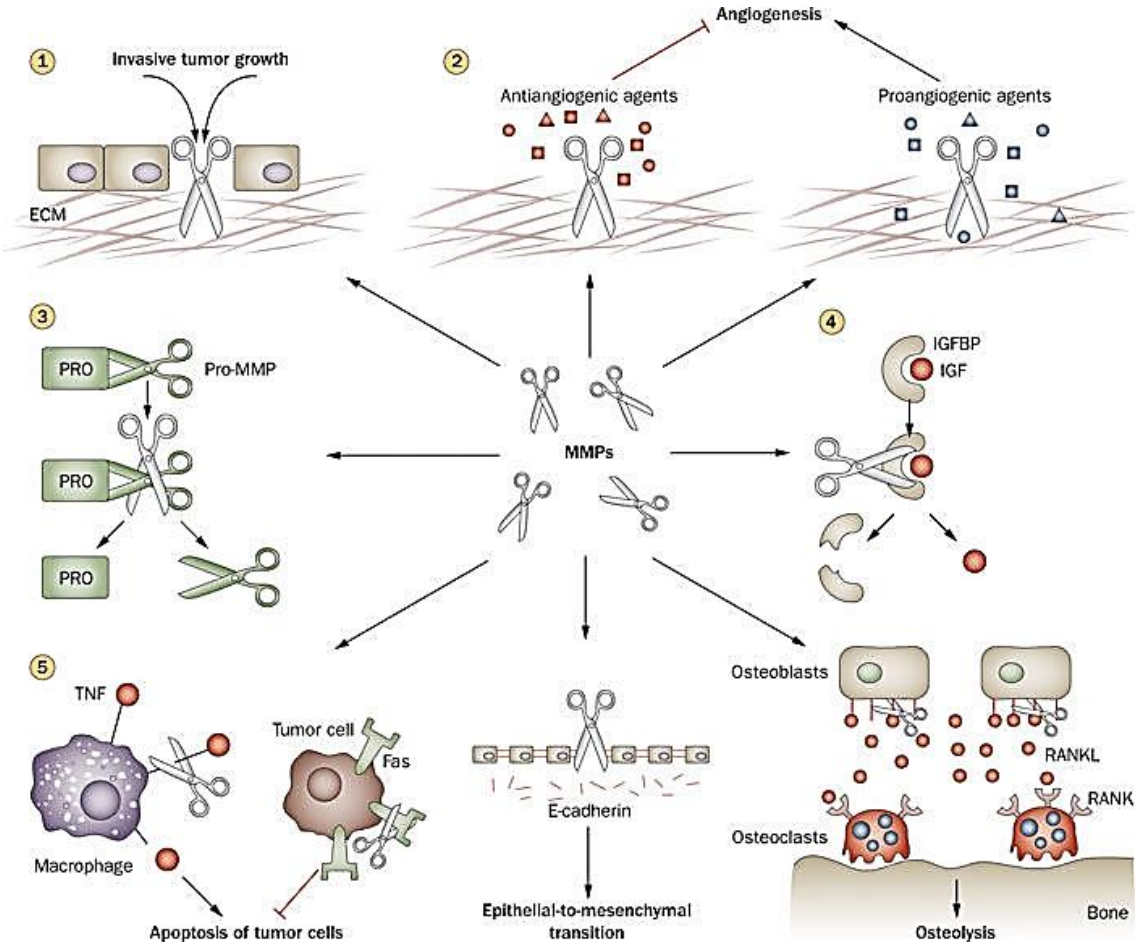

Figure 2.13: Overview of MMP-induced cellular processes and substrate specificity (adapted from [113]). (1) Breakdown of ECM is a prerequisite of cell migration and invasion during tumor metastasis as well as in developmental processes. (2) Proteolytic products of ECM, such as angiostatin, endostatin and neostatin, exhibit potent antiangiogenic properties. However, MMPs can also release proangiogenic factors, such as fibroblast growth factor (FGF) and vascular endothelial growth factor (VEGF), from their bound, inactive form, thus contributing to angiogenesis. (3) MMPs can activate other MMPs from their pro-enzyme forms by removing their prodomain. (4) MMPs can also process various non-bound proteins. For example MMP-mediated inactivation of IGFBPs leads to enhanced IGF activity. (5) MMPs also induce proteolytic shedding of extracellular domains of transmembrane and surface-bound proteins, such as RANKL, E-cadherin, TNF and Fas, enhancing tumor-induced osteolysis and epithelial-to-mesenchymal transition, as well as apoptosis of tumor cells when releasing TNF-α.

In epithelial cancers, however, most of the upregulated MMPs are expressed by the supporting stromal cells rather than by the carcinoma cells themselves [114]. Without the aid of ECM-degrading MMPs, endothelial cells would be unable to penetrate the ECM, and cancer cells would be incapable to cross the matrix barriers that otherwise contain their spread. However, recent data indicate that MMPs do far more to influence cancer progression and metastasis, than solely remove the physical barriers. MMP3 for example can promote late epithelial-to-mesenchymal phenotypic changes, via E-cadherin degradation amongst other things, what leads to a more aggressive malignant behavior [115]. Conversely, some MMPs appear to inhibit cancer progression [91]. Similar to ADAMs (discussed in the next chapter), GPI-linked MT4-MMP can cleave membrane-bound pro-TNF-α to generate active soluble TNF-α, therefore releasing a pro-apoptotic molecule, which acts negatively on tumor cell growth and proliferation [91, 116].

2.5.2 The ADAMs-family

Another important family within the metzincin superfamily are adamalysins. Adamalysins are further divided into the ADAMs-family, the ADAMTS-family (discussed in the next chapter) and the snake venom matrix proteinases (SVMP) [91]. The three subfamilies share similar N-terminal domain structure, but differ in their C-terminal domains. All of them consist of a prodomain, a metalloprotease domain, a disintegrin domain and a cysteine-rich domain. ADAMs (A Disintegrin and Metalloproteinase) have in addition an EGF-like domain, a transmembrane domain, and a cytoplasmic tail (Fig.2.14). At least 40 ADAMs have been described, 25 of which are expressed in humans. Among those, 19 display proteolytic activity. ADAMs are transmembrane proteins, what distinguishes the ADAMs family from the ADAMTSs, which are all fully secreted proteinases [117].

The expression pattern of different ADAMs varies considerably. In mammals, many of them (including ADAMs 2, 7, 18, 20, 21, 29, and 30) are exclusively or predominantly expressed in the testis and/or associated structures. Other members (ADAMs 8, 9, 10, 11, 12, 15, 17, 19, 22, 23, 28, and 33) show a broader distribution pattern [117].

Although ADAMs are kept in an inactive state via their prodomain, similar to MMPs, they are mostly activated by furin and other proprotein convertases (PC) and not by other family members. Indeed, ADAMs have not been shown to activate each other, as it is observed for members of the MMP family [118]. However some ADAMs, mainly ADAM8 and ADAM28, were shown to undergo autocatalytic activation [119, 120]. The prodomain not only keeps the proteinase inactive, but acts in addition as an internal chaperone

supporting the proper folding of a mature ADAM protein [121]. Only human ADAM15 contains an RGD motif within its disintegrin domain and is therefore able to associate with $\alpha_v\beta_3$ and $\alpha_5\beta_1$ in an RGD-dependent manner [122]. However, although missing the RGD motif, some members of the ADAM family are still capable of interacting with certain integrin receptors such as integrin α_4 and α_9, via binding by aspartic acid-containing sequences [123]. The cytoplasmic domain varies considerably in length and sequence between the different members of the ADAMs family. However, the most common motifs within the cytoplasmic domains are binding sites for SH3 domain containing proteins. Several ADAMs also have potential phosphorylation sites for serine-threonine and/or tyrosine kinases [124]. Via their C-terminal cytoplasmic domain ADAMs have a direct role in cell signaling.

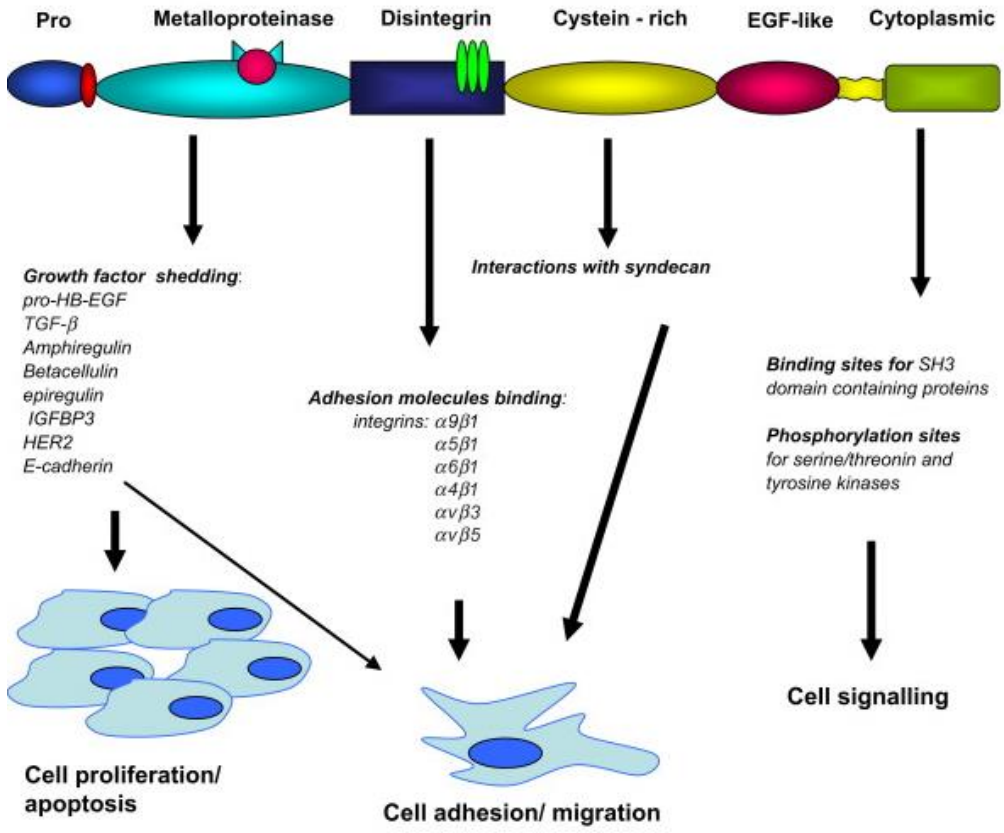

Figure 2.14: Overview of the domain organization and function of ADAM metalloproteinases (adapted from [125])

ADAMs are composed of distinct domains providing the proteins with multiple functions. All ADAM proteins contain a prodomain (Pro) keeping the proteinase in an inactive state. In the case of ADAM15 the disintegrin domain contains the integrin binding motif RGD, allowing integrin receptor binding. Most ADAMs contain a transmembrane domain after the EGF-like domain which anchors them in the cell membrane. The cytoplasmic domains bind to proteins of the cytoskeleton and serves as phosphorylation site of several kinases, therefore participating directly in cell signaling. Via binding and shedding of cell surface receptors and receptor ligands, ADAMs influence cell signaling, adhesion and proliferation.

ADAMs have gained great interest, because of their function in protein ectodomain shedding. In this regard ADAM17, also known as TNF-α converting enzyme (TACE), is the most studied member of the ADAMs family. ADAM17 activates the membrane bound precursor form of TNF-α via its release form the cell surface [117, 126]. Moreover ADAM17 not only activates TNF-α, but is also involved in cytokine receptor shedding mainly in activating the TNF-α receptor and therefore regulating TNF-α signaling in two different ways [127]. Over the years especially ADAM17 has emerged as a major sheddase with an extremely broad substrate range. ADAMs are not just involved in the shedding of cytokines and cytokine receptors, but also have been linked to growth factor, mainly EGFR ligand, shedding. ADAMs have been linked to the shedding of at least 6 EGFR ligands (TNF-α, EGF, HB-EGF, betacellulin, epiregulin and amphiregulin) [128] and play an important role in paracrine, autocrine and juxtacrine signaling (Fig. 2.15) [129]. Although the major interest in ADAMs is due to their sheddase function, they also cleave the amyloid precursor protein [130], cell adhesion molecules such as E-cadherin [131] and process a variety of ECM proteins, mainly within the basement membrane, such as type IV collagen and fibronectin [132, 133].

As previously mentioned, many of the ADAM family members are exclusively expressed in gonad cells where they play an important role regulating fertilization by promoting the fusion of egg and sperm cells. In humans the adhesion of sperm and egg requires the disintegrin domain of ADAM2 [134]. Mutations within this domain strongly inhibit egg binding [135]. However, ADAMs are not just important regulators of fertilization, but have been implicated in a variety of human diseases such as Alzheimer's disease. Alzheimer's disease is caused by the accumulation of β-amyloid peptides. The β-amyloid peptides are formed by stepwise processing of the amyloid precursor protein (APP) by β and γ-secretases. An alternative pathway of APP secretion is through the action of α-secretase activity. The soluble APPα (sAPPα) that results from α-secretase activity has positive neurotrophic effects, and opposes the harmful effects of β-amyloid formation [117]. ADAM9, 10 and 17 have been shown to cleave the amyloid precursor generating the soluble APPα protein [130, 136, 137]. It is therefore assumed that ADAMs act in a protective way preventing the development of Alzheimer's disease.

Due to their sheddase activity towards EFGR ligands and cytokines, ADAMs also regulate cellular processes such as cell proliferation, adhesion and migration (Fig. 2.13). It is therefore not surprising that a variety of members of the ADAM family have been linked to tumor development. ADAM9 and 15 are strongly overexpressed in pancreatic tumors [138] where ADAM28 was shown to be overexpressed in breast carcinomas [139].

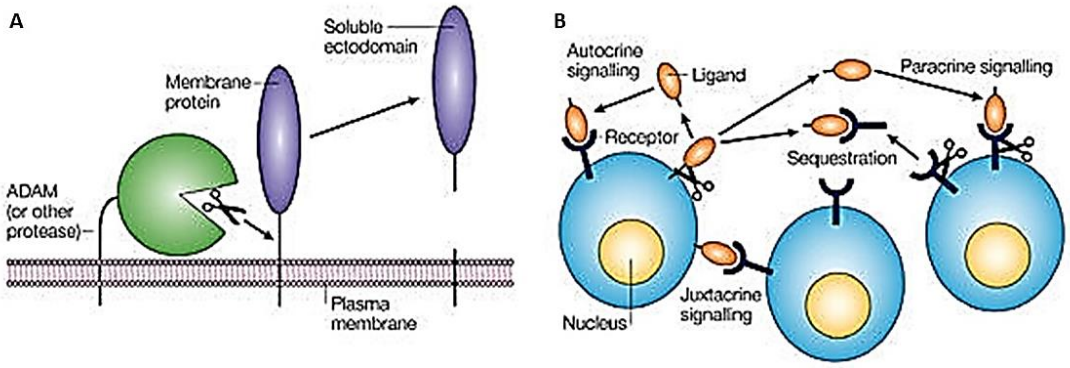

Figure 2.15: Schematic representation of ectodomain shedding and cell signaling by ADAM proteinases (adapted from [129])

A. A schematic representation of an ADAM protein that is engaged in membrane-proximal cleavage of a membrane protein, which results in the release of its soluble ectodomain. Diverse structural and functional molecules are subjected to ectodomain shedding, such as TNFα, HB-EGF and other molecules. **B.** A receptor–ligand pair is used to illustrate possible roles of ectodomain shedding. In the absence of shedding, a membrane-anchored ligand might only engage its receptor in a juxtacrine or autocrine fashion. Receptors might also be shed, which could result in their activation or inactivation.

2.6 The ADAMTS superfamily

2.6.1 Structure and Proteolytic Mechanisms

The ADAMTS (A Disintegrin and Metalloproteinase with Thrombospondin motifs) family is part of the metzincin superfamily. The ADAMTS family is closely related to the ADAM family with regard to their N-terminal domain structure, but lacks the C-terminal transmembrane domain and is therefore fully secreted. Instead ADAMTSs contain at least one thrombospondin (TSR1) domain (Fig. 2.16). The human ADAMTS superfamily includes 19 ADAMTS members and 7 ADAMTS-like (ADAMTSL) proteins. The 19 ADAMTS family members can be further sub-grouped on the basis of their known substrates, namely the aggrecanases or proteoglycanases (ADAMTS1, 4, 5, 8, 9, 15 and 20), the procollagen N-propeptidases (ADAMTS2, 3 and 14), the cartilage oligomeric matrix protein-cleaving enzymes (ADAMTS7 and 12), the von Willebrand Factor proteinase (ADAMTS13) and a group of orphan enzymes (ADAMTS6, 10, 16, 17, 18 and 19) [140]. To date, all known substrates are either ECM proteins and many members of the ADAMTSs family have at least one known substrate, although it is likely that other substrates are yet to be discovered [141]. All ADAMTSs share a common domain organization comprising a signal peptide, a prodomain, a catalytic domain, a disintegrin-like domain, a central TSR1 repeat, a cysteine-rich and a spacer domain. With the exception of ADAMTS4, all other ADAMTS enzymes have further TSR1 repeats and several family members have additional, unique modules (mucin-like domains, Gon-1 domains, protease and lacunin (PLAC) domain and CUB-domains) at their C-terminus [141]. The entire C-terminal region downstream of the central TSR1 is termed the ancillary domain, and this is where the greatest differences between ADAMTS family members occur (Fig. 2.16) [140].

Similar to ADAM family members, ADAMTSs contain a prodomain that keeps the proteinase in its inactive state and acts additionally as an internal chaperone mediating proper folding. Activation of the zymogen into a fully active proteinase requires catalytic processing and release of the prodomain from the catalytic center. It is, however, unlikely and could not be shown so far that ADAMTSs activate each other, as is the case for certain members of the MMP family. Moreover all ADAMTS family members contain a consensus sequence making the protease susceptible for activation by proprotein convertases such as furin. Furin activation can occur within the *trans*-Golgi network as well as extracellularly in close proximity to the cell surface [142, 143]. However, not all members of the ADAMTS family need the removal of the prodomain to be activated. ADAMTS13, for example, does not require cleavage of the prodomain to be fully active [144]. Additionally it could be shown that ADAMTS9 loses its activity towards its substrate versican upon removal

of the prodomain [145]. The catalytic domain of the ADAMTS family members has the highest degree of sequence homology. ADAMTS enzymes have in common with other members of the metzincin superfamily, the active-site consensus sequence HEBxHxBGBxH, in which the three histidine residues coordinate a zinc ion essential for hydrolysis, and where B represents bulky apolar residues (Fig. 2.16). C-terminal to the third histidine is a highly conserved methionine that constitutes the 'Met-turn', a tight turn common to the catalytic domain and the reason for the metzincin nomenclature [146].

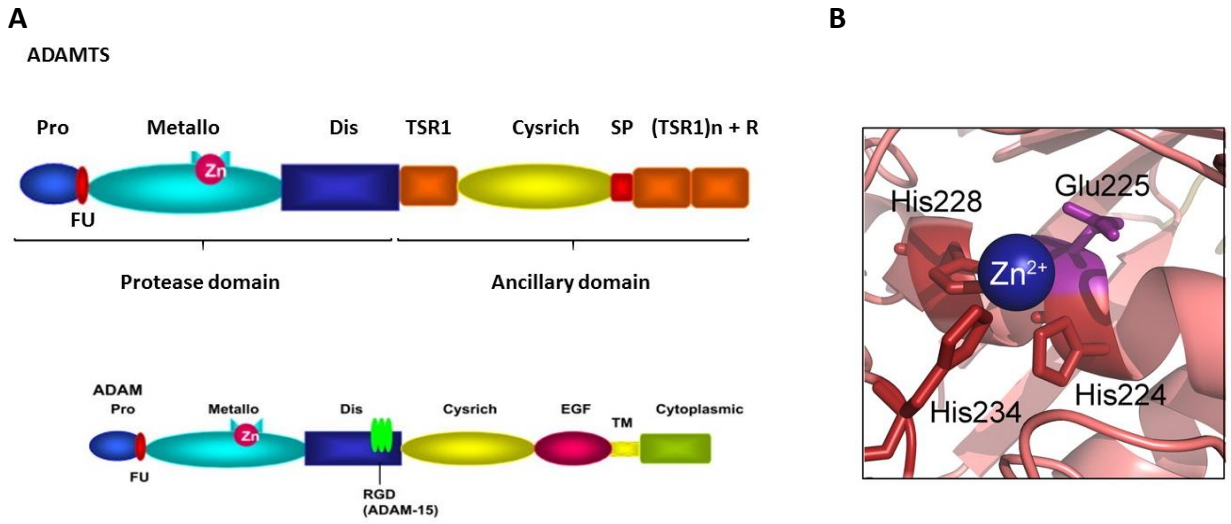

Figure 2.16: Overview of the domain organization and the catalytic center of ADAMTS
A. Structure of ADAM and ADAMTS proteinases. Both proteinase families share common domain structures such as a prodomain (Pro) with a furin cleavage site (FU) for activation, a metalloproteinase domain with a zinc ion bound to the catalytic center, a disintegrin domain (Dis) and a cysteine rich domain. Unlike ADAMs, ADAMTSs contain neither a transmembrane domain (TM), nor a cytoplasmic domain. ADAMTSs contain a first thrombospondin type 1 motif (TSR1) after the Dis domain and a variable amount of TSR1 motifs in their C-terminus. Most ADAMTSs contain an additional domain (R), such as mucine, CUB or PLAC domains at their C-terminus after the last TSR1 motif. Unlike ADAMs, ADAMTSs are fully secreted. Figure adapted from [125] **B.** Cartoon representation of the active site of ADAMTS13. The three histidine (His) residues coordinating the zinc ion (Zn^{2+}) are marked in red. The catalytic Glu225 (purple) polarizes a water molecule that is stabilized by the coordinated Zn^{2+} ion, and is part of the proteolytic machinery. Figure adapted from [147].

Unlike ADAMs none of the ADAMTSs have been reported to interact with integrin receptors via their disintegrin-like domain [140]. Crystal structure data for ADAMTS1, 4 and 5 reveal that the disintegrin-like domain is a cysteine-rich region that stacks against the metalloproteinase active-site cleft, implying that it functions to regulate activity, perhaps by providing an auxiliary substrate-binding surface [148, 149].
While the catalytic domain is strongly conserved among different ADAMTSs, they show less structural homology within their C-terminal ancillary domains. The ancillary domains are responsible for the

association with the ECM, regulation of protease activity, and for specification of substrate-binding preferences. All ADAMTSs contain a TSR1 module after the disintegrin-like domain, a cysteine-rich domain and a spacer domain within their ancillary domains [140]. The cysteine-rich and spacer domains of ADAMTS1, 4, and 5, for example, determine binding to sulphated glycosaminoglycans and tissue localization [150, 151]. With the sole exception of ADAMTS4, the spacer domain is followed by 1 to 14 further TSR1 modules and additional motifs that are characteristic of particular subgroups. The ADAMTS9/20 pair has the largest number of TSRs and each concludes with a GON-1 module (first described in *C. elegans* Gon-1) [152]. ADAMTS13 is unique in having two CUB modules. Several ADAMTSs (ADAMTS2, 3, 6, 7, 10, 12, 14, 16, 17, 18 and 19) possess a PLAC domain. In ADAMTS7 and 12, a mucin/proteoglycan domain is interposed in the middle of the seven C-terminal TSR1s (Fig. 2.17). The sequence of the C-terminal TSR1 modules is more variable than the central thrombospondin module, but their function appears to be ECM binding as well. The ancillary domains of ADAMTSs can be proteolytically processed, affecting secretion, localization, activation and catalytic functions [140, 153, 154].

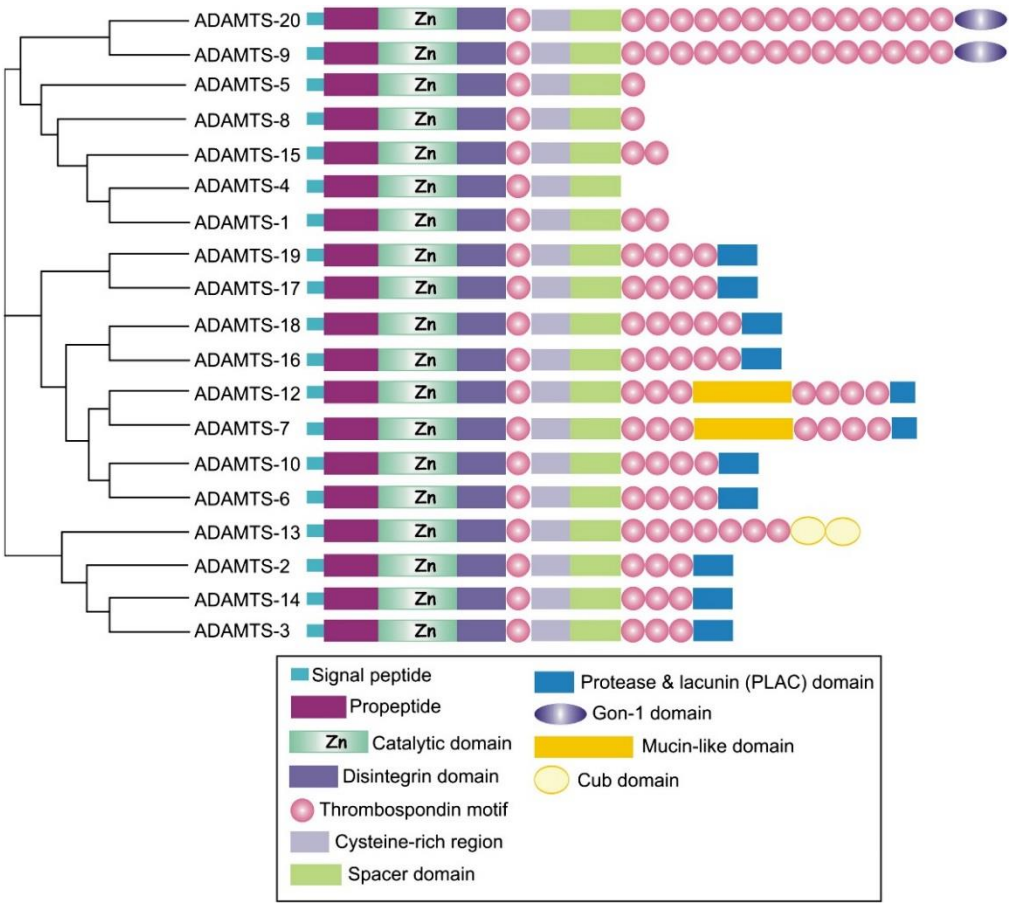

Figure 2.17: Overview of the ADAMTS family (adapted from [141])
The domain structure and phylogenetic analysis of the ADAMTS family. Domains are not to scale.

Like MMPs and ADAMs, ADAMTSs show restricted susceptibility to inhibition by TIMPs, where TIMP3 emerges as the most effective inhibitor [155]. The activity of the ADAMTSs is also controlled by their internalization and degradation. ADAMTS4 and 5, for example, have been shown to be internalized upon binding to LRP-1 [156, 157].

2.6.2 ADAMTSs in Development and Disease

ADAMTSs are not as well characterized with regard to their substrate specificity and mechanisms of action, compared to MMPs and ADAMs. The known substrates of ADAMTSs are mainly ECM proteins and little is known about their potential contribution to cell signaling and how they influence cellular responses and cell behavior upon ECM protein cleavage. However, improving technologies and growing research in the field is revealing an increasing number of substrates and leading to a better understanding of the underlying mechanisms of ADAMTS-mediated substrate processing.

The ADAMTS proteinases have important roles in tissue development and maintenance, and their dysregulation or mutation is associated with a number of diseases. ADAMTS2, ADAMTS3 and ADAMTS14 are procollagen N-proteinases [158-160] and loss-of-function mutations in *ADAMTS2* cause Ehlers–Danlos syndrome type VIIC, a connective tissue disorder characterized by severe skin fragility [161]. The best characterized members and most intensively studied ones however are ADAMTS1, 4, 5 and 13.

The proteoglycan aggrecan is a major constituent of the chondrocyte ECM and excessive degradation can have severe physiological consequences, such as osteoarthritis (OA). Aggrecan is one of the first matrix components to undergo measurable loss that ultimately leads to a loss of cartilage function and OA. Therefore, aggrecan degradation is considered to be a crucial initial event in the development of OA, which is followed by essentially irreversible collagen degradation [162]. Various studies indicate that ADAMTS4 and 5 are the two major aggrecanases in cartilage [163, 164]. A tight regulation of ADAMTS4 and 5 activity is crucial for maintaining a fine balance between aggrecan anabolism and catabolism. In diseases such as OA the regulation of aggrecanase activity is disturbed in favor of catabolism [162-164]. The most significant aggrecan cleavage site for ADAMTS4 and 5 in OA pathogenesis is located at a highly conserved sequence TEGE$^{373}\downarrow^{374}$ARGS. Antibodies that recognize the ^{374}ARGS neo-epitope [165] are important tools for tracking protease activity, OA progression and led to the original discovery of ADAMTS4 and 5 [96, 166].

Particularly ADAMTS5 has been shown to be the major aggrecanase. *In vitro* it has been shown to be about 1,000 times more potent than ADAMTS4 [167]. Therefore ADAMTS5 has emerged as one of the main targets in the treatment of OA and several attempts have been undertaken to generate specific ADAMTS5

inhibitors. Two recent publications demonstrated the efficacy of ADAMTS5 inhibition *in vivo* using monoclonal antibodies. The antibody GSK2394002 developed by researchers at GlaxoSmithKline was shown to protect the cartilage matrix from degradation in both mice and cynomolgus monkeys. Additionally it could reduce pain-associated allodynia in mice [168]. Another promising antibody against ADAMTS5 is CRB0017, a recombinant monoclonal antibody of high affinity and selectivity against the spacer domain of ADAMTS5. Intra-articular injection of CRB0017 in STR/ort male mice, which spontaneously develop OA, resulted in significant chondroprotection [169].

Other ADAMTSs may be physiologically relevant aggrecanases in tissues other than cartilage. ADAMTS1 for example, was shown to be relevant in aggrecan processing during kidney development [170]. Cofactors as well as C-terminal processing may play a functional role in mediating accreganase activity in addition to tissue specific expression. Local cofactors such as fibulin-1 for example, which binds to ADAMTS1 and increases its aggrecanase activity, may be important in determining which enzyme has the principal activity in a particular tissue context [170]. Additionally it could be shown that MMP17-mediated ancillary domain cleavage of ADAMTS4 enhances its ability to cleave aggrecan [171].

Another disease linked to ADAMTSs is thrombotic thrombocytopenic purpura (TTP). TTP is a rare disorder of the blood-coagulation system, causing extensive microscopic clots to form. If untreated the disease leads to the development of severe hemolytic anemia, abundant schistocytes, profound thrombocytopenia, neurological deficits, renal injury, fever and death within the first months of illness [172]. A breakthrough in understanding the pathogenesis of TTP came with the discovery of ADAMTS13 and its main substrate the von Willebrand factor (vWF) [173]. The vWF interacts with blood platelets and thereby promotes blood clotting. However, in the absence of proteolytic cleavage there is an accumulation of unusually large vWF multimers, which triggers intravascular platelet aggregations and microthrombosis [174]. VWF is secreted from endothelial cells as ultra large multimers, and ADAMTS13 progressively reduces the size of those vWF multimers as they circulate in the blood. Under low-shear conditions, vWF multimers adopt a loosely coiled, condensed shape. Above a critical shear rate, vWF multimers extend and unfold the A2 domain exposing a cryptic Tyr-Met bond which is cleaved by ADAMTS13 [175, 176]. Under normal conditions vWF multimers bind platelets on the endothelial cell surface or at sites of vascular injuries. Compared to soluble vWF, bound vWF requires much lower shear stress to induce conformational changes that promote binding to platelets or cleavage by ADAMTS13 [177]. Cleavage of vWF by ADAMTS13 than leads to the release of smaller vWF multimers together with any attached platelets. The proteolytic cleavage of vWF therefore prevents the formation of microvascular thrombosis, tissue ischemia and infarction [172]. ADAMTS13 deficiency can cause the cardinal features of TTP, thrombocytopenia and

microangiopathic hemolytic anemia, by failing to regulate VWF-dependent platelet adhesion (Fig. 2.18). In most cases ADAMTS13 deficiency leading to the development of TTP is caused via autoantibodies to ADAMTS13 (also known as acquired TTP). These anti-ADAMTS13 antibodies usually block the proteolytic activity of ADAMTS13 towards vWF [178]. Another rarer mechanism for ADAMTS13 deficiency is due to loss-of-function mutations within the *ADAMTS13* gene (inherited TTP) [173, 179].

The knowledge whether the patient is suffering from inherited TTP or acquired TTP, is crucial for an effective treatment. In case of inherited TTP, plasma infusions are the most effective way of treatment although connected to a variety of side effects such as severe allergic reactions. Plasma exchange remains the standard therapy for acquired TTP. However, rituximab an antibody that binds and kills all B-cells including the ADAMTS13 autoantibody producing ones, shows to be beneficial in most patients when used in combination with plasma exchange [172].

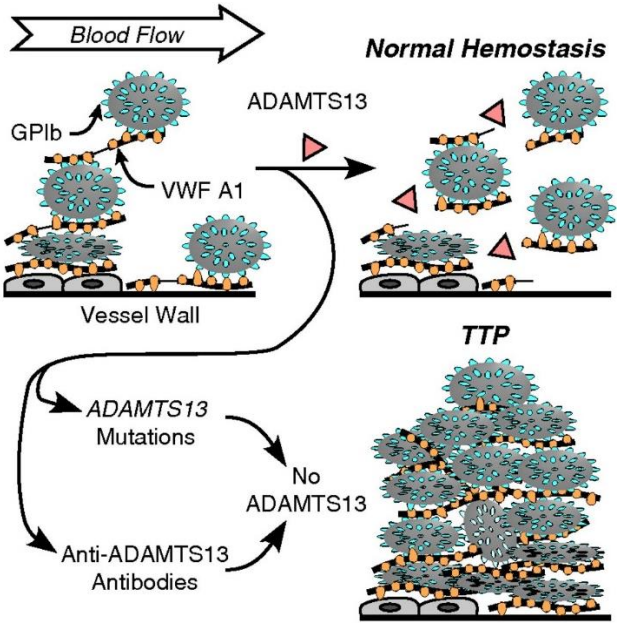

Figure 2.18: Role of ADAMTS13 in platelet adhesion and TTP (adapted from [171])
VWF multimers adhere to endothelial cells or to connective tissue in the vessel wall. Platelets bind to the A1 domain of vWF via GPIb. Shear force applied by the blood flow stretches vWF and exposes a cleavage site for ADAMTS13 in the A2 domain. Cleavage of vWF limits the growth of intravascular thrombi.
Congenital or acquired ADAMTS13 deficiency allows excessive platelet deposition, causing microvascular thrombosis and TTP.

So far ADAMTS13 remains unique in its ability to cleave the soluble plasma protein vWF. However, the C-terminal domain of ADAMTS18 has recently been shown to interact with blood platelets via binding to platelet integrin GPIIIa. Upon secretion of ADAMTS18 by endothelial cells the C-terminus is cleaved by thrombin and interacts with GPIIIa, leading to oxidative platelet fragmentation. Through this process platelet aggregates are dissolved, the in vivo bleeding time is regulated, carotid artery platelet thrombus formation is inhibited, and mice have been shown to be protected against postischemic cerebral stroke [180]. Additionally, various other ADAMTS family members have been shown to play functional roles in vascularization, however rather in controlling angiogenesis than regulating blood coagulation. Studies on

ADAMTS1 reported that the C-terminal spacer domain together with its 3 TSR1s exhibit anti-angiogenic properties by sequestering VEGF and blocking its binding to VEGF receptors [181]. Also other ADAMTS family members such as ADAMTS2, 12 and 15 have been shown to have anti-angiogenetic properties mostly independent of their catalytic domains. Due to their anti-angiogenetic properties these proteinases have also been shown to act negatively on tumor growth and proliferation [182-184]. Although the non-catalytic C-terminal domains of various ADAMTSs have been shown to have anti-angiogenic functions, the substrate specificity and function of the catalytic domain with respect to angiogenesis is of equal if not bigger physiological relevance. In this regard ADAMTS1 is the family member with the most known and the best studied substrates relevant for angiogenesis [185]. Proteolysis of thrombospondin1 and 2 by ADAMTS1 for example, promotes the release of anti-angiogenic TSR fragments with remarkable inhibitory consequences to wound healing and tumor angiogenesis [186]. Not only the cleavage of thrombospondins by ADAMTS1 inhibits angiogenesis, but also the cleavage of the basement membrane glycoproteins nidogen-1 and -2 by ADAMTS1 results in vascular impairment and correlates with tumor suppressive activities in some cancers (Fig. 2.19) [187].

As already mentioned most ADAMTSs have been shown to have anti-tumorigenic properties mostly due to their capability of inhibiting angiogenesis, but also by influencing cell adhesion, migration, proliferation and degradation or interaction with extracellular matrix components. Moreover, several *ADAMTS* genes have been found mutated or epigenetically silenced in specific tumors [188]. This, however, distinguishes them strongly from MMPs where the large majority of the family members exhibit pro-tumorigenic properties and their expression often correlates with poor prognosis and shortened disease-free and overall survival. As already mentioned ADAMTS1 is capable of capturing and inactivating VEGF, by prohibiting its binding to the corresponding receptor. However ADAMTS4 is also able to capture and inactivate VEGF. Moreover ADAMTS4 was shown to inhibit phosphorylation of VEGF receptor 2 (VEGFR2) [189]. Furthermore, and consistent with ADAMTS angio-inhibitory capacities, it has been shown that ADAMTS2 decreases Erk phosphorylation levels in HUVEC cells [182]. Other ADAMTS family members seem to inhibit Erk phosphorylation as well. For example ADAMTS12, which has been shown to inhibit Erk phosphorylation and tubulogenesis in MDCK cells upon stimulation with hepatocyte growth factor (HGF) [190]. Abrogation of Erk phosphorylation has also been linked to ectopic expression of ADAMTS15 in colon cancer cells and ADAMTS8 in epithelial and esophageal carcinoma cells [191, 192]. ADAMTS9 another member of the family, can suppress tumor progression by inhibiting the activity of Akt/mTOR (Fig. 2.19) [193]. Most ADAMTSs are expressed by the tumor cells themselves. However, it is noteworthy that some ADAMTSs can be also found expressed in stromal cells but not in cancer cells. This is the case for ADAMTS12, which

has been detected in cancer-associated fibroblasts but not in tumor cells of colon carcinoma samples. The presence of ADAMTS12 has been related to a stromal response aimed to control tumor progression, thereby it has emerged as a potential marker of good prognosis in this type of tumor [194].

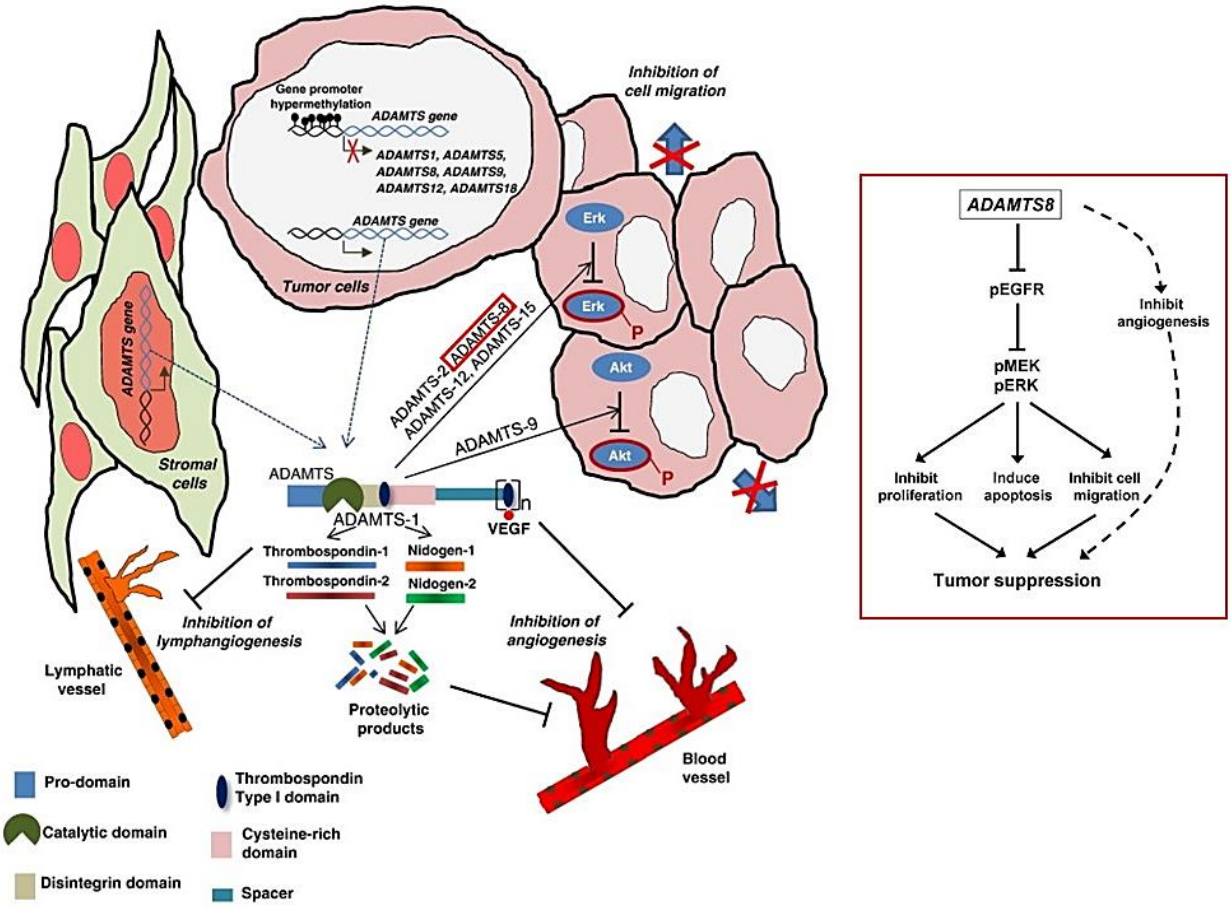

Figure 2.19: Schematic representation of the antitumor effects mediated by ADAMTS metalloproteases (adapted from [188] and [192])

ADAMTSs can be produced by stromal or tumor cells, and exert antitumor properties inhibiting angiogenic or lymphangiogenic processes. Additionally some family members, for example ADAMTS8, block tumor-promoting signaling pathways. These effects may be dependent on the catalytic activity such as degradation of the extracellular components thrombospondin-1 and -2, and nidogen-1 and -2, or independent of the catalytic activity such as VEGF sequestration.

Although they have been shown to have anti-angiogenic properties, ADAMTS1, 4 and 12 have been shown to be pro-tumorigenic as well. Although the proteolytic processing of thrombospondin1 by ADAMTS1 inhibits angiogenesis, ADAMTS1 has been further shown to be involved in the shedding of heparin-binding epidermal growth factor (HB-EGF) and amphiregulin, and the activation of EGFR [195]. Additionally, ADAMTS1 can facilitate the spreading of tumor cells through the degradation of versican, a predictor of metastatic relapse in human breast cancer [196].

ADAMTS4 and ADAMTS5 are proteoglycanases that increase the invasive potential of glioblastoma cancer cells through the degradation of brevican, a highly expressed proteoglycan in this type of malignant brain tumor [197]. ADAMTS12 on the other hand can potentiate trophoblast invasion by regulating adhesion and invasion via a mechanism involving $\alpha_v\beta_3$ integrin and FAK phosphorylation (Fig.2.20) [198].

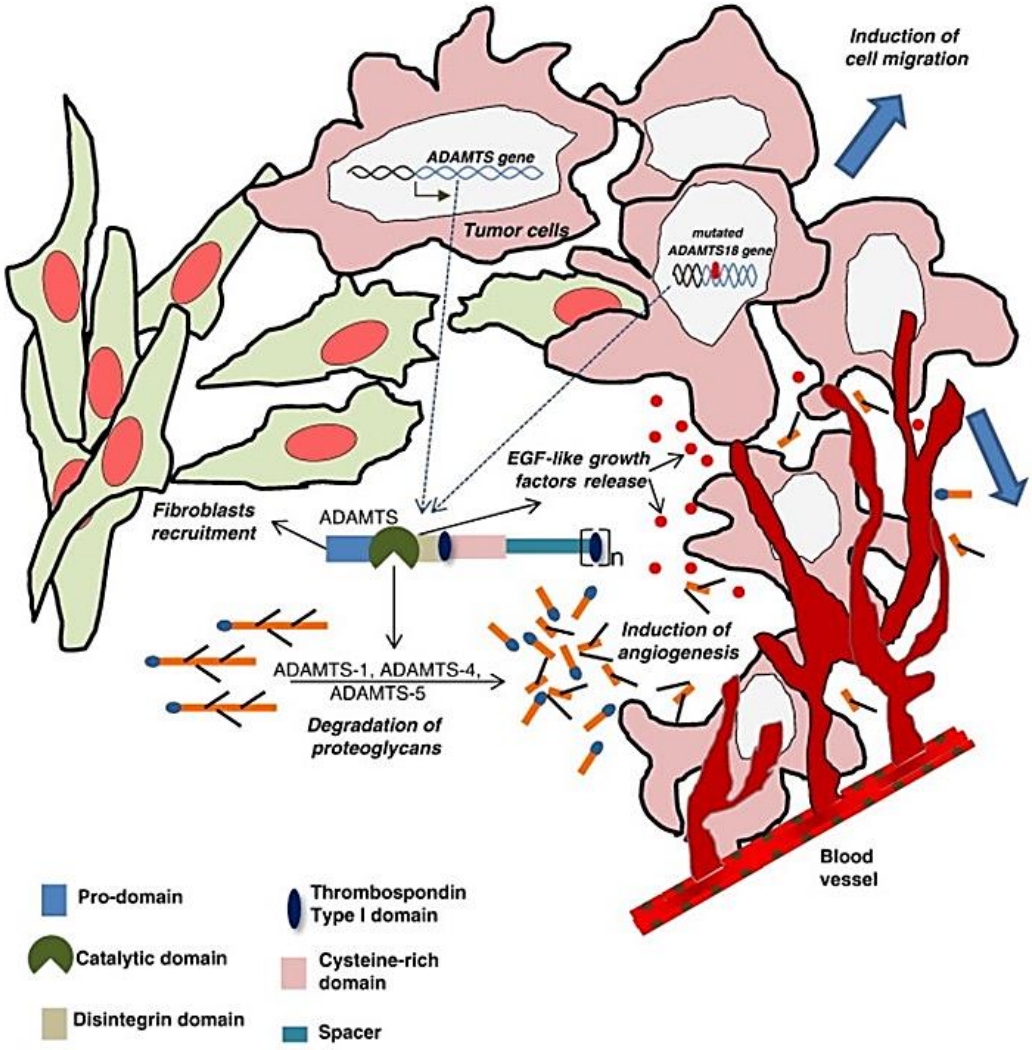

Figure 2.20: Schematic representation of the pro-tumorigenic effects mediated by ADAMTSs (adapted from [188])

ADAMTSs may cleave or induce the release or activation of pro-angiogenic factors (HB-EGF or amphiregulin), and digest extracellular matrix components (proteoglycans) to facilitate tumor cell spreading and metastasis. Pro-tumor effects elicited by ADAMTSs are protease-dependent. Additionally, ADAMTSs can induce the recruitment of fibroblasts involved in tumor growth.

That ADAMTSs can have both pro- and anti-tumorigenic functions depends on the cancer and the context. It also correlates with the processing and activity of the proteinase itself. ADAMTS1 and 4 both undergo autocatalytic processing, which affects the balance between pro-tumorigenic and anti-tumorigenic functions of this metalloproteinase [188, 199]. The N-terminal 53-kDa catalytically active isoform of ADAMTS4 for example promotes B16 melanoma angiogenesis in mice. In clear contrast, the catalytically inactive full-length protein or different truncated fragments containing the C-terminal ancillary domains delay melanoma cell growth and angiogenesis [199]. Also the interaction with other ECM proteins can influence the tumorigenic potential of ADAMTSs. ADAMTS12 was shown to interact with fibulin-2 and concomitant expression of both extracellular proteins considerably reduces pro-tumorigenic capacities of breast tumor cells [200]. Fibulin-2, similarly to fibulin-1, may act as a pro-tumor or anti-tumor glycoprotein respectively [201]. For example, fibulin-2 drives malignant lung cancer progression but reduces breast cancer cell invasion [202, 203]. Therefore, fibulin-2 most likely acts as a modulator between tumor-promoting and anti-oncogenic roles associated to ADAMTS12.

Members of the ADAMTS family are not only involved in the development and progression of various diseases, but play an important role in tissue reorganization during organ development and embryogenesis.

ADAMTS1, 4, 5, 9, 15 and 20 are known versicanases. Versican is an essential ECM component during embryogenesis as it gives rise to a loose, hydrated hyaluronan-rich matrix that provides structural support while allowing dynamic remodeling during morphogenesis. It influences the adhesion, migration and proliferation of many cell types and versican-null mice die around E10 because of cardiac defects [204]. Therefore versican turnover by ADAMTSs is essential during various developmental processes such as cardiac development, limb morphogenesis, palate formation, skin pigmentation and myogenesis [205-209]. During heart formation, the initially immature versican-rich ECM is replaced by a collagen, proteoglycan and elastin-containing matrix. *Adamts9*-null mice die prior to gastrulation, but hemizygous *Adamts9+/−* mice have heart malformations resulting from intact versican accumulation [205].

2.6.3 ADAMTS-like proteins

The ADAMTS superfamily not only comprises of the 19 catalytically active members discussed in the previous chapter, but also includes 7 non-catalytic members known as ADAMTS-like (ADAMTSL) proteins. The structure of ADAMTSLs resembles the non-catalytic domains of ADAMTS proteinases, but they lack a

protease domain (Fig.2.21) [210]. Although members of the ADAMTS superfamily, ADAMTSL proteins are neither proteinases, nor do they arise by alternative splicing of ADAMTS proteinase genes. ADAMTSL are not well characterized and not much is known so far about their function. However, they are fully secreted and are components of the ECM [211]. It is hypothesized that ADAMTSL may have architectural or regulatory functions in the matrix independent of proteolytic activity. Mutations in a variety of *ADAMTSL* genes have been linked to severe human diseases. ADAMTSL2 has been shown to bind to latent TGF-β-binding protein-1 (LTBP1) and fibrillin-1 (FBN1) and mutations in the human *ADAMTSL2* gene cause geleophysic dysplasia, a rare disorder that is characterized by high levels of TGF-β activity and resembles Weill-Marchesani syndrome (WMS) [212]. Moreover a homozygous *ADAMTSL4* mutation was recently identified in isolated ectopia lentis (IEL) (dislocation of the ocular lens) [213]. Interestingly, IEL is a major clinical feature of both WMS and Marfan syndrome, and dominant IEL can also be caused by *FBN1* mutations in addition to *ADAMTSL4* mutations [214]. Therefore, the role of ADAMTSL2 and ADAMTSL4 in TGF-β regulation and maintenance of the lens, respectively, suggests that these ADAMTSL proteins may regulate fibrillin supramolecular assembly and/or architecture [211].

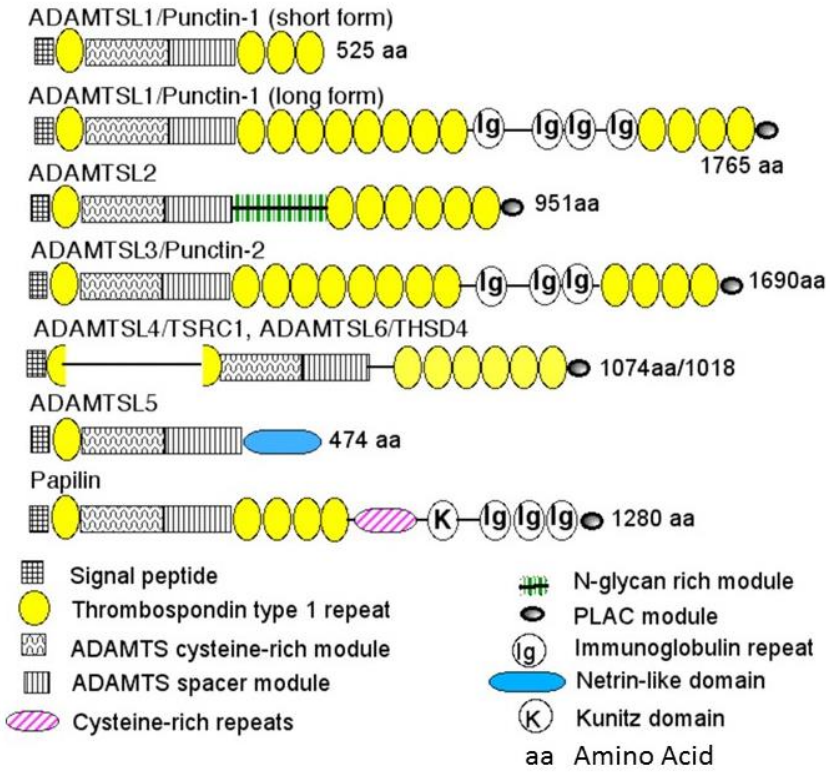

Figure 2.21: Overview of mammalian ADAMTSL proteins (adapted from [211])
The domain structure of each ADAMTSL is shown. The two forms of ADAMTSL1 shown are splice variants of the same gene. The long form of ADAMTSL1 composes a clade with ADAMTSL3. ADAMTSL4 and ADAMTSL6 contain a distinct clade in which TSR1 is split by an insertion.

2.6.4 ADAMTS16

ADAMTS16 is one of the ADAMTS members without a known substrate and is therefore also called an orphan proteinase [140]. Structurally ADAMTS16 is closely related to ADAMTS18 and contains 5 TSR1 repeats and a PLAC domain at its C-terminus. *ADAMTS16* was first discovered and cloned in 2002 by Cal et al. [215]. An expression analysis of various human embryonal and adult tissues showed that *ADAMTS16* is expressed in fetal kidney and lung tissue and in adult brain and ovarian tissue. In addition very low amounts of *ADAMTS16* were found in placenta samples [215]. From its first discovery until know, not much more information on ADAMTS16 has become available. So far no substrate has been identified and its function within the ECM remains mainly unknown. Although studies showed that a recombinant ADAMTS16 construct comprised only of its protease domains, developed very weak aggrecanase activities [154], it remains questionable if these findings are physiologically relevant. Studies addressing the regulation of *ADAMTS16* expression found that *ADAMTS16* is mainly expressed in the ovaries by the parietal granulosa cells of pre-ovulatory follicles. In fully differentiated luteinizing granulosa cells, follicle-stimulating hormone (FSH) and forskolin induce expression of *ADAMTS16*, suggesting that it is regulated via the cAMP pathway [216]. Mutations in the *ADAMTS16* gene were associated with premature ovarian failure [217, 218], indicating that ADAMTS16 plays an important role during ovulation.

Further studies using mouse embryonal kidney and gonad tissues and cell lines indicate the *Adamts16* is transcriptionally regulated by the transcription factor Wilms tumor protein 1 (Wt1) and is involved in the branching process during kidney development [219]. Moreover *ADAMTS16* knockout rats showed morphological defects in the kidney associated with high amounts of protein in the urine in addition to impaired testis development resulting in low sperm production and sterility [220, 221].

ADAMTS16 is not only relevant during kidney and testis development, but was linked to a variety of diseases. Tissue samples of OA patients showed increased expression levels of *ADAMTS16* [222, 223] where the main source of ADAMTS16 seems to be the synovium rather than the cartilage itself [223]. Additional characterization of ADAMTS16 using in vitro cell culture assays showed that *ADAMTS16* expression in chondrocytes is strongly increased in the presence of TGF-β. TGF-β mediated signaling most likely results in the activation of gene transcription by the two transcription factors Sp1 and Egr1 [224]. These factors were previously linked to TGFβ signaling mediated expression of other extracellular matrix genes [225, 226].

Further mutations in the *ADAMTS16* gene have been associated with a higher risk of developing high blood pressure [227].

Additionally *ADAMTS16* was found to be overexpressed in esophageal squamous cell carcinomas [228] and *ADAMTS16* gene mutations influence therapeutic outcome in ovarian cancer patients [229].

Although ADAMTS16 seems to have a functional role in the development of certain diseases and in branching morphogenesis during development, the research done so far focused mainly on gene expression levels and stayed descriptive. So far no substrate has been identified and the mechanism by which ADAMTS16 regulates ovulation, contributes to osteoarthritis or other diseases remains unclear.

3. Aim of the Thesis

ADAMTSs are a family of extracellular metalloproteinases that play key roles during tissue remodeling and regeneration, development and disease. However, their substrate variety and their functional roles in ECM turnover and cell signaling are not well understood for most of the family members. Their C-terminal domain varies strongly within the different family members and distinguishes them from MMPs and ADAMs. Moreover the C-terminal domain of ADAMTSs has a variety of functions, such as regulating activity, ECM binding and substrate recognition. Because of their strong C-terminal variability and the strong influence of the C-terminus on the overall function of ADAMTSs, C-terminal processing is a key element in regulating ADAMTS activity. Therefore certain members can have pro- and anti- tumorigenic properties depending on binding partners and C-terminal processing. This C-terminal variability makes them an ideal therapeutic target, because it allows the design of very specific binders to their C-terminus with minimal cross reaction with other family members or members of the MMP or ADAMs family. However to use them as an efficient therapeutic target, it is necessary to have an in depth understanding of their substrate specificity, and their biochemistry, especially with respect to C-terminal processing and the underlying mechanism of action.

ADAMTS16 is an orphan member of the ADAMTS family. However, recent studies linked mutations in the *ADAMTS16* gene to a variety of diseases such as blood pressure regulation and cancer. Additionally ADAMTS16 seems to play an important role during ovulation and spermatogenesis. Although ADAMTS16 is physiologically relatively well characterized, knowledge of its biochemistry, substrates and underlying mechanisms of action is rather limited.

The aim of this project was to identify a substrate for ADAMTS16, its mechanism of action and its influence on cellular morphology and behavior. For this we developed a novel mass spectrometry approach using a decellularized ECM for substrate identification. A second goal was to gain a better understanding of the ADAMTS16 biochemistry and the functional role of C-terminal processing. For our studies we used wild type ADAMTS16 constructs, but generated an active site mutant in addition as a control. Using the inactive mutant allowed us to further investigate the function of the C-terminal domain separately from the catalytic activity.

4. Results

4.1 Manuscript

"A selective extracellular matrix proteomics approach identifies fibronectin proteolysis by ADAMTS16 and its impact on spheroid morphogenesis "

Rahel Schnellmann, Ragna Sack, Daniel Hess, Douglas S. Annis, Deane F. Mosher, Suneel S. Apte and Ruth Chiquet-Ehrismann

Accepted for publication April 2018 and in press with

Molecular and Cellular Proteomics

My contribution to this paper:

For this study I developed the mass spectrometry approach used for substrate identification. I performed the production and purification of the decellularized ECM and collected and prepared the conditioned medium for mass spectrometry analysis. Together with Ragna Sack I analyzed the mass spectrometry data and identified the relevant potential substrates. I planned, performed and analyzed all cell culture and spheroid assays. I cloned all the used constructs and performed all RT-PCR experiments. With the help of Douglas Annis and Dean Mosher I performed the cleavage assays to prove that fibronectin is a substrate of ADAMTS16. I wrote the manuscript with the input of Suneel Apte.

A Selective Extracellular Matrix Proteomics Approach Identifies Fibronectin Proteolysis by A Disintegrin-like and Metalloprotease Domain with Thrombospondin Type 1 Motifs (ADAMTS16) and Its Impact on Spheroid Morphogenesis*[S]

AQ: A

Rahel Schnellmann‡§¶, Ragna Sack‡, Daniel Hess‡, Douglas S. Annis‖, Deane F. Mosher‖, Suneel S. Apte¶**, and Ruth Chiquet-Ehrismann†‡§**

Secreted and cell-surface proteases are major mediators of extracellular matrix (ECM) turnover, but their mechanisms and regulatory impact are poorly understood. We developed a mass spectrometry approach using a cell-free ECM produced *in vitro* to identify fibronectin (FN) as a novel substrate of the secreted metalloprotease ADAMTS16. ADAMTS16 cleaves FN between its $(I)_5$ and $(I)_6$ modules, releasing the N-terminal 30 kDa heparin-binding domain essential for FN self-assembly. ADAMTS16 impairs FN fibrillogenesis as well as fibrillin-1 and tenascin-C assembly, thus inhibiting formation of a mature ECM by cultured fibroblasts. Furthermore ADAMTS16 has a marked morphogenetic impact on spheroid formation by renal tubule-derived MDCKI cells. The N-terminal FN domain released by ADAMTS16 up-regulates MMP3, which cleaves the $(I)_5$-$(I)_6$ linker of FN similar to ADAMTS16, therefore creating a proteolytic feed-forward mechanism. Thus, FN proteolysis not only regulates FN turnover, but also FN assembly, with potential long-term consequences for ECM assembly and morphogenesis. ***Molecular & Cellular Proteomics 16: 1–15, 2018. DOI: 10.1074/mcp.RA118.000676.***

AQ: B

AQ:C-J, Fn1

The extracellular matrix (ECM)[1] is a network of proteins, glycoproteins and complex carbohydrates that normally undergoes continuous remodeling via coupled proteolytic degradation and biosynthesis. Deposition of a provisional ECM during morphogenesis, tissue regeneration or ECM assembly by cultured cells is known to rely heavily on the assembly of FN, an ECM glycoprotein, which is a crucial cell adhesion molecule and pro-migratory substrate (1, 2). Plasma and cellular FN are secreted as disulfide-bonded dimers that bind to cell surface integrins. Subsequently, cell contractility and centripetal integrin translocation expose cryptic binding sites in the FN dimers that allow their association and promote FN fibril assembly (1, 3). A major FN domain mediating initial self-assembly and promoting fibrillogenesis is the N-terminal heparin-binding domain spanning the first five type I repeats (4–7). The FN network serves as a template for the assembly of fibrillins, collagens, tenascin-C, latent TGFβ-binding proteins and other molecules and therefore has a crucial role in the formation of mature ECM (8–11). Consistent with the observed significant impact on ECM ontogeny, cell adhesion and migration *in vitro*, inactivation of the *Fn1* gene in mice leads to embryonic lethality by 8.5 days of gestation, with embryos showing impaired cardiovascular development and other morphogenetic defects (12).

Whereas initiation of FN fibril assembly has been extensively investigated, mechanisms regulating fibril turnover and maturation, are poorly understood (1, 13). Even though a number of proteases are known to cleave FN (4, 13–17) little is known about how they affect FN networks and so far, the relationship between FN proteolysis and assembly has not been specifically investigated. The ADAMTS (a disintegrin-like and metalloproteinase domain with thrombospondin type I motif) family includes 19 secreted proteases, most of which act on ECM and are crucial regulators of morphogenesis (18, 19). ADAMTS16 is a poorly characterized family member without a known substrate, although it was reported to play a role during renal and gonadal development. Homozygous *Adamts16* knockout male rats are infertile, with reduced testicular size and cryptorchidism (20) and

From the ‡Friedrich Miescher Institute for Biomedical Research, Basel, Switzerland; §Faculty of Science, University of Basel, Basel, Switzerland; ¶Department of Biomedical Engineering (ND20), Cleveland Clinic Lerner Research Institute, 9500 Euclid Avenue, Cleveland, Ohio 44195; ‖Department of Biomolecular Chemistry, University of Wisconsin, Madison, Wisconsin

Received February 8, 2018, and in revised form, March 21, 2018
Published, MCP Papers in Press, April 18, 2018, DOI 10.1074/mcp.RA118.000676

ADAMTS16 was linked to branching morphogenesis during renal development (21). In addition to its role during embryogenesis, *ADAMTS16* was implicated in blood pressure regulation in rats and humans (22, 23) and linked to ovarian cancer and esophageal squamous cell carcinoma (24, 25). Thus, ADAMTS16 is well-connected to morphogenesis and human diseases, but without knowledge of its underlying mechanisms, *i.e.* its molecular characteristics, substrates, and the molecular pathways in which it participates.

Here, we identified FN as an ADAMTS16 substrate via a novel mass spectrometry (MS) approach, using a decellularized ECM produced *in vitro* by fibroblasts for substrate discovery. We show that ADAMTS16 cleaves FN near its N terminus with an immediate and long-term impact on ECM assembly. By upregulating MMP3 in the epithelial cell line MDCKI, ADAMTS16 creates an intriguing dual protease feed-forward loop that may serve to limit and fine-tune FN assembly and control tubular morphogenesis.

EXPERIMENTAL PROCEDURES

ZSI *Antibodies*—All antibodies and used dilutions are listed in supplemental Table S1.

Expression Plasmids—Mouse *Adamts16* cDNA clone (with sequence NM_172053) was purchased from Creative Biogene (Shirley, NY). All constructs were generated by PCR using this clone as a template and HiFidelity Polymerase (Qiagen, Hombrechtikon, Switzerland) following the manufacturer's protocol. All constructs were C-terminally myc_His_6 tagged and cloned into pCEP_pu (Invitrogen, Carlsbad, CA) for expression and verified by Sanger sequencing. ADAMTS16 mutant constructs were obtained by site directed mutagenesis PCR following a previously published protocol (26). For
ZSI cloning and mutagenesis primer sequences see supplemental Table S2.

Cell Culture—HEK293-EBNA (CRL-10852, ATCC, Manassas, VA) cells were grown in DMEM supplemented with 10% FBS. To generate HEK293-EBNA cells stably expressing mouse ADAMTS16, mouse ADAMTS16-sh, mouse ADAMTS16-EA, or mouse ADAMTS16-sh-EA, cells were seeded on 0.1% gelatin-coated dishes (0.1% gelatin (Sigma Aldrich, St. Louis, MO) in H_2O), transfected using jetPei® (Polyplus transfection, Illkirch, France) following manufacturer's instructions and selected with puromycin (2 μg/ml, Sigma Aldrich) for 14 days. Mouse BALB/c 3T3 fibroblasts (CCL-163, ATCC), human dermal fibroblasts (HDF, ATCC) and LN229 cells (CRL-2611, ATCC) were grown in DMEM supplemented with 10% FBS. MDCK strain I (MDCKI) cells, kindly provided by Dr. Martin Spiess (Basel, Switzerland), were grown in α-MEM supplemented with 10% FBS. To obtain MDCKI cells stably expressing mouse ADAMTS16, mouse ADAMTS16-sh, mouse ADAMTS16-EA, or mouse ADAMTS16-sh-EA, cells were transfected using FuGENE® 6 (Roche, Basel, Switzerland) and selected with puromycin for 14 days. All cell lines used in the experiments were tested for mycoplasma contamination by MycoAlert™ Mycoplasma Detection Kit (LT07–218, Lonza Basel, Switzerland).

[1] The abbreviations used are: ECM, Extracellular Matrix; FBN1, Fibrillin1; FN, Fibronectin; GELS, Gelsolin; LTBP1, Latent-transforming growth factor beta-binding protein 1; PG-S1, Biglycan; PLEC, Plectin; PLAC, Protease and lacunin domain; POSTN, Periostin; SERPH, Serpin H1; TNC, Tenascin-C; TSR, Thrombospondin type 1 repeats.

Western Blotting—Cell extracts and conditioned media were prepared in Laemmli loading buffer with or without 2-mercaptoethanol and separated by SDS-PAGE. Proteins were transferred to PVDF membranes (Immobilon FL for fluorescence detection, EMD Millipore, Billerica, MA) and probed with primary antibody (supplemental Table S1) and detected by an enhanced fluorescence technique using an Odyssey CLx scanner (LI-COR Biosciences, Lincoln, NE). ZSI

Protein Purification—1 L of conditioned medium was filtered through a 0.22 μm filter (Corning, Corning, NY). After filtration the solution was applied to a pre-equilibrated 1 ml IMAC column (Ni-NTA agarose, Qiagen, Hombrechtikon, Switzerland) at 4 °C. Bound protein was eluted with 250 mM imidazole in 50 mM Tris-buffer (pH 7.5). For removal of imidazole, the protein solution was dialyzed against TBS (50 mM Tris-HCl, 150 mM NaCl, pH 7.5) supplemented with 5 μM $ZnCl_2$. Protein concentration was determined with a NanoDrop ND-1000 spectrometer (ThermoFisher Scientific, Reinach, Switzerland). Protein absorption coefficients were calculated using the PDB ProtParam tool. The protein solution was stored in 50% (v/v) glycerol at −20 °C.

Immunofluorescence—HEK293-EBNA cells were seeded on 8-well glass chamber slides (Falcon Culture Slides, Thermo Fisher Scientific) and cultured in DMEM containing 10% FBS until they reached 80% confluence. Cells were transiently transfected with ADAMTS16-sh and ADAMTS16-CT, ADAMTS16 or empty vector only using Lipofectamine 3000 (Invitrogen/Life Technologies, CA). After 48 h under serum-free conditions the cells were fixed with 4% formaldehyde (PFA) for 20 min. The samples were incubated with anti-myc and anti-laminin for 1h at room temperature, followed by incubation with Alexa conjugated secondary antibody. Samples were mounted in ProLong Gold with DAPI (Life Technologies) and imaged with a Leica TCS5 SPII confocal microscope. Images comparing conditions were acquired under identical camera settings and analyzed using ImageJ software (U. S. National Institutes of Health, Bethesda, Maryland). LN229 cells were seeded on 8 well glass chamber slides and cultured in DMEM containing 10% FBS until they reached 90% confluence. Cells were transiently transfected using Lipofectamine 3000. Cells were maintained in DMEM with 10% FBS for another 48 h before fixation and staining.

Preparation of Cell-free ECM from HEK-EBNA Cells—HEK-EBNA cells were transiently transfected and cultured for 48 h in DMEM/10% FBS. Cells were removed using extraction buffer (0.5% Na-deoxycholate, 10 mM Tris-HCl, pH 7.5) supplemented with protease inhibitor (cOmplete™, Mini Protease Inhibitor Mixture, Sigma-Aldrich) for 30 min at 4 °C. ECM was washed with 2 mM Tris- HCl (pH 7.5). Total protein was analyzed by SDS-PAGE under reducing conditions.

Preparation of ECM Produced by Cultured BALB/c 3T3 Fibroblasts—BALB/c 3T3 fibroblasts were cultured in DMEM supplemented with 10% FBS for preparation of cell-free ECM as previously described (27). Briefly, 1×10^6 fibroblasts were seeded on a 6 cm culture dish (Corning) precoated with 0.1% gelatin and allowed to attach for 24 h. After 24 h the medium was replaced with fresh culture medium containing 10% FBS and 50 μg/ml ascorbic acid (Merck Millipore, Darmstadt, Germany). The medium was replaced every 24 h for 5 days. The cells were extracted from the matrix using PBS containing 0.5% Triton X-100 and NH_4OH. PBS was added to dilute the cellular debris and the plate was stored overnight at 4 °C. Debris were removed, and ECM was washed with cold PBS. 5×10^5 HEK cells stably expressing mouse ADAMTS16, mouse ADAMTS16-sh, mouse ADAMTS16-sh-EA or transfected with empty vector as a control, were seeded on this matrix and cultured for 24 h in serum-free medium. ADAMTS16-sh-EA served as the control for both wt-ADAMTS16 and ADAMTS16-sh. The conditioned medium was analyzed by LC-MS/MS.

Sample Preparation and Analysis of the Digested ECM by Mass Spectrometry—The proteins in the medium were precipitated using trichloroacetic acid (TCA), washed with HPLC grade ice-cold acetone and dissolved in 0.5 M Tris pH 8.6 containing 6 M guanidine hydrochloride and aliquoted into four fractions for treatment with the endopeptidase Lys-C (Wako, Neuss, Germany) or trypsin (sequencing grade modified, Promega, Dübendorf, Switzerland), Asp-N (Roche) and combinations thereof after reduction with TCEP and alkylation with iodoacetamide (both Fluka, Buchs, Switzerland) and further addition of digestion buffer (50 mM Tris/HCl pH 8.6, 5 mM $CaCl_2$). Peptides were separated on an EASY n-LC 1000 liquid chromatography system equipped with a C18 Acclaim PepMap 100 trap-column (75 μm × 2 cm, 3 μm, 100 Å) and a C_{18} New Objective analytical column (75 μm × 25 cm, Reprosil, 3 μm) coupled to a Thermo Orbitrap Fusion mass spectrometer (Thermo Scientific) equipped with a New Objective Digital Pico View source. Data were collected over a 30 min linear gradient from 2% buffer B (0.1% formic acid in acetonitrile) to 25% buffer B, followed by a 5 min linear gradient from 25% to 40% buffer B. Buffer A contained 0.1% formic acid in water. Sample digests were acidified with trifluoroacetic acid (Pierce) to a final concentration of 0.1% TFA.

Analysis and Peptide Identification by LC-MS/MS—Peptides were identified by searching SwissProt restricted to mammalian proteins (version 2015–01, # of entries searched for: 16920 mouse proteins) using Mascot Distiller (version 2.5.1, Matrix Science) and Mascot (version 2.5.1, Matrix Science) allowing the following post-translational modifications; fixed modifications: Carbamidomethyl (C), variable modifications: acetylation at protein N termini, deamidation at asparagine and glutamine, oxidation at methionine and phosphorylation at serine/threonine and no enzyme specificity. The number of max. missed cleavages was set to 1, with a peptide mass tolerance ± 10 ppm and a fragment mass tolerance ± 0.6 Da. Data were compiled and evaluated with Scaffold (version Scaffold_4.4.1.1, Proteome Software), considering proteins identified with at least five peptides and having thresholds for protein and peptides of 90%, with peptide FDR 2.1% (Prophet) and protein FDR 0% (Prophet). The FDR was calculated using Scaffold software using the following parameters: Protein Grouping Strategy: Experiment-wide grouping with binary peptide-protein weights. Peptide Thresholds: 90.0% minimum and Protein Thresholds: 90.0% minimum and 5 peptides minimum. Scaffold software was used for a qualitative analysis of ADAMTS16 cleavage products. For a quantitative analysis of single peptides, the area under the curves of the MS1 spectra of single peptides was analyzed using a label free approach. For this, the corresponding data files were loaded into Progenesis QI for proteomics (version 2.0.5556.29015, Waters) and analyzed using the default settings of the program (medium sensitivity and peptide charge: 1–20). All the raw data files of the single runs, the scaffold file (.sf3) and the corresponding Mascot result files (file name: F077701–5.dat) as well as the Mascot peak list (mgf files) and the corresponding search files (xml files) for the Progenesis quantification are available via ProteomeXchange with identifier PXD007284.

Sample Preparation and LC-MS/MS Analysis of Human Fibronectin Cleavage Products—12-well tissue culture dishes were coated with purified human plasma fibronectin (FC010–10MG, Merck Millipore) in a final concentration of 30 μg/ml in PBS. HEK293-EBNA cells stably expressing various ADAMTS16 constructs were seeded on top of the FN under serum-free conditions and incubated for 24 h. The supernatant was analyzed by Western blotting or by LC-MS/MS for potential cleavage products. Prior to LC-MS/MS analysis the conditioned medium was TCA-precipitated and digested with LysC following the protocol described in the previous section. The generated peptides were acidified with 1 μl of 20% TFA and analyzed by capillary liquid chromatography tandem mass spectrometry with an EASY-nLC 1000 using a two-column set up (Thermo Scientific). The peptides were loaded with 0.1% formic acid, 2% acetonitrile in H_2O onto a peptide trap (Acclaim PepMap 100, 75 μm × 2 cm, C18, 3 μm, 100 Å) at a constant pressure of 800 bar. Peptides were separated at a flow rate of 150 μl/min with a linear gradient of 2–6% buffer B in buffer A in 3 min followed by an linear increase from 6 to 22% in 40 min, 22–28% in 9 min, 28–36% in 8 min, 36–80% in 1 min and the column was finally washed for 14 min at 80% B (Buffer A: 0.1% formic acid, buffer B: 0.1% formic acid in acetonitrile) on a 50 μm x 15 cm ES801 C18, 2 μm, 100 Å column mounted on a DPV ion source (New Objective) connected to an Orbitrap Fusion mass spectrometer (Thermo Scientific). The data were acquired using 120,000 resolution for the peptide measurements in the Orbitrap and a top T (3s) method with HCD fragmentation for each precursor and fragment measurement in the LTQ according the recommendation of the manufacturer (Thermo Scientific).

Peptides were identified using Mascot (version 2.5.1, Matrix Science) and Mascot Distiller (version 2.5.1, Matrix Science) allowing the following post-translational modifications; fixed modification: Carbamidomethyl (C), variable modifications: acetylation at protein N termini, deamidation at asparagine and glutamine, oxidation at methionine and phosphorylation at serine/threonine. The number of max. missed cleavages was set to 1, with a peptide mass tolerance ± 5 ppm and a fragment mass tolerance ± 0.6 Da and quantified using Progenesis QI for proteomics (version 2.0.5556.29015, Waters). All raw data files of the single runs, a Scaffold file (.sf3) as well as the Mascot peak list (mgf files) and the corresponding search files (xml files) for the Progenesis QI quantification are available via ProteomeXchange with identifier PXD007284.

In Vitro Fibrillogenesis—HDF and HEK293 cells were co-cultured in a 3:5 (fibroblasts: HEK cells) ratio in DMEM containing 10% FBS for 24 h, 48 h, or 4 days respectively. For 8-day co-cultures the cells were seeded in a 4:1 (fibroblasts: HEK cells) ratio. Cells were fixed in 4% PFA, stained and imaged using a Leica TCS5 SPII confocal microscope. Images were analyzed using ImageJ software.

3D-culture Staining and Imaging—MDCKI cells were embedded in 3D collagen gels. Acid-solubilized collagen (Corning Collagen I) was mixed with 10X PBS in a 1:1 ratio, followed by pH adjustment to 7.5 with 0.1 M NaOH. The collagen concentration was adjusted to a final concentration of 2.5 mg/ml using α-MEM/10%FBS. 150 μl of collagen containing 1.5×10^4 cells was poured into each well of an 8-well glass chamber slide and allowed to solidify at 37 °C. After gelation α-MEM containing 10% FBS was added and replaced every 24 h.

After 4 days or 8 days of culture, the 3D gels were fixed using 4% PFA for 30 min and permeabilized 3X 15 min at room temperature using 0.3% Triton X-100 in PBS. Primary antibodies were diluted in PBST and applied overnight at 4 °C. Gels were washed with PBST and incubated with secondary antibodies in PBST for 2 h at room temperature. Images were taken with a Leica TCS5 SPII confocal microscope and analyzed with ImageJ software.

RNA Analysis by qRT-PCR—Total RNA was isolated using the RNeasy Plus Micro Kit (Quiagen). RNA was reversed transcribed and relative mRNA levels were detected as described (28). Relative mRNA levels for the genes, normalized to TBP, were measured using Platinum® SYBR® Green qPCR SuperMix-UDG with ROX (Invitrogen). Real-time PCR was performed in a StepOnePlus Real-Time PCR System (Applied Biosystems, Rotkreuz, Switzerland) using a standard cycling profile. All samples were run in triplicates. Data were analyzed by the ΔΔCt method (29). RT-PCR primers are listed in supplemental Table S3.

AQ: K

ZSI

Labeling of FN—0.5 mg of plasma FN (F0895, Sigma-Aldrich) was labeled using the Alexa Fluor 488 protein labeling kit (A10235, Thermo Fisher Scientific) following the manufacturer's instructions. 30 μg/ml of the labeled FN were plated on 8-well glass

chamber slides. HEK-EBNA cells stably expressing wtADAMTS16, ADAMTS16-EA or empty vector were seeded under serum-free conditions and allowed to attach for 48 h prior to fixation and phalloidin staining.

FN Cleavage—Purified ADAMTS16-sh was incubated with plasma FN (Sigma-Aldrich) or 500 ng of the 70 kDa N-terminal FN fragment or the 4F1–2F2 produced in insect cells (30) for 4 h at 37 °C in TBS (pH 7.5) supplemented with 10 mM $CaCl_2$. Cleavage products were analyzed by immunoblotting under reducing conditions.

Experimental Design and Statistical Rational—All grouped data are means ± S.E. The statistical analysis was performed using GraphPad InStat version 3.05. Differences between two groups were evaluated using a two-tailed Student *t* test for parametric data. Values of $p < 0.05$ were considered statistically significant. Empty vector and an inactive mutant of ADAMTS16 were used as control for all experiments. All qRT-PCR experiments were done in triplicates. Relative amount of FN was quantified using ImageJ software. Each condition was done in triplicate and a total of 12 images per condition were analyzed. For spheroid size quantification a total number of 50 spheroids per condition from three independent experiments together were evaluated. For lumen quantification a total of 16 spheroids per condition from 3 independent experiments were quantified.

Human FN digestion was done in biological triplicates and all triplicates were analyzed by LC-MS/MS to get statistically relevant quantifications of the cleavage peptides. The presence of the identified mouse FN peptide from decellularized ECM was verified in two individual runs using different working proteases and was further verified by a complete repetition of the experiment using the same experimental setup for ADAMTS16-sh, ADAMTS16-sh-EA and vector control.

RESULTS

ADAMTS16 is Secreted and Binds to ECM via its C-terminal Modules—Constructs expressing wt myc-tagged ADAMTS16 and their corresponding active site mutants (E432A) (Fig. 1*A*) were transiently or stably expressed in HEK293-EBNA cells. Neither active full-length ADAMTS16 (wtADAMTS16) nor inactive ADAMTS16 (ADAMTS16-EA) were detectable in the conditioned medium of either stably or transiently transfected HEK-EBNA cells (Fig. 1*B*). In contrast, liquid chromatography-tandem mass spectrometry (LC-MS/MS) analysis of the medium of these cells detected an abundance of peptides spanning the catalytic domain to the spacer, but none derived from the C-terminal thrombospondin (TSR) repeats and the protease and lacunin (PLAC) domain (Fig. 1*A*, supplemental Fig. S1, supplemental Table S4). These findings suggested that wtADAMTS16 was C-terminally processed with release of a form containing the catalytic domain through the spacer module into the medium, whereas the remaining C-terminal modules were retained within the ECM and or the cell surface.

To gain further insights into C-terminal processing of ADAMTS16, we designed a construct lacking the C-terminal TSRs and PLAC domain (ADAMTS16-sh) thereby mimicking wtADAMTS16 after C-terminal processing and release into the medium (Fig. 1*A*). In contrast to ADAMTS16, ADAMTS16-sh as well as its proteolytically inactive counterpart (ADAMTS16-sh-EA), were readily detectable in the conditioned medium using anti-myc (Fig. 1*B*). A reported isoform of ADAMTS16, lacking the C-terminal PLAC domain (ADAMTS16-TS6) (31) (Fig. 1*A*) was also detected in the conditioned medium of transfected HEK-EBNA cells (Fig. 1*B*), suggesting that the C-terminal modules, such as PLAC may regulate binding of ADAMTS16 to the cell surface and/or the ECM. Smaller than expected ADAMTS16-sh and ADAMTS16-TS6 molecular fragments in the medium are indicative of autocatalysis, in addition to proteolysis by ambient proteases within the TSR2- PLAC region (ancillary domain) (Fig. 1*B*, 1*C*). These findings support the assumption of C-terminal processing of ADAMTS16 between the spacer and TSR2, with retention of C-terminal modules in the cell layer and release of the remaining ADAMTS16 into the medium.

In addition, like other ADAMTS proteases, ADAMTS16 likely undergoes furin-processing at a consensus site, $RHKR^{279}$, releasing the N-terminal propeptide. Consistent with this, the ADAMTS16 constructs observed in the medium by antibodies to the C-terminal myc tag were ~30 kDa smaller than in the cell lysates (Fig. 1*B,* 1*C*). To determine if full-length ADAMTS16 binds to and retains in the ECM we performed a DOC insolubility assay using transiently transfected HEK-EBNA cells. All ADAMTS16 constructs could be detected within the cell-free ECM (Fig. 1*D*). In contrast to ADAMTS16-EA, ADAMTS16-TS6, ADAMTS16-TS6-EA, and ADAMTS16-sh, wtADAMTS16 was detected at markedly lower levels in the cell-free ECM of transfected HEK293-EBNA cells (Fig. 1*D*). This further confirms the finding that autoproteolysis likely had complex effects on full-length ADAMTS16 with increased lability compared with the other constructs. Immunostaining of ADAMTS16 transfected cells with laminin (a marker for ECM) showed that the C-terminal domain of ADAMTS16 (ADAMTS16-CT) was strongly localized to the ECM. ADAMTS16-sh was localized to the ECM as well, but at considerably reduced levels compared with ADAMTS16-CT (Fig. 1*E*). Together, these findings provide evidence that cell and ECM binding of ADAMTS16 is primarily mediated by its C-terminal ancillary domain, and that ADAMTS16 is released into the medium because of complex proteolytic processing, including autocatalysis (Fig. 1*B*–1*E* supplemental Fig. S1).

Mass Spectrometry Identifies FN as an ADAMTS16 Substrate—Because ADAMTS16 binds to the ECM and is extensively processed, purification of full-length catalytically active enzyme was not feasible. Therefore, to identify ADAMTS16 substrates, we designed a strategy in which a decellularized ECM, deposited by mouse BALB/c 3T3 fibroblasts *in vitro*, was digested by HEK293-EBNA cells expressing wtADAMTS16, ADAMTS16-sh or its catalytically inactive mutant ADAMTS16-sh-EA. The medium from these cultures was analyzed by LC-MS/MS to identify ADAMTS16 substrates (Fig. 2*A*, Table I, II) by searching for peptides with cleavage sites that did not arise from the proteases used to generate peptides for LC-MS/MS. This analysis identified a mouse FN peptide ^{270}CERHALQSASAGSGS^{285} (GenBank ID NP_034363) exclusively in digests of ECM by the two active ADAMTS16 constructs but not the catalytically inactive

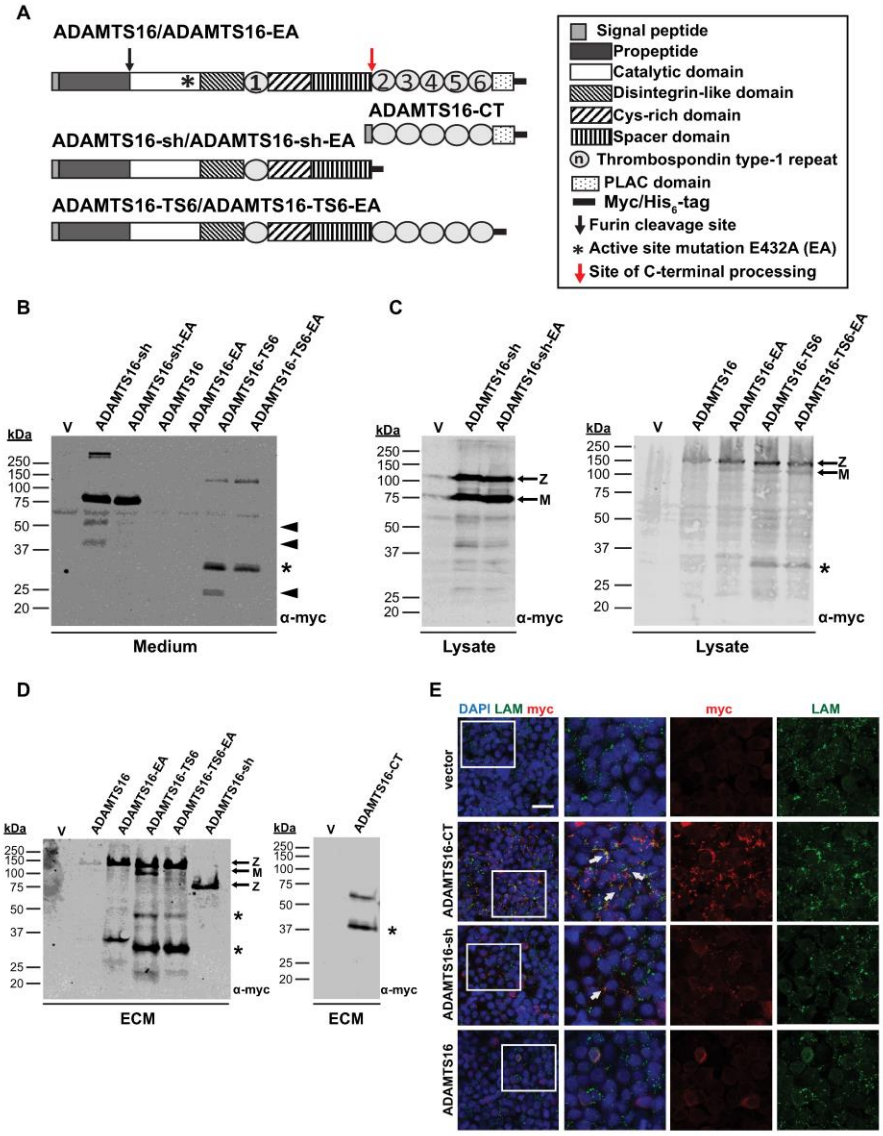

COLOR

FIG. 1. **ADAMTS16 binds ECM and is C-terminally processed.** *A*, Domain organization of ADAMTS16 constructs. *B*, Western blot analysis of conditioned medium from HEK293-EBNA cells transfected with the indicated constructs or empty vector (v) using anti-myc antibody and enhanced chemiluminescence. The black arrowheads and asterisk indicate autocatalytic and non-autocatalytic C-terminal fragments of ADAMTS16 respectively. *C*, Western blot analysis of HEK293-EBNA cell lysate transfected with the indicated constructs or empty vector (v). The asterisks indicate autocatalytic and non-autocatalytic C-terminal fragments of ADAMTS16. Z and M indicate the zymogen and mature forms arising from furin processing. *D*, Western blot analysis of cell-free ECM from HEK293-EBNA cells expressing various ADAMTS16 constructs or transfected with empty vector (v). The asterisks indicate C-terminal fragments. Z and M indicate the zymogen and mature forms arising from furin processing. *E*, HEK293-EBNA monolayers were stained for wtADAMTS16, ADAMTS16-CT and ADAMTS16-sh with anti-myc (red) and laminin (green) as ECM marker. The images show stronger localization of ADAMTS16-CT to the cell layer than ADAMTS16-sh. White arrows indicate co-localization of ADAMTS16 and laminin. The scale bar is 50 μm. The right-hand panels are 2X amplification of the boxed areas in the left-hand column.

AQ: R

tapraid4/zjw-macp/zjw-macp/zjw00818/zjw5767-18a xppws S=3 31/5/18 13:33 4/Color Figure(s) F1–6 ARTNO: RA118.000676

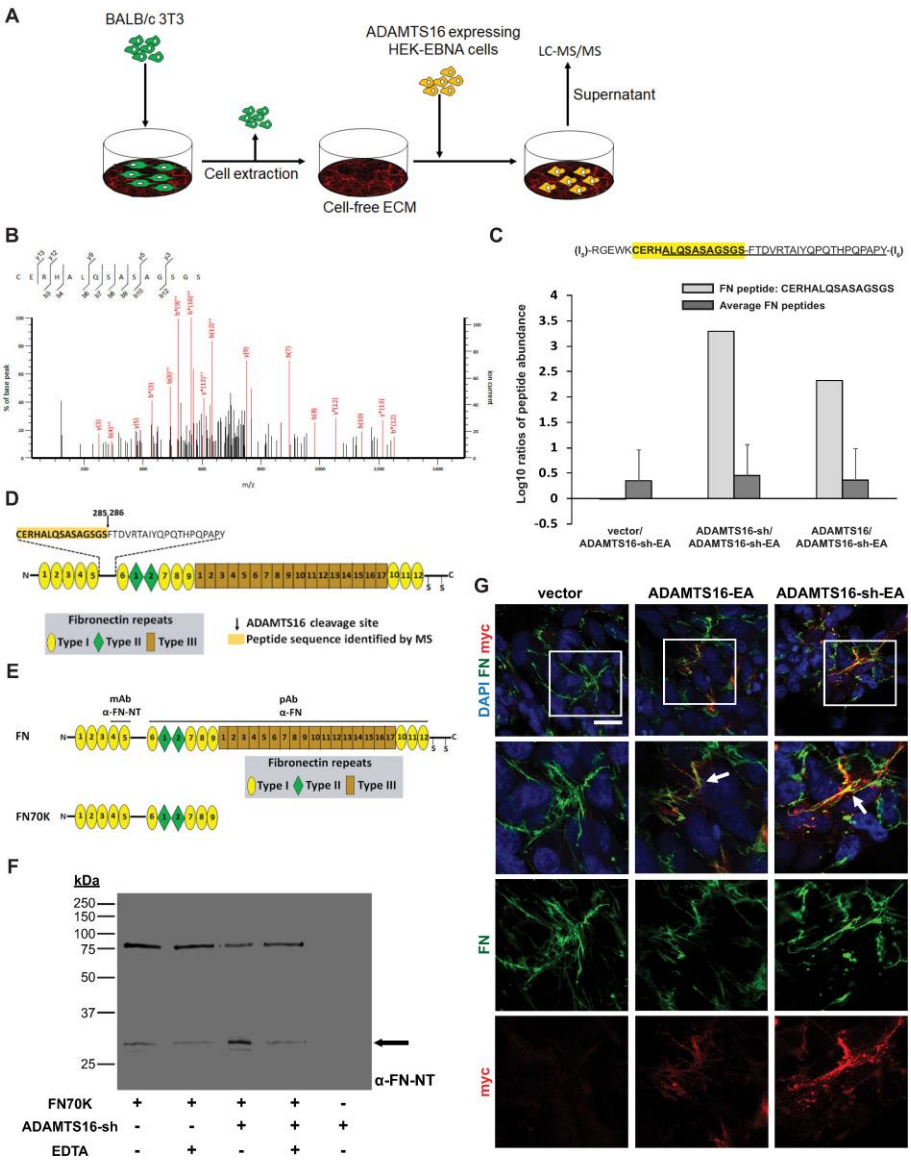

COLOR

FIG. 2. **Identification and validation of FN as an ADAMTS16 substrate.** *A*, Schematic of the proteomic strategy used to identify ADAMTS16 substrates. *B*, MS2 spectrum of the doubly charged FN peptide CERHALQSASAGSGS identified in the LysC-AspN digest of wtADAMTS16. *C*, Histogram of log10 ratios of relative abundance of the FN peptide CERHALQSASAGSGS identified by LC-MS/MS in the LysC/AspN digest showing its presence exclusively in matrix incubated with active ADAMTS16 and ADAMTS16-sh expressing cells, but not in the control samples. Log10 ratios compare wtADAMTS16 with ADAMTS16-sh-EA, ADAMTS16-sh with ADAMTS16-sh-EA and vector with ADAMTS16-sh-EA. Average of log10 ratios of all identified FN peptides, showed similar values between the samples, indicating equal amounts of FN in each sample. *D*, Domain structure of FN with expanded view of the amino acid sequence of the linker between domains $(I)_5$ and $(I)_6$ showing the peptide identified by LC-MS/MS (yellow highlight) and the potential ADAMTS16 cleavage site. *E*, The domain structure of FN and the N-terminal 70 kDa FN fragment (FN70K). Antibody binding sites of the monoclonal anti FN-NT (MAB1936) and the polyclonal anti-FN (Ruth

mutant and/or the vector control (Fig. 2*B*, 2*C*, supplemental Fig. S2*A*). The presence of the FN peptide ^{270}CERHALQSASAGSGS^{285} was found in both active samples (wtADAMTS16 and ADAMTS16-sh) using LysC alone as working protease or LysC in combination with AspN (Table I, supplemental Table S5–S7). The findings could be reproduced in a second independent experiment (data available in ProteomeXchange with identifier PXD007284). This finding suggests that ADAMTS16 cleaves FN within its N-terminal linker sequence between domain $(I)_5$ and $(I)_6$ (Fig. 2*C*). We identified additional peptides showing cleavage sites that did not arise from the sample preparation process (Table I). Because these peptides were also identified in the control samples, but at lower abundance, we conclude that they were not uniquely targeted by ADAMTS16 and were not pursued further (Table I, II, supplemental Table S5, S7, supplemental Fig. S2*C*, S2*D*). The similar results obtained for wtADAMTS16 and ADAMTS16-sh indicate that although C-terminal processing influences enzyme localization, it does not significantly influence FN recognition and proteolysis. Although a unique peptide identified FN as a potential substrate of ADAMTS16, the FN sequence coverage did not vary between the different samples, indicating the same overall amount of FN in the conditioned medium (Fig. 2*C*, supplemental Fig. S2*C*, supplemental Table S7). On the other hand, differential sequence coverage was noted for biglycan, plectin, and serpinH1, but no unique peptides arising from ADAMTS16 cleavage were identified (Table II, supplemental Table S7). These molecules could also be potential ADAMTS16 substrates where unique cleaved peptides were not detected by LC-MS/MS.

For further validation of FN as substrate of ADAMTS16, cell culture dishes were coated with human plasma FN and cells stably expressing different ADAMTS16 constructs were seeded under serum-free conditions. ADAMTS16-mediated FN proteolysis was allowed for 24 h. The conditioned medium was analyzed for FN cleavage products by Western blotting using an antibody specific to the N-terminal domain of human FN. Samples incubated with ADAMTS16-sh showed a strong increase of the 30 kDa FN N-terminal heparin binding domain after 24 h of incubation in the conditioned medium compared with inactive mutant and vector control (supplemental Fig. S3*A*). To further validate FN as a substrate the conditioned medium was analyzed by mass spectrometry for specific FN cleavage peptides after 24 h of incubation with ADAMTS16-sh. The specific cleavage peptides ^{270}CERHTSVQTTSSGSGPFTDVRAA^{292} from the $(I)_5$-$(I)_6$ linker sequence of FN was identified in very high abundance in the active ADAMTS16-sh sample but not in the inactive ADAMTS16-sh-EA and vector control samples, although overall FN peptide abundance was comparable supplemental Fig. S3*B*–S3*D*; supplemental Table S8, S9). This finding further suggests that ADAMTS16 cleaves FN within the N-terminal $(I)_5$-$(I)_6$ linker. We identified additional human FN cleavage peptides toward the C-terminal side of this cleavage indicating that ADAMTS16 might cleave FN elsewhere in addition to the characterized N-terminal cleavage site (supplemental Table S8).

Because of the extensive post-secretion processing, purification of full-length ADAMTS16 was not feasible using the C-terminal tags, but ADAMTS16-sh was purified and its proteolytic activity was demonstrated by cleavage of the generic protease substrate α2-macroglobulin (supplemental Fig. S4*A*) as previously demonstrated (32). To obtain biochemical validation that fibronectin is a substrate of ADAMTS16 and to determine the requirements for proteolysis, we incubated purified ADAMTS16-sh with different FN constructs. A recombinant 70 kDa FN fragment extending from module $(I)_1$ to module $(I)_9$ was cleaved to generate a 30 kDa N-terminal fragment (Fig. 2*E*, 2*F*). Full-length plasma FN, whose globular structure potentially masks susceptible peptide bonds, was not cleaved by purified ADAMTS16-sh *in vitro* (supplemental Fig. S4*B*). ADAMTS16-sh failed to cleave the linker of a shorter recombinant FN fragment spanning the $(I)_4$ to $(II)_2$ modules suggesting that binding of ADAMTS16 to FN may occur via domains distant from the cleavage site (Fig. S4*C*, S4*D*). We also tested the ability of wtADAMTS16 to cleave FN using a cell-based approach. Seeding of HEK-EBNA cells expressing wtADAMTS16, but not ADAMTS16-EA on Alexa488 labeled FN showed a loss of FN fluorescence underlying the cells (supplemental Fig. S4*E*), suggesting that in contrast to plasma FN in solution, bound plasma FN could be cleaved by ADAMTS16-expressing cells. In transiently transfected LN-229 glioblastoma cells, ADAMTS16 co-localized with FN fibrils *in vitro* (Fig. 2*G*) and the FN network was reduced in cells expressing wtADAMTS16 (supplemental Fig. S4*F*). Together, these findings indicate that FN is directly cleaved by ADAMTS16, but that cleavage requires a distant binding region on FN and exposure of the scissile bond by traction provided by cell contraction.

ADAMTS16 Inhibits FN Assembly and Elaboration of a Mature FN-dependent ECM—The 30 kDa N-terminal heparin binding domain released by wtADAMTS16 was previously shown to regulate FN self-association during fibrillogenesis (5,

Chiquet) are indicated above full-length FN. *F*, Western blot analysis of FN70K incubated with purified active ADAMTS16-sh in the presence or absence of EDTA. Anti-FN antibody (MAB1936) specific to the N-terminal heparin-binding domain of FN was used to identify release of the 30 kDa N-terminal heparin-binding domain (black arrow). *G*, Co-localization of ADAMTS16 with FN fibrils. Transiently transfected LN229 cells were cultured for 48 h and stained for ADAMTS16-EA and ADAMTS16-sh-EA with anti-myc (red) and FN (green). The images show co-localization of ADAMTS16-EA and ADAMTS16-sh-EA with FN fibers, indicating that the C terminus of ADAMTS16 is not essential for FN binding. White arrows show co-localization of ADAMTS16 with FN. Scale bar is 50 μm. Lower panels show 2× amplification of the boxed areas in the top row.

TABLE I

Peptides and peptide ratios obtained from ADAMTS16 digestion of BALB/c 3T3 extracellular matrix

Protein name	Preceding amino acid	Peptide seq.	Succeeding amino acid	Precursor charge	mass/charge (*m/z*)	Working protease	log10 wtADAMTS16/ ADAMTS16-sh-EA	Sequence coverage % (ADAMTS16-sh)	log10 ADAMTS16-sh/ ADAMTS16-sh-EA	Sequence coverage % (ADAMTS16-sh-EA)	log10 vector/ ADAMTS16-sh-EA
FN	K	^{271}CERHALQSASAGSGS^{285}	F	2+	759.34	LysC/AspN	2.33	66	3.29	70	−0.01
FN	K	^{271}CERHALQSASAGSGS^{285}	F	2+	759.34	LysC	3.51	20	4.50	17	1.66
FN	K	^{271}CERHALQSASAGSGS^{285}	F	3+	506.56	LysC	3.42	33	4.29	37	1.66
FN	D	^{557}PIDQCQDSETR^{567}	T	2+	674.79	LysC/Trypsin	0.65	45	0.37	58	0.15
LTBP-1	Y	^{1581}GRDALVDFSEQYGPETDPYFIQDR^{1604}	F	3+	940.10	LysC/Trypsin	0.62	33	0.32	30	0.07
POSTN	T	^{604}LLVNELK^{610}	S	2+	415.25	LysC	0.2	17	0.14	39	−0.08
GELS	R	^{450}IEGSNKVPVDPATY^{463}	G	2+	745.38	AspN/Trypsin	0.37	6.4	−0.01	4.2	0.18

Comparison of peptides released from digests of decellularized BALB/c 3T3 ECM (mouse) with HEK-EBNA cells stably expressing wtADAMTS16, ADAMTS16-sh-EA, ADAMTS16-sh, and vector control as indicated in column headings. Peptides arising from cleavage by proteases different from the ones used for sample preparation (working proteases) are shown. No change in peptide abundance gives a ratio near 0. Increased peptide abundance in active samples gives a ratio >0. Ratios were calculated using Progenesis QI software. All peptides shown in the table are of murine (BALB/c 3T3) origin.

All Mascot peak lists and search files used to quantify peptide ratios and abundance are available via ProteomeXchange with identifier PXD007284.

TABLE II

Unique peptide count and sequence coverage of ECM proteins obtained from ADAMTS16 digestion of BALB/c 3T3 extracellular matrix

Protein name	Accession Nr.	Unique peptide count (wtADAMTS16)	Unique peptide count (ADAMTS16-sh)	Unique peptide count (ADAMTS16-sh-EA)	Unique peptide count (vector)	Sequence coverage % (wtADAMTS16)	Sequence coverage % (ADAMTS16-sh)	Sequence coverage % (ADAMTS16-sh-EA)	Sequence coverage % (vector)
FN	**P11276**	206	150	186	180	71	66	70	72
LTBP1	**Q8CG19**	41	27	21	25	28	20	17	21
POSTN	**Q62009**	23	23	25	23	32	33	37	30
GELS	**P13020**	46	32	46	40	57	45	58	50
PGS1	**P28653**	5	8	10	12	16	33	30	39
SERPH	**P19324**	3	4	12	14	12	17	39	39
PLEC	**Q9QXS1**	43	23	14	11	11	6.4	4.2	3.3

Differences in sequence coverage as well as in peptide counts were obtained for other ECM proteins. Sequence coverage and unique peptide counts were calculated using Scaffold software, the following posttranslational modifications were included in the Mascot search: acetylation at the protein N-terminus, oxidation, phosphorylation and deamidation. No enzyme specificity was applied to the search parameters to identify potential ADAMTS16 cleavage products. All ECM proteins shown in the table are of murine (BALB/c 3T3) origin. The original scaffold file and the corresponding Mascot search files are available via ProteomeXchange with identifier PXD007284.

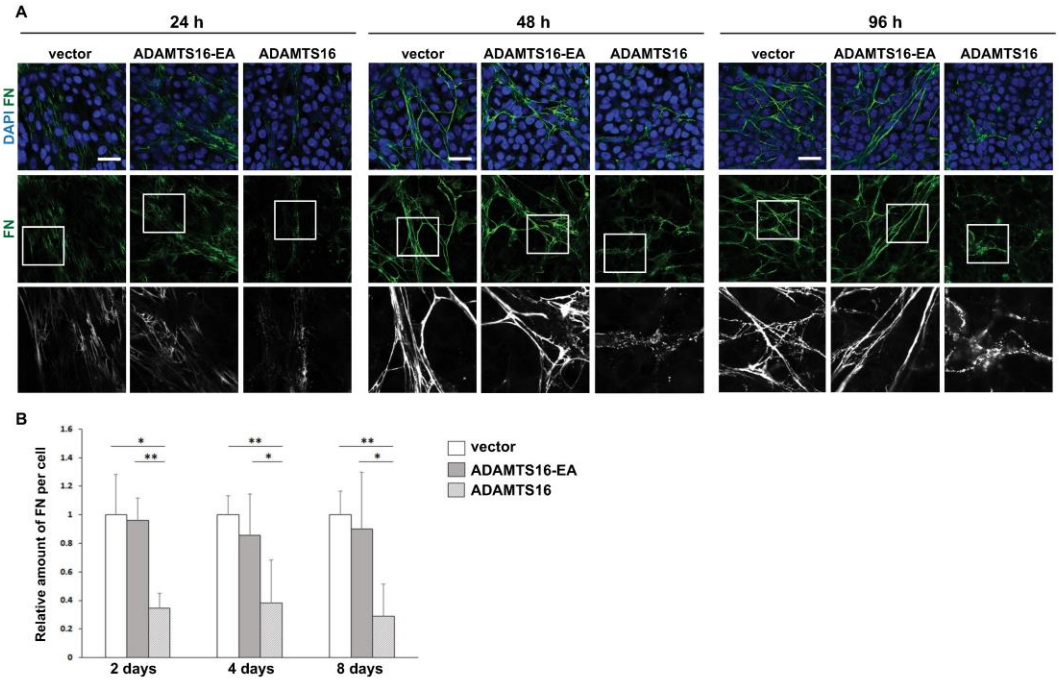

COLOR

FIG. 3. **ADAMTS16 affects FN fibril assembly by human dermal fibroblasts (HDF).** *A*, Confocal analysis of FN networks after 24, 48 or 96 h of co-culture of HDF with ADAMTS16-expressing HEK293-EBNA cells, shows reduced FN fibril staining (green). Scale bars are 50 μm. Lower panels are 3X amplifications of the boxed areas in the upper row. *B*, The relative amount of fibrillar FN per cell was measured in wtADAMTS16, ADAMTS16-EA, and vector control co-cultures. Data are mean ± S.E., $n = 12$ images from 3 independent experiments. (*) $p <$ 0.05 by Student t test, (**) $p < 0.01$, Student t test.

6). To investigate whether ADAMTS16 had a direct effect on FN fibril networks, we investigated the temporal effect of ADAMTS16 on the FN network. Human dermal fibroblasts (HDF) co-cultured with HEK cells stably transfected with either vector or inactive ADAMTS16-EA established a robust FN network within 24 h in culture medium containing 10% FBS. In contrast, a profound reduction of FN fibrils was observed in the presence of wtADAMTS16 after 24 h despite comparable cell density (Fig. 3*A*). Indeed, in the presence of wtADAMTS16, FN was visible as punctate structures localized near the surface of fibroblasts, rather than in a well-defined fibrillar network. Upon continuing co-culture to 2, 4, and 8 days, a similar impact on the network was observed, indicative of a continuing impact on FN assembly, although digestion of preformed fibrils cannot be ruled out (Fig. 3*A*, 3*B*, Fig. 4). This temporal sequence in reduction of FN fibrillogenesis suggested that ADAMTS16 affected FN fibril maturation at the point of, or shortly after initial fibril assembly and therefore reduced further assembly and fibril maturation. *FN1* mRNA levels were comparable in the various co-cultures (supplemental Fig. S5*A*), suggesting that reduction of fibrils in the presence of active ADAMTS16 did not have a transcriptional basis. The C-terminally truncated construct, ADAMTS16-sh had a similar effect on fibril maturation as full-length ADAMTS16, showing that the catalytic specificity for FN and inhibition of fibrillogenesis did not rely on the C terminus of the protease (supplemental Fig. S5*B*, S5*C*). Moreover, a similar impact was observed on FN networks formed by mouse BALB/c-3T3 fibroblasts, which were used for substrate identification, when co-cultured with wtADAMTS16 expressing HEK-EBNA cells (supplemental Fig. S5*D*). Impairment of FN assembly in LN-229 cells, HDF and 3T3 cells suggested that the effect of ADAMTS16 was independent of cell type.

Because fibrillin-1 (FBN1) and tenascin-C (TN-C) assembly requires a preformed FN network, we used them as reporters for the formation of a stable, mature ECM after formation of the primordial FN matrix. The 8-day co-culture was investigated for proper FBN1 and TN-C assembly, in addition to FN fibrillogenesis. Whereas the ADAMTS16 active-site mutant had no effect on the formation of FBN1 and TN-C fibrils, active ADAMTS16 strongly impaired the formation of FBN1 and TN-C networks (Fig. 4*A*, 4*B*). Whereas collagen IV formed

COLOR

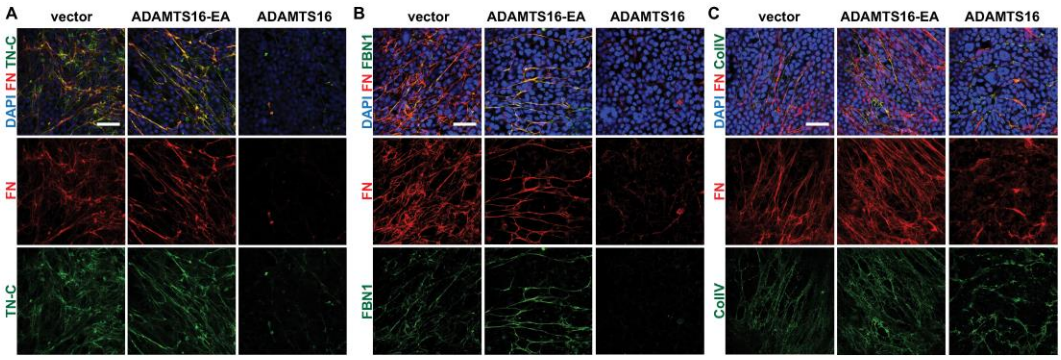

FIG. 4. **Reduction of FN fibrillogenesis in the presence of ADAMTS16 inhibits ECM maturation.** *A*, 8 day co-culture of HDF with ADAMTS16-expressing HEK cells, shows reduction of the formation of FN (red, monoclonal FN-NT) and tenascin-C (green) networks. *B*, 8-day co-culture of HDF with ADAMTS16-expressing HEK cells, shows reduction of the formation of a FN (red) and fibrillin- 1 (green) network. *C*, 8 day co-culture of HDF with ADAMTS16-expressing HEK cells, shows thickening and shortening of collagen IV bundles. FN (red, monoclonal FN- NT (7D5)) and collagen IV (green). Scale bars are 50 μm.

a network with long thin fibers in the presence of ADAMTS16-EA, thicker and shorter collagen IV fibers accumulated in HDF cultures exposed to wtADAMTS16 (Fig. 4*C*). Therefore, we conclude that ADAMTS16 overexpression can influence the integrity of other ECM assemblies by interference with FN assembly.

ADAMTS16 Impairs Spheroid Morphogenesis by MDCKI Cells in 3D Collagen Gels Via FN Proteolysis—Because of prior work indicating a role for ADAMTS16 in renal development (21, 22), renal tubule-derived MDCKI cells, which have very low levels of *ADAMTS16* mRNA were used as a model to investigate the effect of ADAMTS16 on tubulogenesis. MDCKI cells stably transfected with ADAMTS16 constructs did not show any obvious morphological differences in monolayer culture (data not shown). When grown in 3-dimensional collagen gels, MDCKI cells form spheroids in which the cells are arranged with strict apical-basal polarity. In this spheroid-formation assay, wtADAMTS16 transfected cells showed less intense FN staining in the basement membrane whereas the ADAMTS16-EA expressing spheroids had stronger FN staining compared with vector control after 4 days and 8 days in 3D culture (Fig. 5*A*, 5*B*). This finding suggested increased FN digestion in the presence of ADAMTS16 and that ADAMTS16-EA may stabilize FN fibers in 3D cultures (Fig. 5*A*, 5*B*), or that binding to ADAMTS16-EA protects them from cleavage. Additionally we observed reduced laminin staining in spheroids expressing wtADAMTS16 after 8 days in culture compared with vector or ADAMTS16-EA expressing spheroids (supplemental Fig. S6*A*). Consistent with the reduction of FN, wtADAMTS16-expressing spheroids were significantly smaller after 4 days and 8 days compared with vector control and ADAMTS16-EA expressing cells (Fig. 5*A*, 5*B*). In addition to the obvious size difference, wtADAMTS16-expressing spheroids formed multiple lumina compared with spheroids made by MDCKI cells transfected with empty vector. Moreover, spheroids expressing ADAMTS16-EA failed to form a lumen (Fig. 5*C*). E-cadherin staining of spheroids expressing wtADAMTS16 showed weaker E-cadherin staining than spheroids expressing empty vector (Fig. 5*D*) although *CDH1* mRNA was unaltered (supplemental Fig. S6*B*). In spheroids expressing ADAMTS16-EA, E-cadherin was localized to the membrane of cells attached to the basolateral FN matrix, whereas cells in the center of the spheroids showed no E-cadherin expression (Fig. 5*D*). To further investigate the polarity of these cells, we stained the spheroids for the Golgi marker gm130 after 8 days in culture. Whereas spheroids formed by vector-transfected cells showed a clear apical gm130 distribution, spheroids formed by cells expressing ADAMTS16-EA lacked polarity as evidenced by random distribution of gm130 (Fig. 5*E*). Spheroids formed by cells expressing wtADAMTS16 showed polarized gm130 staining in sections containing a single layer of cells, which was disrupted where multiple lumina were formed (Fig. 5*E*). Western blot analysis of the MDCKI monolayers showed similar E-cadherin levels when cultured in 2D and acquisition of N-cadherin expression in cells expressing ADAMTS16-EA (Fig. 5*F*). Together, these findings suggest that wtADAMTS16 overexpression reduces spheroid growth and promotes formation of multiluminal spheroids, whereas over-expression of ADAMTS16-EA promotes epithelial-mesenchymal transition in spheroids, evidenced by loss of cell polarity and acquisition of N-cadherin.

ADAMTS16 Overexpression Up-regulates MMP3 Expression by MDCKI Cells—Although Western blot analysis of the cell lysate of the MDCKI cells cultured in 2D did not show a significant differences in FN levels between cells expressing different ADAMTS16 constructs (Fig. 5*F*), the N-terminal 30 kDa FN fragment was evident in the concentrated medium of the wtADAMTS16- expressing cells (Fig. 6*A*). To ask whether

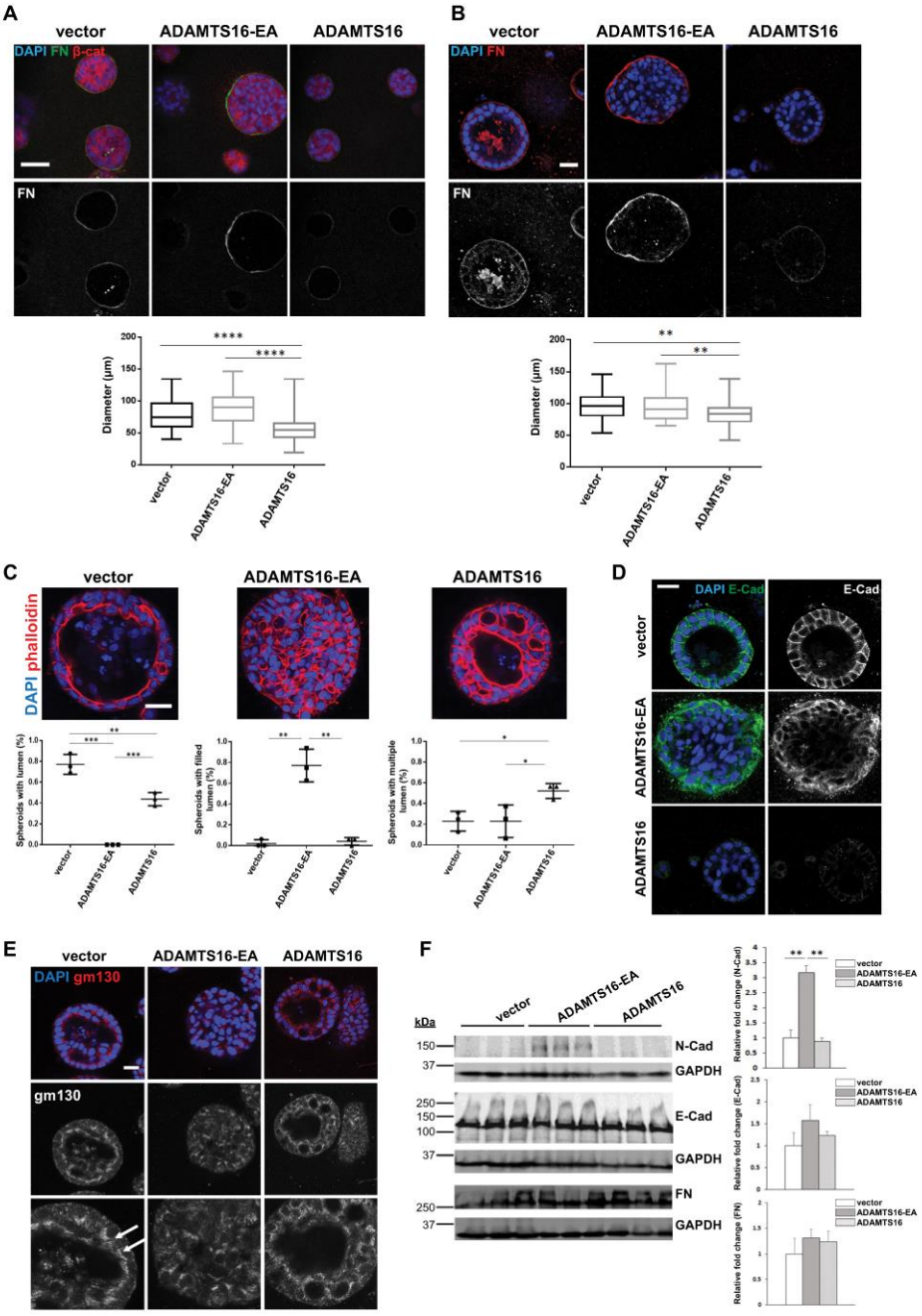
A
vector
ADAMTS16-EA
ADAMTS16
DAPI FN β-cat
FN
Diameter (μm)
B
DAPI FN
C
DAPI phalloidin
Spheroids with lumen (%)
Spheroids with filled lumen (%)
Spheroids with multiple lumen (%)
D
DAPI E-Cad
E-Cad
E
DAPI gm130
gm130
F
kDa
N-Cad
GAPDH
E-Cad
FN
Relative fold change (N-Cad)
Relative fold change (E-Cad)
Relative fold change (FN)

COLOR

this FN fragment induced MMP3 expression in MDCKI cells, as previously noted in chondrocytes (33), we added it to MDCKI monolayers and quantified *MMP3* mRNA expression. We found a significant up-regulation of *MMP3* mRNA after 24 h in treated MDCKI cells (Fig. 6*B*) and *MMP3* mRNA levels were also significantly increased in cells expressing wtADAMTS16 for 6 days in 3D cultures (Fig. 6*C*). Because MMP3 cleaves FN within the $(1)_5$-$(I)_6$ linker *i.e.* generating the 30 kDa fragment similar to ADAMTS16 (34), it is likely that the observed *MMP3* mRNA up-regulation leads to a feed-forward loop that may enhance FN proteolysis in MDCK I spheroids.

DISCUSSION

Identifying new substrates for proteases is a challenging yet crucial undertaking that is necessary for a better understanding of their function in diverse cellular and disease processes such as development, tissue repair, cancer, and inflammation. Because proteolysis is an irreversible post-translational modification, substrate identification can define pathways that are substantially modified by a protease with lasting consequences. Until now ADAMTS16 has been an orphan protease, *i.e.* one without known substrates. Although it has been linked to several human diseases, such as cancer and hypertension, its substrates and its mechanism of action were so far unknown. Our data shows that ADAMTS16 is a secreted metalloprotease that acts in a cell-proximate location. After secretion, ADAMTS16 is extensively cleaved within its C-terminal domains such that mature full-length ADAMTS16 is undetectable with antibodies to the C-terminal epitope tags. This results in release of a truncated form of ADAMTS16, which we modeled using the ADAMTS16-sh construct. ADAMTS16-sh had similar activity as ADAMTS16 in the assays utilized, suggesting that the TSR2-PLAC domain is primarily necessary for localizing ADAMTS16 to ECM through yet undetermined interactions, although ADAMTS16-sh clearly also retained some ECM-binding ability.

Here, the use of a cell-free ECM produced *in vitro* by BALB/c fibroblasts allowed substrate discovery using LC-MS/MS without prior purification of ADAMTS16. This approach is suitable for investigating other ECM-degrading proteases whose purification, like ADAMTS16, is challenging. The ECM used in this approach provided a physiological ECM containing a broad spectrum of potential substrates because fibroblasts typically produce several secreted molecules which are assembled into a well-organized ECM. The mass spectrometry strategy not only identified FN as a potential substrate of ADAMTS16, but also identified a cleavage site in the linker region between repeat $(I)_5$ and $(I)_6$ of FN. Release of the 30 kDa N-terminal heparin binding domain, likely affects FN assembly in two ways: FN dimers lacking this region may not assemble properly, and the 30 kDa fragment may interfere with the assembly of intact FN dimers by occupying cell-surface receptors or sites relevant for FN self-assembly (Fig. 6*E*). The temporal analysis of FN assembly in the presence of wild-type or catalytically inactive ADAMTS16, specifically at an early 24 h time point, suggests that ADAMTS16 primarily interferes with initiation and maturation of FN fibrils. However, release of the 30 kDa FN fragment, as observed by LC-MS/MS after digestion of a pre-formed ECM, indicates that ADAMTS16 is also capable of degrading FN fibrils. The conformation of FN dimers appears to be crucial for regulating proteolytic susceptibility, because ADAMTS16-sh did not cleave soluble plasma FN, which assumes a globular conformation (35) in which the $(I)_5$-$(I)_6$ linker region may be concealed. The cryptic site is likely exposed in the presence of cells, which apply tensile forces to FN and FN fibrils upon attachment (36). Other proteases, such as ADAMTS2 and ADAMTS3 (17), have been shown to cleave FN within its $(I)_5$-$(I)_6$ linker sequence, indicating its high susceptibility to proteolysis. The findings suggest that there is considerable redundancy in fibronectin processing by proteases. Thus, release of the 30 kDa fragment of FN by proteases is likely to be a widespread mechanism of regulation of FN assembly that has not been extensively studied.

The cell-proximate location of ADAMTS16 is relevant because FN assembly is initiated at the cell surface by integrin-binding to secreted dimers (37), and thus FN proteolysis by

FIG. 5. **ADAMTS16 impairs spheroid morphogenesis by MDCKI cells in 3D collagen gels.** *A*, Confocal microscopy of spheroids formed by ADAMTS16-expressing MDCKI cells in 3D collagen gels after 4 days. Spheroids were stained for β-catenin (red), FN (green) and nuclei (DAPI, blue). Quantitative analysis of spheroid diameter in 3D collagen gels shows size reduction upon wtADAMTS16 overexpression compared with vector and ADAMTS16-EA control after 4 days. $n = 50$ spheroids from 3 independent experiments. (****) $p < 0.0001$, Student *t* test *B*, Confocal microscopy of spheroids formed by ADAMTS16-expressing MDCKI cells in 3D collagen gels after 8 days. Spheroids were stained for FN (red) and nuclei (DAPI, blue). Reduction of FN staining in spheroids expressing wtADAMTS16 was observed whereas spheroids expressing ADAMTS16-EA had increased FN staining. Quantitative analysis of spheroid diameter shows size reduction upon ADAMTS16 overexpression compared with vector and ADAMTS16-EA control after 8 days. $n = 50$ spheroids from 3 independent experiments. (**) $p < 0.01$, Student *t* test. *C*, Spheroids were stained for phalloidin (red) and DAPI (blue) after 8 days in culture. Quantification of lumen formation in spheroids after 8 days in culture. $n = 16$ per experiment and construct, experiments were repeated 3 times. (*) $p < 0.05$, (**) $p < 0.01$, (***) $p < 0.001$ *D*, Confocal microscopy of MDCKI spheroids in 3D collagen gels after 8 days showing perturbation of E-cadherin staining in spheroids expressing wtADAMTS16. Spheroids were stained for E-cadherin (green) and nuclei (DAPI, blue). *E*, Confocal microscopy of spheroids formed by ADAMTS16-expressing MDCKI cells in 3D collagen gels after 8 days. Spheres were stained for gm130 (red) and nuclei (DAPI, blue). White arrows show polarized gm130 staining. Lower images are 2× amplifications upper panel. *F*, Western blot analysis of MDCKI cells in monolayer culture. N-cadherin expression was strongly increased in cells expressing ADAMTS16-EA. No changes in E-cadherin or FN levels were observed. Scale bars are 50 μm in *A*, *B* and *E* and 25 μm in *C*, *D*. **, $p < 0.01$ by student *t*-test.

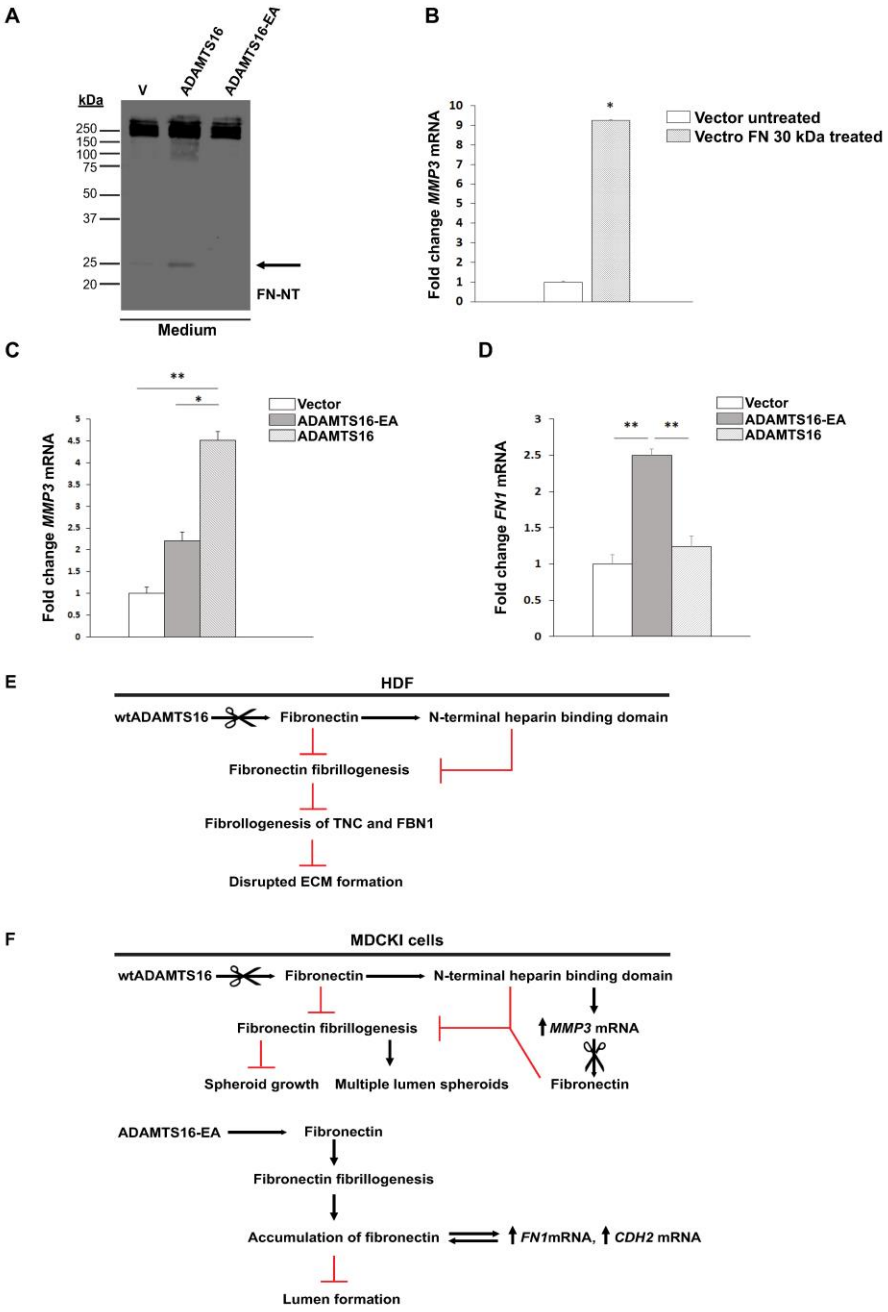
A
V
ADAMTS16
ADAMTS16-EA
kDa
250
150
100
75
50
37
25
20
FN-NT
Medium
B
Fold change MMP3 mRNA
Vector untreated
Vectro FN 30 kDa treated
C
Fold change MMP3 mRNA
Vector
ADAMTS16-EA
ADAMTS16
D
Fold change FN1 mRNA
Vector
ADAMTS16-EA
ADAMTS16
E
HDF
wtADAMTS16
Fibronectin
N-terminal heparin binding domain
Fibronectin fibrillogenesis
Fibrollogenesis of TNC and FBN1
Disrupted ECM formation
F
MDCKI cells
wtADAMTS16
Fibronectin
N-terminal heparin binding domain
Fibronectin fibrillogenesis
MMP3 mRNA
Spheroid growth
Multiple lumen spheroids
Fibronectin
ADAMTS16-EA
Fibronectin
Fibronectin fibrillogenesis
Accumulation of fibronectin
FN1mRNA, CDH2 mRNA
Lumen formation

COLOR

ADAMTS16 may occur pericellularly. WtADAMTS16 overexpression in MDCKI cells led to a significant reduction in the size of MDCK-derived spheroids associated with reduced FN staining and detection of the 30 kDa FN fragment. Additionally, we observed formation of multiluminal spheroids. These findings are consistent with a previously described reduction of spheroid size and multiple lumen formation in MDCKI cells upon FN knockdown (38, 39), suggesting that the observed impact is a result of reduction of FN in the spheroid ECM. Loss of FN in 3D cultures was also previously linked to loss of cell polarity (40). The 70 kDa N-terminal FN fragment, which blocks FN fibril assembly has been shown to impair angiogenesis in 3D cultures of vascular endothelium in collagen gels (40) and to promote loss of cell polarity during gastrulation (41). Interestingly, spheroids expressing the catalytically inactive ADAMTS16-EA had increased FN accumulation in their basement membrane. Most likely ADAMTS16-EA binds to FN without proteolysis of the protein and acts in a dominant negative manner to prevent other proteases from binding. The resulting accumulation of FN may change matrix stiffness leading to an up-regulation of *FN1* expression, which further contributes to the extensive accumulation of FN. Overall these spheroids were larger and failed to form a lumen, in contrast to the vector or wtADAMTS16-expressing spheroids. The cells of ADAMTS16-EA expressing spheroids showed characteristics of epithelial-mesenchymal transition (EMT) upon FN accumulation as shown by the up-regulation of N-Cadherin (Fig. 5*F*). Previous studies showed that TGFβ overexpression in MDCK cells blocked lumen formation via induction of EMT (42, 43) and that the levels of laminin, fibronectin and collagen IV in the ECM of MDCK spheroids could influence their ability to form a proper lumen (42). FN turnover by ADAMTS16 can therefore potentially influence cell polarity, EMT and morphogenesis in 3D culture systems. The reduction of laminin staining in wtADAMTS16-expressing MDCKI spheroids, taken together with overlapping staining of ADAMTS16 and laminin in HEK293-EBNA cultures, suggests that laminins could also be potential ADAMTS16 substrates; however, BALB/c 3T3 cells produce very low levels of laminin and we did not identify unique laminin peptides in our LC-MS/MS screen.

The 30 kDa N-terminal heparin-binding domain of FN released by ADAMTS16 is not only functionally relevant to FN fibrillogenesis but was previously shown to activate *MMP3* expression via integrin signaling in chondrocytes (33). MMP3 and its activation have been extensively studied during branching morphogenesis and cancer (44)·(45,46), but little is known about regulation of *MMP3* expression by other proteases. Our data showed that the 30 kDa fragment of FN released by ADAMTS16 increased *MMP3* expression in MDCKI cells. FN cleavage by MMP3 within the linker region between domain $(I)_5$ and $(I)_6$, like ADAMTS16, was previously shown to release the 30 kDa N-terminal heparin binding domain (33, 34). We therefore propose that induction of *MMP3* upon ADAMTS16 overexpression creates a feed-forward loop augmenting FN proteolysis (Fig. 6*F*). Thus, ADAMTS16 and MMP3 might work synergistically in regulation of FN fibril maturation and ECM assembly (Fig. 6*F*). Although the data suggest that ADAMTS16 cleaves fibronectin directly, *i.e.* by showing it binds to fibronectin and that purified ADAMTS16 cleaves fibronectin, it is possible that ADAMTS16 may act not only as a terminal protease, but also via activation of an earlier step in a proteolytic pathway, such as by up-regulation of MMP3 or activation of other proteases.

In summary, we have demonstrated that FN turnover by ADAMTS16 has a profound effect on the formation of FN networks and therefore has the potential to modify cell behavior and influence ECM composition and integrity over extended time-scales. Additionally, we have shown that ADAMTS16 drives a feed-forward proteolytic loop, because the N-terminal FN fragment generated increases *MMP3* expression in MDCKI cells. Although proteases are typically considered in the context of ECM turnover, the present work supports a major role for ADAMTS16 in regulating ECM assembly. These findings have broad ramifications for understanding cell behavior and extend the concept of the protease web (47, 48) to illustrate the complexity and interdependence of proteases in discrete cascades and circuits.

FIG. 6. **Release of the 30 kDa N-terminal heparin binding domain by ADAMTS16 up-regulates *MMP3* mRNA in MDCKI cells to generate a proteolysis feed-forward loop.** *A*, Western blot analysis of conditioned medium of MDCKI monolayers expressing wtADAMTS16, ADAMTS16-EA and empty vector control after 48 h under serum-free conditions, shows a 30 kDa FN fragment released by wtADAMTS16 activity (black arrow). *B*, *MMP3* mRNA expression is significantly increased in MDCKI cells treated with recombinant 30 kDa N-terminal heparin binding domain (1F1–5F1). (*) $p < 0.05$ by Student *t* test. Experiments were done in duplicates. *C*, Quantitative RT-PCR analysis of *MMP3* expression in MDCKI cells stably expressing ADAMTS16, ADAMTS16-EA and vector control after 6 days of culture in collagen gels. The expression of *MMP3* is up-regulated in cells expressing active ADAMTS16. (*) $p < 0.05$, (**) $p < 0.01$ by Student *t* test.; $n = 3$ independent experiments per construct. *D*, Quantitative RT-PCR analysis of *FN1* expression in MDCKI cells stably expressing ADAMTS16, ADAMTS16-EA and vector control after 6 days of culture in collagen gels. *FN1* mRNA is up-regulated in cells expressing ADAMTS16-EA. (**) $p < 0.01$ by Student *t* test; $n = 3$ independent experiments per construct. *E*, *F*, Schematics depicting the proposed pathway and impact of ADAMTS16 in HDF and MDCKI cells respectively. ADAMTS16 is furin-processed and secreted into the extracellular space, where it binds to the ECM and is further C-terminally processed. ADAMTS16 cleaves FN at its N terminus releasing a 30 kDa N-terminal heparin-binding domain that inhibits FN fibrillogenesis and ECM maturation in fibroblast cultures (*E*). In MDCKI spheroids (*F*), the 30 kDa N-terminal heparin-binding domain of FN released by ADAMTS16 induces *MMP3* expression, generating a feed-forward proteolytic loop. In contrast to active ADAMTS16, the inactive mutant ADAMTS16-EA binds to FN preventing its degradation. This enhances FN accumulation in the ECM, likely interfering with ECM stiffness and leading to increased *FN1* and *CDH2* expression.

Acknowledgments—The authors express their appreciation of the many contributions of the late Ruth Chiquet-Ehrismann (deceased September 4, 2015) to whom this manuscript is dedicated. We thank Prof. Nancy E. Hynes for critical reading of the manuscript and members of the Chiquet-Ehrismann and Apte laboratory for constructive comments. We further thank Dr. Martin Spiess for the MDCKI cells and Dr. Jan Seebacher for input on MS analysis.

DATA AVAILABILITY

The authors declare that all data supporting the findings of this study are available within the article and its Supplementary Information files or are available from R.Sc upon request. The mass spectrometry proteomics data have been deposited to the ProteomeXchange Consortium via the PRIDE partner repository (https://www.ebi.ac.uk/pride/archive/) with the dataset identifier PXD007284. Project Webpage: http://www.ebi.ac.uk/pride/archive/projects/PXD007284; FTP Download: ftp://ftp.pride.ebi.ac.uk/pride/data/archive/2018/04/PXD007284; PubMed ID: 29669734.

* This work was supported by grants from: Schweizerischer Nationalfonds zur Förderung der Wissenschaftlichen Forschung (SNF, Project funding in biology and medicine (division III)) grant no. 31003A_156740 (to R. C-E), HHS/NIH awards HL107147 and EY024943 (to S.A.), and American Heart Association-Paul G. Allen Frontiers Group Distinguished Investigator Award (to S.A.).

ZSI

S This article contains supplemental material. The authors declare no competing financial interests.

** To whom correspondence should be addressed: Department of Biomedical Engineering (ND20), Cleveland Clinic Lerner Research Institute, 9500 Euclid Avenue, Cleveland, OH 44195. Tel.: (216) 445-3278; FAX (216) 444-9198; E-mail: aptes@ccf.org or Friedrich Miescher Institute for Biomedical Research, Maulbeerstrasse 66, 4058 Basel, Switzerland. Tel.: +41-61-697-66-51; FAX +41-61-697-397; Email: rahel.schnellmann@fmi.ch.

† Deceased.

Author contributions: R.S., R.C.-E. and S.A. designed the research; R.C.-E. and S.A. supervised the research, R.S. performed the research and analyzed the data. R.S. and D.H. performed the LC-MS/MS analysis. D.A. and D.M. provided FN protein constructs and antibodies. R.S. and S.A. wrote the manuscript.

REFERENCES

1. Schwarzbauer, J. E., and DeSimone, D. W. (2011) Fibronectins, their fibrillogenesis, and in vivo functions. *Cold Spring Harb. Prospect. Biol.*
2. Hynes, R. O. (1990) Fibronectins. *Springer- Verlag, New York*
3. Grudzenko, T., and Franz, C. M. (2015) Studying early stages of fibronectin fibrillogenesis in living cells by atomic force microscopy. *Mol. Biol. Cell* **26,** 3190–3204
4. Pankov, R., and Yamada, K. M. (2002) Fibronectin at a glance. *J. Cell Sci.* **115,** 3861–3863
5. Schwarzbauer, J. E. (1991) Identification of the fibronectin sequences required for assembly of a fibrillar matrix. *JCB* **113,** 1463–1473
6. McDonald, J. A., Quade, B. J., Broekelman, T. J., LaChance, R., Forsman, K., Hasegawa, E., and Akiyama, S. (1987) Fibronectin's cell-adhesive domain and an amino-terminal matrix assembly domain participate in its assembly into fibroblast pericellular matrix. *J. Biol. Chem.* **262,** 2957–2967
7. McKEOWN-LONGO, P. J., and MOSHERDF. (1985) Interaction of the 70,000-mol-wt Amino-terminal Fragment of Fibronectin with the Matrix-assembly Receptor of Fibroblasts. *J. Cell Biol.* **100,** 364–374
8. Sabatier, L., Chen, D., Fagotto-Kaufmann, C., Hubmacher, D., McKee, M. D., Annis, D. S., Mosher, D. F., and Reinhardt, D. P. (2009) Fibrillin assembly requires fibronectin. *Mol. Biol. Cell* **20,** 846–856
9. Chiquet-Ehrismann, R., Matsuoka, Y., Hofer, U., Spring, J., Bernasconi, C., and Chiquet, M. (1991) Tenascin variants: differential binding to fibronectin and distinct distribution in cell cultures and tissues. *Cell Regul.* **11,** 927–938
10. Kubow, K. E., Vukmirovic, R., Zhe, L., Klotzsch, E., Smith, M. L., Gourdon, D., Luna, S., and Vogel, V. (2015) Mechanical forces regulate the interactions of fibronectin and collagen I in extracellular matrix. *Nat. Commun.* **6,** 8026 AQ: L
11. Dallas, S. L., Sivakumar, P., Jones, C. J., Chen, Q., Peters, D. M., Mosher, D. F., Humphries, M. J., and Kielty, C. M. (2005) Fibronectin regulates latent transforming growth factor-beta (TGF beta) by controlling matrix assembly of latent TGF beta-binding protein-1. *J. Biol. Chem.* **280,** 18871–18880
12. George, E. L., Georges-Labouesse, E. N., Patel-King, R. S., Rayburn, H., and Hynes, R. O. (1993) Defects in mesoderm, neural tube and vascular development in mouse embryos lacking fibronectin. *Development* **119,** 1079–1091
13. Shi, F., and Sottile, J. (2011) MT1-MMP regulates the turnover and endocytosis of extracellular matrix fibronectin. *J. Cell Sci.* **124,** 4039–4050
14. Mosher, D. F. (1989) Fibronectin. *Academic Press. Inc.*
15. Gronski, T. J. J., Martin, R. L., Kobayashi d, Walsh, K. B. C., Holman, M. C., Huber, M., Wart, H. E. V., and Shapiro, S. D. (1997) Hydrolysis of a broad spectrum of extracellular matrix proteins by human macrophage elastase. *J. Biol. Chem.* **272,** 12189–12194
16. Marchina, E., and Barlati, S. (1996) Degradation of human plasma and extracellular matrix fibronectin by tissue type plasminogen activator and urokinase. *Int. J. Biochem. Cell Biol.* **28,** 1141–1150
17. Bekhouche, M., Leduc, C., Dupont, L., Janssen, L., Delolme, F., Goff, S. V.-L., Smargiasso, N., Baiwir, D., Mazzucchelli, G., Zanella-Cleon, I., Dubail, J., Pauw, E. D., Nusgens, B., Hulmes, D. J., Moali, C., and Colige, A. (2016) Determination of the substrate repertoire of ADAMTS2, 3, and 14 significantly broadens their functions and identifies extracellular matrix organization and TGF-β signaling as primary targets. *FASEB J.* **30,** 1741–1756
18. Kern, C. B., Wessels, A., McGarity, J., Dixon, L. J., Alston, E., Argraves, W. S., Geeting, D., Nelson, C. M., Menick, D. R., and Apte, S. S. (2010) Reduced versican cleavage due to Adamts9 haploinsufficiency is associated with cardiac and aortic anomalies. *Matrix Biol.* **29,** 304–316
19. Kelwick, R., Desanlis, I., Wheeler, G. N., and Edwards, D. R. (2015) The ADAMTS (A Disintegrin and Metalloproteinase with Thrombospondin motifs) family. *Genome Biol.* **16,** 113 AQ: M
20. Abdul-Majeed, S., Mell, B., Nauli, S. M., and Joe, B. (2014) Cryptorchidism and infertility in rats with targeted disruption of the Adamts16 locus. *PLoS ONE* **9,** e100967 AQ: N
21. Jacobi, C. L., Rudigier, L. J., Scholz, H., and Kirschner, K. M. (2013) Transcriptional regulation by the Wilms tumor protein, Wt1, suggests a role of the metalloproteinase Adamts16 in murine genitourinary development. *J. Biol. Chem.* **288,** 18811–18824
22. Gopalakrishnan, K., Kumarasamy, S., Abdul-Majeed, S., Kalinoski, A. L., Morgan, E. E., Gohara, A. F., Nauli, S. M., Filipiak, W. E., Saunders, T. L., and Joe, B. (2012) Targeted disruption of Adamts16 gene in a rat genetic model of hypertension. *Proc. Natl. Acad. Sci. U.S.A.* **109,** 20555–20559
23. Joe, B., Saad, Y., Dhindaw, S., Lee, N. H., Frank, B. C., Achinike, O. H., Luu, T. V., Gopalakrishnan, K., Toland, E. J., Farms, P., Yerga-Woolwine, S., Manickavasagam, E., Rapp, J. P., Garrett, M. R., Coe, D., Apte, S. S., Rankinen, T., Pérusse, L., Ehret, G. B., Ganesh, S. K., Cooper, R. S., O'Connor, A., Rice, T., Weder, A. B., Chakravarti, A., Rao, D. C., and Bouchard, C. (2009) Positional identification of variants of Adamts16 linked to inherited hypertension. *Hum. Mol. Genet.* **18,** 2825–2838
24. Sakamoto, N., Oue, N., Noguchi, T., Sentani, K., Anami, K., Sanada, Y., Yoshida, K., and Yasui, W. (2010) Serial analysis of gene expression of esophageal squamous cell carcinoma: ADAMTS16 is upregulated in esophageal squamous cell carcinoma. *Cancer Sci.* **101,** 1028–1044
25. Yasukawa, M., Liu, Y., Hu, L., Cogdell, D., Gharpure, K. M., Pradeep, S., Nagaraja, A. S., Sood, A. K., and Zhang, W. (2016) ADAMTS16 mutations sensitize ovarian cancer cells to platinum-based chemotherapy. *Oncotarget* **8,** 88410–88420 AQ: O
26. Zheng, L., Baumann, U., and Reymond, J. L. (2004) An efficient one-step site-directed and site-saturation mutagenesis protocol. *Nucleic Acids Res.* **32,** e115 AQ: P
27. Beacham, D. A., Amatangelo, M. D., and Cukierman, E. (2007) Preparation of Extracellular Matrices Produced by Cultured and Primary Fibroblasts. *Curr. Protoc. Cell Biol.*, 10.19.11–10.19.21

28. Asparuhova, M. B., Ferralli, J., Chiquet, M., and Chiquet-Ehrismann, R. (2011) The transcriptional regulator megakaryoblastic leukemia-1 mediates serum response factor- independent activation of tenascin-C transcription by mechanical stress. *FASEB J.* **25,** 3477–3488
29. Schmittgen, T. D., and Livak, K. J. (2008) Analyzing real- time PCR data by the comparative C(T) method. *Nat. Protoc.* **3,** 1101–1108
30. Maurer, L. M., Tomasini-Johansson, B. R., Ma, W., Annis, D. S., Eickstaedt, N. L., Ensenberger, M. G., Satyshur, K. A., and Mosher, D. F. (2010) Extended Binding Site on Fibronectin for the Functional Upstream Domain of Protein F1 of Streptococcus pyogenes. *J. Biol. Chem.* **285,** 41087–41099
31. Cal, S., Obaya, A. J., Llamazares, M., Garabaya, C., Quesada, V., and López-Otín, C. (2002) Cloning, expression analysis, and structural characterization of seven novel human ADAMTSs, a family of metalloproteinases with disintegrin and thrombospondin-1 domains. *Gene* **283,** 49–62
32. Gao, S., Geyter, C. D., Kossowska, K., and Zhang, H. (2007) FSH stimulates the expression of the ADAMTS-16 protease in mature human ovarian follicles. *Mol. Hum. Reprod.* **13,** 465–471
33. Ding, L., Guo, D., and Homandberg, G. A. (2008) The cartilage chondrolytic mechanism of fibronectin fragments involves MAP kinases: comparison of three fragments and native fibronectin. *Osteoarthritis Cartilage* **16,** 1253–1262
34. Muir, D., and Manthorpe, M. (1992) Stromelysin generates a fibronectin fragment that inhibits Schwann cell proliferation. *J. Cell Biol.* **116,** 177–185
35. Maurer, L. M., Ma, W., and Mosher, D. F. (2016) Dynamic structure of plasma fibronectin. *Crit. Rev. Biochem. Mol. Biol.* **51,** 213–227
36. Sivakumar, P., Czirok, A., Rongish, B. J., Divakara, V. P., Wang, Y. P., and Dallas, S. L. (2006) New insights into extracellular matrix assembly and reorganization from dynamic imaging of extracellular matrix proteins in living osteoblasts. *J. Cell Sci.* **119,** 1350–1360
37. Sechler, J. L., Corbett, S. A., and Schwarzbauer, J. E. (1997) Modulatory roles for integrin activation and the synergy site of fibronectin during matrix assembly. *Mol. Biol. Cell* **8,** 2563–2573
38. Jiang, S. T., Chiang, H. C., Cheng, M. H., Yang, T. P., Chuang, W. J., and Tang, M. J. (1999) Role of fibronectin deposition in cystogenesis of Madin-Darby canine kidney cells. *Kidney Int.* **56,** 92–103
39. Jiang, S. T., Chuang, W. J., and Tang, M. J. (2000) Role of fibronectin deposition in branching morphogenesis of Madin-Darby canine kidney cells. *Kidney Int.* **57,** 1860–1867
40. Zhou, X., Rowe, R. G., Hiraoka, N., George, J. P., Wirtz, D., Mosher, D. F., Virtanen, I., Chernousov, M. A., and Weiss, S. J. (2008) Fibronectin fibrillogenesis regulates three-dimensional neovessel formation. *Genes Dev.* **22,** 1231–1243
41. Rozario, T., Dzamba, B., Weber, G. F., Davidson, L. A., and DeSimone, D. W. (2009) The physical state of fibronectin matrix differentially regulates morphogenetic movements in vivo. *Dev. Biol.* **327,** 386–398
42. Santos, O. F., and Nigam, S. K. (1993) HGF-induced tubulogenesis and branching of epithelial cells is modulated by extracellular matrix and TGF-beta. *Dev. Biol.* **16,** 293–302
43. Sakurai, H., and Nigam, S. K. (1997) Transforming growth factor-beta selectively inhibits branching morphogenesis but not tubulogenesis. *Am. J. Physiol.* **272,** 139–146
44. Talhouk, R. S., Chin, J. R., Unemori, E. N., Werb, Z., and Bissell, M. J. (1991) Proteinases of the mammary gland: developmental regulation in vivo and vectorial secretion in culture. *Development* **112,** 439–449
45. Nagase, H., Enghild, J. J., Suzuki, K., and Salvesen, G. (1990) Stepwise activation mechanisms of the precursor of matrix metalloproteinase 3 (stromelysin) by proteinases and (4-aminophenyl)mercuric acetate. *Biochemistry* **29,** 5783–5789
46. Overall, C. M., and Kleifeld, O. (2006) Tumour microenvironment—opinion: Validating matrix metalloproteinases as drug targets and anti-targets for cancer therapy. *Nat. Rev. Cancer* **6,** 227–239
47. Keller Ua. d., Doucet, A., and CMO. (2007) Protease research in the era of systems biology. *Biol. Chem.* **388,** 1159–1162
48. Fortelny, N., Cox, J. H., Kappelhoff, R., Starr, A. E., Lange, P. F., Pavlidis, P., and Overall, C. M. (2014) Network analyses reveal pervasive functional regulation between proteases in the human protease web. *PLos Biol.* **12,** e1001869

AQ: Q

Supplementary figure legends, figures and tables:

Fig.S1. The C-terminal TSR2-PLAC domain was not detectable by LC-MS/MS. Full length ADAMTS16 sequence (Uniprot Accession Nr. **Q69Z28-1**) is underlined with the peptides identified by LC-MS/MS of conditioned medium of HEK-EBNA cells stably expressing wtADAMTS16, ADAMTS16-sh, ADAMTS16-sh-EA as indicated. Peptides arising from the C-terminus of ADAMTS16 were not identified. ^{862}TPAAQPSYSWAIVR^{876} is the most C-terminal peptide of ADAMTS16 identified, suggesting C-terminal processing in the vicinity of Arg^{876}.

Fig.S2. LC-MS/MS identified FN as potential substrate of ADAMTS16. A. Extracted ion chromatograms (MS1 spectra) for the doubly charged FN peptide CERHALQSASAGSGS (*m/z* 739.3402) after digestion with Lys-C/AspN digests. The peptide elutes at about 11.3 min (see red box). It was observed only with wtADAMTS16 and ADAMTS16-sh but not with ADAMTS16-sh-EA and empty vector. **B-F.** Histograms of the log10 ratios of wtADAMTS16 with ADAMTS16-sh-EA, ADAMTS16-sh with ADAMTS16-sh-EA and vector with ADAMTS16-sh-EA. LTBP-1 (B), FN (C,D), GELS (E) and POSTN (F). Peptides showing potential cleavage sites are marked by a red box.

Fig. S3. LC-MS/MS identified human FN cleavage products upon digestion by ADAMTS16. A. HEK293-EBNA cells stably expressing ADAMTS16-sh, ADAMTS16-sh-EA and empty vector control were seeded on FN coated cell culture dishes under serum-free conditions for 24 h. 1 µg of total protein was loaded and western blot was probed with anti-FN-NT antibody specific to the N-terminus of FN. Release of the 30 kDa N-terminal fragment into the medium could be observed in the sample incubated with ADAMTS16-sh (arrow). **B.** MS2 spectrum of the human FN peptide ^{270}CERHTSVQTTSSGSGPFTDVRAA^{292} identified in the digest of ADAMTS16-sh. **C.** Histogram of the normalized average abundance of the peptide ^{270}CERHTSVQTTSSGSGPFTDVRAA^{292}. The peptide was found with different charges (3+, 4+). The abundance of all charged forms of the peptides was therefore summarized and normalized against total FN. Each bar represents the averaged abundance from biological triplicates normalized against total FN. Data are mean ± S.E.M with n=3. (***) P<0.001, Student *t*- test. **D.** Domain structure of human FN with expanded view of the amino acid sequence of the linker between domains $(I)_5$ and $(I)_6$ showing the peptide identified by LC-MS/MS (underlined) and the potential ADAMTS16 cleavage site.

Fig. S4. FN is a substrate of ADAMTS16. A. Activity assay of ADAMTS16-sh using alpha2-macroglobulin as a substrate showed activity of purified ADAMTS16-sh. ADAMTS16-sh was incubated with alpha2-macroglobulin and the cleavage products were analyzed by SDS-PAGE under reducing conditions, but without heating prior to loading. **B.** Western blot analysis of digests of full-length plasma FN by recombinant ADAMTS16-sh with and without EDTA in the reaction buffer. Western blot was probed with an antibody specific to the N-terminus of FN (anti-FN-NT, MAB1936). No cleavage product was identified. **C.** Schematic of the domain structure of FN and a recombinant FN construct spanning domain $(I)_4$ until $(II)_2$ including the predicted ADAMTS16 cleavage site within the FN-linker domain. **D.** Western blot analysis of digest of recombinant FN-linker by purified ADAMTS16-sh with or without EDTA in the reaction buffer. Western blot was probed with anti- FN- NT antibody (MAB1936). No cleavage product was identified. **E.** HEK-EBNA cells stably expressing wtADAMTS16, ADAMTS16-EA or empty vector control were seeded under serum free conditions on a culture dish pre-coated with FITC-labelled FN (FITC-FN, green). Degradation of FITC-FN, visible as loss in green fluorescence signal, was observed in the presence of wtADAMTS16 (white arrows). Cells were stained with TR-phalloidin (red), and DAPI (blue). Scale bars are 50 µm. Lower panels show 2X magnifications of the boxed areas. **F.** Staining of FN in the cell layer of

transiently transfected LN229 cells shows reduction of FN in the cells expressing wtADAMTS16. Cells were stained for FN using polyclonal anti-FN antibody (green) and nuclei (DAPI, blue). Scale bars are 50 µm. Lower panels show 3X amplification of the boxed areas in the upper panels**.**

Fig. S5. ADAMTS16 influences FN fibril formation and maturation in co-culture with human dermal fibroblasts (HDF) and BALB/c 3T3 fibroblasts. A. Quantitative RT-PCR of HDF co-cultured with HEK293-EBNA cells for 4 days and 8 days. No difference in *FN1* mRNA was observed after 4 days. 1.6 fold increase in *FN1* mRNA was observed in cells co cultured in the presence of ADAMTS16-EA after 8 days of co-culture. No reduction of *FN1* mRNA levels, in the presence of ADAMTS16 could be observed at any time point. n=3 independent experiments. **B.** Co-culture of HDF with HEK-EBNA cells stably expressing ADAMTS16-sh showed strong reduction of FN fibrils compared to HDF co-cultured with HEK-EBNA cells stably expressing the inactive mutant ADAMTS16-sh-EA after 2 days. Scale bars are 50 µm. Lower panels are 3X magnifications of boxed areas. **C.** Co-culture of HDF cells with ADAMTS16-sh expressing cells shows reduction of fibrillin-1 fibrils after 8 days of culture. HDF co-cultured with ADAMTS16-sh-EA expressing cells did not show differences in the FN and fibrillin-1 networks compared to the vector control. Cells were stained for FN (polyclonal, red), FBN1 (green) and nuclei (DAPI, blue). Scale bars are 50 µm. **D.** Co- culture of BALB/c 3T3 cells and HEK-EBNA cells stably expressing ADAMTS16 show reduction of FN fibrils after 4 days similar to co-culture experiments using HDF. No FN fibril reduction was observed when BALB/c 3T3 cells were co-cultured with ADAMTS16-EA and vector control. Cells were stained for FN (polyclonal, green) and nuclei (DAPI, blue). Scale bars 50 µm. Lower panels show 3X magnification of the boxed areas.

Fig. S6. ADAMTS16 influences morphology of MDCKI cells in 3D culture. A. Laminin (LAM) staining of MDCKI spheroids stably expressing wtADAMTS16, ADAMTS16-EA or vector control. The spheroids expressing wtADAMTS16 have less laminin staining than spheroids expressing the inactive ADAMTS16-EA or vector control. Spheroids were stained for laminin (red) and nuclei (DAPI, blue) after 8 days in culture. Scale bars are 50 µm. **B.** Quantitative RT-PCR shows no significant difference for *CDH1* expression in spheroids expressing either wtADAMTS16, ADAMTS16-EA or vector control after 6 days in 3D cultures. n=3 independent experiments. **C.** Uncropped western blot analyzing FN expression in MDCKI monolayer cultures. Western blot was probed with anti-FN (polyclonal, red) and anti-GAPDH (green). **D.** Uncropped western blot analyzing FN expression in MDCKI monolayer cultures. Western blot was probed with anti-N-Cad (red) and re-probed anti-GAPDH (green). **F.** Uncropped western blot analyzing FN in MDCKI monolayer cultures. Western blot was probed with anti- E-Cad (red) and re-probed with anti-GAPDH (green).

Table S1: Antibodies used in the present work

primary antibodies		catalog no.	vendor	WB	IF	3D
mouse monoclonal	anti-myc	clone 9E10	Lerner Research Institute Hybridoma Core	1:1000	1:100	
rabbit monoclonal	anti-FN		Generated by Ruth Chiquet- Ehrismann	1:10000	1:1000	1:500
mouse monoclonal	anti-FN-NT	*MAB1936*	Merck Millipore, Darmstadt, Germany	1:1000		
mouse monoclonal	anti-FN-4F1	7D5	Generated by Dean Mosher, Madison Wisconsin	1:1000	1:500	
rabbit polyclonal	anti-hTenC		Generated by Ruth Chiquet- Ehrismann, FMI, Basel		1:1000	
mouse monoclonal	anti-FBN1 (11C1.3)	MAB1919	EMD Millipore, Billerica, MA		1:200	
rabbit polyclonal	anti-laminin	L9393	Sigma Aldrich, St. Louis, MO		1:200	
rabbit polyclonal	anti-Collagen Type IV	600-401-106-0.5	Rockland, Limerick, PA			
mouse monoclonal	anti-β catenin	610154	BD Biosciences, San Jose, CA			1:200
mouse monoclonal	anti-E-Cadherin	610181	BD Biosciences, San Jose, CA	1:1000		1:200
rabbit polyclonal	anti-gm130	ab31561	Abcam, Cambridge, UK			1:200
mouse monoclonal	anti-GAPDH	MAB374	EMD, Millipore, Billerica, MA	1:1000		
rabbit polyclonal	anti-GAPDH	NB-300-323	Novus Biologicals, Littleton CO	1:1000		

sec. antibodies		catalog no.	vendor	WB	IF	3D
Goat	anti-rabbit	IRDye 680RD	LI-Core, Lincoln, NE	1:1000		
Goat	anti-mouse	IRDye 680RD	LI-Core, Lincoln, NE	1:1000		
Goat	anti-rabbit	Alexa Fluor 568	Invitrogen, Carlsbad, CA		1:1000	1:400
Goat	anti-mouse	Alexa Fluor 568	Invitrogen, Carlsbad, CA		1:1000	1:400
Goat	anti-rabbit	Alexa Fluor 488	Invitrogen, Carlsbad, CA		1:1000	1:400
Goat	anti-mouse	Alexa Fluor 488	Invitrogen, Carlsbad, CA		1:1000	1:400
	phalloidin	Alexa Fluor 568	Life technologies, Carlsbad, CA		1:400	1:400

Table S2: Cloning primers used to generate ADAMTS16 constructs described in the paper

	Sequence
ADAMTS16 for	5′-ACGTGGTACCGCTAGCGCCACCATGGAGTCCCGAGGTTGTGCT-3′
ADAMTS16-sh rev.	5′-ACGTGCGGCCGCTCAATGATGATGATGATGATGCAGATCCTCTTCTGAGATGAGTTTCTGCTCCCATGAGTA GCTGGGCTGGGCAG-3′
ADAMTS16 rev.	5′-ACGTGCGGCCGCTCAATGATGATGATGATGATGCAGATCCTCTTCTGAGATGAGTTTCTGCTCCAGGTTGGATT TGGAGCAGGT-3′
ADAMTS16 w/o PLAC rev	5′-ACGTGCGGCCGCTCAATGATGATGATGATGATGATGCAGATCCTCTTCTGAGATGAGTTTCTGCTCCTTCTCTGC AAGGGGCAGAA-3′
CT-ADAMTS16 for	5′-ACGTGCTAGCACCGCCATGGAGTCCCGAGGTTGTGCTGCGCTCTGGGTGCTGCTGCTGGCGCAGGTCAGTGAG CAGTGGGCCATCGTACGCTCTGA-3′
ADAMTS16 mut for	5′-CGTGGGGGAAGAGCTGTGACCCAGCCA-3′
ADAMTS16 mut rev	5′-TCTTCCCCCACGCCTCCGCTGGTAGTG-3′

Table S3: RT-PCR primer

Species	target	Forward primer	Reverse Primer
human	*FN1*	5′-GAACTATGATGCCGACCAGAA-3′	5′-GGTTGTGCAGATTTCCTCGT-3′
human	*TBP*	5′-TGCACAGGAGCCAAGAGTGAA-3′	5′-CACATCACAGCTCCCCACCA-3′
dog	*MMP3*	5′-CCTGGGTCTCTTTCACTCGG-3′	5′-AGGGAGGTCCACCATACAGG-3′
dog	*TBP*	5′-AACAGTTTAGCAGTTACGAGCC-3′	5′-ACAGCCATTACGTTGTCTTCC-3′
dog	*FN*	5′-TACAGTTCCGAGTTCCTGGC-3′	5′-GTTTAGGCCTTGGTCCACAGA-3′
dog	*CDH1*	5′-GTACAATGACCCAGCTCGTGA-3′	5′-TCCGAGAATGCCCAAGATGC-3′

Table S4: Detection of full length ADAMTS16 in the conditioned medium.

construct	unique peptides detected	exclusive spectrum count	sequence coverage %
ADAMTS16-sh-EA	35	60	32
ADAMTS16-sh	43	91	38
ADAMTS16	29	49	26

Scaffold analysis of the LC-MS/MS results showed comparable sequence coverage and peptide counts of peptides of wtADAMTS16, ADAMTS16-sh and ADAMTS16-sh-EA in the conditioned medium of stably expressing HEK-EBNA cells seeded on decellularized ECM.

Table S5: Peptide abundance of mouse peptides showing proteolytic cleavage not resulting from sample preparation prior to LC-MS/MS analysis

Protein name	Peptide mass	Charge	modifications	Peptide seq.	Position (Start-End)	Working protease	Abundance wtADAMTS16	Abundance ADAMTS16-sh	Abundance ADAMTS16-sh-EA	Abundance vector
FN	1516.665	2	none	(K)CERHALQSAS AGSGS(F)	271-285	LysC/AspN	1.15E+04	1.05E+05	5.31E+01	5.19E+01
FN	1516.666	2	none	(K)CERHALQSAS AGSGS(F)	271-285	LysC	2.68E+04	2.62E+05	8.32E+00	3.77E+02
FN	1516.666	3	none	(K)CERHALQSAS AGSGS(F)	271-285	LysC	2.64E+04	1.93E+05	0.00	4.45E+02
FN	1347.5691	2	none	(D)PIDQCQDSET R(T)	557-567	LysC/Trypsin	1.20E+04	6.30E+03	2.66E+03	3.80E+03
LTBP-1	2817.2816	3	none	(Y)GRDALVDFSE QYGPETDPYFIQ DR(F)	1580-1603	LysC/Trypsin	1.39E+04	6.88E+03	3.32E+03	3.57E+03
POSTN	828.4933	2	[4] Deamidated (NQ)	(T)LLVNELK(S)	604-610	LysC	1.53E+05	1.33E+05	9.57E+04	7.94E+04

Peptide abundance of peptides showing proteolytic cleavage not resulting from sample preparation. Abundancies were calculated using Progenesis QI software.

Table S6: Abundance of mouse FN peptides in comparison to the abundance of CERHALQSASAGSGS

Protein name	Peptide mass	Charge	modifications	Peptide seq.	Working protease	Abundance wtADAMTS16	Abundance ADAMTS16-sh	Abundance ADAMTS16-sh-EA	Abundance vector
FN	**1516.665**	**2**	**none**	**(K)CERHALQSASAGSGS(F)**	**LysC/AspN**	**1.15E+04**	**1.05E+05**	**5.31E+01**	**5.19E+01**
FN	1097.581	2	none	(K)YIVNVYQIS(E)	LysC/AspN	8.58E+03	7.53E+03	8.24E+03	4.78E+03
FN	1594.856	2	none	(F)AEITGLSPGVTYLFK(V)	LysC/AspN	3.08E+04	3.35E+04	2.18E+04	1.92E+04
FN	1087.040	2	none	(H)LEANPDTGVLTVSWERSTTP (D)	LysC/AspN	6.81E+03	8.28E+03	4.88E+03	3.38E+03
FN	**1516.666**	**2**	**none**	**(K)CERHALQSASAGSGS(F)**	**LysC**	2.68E+04	2.62E+05	8.32E+00	3.77E+02
FN	**1516.666**	**3**	**none**	**(K)CERHALQSASAGSGS(F)**	**LysC**	2.64E+04	1.93E+05	0.00	4.45E+02
FN	5931.781	5	none	(K)CERHALQSASAGSGSFTDVRTAIY QPQTHPQPAPYGHCVTDSGVVYSV GMQWLK(S)	LysC	3.57E+04	6.48E+04	2.01E+05	1.13E+05
FN	1499.653	2	[10] Phospho (ST)	(P)HVPGLNPNASTGQE(A)	LysC	4.32E+06	6.25E+06	2.44E+06	2.89E+06
FN	1198.675	3	[10] Deamidated (NQ)	LTAGLTRGGQPK	LysC	7.08E+04	8.12E+04	7.24E+04	3.49E+04

Abundance of FN peptides showing that only the peptide CERHALQSASAGSGS is markedly different between control and active samples where other peptides identified show small to no differences in abundance between control and active samples. Abundancies were calculated using Progenesis QI software

Table S7: Abundance of identified mouse proteins in the analyzed samples

Protein Name	Accession Nr.	Working Protease	Abundance wtADAMTS16	Abundance ADAMTS16-sh	Abundance ADAMTS16-sh-EA	Abundance vector
Fibronectin	P11276	LysC	4.97E+07	6.80E+07	2.52E+07	7.32E+07
Fibronectin	P11276	LysC/AspN	3.10E+07	3.59E+07	1.43E+07	2.95E+07
Fibronectin	P11276	LysC/Tryp	4.03E+07	5.04E+07	2.25E+07	4.94E+07
Fibronectin	P11276	AspN/Tryp	1.65E+07	1.42E+07	6.73E+06	1.37E+07
LTBP1	Q8CG19	LysC	3.68E+06	6.99E+06	1.15E+06	5.26E+06
LTBP1	Q8CG19	LysC/AspN	1.25E+06	2.11E+06	3.83E+05	1.19E+06
LTBP1	Q8CG19	LysC/Tryp	2.22E+06	2.96E+06	7.16E+05	1.73E+06
LTBP1	Q8CG19	AspN/Tryp	6.92E+05	4.09E+05	2.67E+05	6.81E+05
POSTN	Q62009	LysC	5.31E+06	9.49E+06	7.81E+06	1.21E+07
POSTN	Q62009	LysC/AspN	2.01E+06	3.13E+06	1.35E+06	4.10E+06
POSTN	Q62009	LysC/Tryp	1.66E+06	2.92E+06	1.68E+06	3.66E+06
POSTN	Q62009	AspN/Tryp	8.03E+05	2.20E+07	5.15E+05	1.08E+06
GELS	P13020	LysC	5.19E+06	8.13E+06	4.98E+06	8.99E+06
GELS	P13020	LysC/AspN	2.29E+06	3.23E+06	2.12E+06	2.79E+06
GELS	P13020	LysC/Tryp	2.28E+06	3.05E+06	2.30E+06	3.01E+06
GELS	P13020	AspN/Tryp	1.57E+06	1.53E+06	1.55E+06	1.70E+06
PGS1	P28653	LysC	2.73E+05	7.07E+05	3.32E+05	1.72E+06
PGS1	P28653	LysC/AspN	6.79E+04	2.16E+05	9.24E+04	2.45E+05
PGS1	P28653	LysC/Tryp	1.48E+05	3.66E+05	1.62E+05	2.85E+05
PGS1	P28653	AspN/Tryp	2.96E+04	2.61E+05	1.16E+05	1.15E+05
SERPH	P19324	LysC	3.00E+05	4.72E+05	3.95E+05	1.55E+06
SERPH	P19324	LysC/AspN	1.55E+05	2.04E+05	2.20E+05	3.78E+05
SERPH	P19324	LysC/Tryp	1.80E+05	4.02E+05	4.61E+05	6.80E+05
SERPH	P19324	AspN/Tryp	2.30E+04	8.15E+04	3.34E+04	5.96E+04
PLEC	Q9QXS1	LysC	4.25E+06	4.96E+06	1.58E+06	3.04E+06
PLEC	Q9QXS1	LysC/AspN	6.01E+05	6.37E+05	2.35E+05	5.34E+05
PLEC	Q9QXS1	LysC/Tryp	1.52E+06	1.36E+06	8.74E+05	1.25E+06
PLEC	Q9QXS1	AspN/Tryp	2.99E+05	1.14E+06	1.90E+05	1.90E+05

Abundance of Progenesis QI analysis of the digests using different working proteases. The results show comparable normalized abundance in the different digests of the analyzed proteins from Table 1 and 2 of the main manuscript.

Table S8: Normalized average abundance of the human FN peptides identified in the ADAMTS16 digest.

Peptide mass	Charge	modifications	Peptide seq.	Position (Start-End)	Averaged normalized abundance ADAMTS16-sh	Averaged normalized abundance ADAMTS16-sh-EA	Averaged normalized abundance vector
2450.1275	3	none	(K)CERHTSVQTTSSGSGPFTDVRAA(V)	270-292	2.41E-04 ± 0.26E-04	0	3.2E-06 ± 5.5E-06
2450.128	4	none	(K)CERHTSVQTTSSGSGPFTDVRAA(V)	270-292	6.64E-04 ± 0.9E-04	3.17E-05 ± 1.2E-05	3.89E-05 ± 4.8E-05
2412.181	3	none	(Y)AVEENQESTPVVIQQETTGTPR(S)	882-903	6.33E-03 ± 2.6E-03	1.13E-04 ± 8.1E-05	1.05E-03 ± 1.5E-03
3251.5967	3	none	(Y)AVEENQESTPVVIQQETTGTPRSDTV PSPR(D)	882-911	1.54E-03 ± 2.2E-03	0	0
3299.6712	3	none	(K)LGVRPSQGGEAPREVTSDSGSIVVSG LTPGVEY(V)	1117-1149	1.44E-03 ± 0.89E-03	0	4.54E-06 ± 7.8E-06
3561.7996	3	none	(K)LGVRPSQGGEAPREVTSDSGSIVVSG LTPGVEYVY(T)	1117-1151	7.09E-03 ± 2.4E-03	4.05E-05 ± 7E-05	1.52E-04 ± 2.4E-04

Averaged abundance of FN peptides with cleavage sites other than LysC (working protease) and stronger abundance compared to the control samples. The N-terminal peptide CERHTSVQTTSSGSGPFTDVRAA was identified with two different charges. The displayed abundance are average values of biological triplicates. The samples were LysC digested prior to LC-MS/MS analysis and abundance were calculated using ProgenesisQI for proteomics. Individual peptide abundance was normalized towards total FN. Data are mean ± S.E.M. A complete list of all identified peptides and abundance of each single run can be found on Proteomexchange.

Table S9: Average abundance of total human FN in ADAMTS16 digest samples

Protein Name	Accession Nr.	Averaged Abundance ADAMTS16-sh	Averaged Abundance ADAMTS16-sh-EA	Averaged Abundance vector
Fibronectin	P02751	8.63E+06 ± 1.5E+06	3.10E+06 ± 6.3E+05	9.27E+06 ± 9.9E+06

Averaged abundance of human FN in ADAMTS16 digest samples, shows comparable amounts of overall FN in all samples. The displayed abundance are average values of biological triplicates. The samples were LysC digested prior to LC-MS/MS analysis and abundance were calculated using ProgenesisQI for proteomics. Data are mean ± S.D. A list with the FN abundance of each single run can be found on Proteomexchange.

Figure S1

>sp|Q69Z28|ATS16_MOUSE A disintegrin and metalloproteinase with thrombospondin motifs 16 OS=Mus musculus GN=Adamts16 PE=2 SV=2

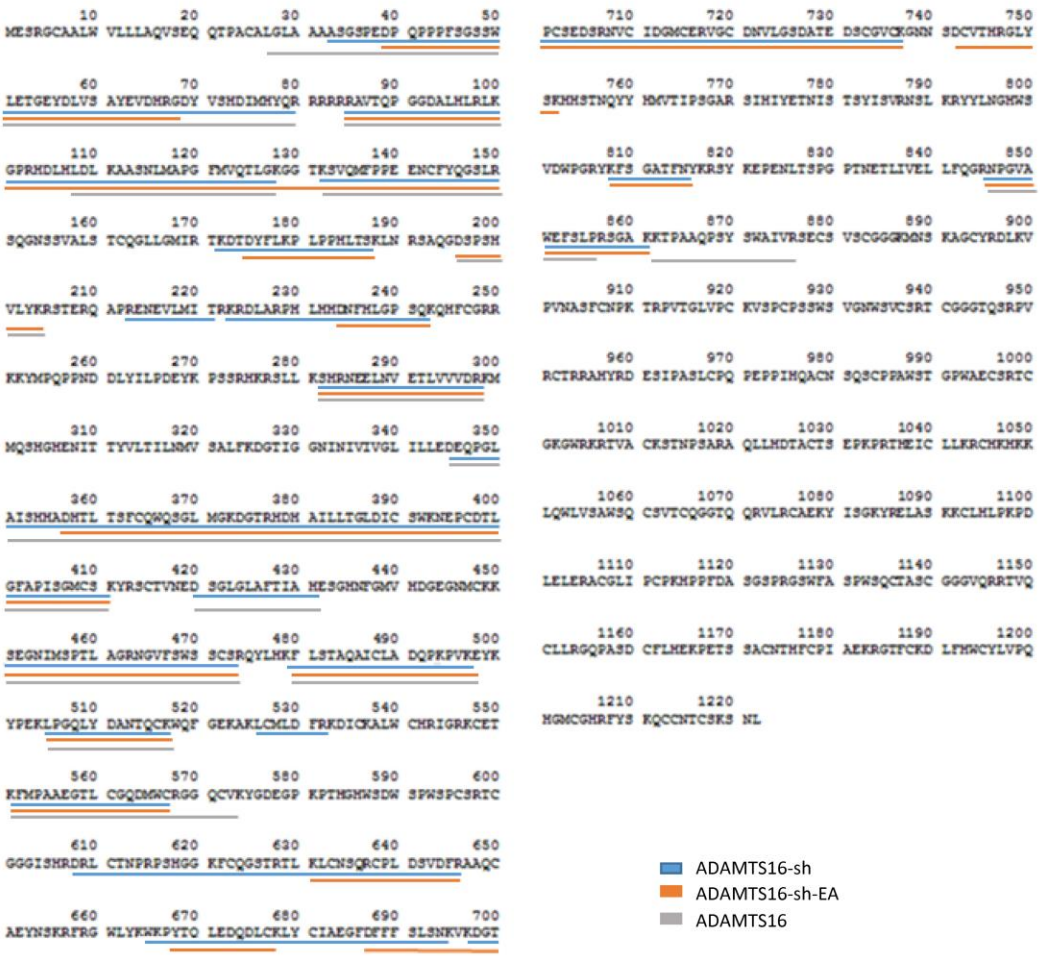

Figure S2

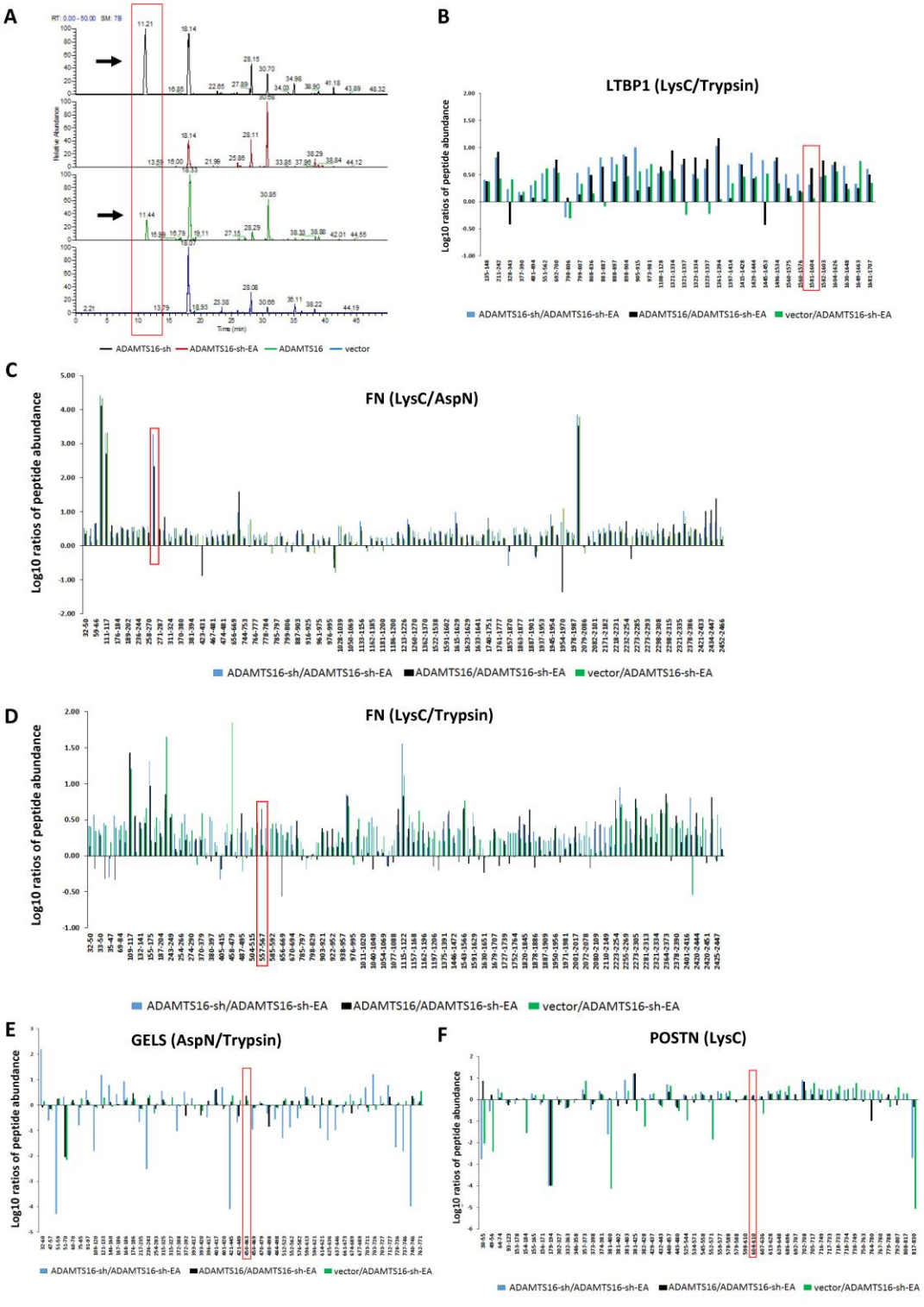
A
B
LTBP1 (LysC/Trypsin)
Log10 ratios of peptide abundance
ADAMTS16-sh/ADAMTS16-sh-EA
ADAMTS16/ADAMTS16-sh-EA
vector/ADAMTS16-sh-EA
ADAMTS16-sh
ADAMTS16
vector
C
FN (LysC/AspN)
D
FN (LysC/Trypsin)
E
GELS (AspN/Trypsin)
F
POSTN (LysC)

Figure S3

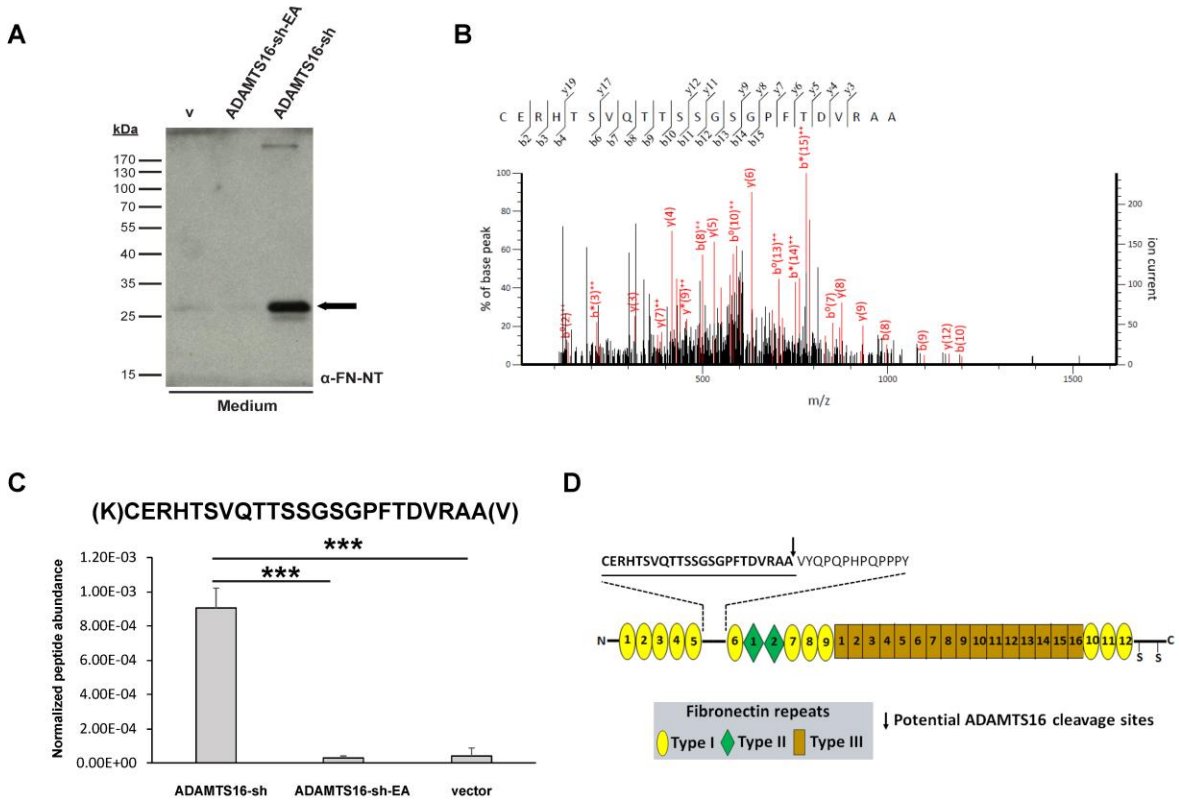
A
v
ADAMTS16-sh-EA
ADAMTS16-sh
kDa
170
130
100
70
55
40
35
25
15
α-FN-NT
Medium
B
C E R H T S V Q T T S S G S G P F T D V R A A
% of base peak
ion current
m/z
C
(K)CERHTSVQTTSSGSGPFTDVRAA(V)
Normalized peptide abundance
1.20E-03
1.00E-03
8.00E-04
6.00E-04
4.00E-04
2.00E-04
0.00E+00
***
***
ADAMTS16-sh
ADAMTS16-sh-EA
vector
D
CERHTSVQTTSSGSGPFTDVRAA VYQPQPHPQPPPY
N
C
Fibronectin repeats
Type I
Type II
Type III
Potential ADAMTS16 cleavage sites

Figure S4

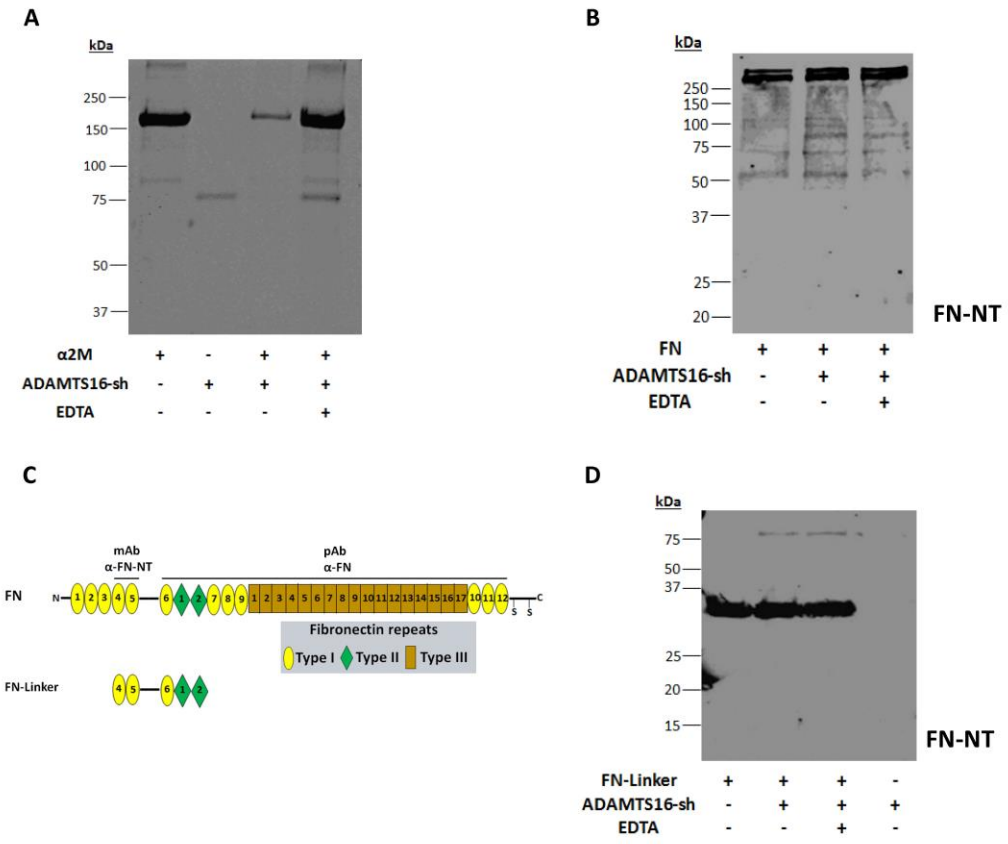
A
kDa
250
150
100
75
50
37
α2M + - + +
ADAMTS16-sh - + + +
EDTA - - - +
B
kDa
250
150
100
75
50
37
25
20
FN-NT
FN + + +
ADAMTS16-sh - + +
EDTA - - +
C
mAb
α-FN-NT
pAb
α-FN
FN
N
C
S S
Fibronectin repeats
Type I
Type II
Type III
FN-Linker
D
kDa
75
50
37
25
20
15
FN-NT
FN-Linker + + + -
ADAMTS16-sh - + + +
EDTA - - + -
E
vector
ADAMTS16-EA
ADAMTS16
DAPI FN phalloidin
FN
F
vector
ADAMTS16-EA
ADAMTS16
DAPI FN
FN

Figure S5

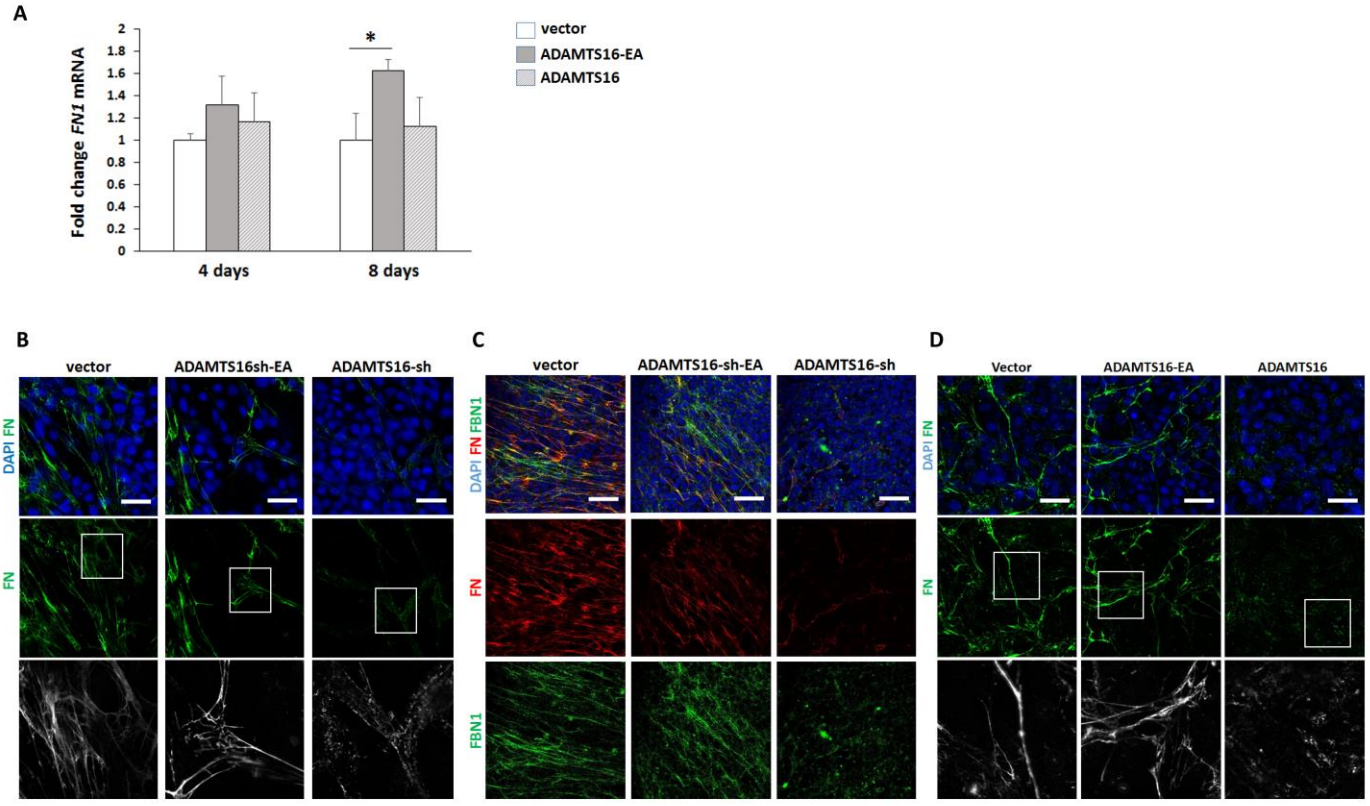
A
Fold change FN1 mRNA
2
1.8
1.6
1.4
1.2
1
0.8
0.6
0.4
0.2
0
*
4 days
8 days
vector
ADAMTS16-EA
ADAMTS16
B
vector
ADAMTS16sh-EA
ADAMTS16-sh
DAPI FN
FN
C
vector
ADAMTS16-sh-EA
ADAMTS16-sh
DAPI FN FBN1
FN
FBN1
D
Vector
ADAMTS16-EA
ADAMTS16
DAPI FN
FN

Figure S6

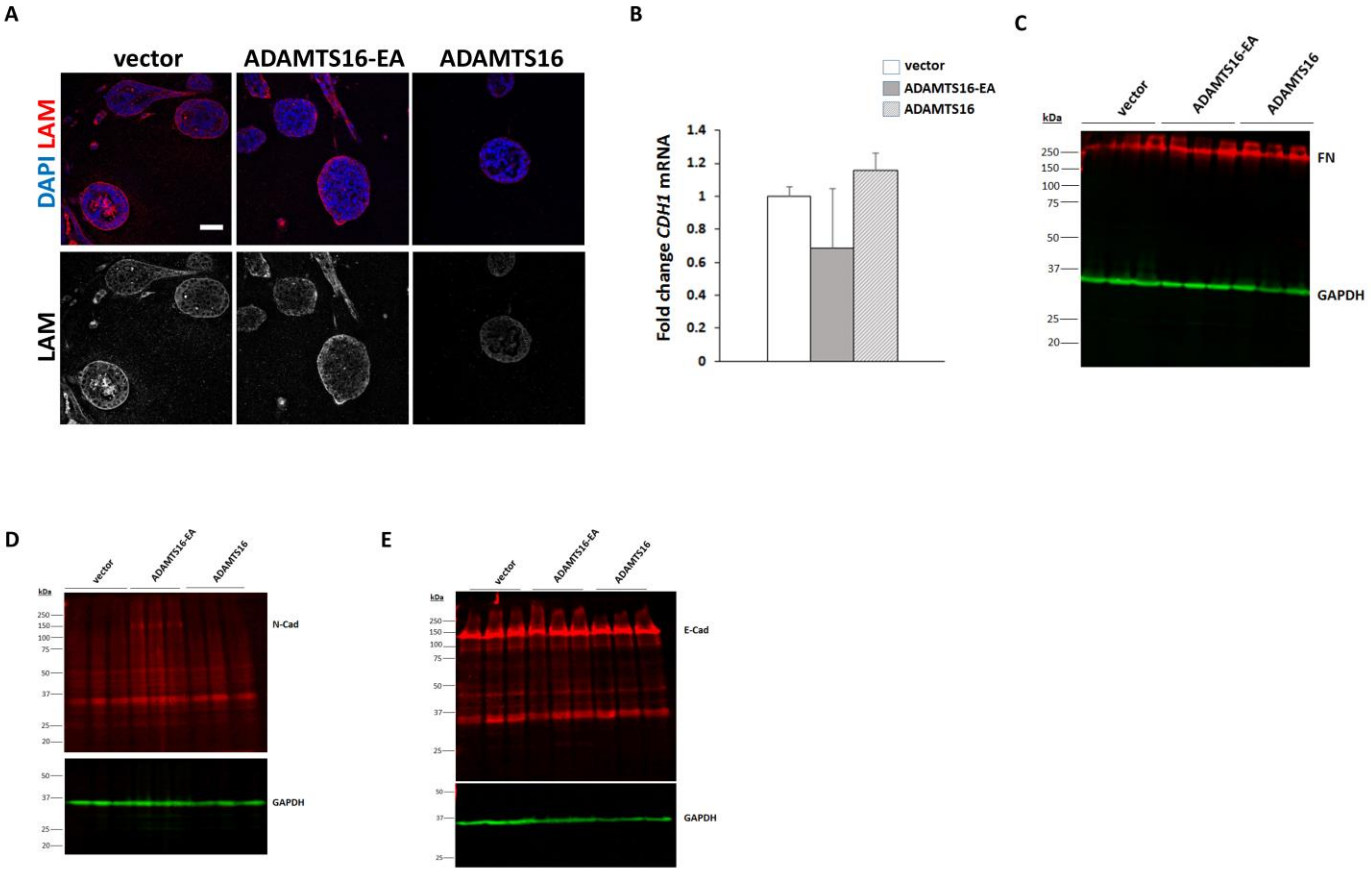
A
vector
ADAMTS16-EA
ADAMTS16
DAPI LAM
LAM
B
vector
ADAMTS16-EA
ADAMTS16
Fold change CDH1 mRNA
1.4
1.2
1
0.8
0.6
0.4
0.2
0
C
vector
ADAMTS16-EA
ADAMTS16
kDa
250
150
100
75
50
37
25
20
FN
GAPDH
D
vector
ADAMTS16-EA
ADAMTS16
kDa
250
150
100
75
50
37
25
20
N-Cad
50
37
25
20
GAPDH
E
vector
ADAMTS16-EA
ADAMTS16
kDa
250
150
100
75
50
37
25
E-Cad
50
37
25
GAPDH

5. Unpublished Results

5.1 Materials and Methods

All reagents and chemicals used in the following experiments were obtained from either Sigma Aldrich or Merck Millipore unless stated otherwise.

Cell culture, cloning and transfection

Human embryonic kidney HEK293-EBNA cells, African Green Monkey kidney cells COS-7 and the glioblastoma cell line LN229 were grown in DMEM medium supplemented with 10% FCS. The epithelial Madyn-Darby canine kidney type I cells (MDCKI) were grown in α-MEM supplemented with 10% FCS. All cell culture experiments were done in medium supplemented with 10% FCS unless stated otherwise.

Mouse ADAMTS16 cDNA ORF clone (with ref. sequence NM_172053), was obtained from Creative Biogene (Shirley, NY). All constructs were C-terminally myc_His_6 tagged and subcloned into pCEP_pu (Invitrogen, *Carlsbad, CA*). Cloning primers and protocols are described previously. Briefly truncated ADAMTS16-sh was amplified by PCR adding KpnI and NheI restrictions sites 5' and a NotI restriction site 3'. Additionally the construct was C-terminally myc_His_6 tagged. The constructs was cloned into the pCEP_pu via the KpnI and NotI restriction sites (pCEP_pu_ADAMTS16-sh). WtADAMTS16 was amplified by PCR adding NheI and NotI restrictions sites 5' and 3' respectively and a C-terminal myc_His_6 tag. WtADAMTS16 was cloned into pCEP_pu_ADAMTS16-sh via the NheI and NotI restriction sites, thereby replacing ADAMTS16-sh. All clones were verified by DNA sequencing. For vector maps and DNA sequences see Appendix.

Human MMP14 cDNA ORF clone (with ref. sequence NM_008608.3) was obtained from Sino Biological (Sino biological Inc., Beijing, China). MMP14 was amplified by PCR adding a C-terminal HA tag and cloned into pCDNA-3.1 vector. The following primers were used: 5'- ACG TAA GCT TGC CAC CAT GTC TCC CGC CCC TCA ACC (forward primer) and 5'- ACG TGG ATC CTC AAG CGT AAT CTG GAA CAT CGT ATG GGT AGA CCT TGT CCA GCA GCG AAC-3' (reverse primer).

COS-7, HEK-EBNA, MDCKI and LN229 cells were transfected using FuGENE® 6 (Roche, Basel, Switzerland) or jetPEI® DNA transfection reagent (Polyplus), respectively according to the manufacturers' instructions. To obtain stably expressing cell lines, the cells were treated after transfection with puromycin for 14 days.

Protein analysis by western blotting

Cell extracts and conditioned media were prepared in Laemmli loading buffer with or without 2-mercaptoethanol, separated by SDS-PAGE and transferred to a nitrocellulose membrane. Amido black staining of the membranes was used to visualize bands as loading control. Blots were probed with the following antibodies: anti-MMP14 (diluted 1:2000 in 5% milkpowder/ TBS-T, rabbit polyclonal, ab88618, Abcam), anti-myc (diluted 1:100 in 5% milkpowder/ TBS-T, mouse monoclonal, Clone: 9E10, homemade FMI), anti-HA (diluted 1:10 in 5% milkpowder/TBS-T, mouse monoclonal, homemade FMI), anti-MMP3 (diluted 1:1000 in 5% milkpowder/ TBS-T, rabbit monoclonal, EP1186Y, Abcam). The blots were further treated using horseradish peroxidase-conjugated secondary antibodies (1:10,000; MP Biomedicals, France) for detection with the ECL Western blotting System (Amersham, Switzerland), and exposed to Kodak X-ray film.

MMP14 cleavage assay

COS-7 cells were co-transfected with MMP14 and various ADAMTS16 constructs using jetPEI® DNA transfection reagent (Polyplus) according to manufacturers' instructions. After transfection the cells were incubated under serum-free conditions for 24 h at 37°C. The cell lysate and conditioned medium were prepared in Laemmli loading buffer containing 2-mercaptoethanol and analyzed by western blot as described previously.

MMP3 cleavage assay

HEK-EBNA cells were co-transfected with MMP3 and either wtADAMTS16, ADAMTS16-EA or vector control using FuGENE® 6 (Roche, Basel, Switzerland) according to manufacturers' instructions. After transfection cells were incubated under serum-free conditions for 24 h at 37°C. Conditioned medium was prepared in Laemmli loading buffer with or without 2-mercaptoethanol and analyzed by western blot as described above.

HEK-EBNA cells were transiently transfected with MMP3. After 24 h of incubation under serum-free conditions, the conditioned medium was collected and incubated with purified recombinant ADAMTS16-sh. 50 µl of conditioned medium containing MMP3 was incubated with ADAMTS16-sh in the presence or absence of 50 mM EDTA for 4 h at 37°C. The sample was prepared in Laemmli loading buffer without 2-mercaptoethanol and analyzed by western blot as described above.

Immunofluorescence (IF)

HEK-EBNA cells stably expressing wtADAMTS16 and ADAMTS16-EA were plated on 35×10 mm cell culture dishes with 4 inner rings (Greiner Bio-One GmbH, Germany) in DMEM supplemented with 10% FCS and EDTA-free protease inhibitor (cOmplete™, Mini Protease Inhibitor Cocktail, Sigma-Aldrich). Cells were incubated for 24 h at 37°C and fixed with Zinc Formal-Fixx™ (Thermo Fisher Scientific) for 30 minutes and permeabilized with 0.1% Triton X-100 for 5 minutes. Cells were incubated at room temperature with anti-myc mouse monoclonal antibody (diluted 1:20 in PBS, Clone: 9E10) for 90 minutes and then incubated with Alexa488-labeled secondary antibody (diluted 1:1000 in PBS) for 60 minutes. Cell nuclei were stained using Hoechst staining solution (diluted 1:1000, Hoechst 33342 Solution, Thermo Fisher Scientific). Cells were mounted in Prolong Gold antifade reagent (Invitrogen, Switzerland) and images were taken using a Zeiss-Axioscope fluorescent microscope equipped with a 20X objective and Hamamatsu ORCA-ER camera.

HEK-EBNA cells stably expressing wtADAMTS16, ADAMTS16-EA or vector control were seeded on 8-well glass chamber slides (Falcon Culture Slides, Thermo Fisher Scientific) previously coated with FN (30 µg/ml in PBS) and allowed to attach for 24 h at 37°C. Cells were fixed using 4% paraformaldehyde (PFA) for 20 min at room temperature. Cells were stained using phalloidin (diluted 1:1000, Alexa Fluor™ 568 Phalloidin, Thermo Fisher Scientific). Samples were mounted in ProLong Gold with DAPI (Life Technologies, Carlsbad, CA) and imaged with a Leica TCS5 SPII confocal microscope. Images were acquired under identical camera settings and analysed using ImageJ software (U. S. National Institutes of Health, Bethesda, Maryland, USA).

Mass spectrometry analysis

To identify the additional proteins co-purified with ADAMTS16-sh, we performed an in gel digest and analyzed the samples by mass spectrometry (MS). 50 µl of ADAMTS16-sh protein elute, described in the manuscript, was separated by SDS-PAGE. The gel was further stained using ready-to-use protein stain based on colloidal coomassie dye G-250 (GelCode™ Blue Stain Reagent, Thermo Fisher Scientific). Protein bands were cut and the coomassie was excised by washing the gel pieces in 50 µL AmBic (25 mM NH_4HCO_3 in 50% acetonitrile) for 30 min at room temperature. Samples were reduced with tris(2-carboxyethyl)phosphine (TCEP), alkylated with Iodoacetamide and digested with Trypsin overnight at 37°C. Peptides were analyzed by liquid chromatography mass spectrometry (LTQ Orbitrap Velos, Thermo Fisher Scientific). The results were analyzed using Scaffold 4.4.8 software (Proteome Software, Portland, Oregon, USA).

Phage display

To identify potential substrates of ADAMTS16 a commercially available phage library was used (NEB Ph.D 7 phage display library, NEB). Purified ADAMTS16-sh and its inactive mutant ADAMTS16-sh-EA was used as template. The experiment was performed according to manufacturers' instructions. Although the target protein was diluted in TBS buffer and not in $NaHCO_3$ as recommended by the protocol. After three rounds of panning 20 clones were picked and sequenced. The 20 protein sequences were analyzed for a potential consensus sequence. A protein blast was performed with the resulting consensus sequence using NCBI/BLASTP (National Center for Biotechnology Information (NCBI), Bethesda MD). UniProtKB/Swiss-Prot was used as search database with a maximum of 500 target sequences. The search was restricted to human and mouse proteins. Only ECM proteins and the extracellular domain of membrane proteins were considered as potential substrates.

Protein zymogram

After reaching 90% confluency, MDCKI and HEK-EBNA cells stably expressing various ADAMTS16 constructs were incubated under serum-free conditions for 48 h at 37°C. The conditioned medium was collected, concentrated and analyzed by zymography. For casein zymography, 2 ml of media was concentrated using amicon centrifugal filter units (Amicon Ultra-0.5 mL Centrifugal Filters, Merck Millipore)). 5 µg of total protein was loaded on a 10% polyacrylamide gel containing 0.1% casein. The gels were soaked in wash buffer (2.5% Triton X-100, 50 mM Tris (pH 7.5), 5 mM $CaCl_2$, 1 uM $ZnCl_2$) for 60 minutes at room temperature to remove the SDS and incubated in reaction buffer (50 mM Tris-HCl (pH 7.5), 5 mM $CaCl_2$ and 1 uM $ZnCl_2$) at 37°C overnight. Gels were rinsed again in distilled water, stained with 0.5% Coomassie brilliant blue R-250 in 30% methanol and 10% acetic acid for 30 min, and destained with 30% methanol and 10% acetic acid. Proteolytic activities appeared as clear bands of lysis against a dark background of stained casein.

For gelatin zymography 2 ml of media form HEK-EBNA cell or MDCKI cells respectively was concentrated using amicon centrifugal filter units. 10 µg of total protein was loaded on a 10% polyacrylamide gel containing 0.1% gelatin. The same staining protocol as described above was used.

Quantitative Reverse-Transcriptase PCR

Total RNA was isolated using the RNeasy Plus Micro Kit (50) (Quiagen). RNA was reverse transcribed and relative *ADAMTS16* mRNA levels normalized to *TBP* were measured using Platinum® SYBR® Green qPCR

SuperMix-UDG with ROX (Invitrogen). The following *ADAMTS16* primers were used: 5'-CGC AAG AAA TAC ATG CCC CAG-3' (forward primer) and 5'-AGA AGA GAG CGC TTA TGC CG-3' (reverse primer). Real-time PCR was performed in StepOnePlus Real-Time PCR System (Applied Biosystems, Rotkreuz, Switzerland) using a standard cycling profile. All samples were run in duplicates. Endogenous *ADAMTS16* mRNA expression levels were analyzed by the ΔCt method [230]. Data represent means ± S.E.M from technical replicates.

RNA in situ hybridization

16.5 day-old (E16.5) mouse embryos and kidneys of newborn, 10 days, 4 week- and 8 week-old mice were fixed in 4% PFA at 4°C for 48h prior to paraffin embedding. Fresh 10 µm sections for the embryo tissue and 7 µm sections for the kidney tissue were used for in-situ hybridization using RNASccope (Advanced Cell Diagnostics, Newark, CA)) following the manufacturer's protocol. All steps requiring incubation at 40°C were performed in a HybEZ Oven (Advanced Cell Diagnostics). Tissue localization of specific probe against mouse *Adamts16* mRNA (#474881, Advanced Cell Diagnostics) was detected with the RNAscope 2.0 HD detection kit "RED"(Advanced Cell Diagnostics).

Boyden chamber cell migration assay

Directed migration of MDCKI and HEK-EBNA cells stably expressing various ADAMTS16 constructs was analyzed using transwell polycarbonate membrane inserts (6.5 mm; Corning, Amsterdam, The Netherlands) with 8 µm pore size. The transwell inserts were either left untreated or the lower membrane site was FN coated (100 µg/ml in PBS) prior to use. $3.5 * 10^4$ cells were plated in 100 µl serum-free DMEM into the transwell inserts. The lower chamber was filled with 600 µl 10% FCS/DMEM. Cells were incubated at 37°C and were allowed to migrate across the transwell filters for 24 h. Migrated cells were fixed and stained with crystal violet. 4 Images/ insert were taken using a Zeiss-Axioscope fluorescent microscope equipped with a 10X objective and Hamamatsu ORCA-ER camera. Migration was quantified by measuring the area covered by migrated cells using ImageJ software (U. S. National Institutes of Health, Bethesda, Maryland, USA). Data represent means ± S.E.M from technical replicates.

Cell proliferation assay

Proliferation rates of MDCKI cells stably expressing wtADAMTS16, ADAMTS16-EA and vector control and LN229 cells transiently expressing wtADAMTS16, ADAMTS16-EA and vector control were determined

using the MTT cell proliferation assay kit (Vybrant® MTT Cell Proliferation Assay Kit, Thermo Fisher Scientific). MDCKI and LN229 cells were plated in triplicates on 96-well microtiter plates (PerkinElmer) in 10% FCS/DMEM at $3*10^3$ cells/well and $5*10^3$ cells/well, respectively, were incubated at 37°C and allowed to proliferate for 24 h, 48 h, 3 days, 4 days, 5 days, 6 days and 7 days. At each time point cells were labelled with the MTT reagents following the manufacturer's instructions and the absorbance was measured at 540 nm using an absorbance spectrophotometer (PowerWave HT microplate spectrophotometer, BioTeK). Data represent means ± S.E.M from technical triplicates.

5.2 Results

5.2.1 ADAMTS16 is C-terminally processed and forms high order oligomers

Due to the observed C-terminal processing of wtADAMTS16, HEK-EBNA cells stably expressing wtADAMTS16 and ADAMTS16-EA were treated with an EDTA-free protease inhibitor cocktail and analyzed for secretion and accumulation of ADAMTS16 by western blot and immunofluorescence (IF). Cells treated with protease inhibitor strongly accumulate ADAMTS16 within the secretory pathway, mainly within the *trans*-Golgi network (TGN). This indicates that ADAMTS16 is fully translated and the C-terminus is either cleaved by proteases within the TGN, in the secretory pathway or extracellularly in close proximity to the cell surface (Fig. 1A). Analysis of the cell lysate of inhibitor treated cells by western blot conforms the accumulation of full length ADAMTS16. Due to the extremely low amount of full length ADAMTS16 in the cell lysate of untreated cells we can conclude that under normal conditions ADAMTS16 is very efficiently C-terminally processed shortly after translation. Moreover, although we treated the cells with protease inhibitor we still could observe a low amount of mature ADAMTS16 indicating that the protein convertase furin, responsible for prodomain processing was not completely inhibited, or another protease is processing the prodomain as well (Fig. 1B).

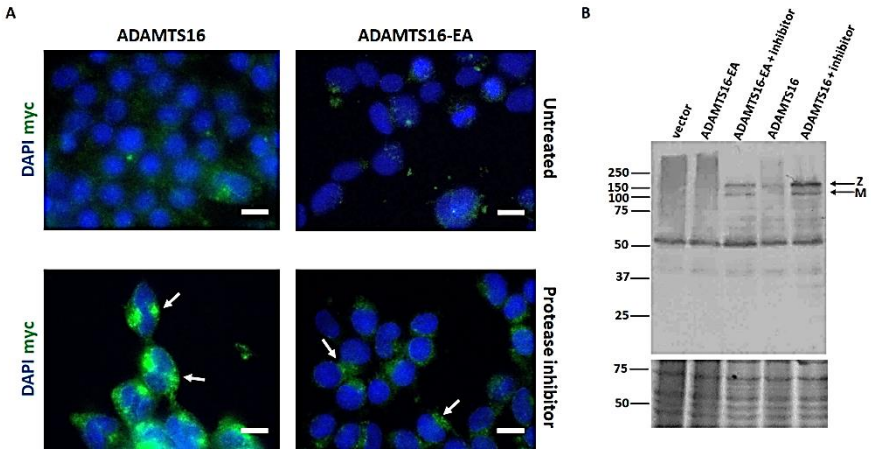

Figure 1: Upon treatment with EDTA-free protease inhibitor strong accumulation of ADAMTS16 in the secretory pathway was observed. **A.** HEK-EBNA cells stably expressing wtADAMTS16 or ADAMTS16-EA were treated with protease inhibitor. After 24 h the cells were stained for ADAMTS16 expression using an anti-myc antibody against the C-terminal tag of ADAMTS16 (green). Strong accumulation of ADAMTS16 within the *trans*-Golgi network could be observed (white arrows). Scale bars 50 µm **B.** Western blot analysis of cell lysate of protease inhibitor treated HEK-EBNA cells. The blot was probed with anti-myc antibody. Strong accumulation of ADAMTS16 could be observed within the cell lysate of inhibitor treated cells. Zymogen (Z) and mature (M) ADAMTS16 are indicated by black arrows. Amido black staining of the membrane was used to visualize protein bands as loading control.

A recent publication by Kosasihet al. on ADAMTS5 showed that the C-terminal ancillary domain can influence the protease activity without being covalently attached to the protease domain. They showed that ADAMTS5 is a higher order oligomer and that oligomerization is required for full aggrecanase activity. However the ancillary domain can block full length ADAMTS5 oligomerization and therefore inhibit ADAMTS5 activity. To show the effect of the ancillary domain on ADAMTS5 activity in vivo they compared the aggrecanolysis in cartilage explanted from mice that were either heterozygous for the ADAMTS5Δcat (TS5Δcat) mutation (TS5+/Δcat) or the ADAMTS5 null mutation (TS5+/−). TS5Δcat mice express the full suite of ancillary domains but lack ADAMTS5 activity, where ADAMTS5 null mice expressed neither catalytic nor ancillary domains. Where the TS5+/− mice had the same level of aggrecanase activity as wild type mice, TS5+/Δcat mice had significantly reduced aggrecanase activity. This result suggested the possibility of an interaction between wild type and mutant ADAMTS5 molecules in TS5+/Δcat cartilage, in which binding of the mutant TS5Δcat protein, with its full set of ancillary domains, to wild type ADAMTS5 inhibits enzyme activity in a dominant-negative manner. [231].

Based on the published results on ADAMTS5 oligomerization we tested whether ADAMTS16 forms oligomers in vitro as well. For this we analyzed the supernatant of HEK-EBNA cells transiently expressing various ADAMTS16 constructs under reducing, and non-reducing conditions, by western blot. Because of the strong C-terminal processing of wtADAMTS16 we were not able to detect any full length protein in the conditioned medium using antibodies against the C-terminal myc-tag. Therefore, we used the short form of ADAMTS16 lacking the C-terminal TSR1 and PLAC domains (ADAMTS16-sh, construct details are described in the manuscript) and its inactive mutant (ADAMTS16-sh-EA) to screen for oligomerization. We could observe the formation of higher order oligomers in the conditioned medium of cells expressing ADAMTS16-sh. Further we observed that oligomerization is not dependent on enzyme activity, because the inactive mutant ADAMTS16-sh-EA showed the formation of oligomers as well. However, we observed a lower overall amount of secreted ADAMTS16-sh-EA (Fig.2A).

To investigate the influence of the C-terminal domain on oligomerization we co-expressed wtADAMTS16 and its inactive mutant ADAMTS16-EA together with the truncated constructs ADAMTS16-sh and ADAMTS16-sh-EA. The presence of full length ADAMTS16 neither interferes with the oligomer formation of ADAMTS16-sh nor its inactive mutant ADAMTS16-sh-EA. However, we could observe a reduction in oligomer formation by ADAMTS16-sh in the presence of active ADAMTS16, but not in the presence of ADAMTS16-EA (Fig. 2B). As expected, we could not detect any bands in the conditioned medium of cells co-expressing wtADAMTS16 and ADAMTS16-EA (Fig. 2B). Moreover we could see strong C-terminal

processing of ADAMTS16 in the cell lysate of transiently transfected cells. Co-expression of wtADAMTS16 with either inactive ADAMTS16-sh-EA or ADAMTS16-EA did not influence the C-terminal processing, indicating that neither the truncated ADAMTS16-sh-EA nor the full length inactive ADAMTS16-EA interfere with the activity of ADAMTS16 and its ability for autoproteolysis. Additionally neither ADAMTS16-EA nor ADAMTS16-sh-EA interfered with the activity and the ability of other proteinases to C-terminally process ADAMTS16. (Fig.2B).

Because of its C-terminal processing it was not possible to purify full length ADAMTS16. Therefore we decided to express and purify the C-terminally truncated ADAMTS16-sh, as described previously. The eluted protein fractions containing purified recombinant ADAMTS16-sh were analyzed by SDS-Page. Beside the most abundant band corresponding to ADAMTS16-sh at approximately 75 kDa, we observed several other bands at lower molecular weights. To investigate whether these bands are degradation products of ADAMTS16-sh, or other co-purified proteins, we performed an in gel digest and analyzed the fractions by mass spectrometry (MS). We could not see any degradation of ADAMTS16-sh, instead we found a couple of human proteins co-purified with ADAMTS16-sh, such as clusterin (CLUS) and heat shock 70 kDa protein 1A/1B (HSP71). Both proteins are known chaperones where CLUS can act intracellularly as well as in the extracellular space. Additionally CLUS is involved in the internalization of bound proteins via cell surface receptor binding. Further we identified tubulin beta chain (TBB5) and zinc transporter ZIP10 (S39AA) amongst the co-purified proteins (Fig. 3A). This either indicates that the identified co-purified proteins bind unspecifically to the Ni-column or bind non-covalently to ADAMTS16 and are therefore co-purified with the proteinase.

Moreover we had a closer look at the purified ADAMTS16-sh. We did not find any peptides belonging to the N-terminal propeptide indicating that the prodomain of purified recombinant ADAMTS16-sh is fully removed by furin prior to or after secretion and that the proteinase should therefore be fully active (Fig. 3B).

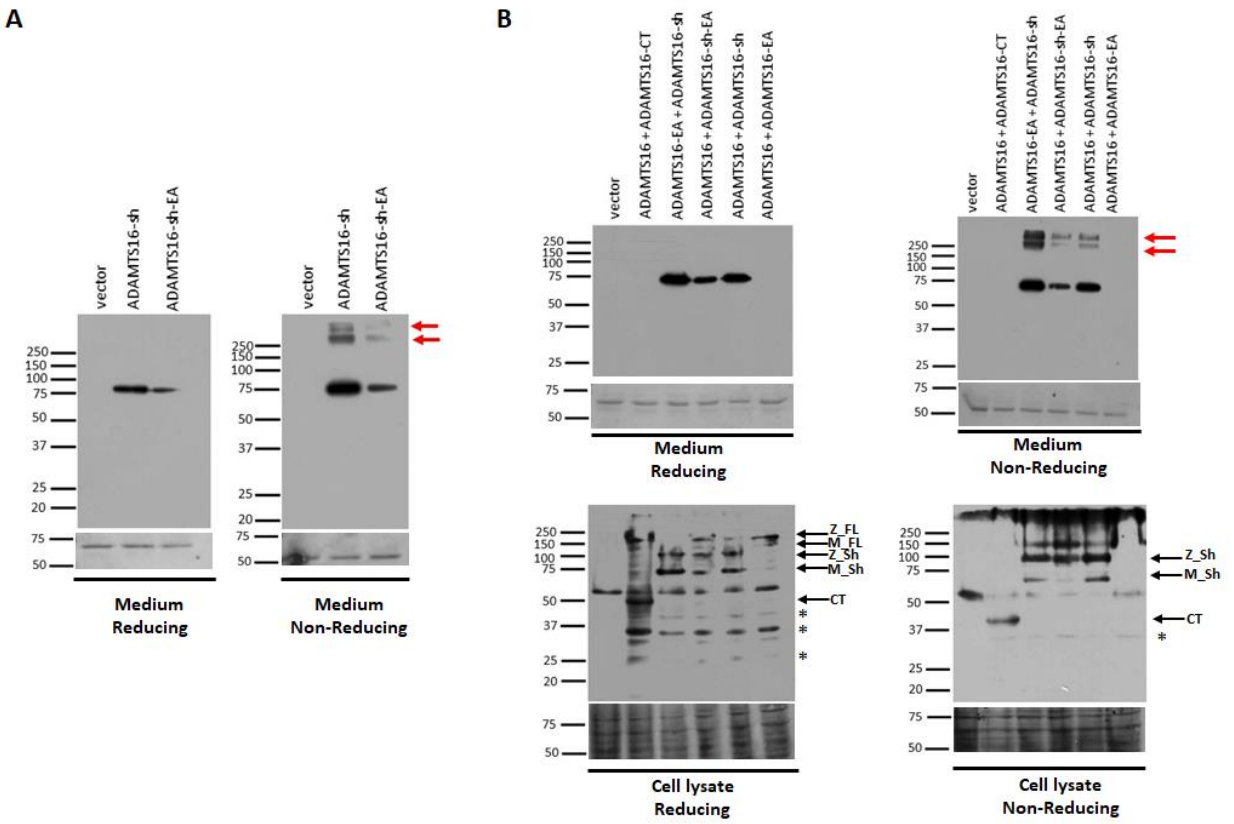

Figure 2: Western blot analysis of supernatant of transiently transfected HEK-EBNA cells showed oligomerization of ADAMTS16 **A.** The conditioned medium of transiently transfected cells with the C-terminally truncated ADAMTS16-sh and its inactive mutant (ADAMTS16-sh-EA) showed oligomerization of the catalytic domains of ADAMTS16 (red arrow). The ADAMTS16-sh-EA showed a lower overall amount of secreted protein and oligomerization. The conditioned medium was analyzed by western blot under reducing and non-reducing conditions. All constructs are C-terminally myc-tagged and an anti-myc antibody was used for detection of ADAMTS16. Amido-black staining of the membrane was used as loading control. **B.** The C-terminally truncated constructs ADAMTS16-sh and ADAMTS16-sh-EA were either co-transfected with wtADAMTS16 or its inactive mutant ADAMTS16-EA respectively. The cell lysate as well as the conditioned medium were analyzed by western blot under reducing and non-reducing conditions. The presence of the full length ADAMTS16 did not influence the ability of the truncated ADAMTS16-sh, or ADAMTS16-sh-EA to form oligomers (red arrow). The zymogen (Z) and mature (M) forms of wtADAMTS16 (FL) and the truncated ADAMTS16-sh (Sh) are indicated by black arrows. C-terminal processing is indicated by asterisks and the ADAMTS16 constructs just comprising of the C-terminal TSR1 and PLAC domain (ADAMTS16-CT) is indicated by a black arrow labelled CT.

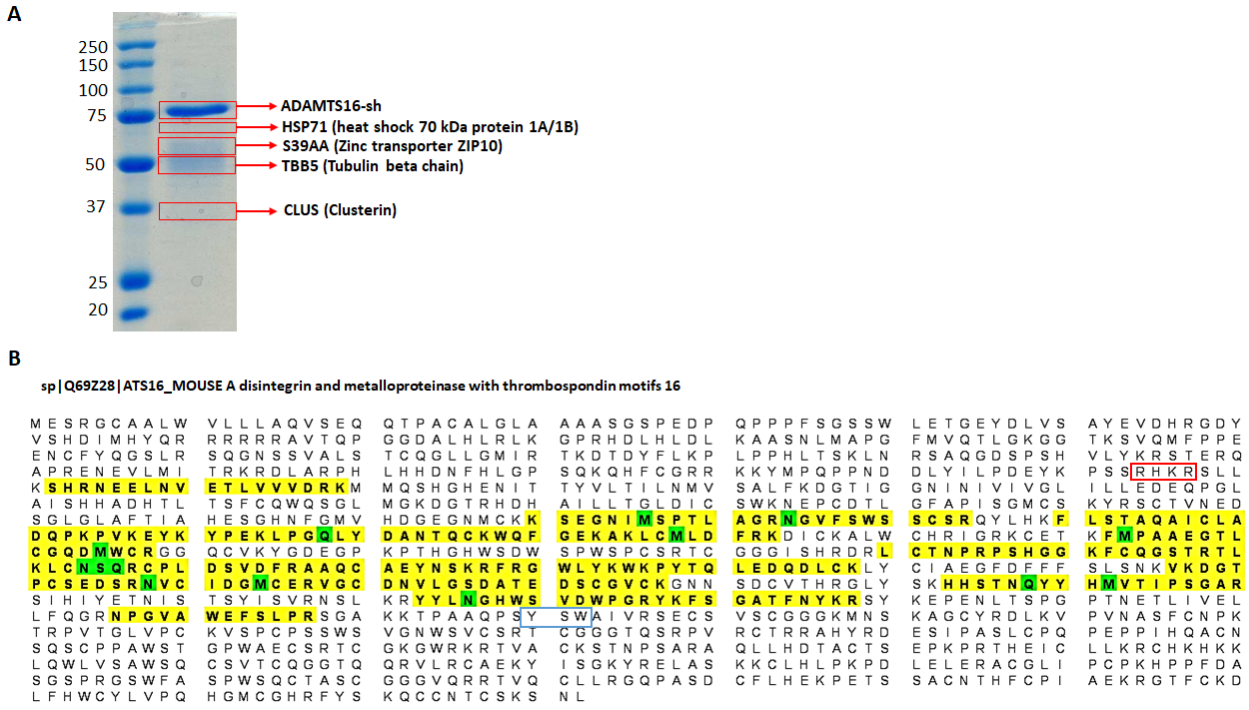

Figure 3: In gel digest and MS analysis of purified mouse ADAMTS16-sh by MS. **A.** 50 µl of the main protein elute of purified ADAMTS16-sh was separated by 10% SDS-Page. The visible bands were cut and an in gel digest was performed for protein identification by MS. Clusterin (CLUS), tubulin beta chain (TBB5), zinc transporter ZIP10 (S39AA) and heat shock 70 kDa protein (HSP71) were identified as being co-purified with ADAMTS16. The data was analyzed using Scaffold software **B.** The purified recombinant ADAMTS16-sh was analyzed by MS for peptide coverage. No peptides belonging to the prodomain were identified. The red box marks the furin cleavage site RHKR. The blue box indicates the last three amino acids of the truncated ADAMTS16-sh. The data was analyzed using Scaffold software.

5.2.2 Phage display for identification of ADAMTS16 substrates

In a first attempt we tried to identify substrates by phage display. For this we used a commercially available phage library (NEB Ph.D 7 phage display library), where each phage displays a 7 amino acid long peptide (Fig. 4). As target proteins, purified mouse ADAMTS16-sh and its inactive mutant ADAMTS16-sh-EA were used. The consensus sequence KVWXXPZ and XMMHHPH where X can be any amino acid and Z has to be either R, N or Q, could be identified in both targets independently from each other. A protein blast was performed using the consensus sequences to screen for potential binding partners. The search was restricted to extracellular and membrane proteins. Using those criteria, 10 potential binding partners and therefore potential substrates for ADAMTS16 could be identified (Table 1). Some proteins such as MMP14 were further analyzed for their ability to be a substrate of ADAMTS16. Additionally the identified binder FN was proven to be a substrate of ADAMTS16. Interestingly most glycoproteins and proteoglycans identified by phage display have the same overlapping consensus sequence WXXPZ. This could be a shared binding motif for ADAMTS16 and or other members of the ADAMTS family.

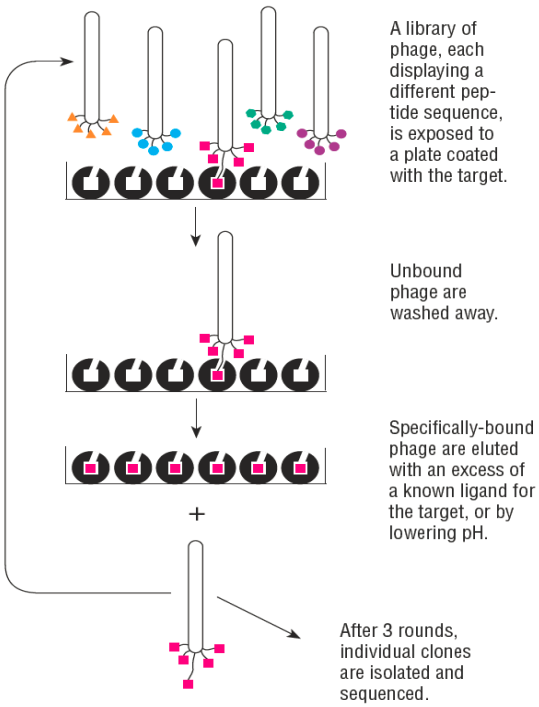

Figure 4: Schematic overview of the phage display workflow. Recombinant ADAMTS16-sh was used as target. After 3 rounds of panning 20 clones were send for sequencing.

Protein Name	Consensus Sequence	Matching Sequence	AA position
Jagged 1	KVWXXPZ	**KVW**CG**PR**	894-900
Usherin	KVWXXPZ	**VW**VT**PR**	3676-3681
MMP14	KVWXXPZ	**KVW**EGIPES**PR**	454-464
Laminin subunit alpha 5	KVWXXPZ	WGF**PN**	1481-1485
Tenascin	KVWXXPZ	WKG**PN**	180-184
Collagen alpha-1 (V)	KVWXXPZ	WVD**PN**	1655-1659
Fibronectin	KVWXXPZ	WTP**PR**	1016-1020
Aggrecan	KVWXXPZ	**W**EE**PR**	2098-2102
Neurocan	KVWXXPZ	WDR**PQ**	1216-1220
ADAMTS18	MMHHPHX	**HHPH**	197-200

Table 1: Identified binders of ADAMTS16-sh. A protein blast was performed with the identified consensus sequences. Only ECM proteins and the extracellular domains of membrane proteins were considered as potential binders. The overlapping amino acids (AA) in the potential binding partners are marked in bold.

5.2.3 ADAMTS16 potentially processes MMP14 and MMP3

To see whether MMP14 is a substrate of ADAMTS16, C-terminally HA-tagged MMP14 was co-expressed with various ADAMTS16 constructs in COS-7 cells. In addition to the anti-HA antibody recognizing the C-terminus of MMP14, we used an anti-MMP14 antibody specific to the N-terminal domains of MMP14. Alternatively, to see whether ADAMTS16 is processed by MMP14, we also analyzed the cell lysate and conditioned medium using an anti-myc antibody recognizing the tagged C-terminus of ADAMTS16. As control, COS-7 cells were either transfected with MMP14 alone or in combination with inactive ADAMTS16-EA. Although we could not see any cleavage products in the conditioned medium using anti-MMP14 antibody we found a profound reduction in the intensity of a protein band at approximately 50 kDa when analyzing the cell lysate for MMP14 cleavage products (Fig. 5A). Moreover we observed high molecular weight bands in the lysate of cells co-expressing MMP14 and the inactive ADAMTS16 mutants, using anti-HA antibody (Fig. 5B). Interestingly the possible degradation of MMP14 by ADAMTS16 seems to be independent of its C-terminus, because the same results were obtained by using ADAMTS16-sh instead of wtADAMTS16. Further we neither observed any bands in the cell lysate, nor in the conditioned medium of co-expressing cells, indicating degradation of ADAMTS16 by MMP14 when staining with anti-myc antibody (Fig. 5C). However, we observed the secretion of the inactive zymogen of ADAMTS16-sh and ADAMTS16-sh-EA into the conditioned medium. This observation is unique to COS-7 cells and did not occur using ADAMTS16-sh expressing HEK-EBNA cells. Additionally a faint band corresponding to the wtADAMTS16 zymogen could be observed in the conditioned medium. Again secretion of full length ADAMTS16 could not be observed using HEK-EBNA cells (Fig. 5C). However, the secretion of the ADAMTS16 zymogen does not seem to correlate with the expression of MMP14, but seems to be COS-7 cell specific.

Due to the fact that MMP14 directly activates MMP2, measuring the activity of MMP2 via gelatin zymography gives valuable information about the activity of MMP14. Because COS-7 cells do not express endogenous MMP14 [232] we used HEK-EBNA cells and MDCKI cells stably transfected with various ADAMTS16 constructs to perform a gelatin zymography. However, we could not detect any changes in MMP2 activity neither in HEK-EBNA cells nor in MDCKI cells (Fig. 6). Therefore, we conclude that ADAMTS16 does not have a direct influence on MMP14 activity, or the effects are too small to be detected by zymography. Additionally, no changes in MMP9 activity could be observed in HEK-EBNA cells expressing wtADAMTS16 compared to vector control.

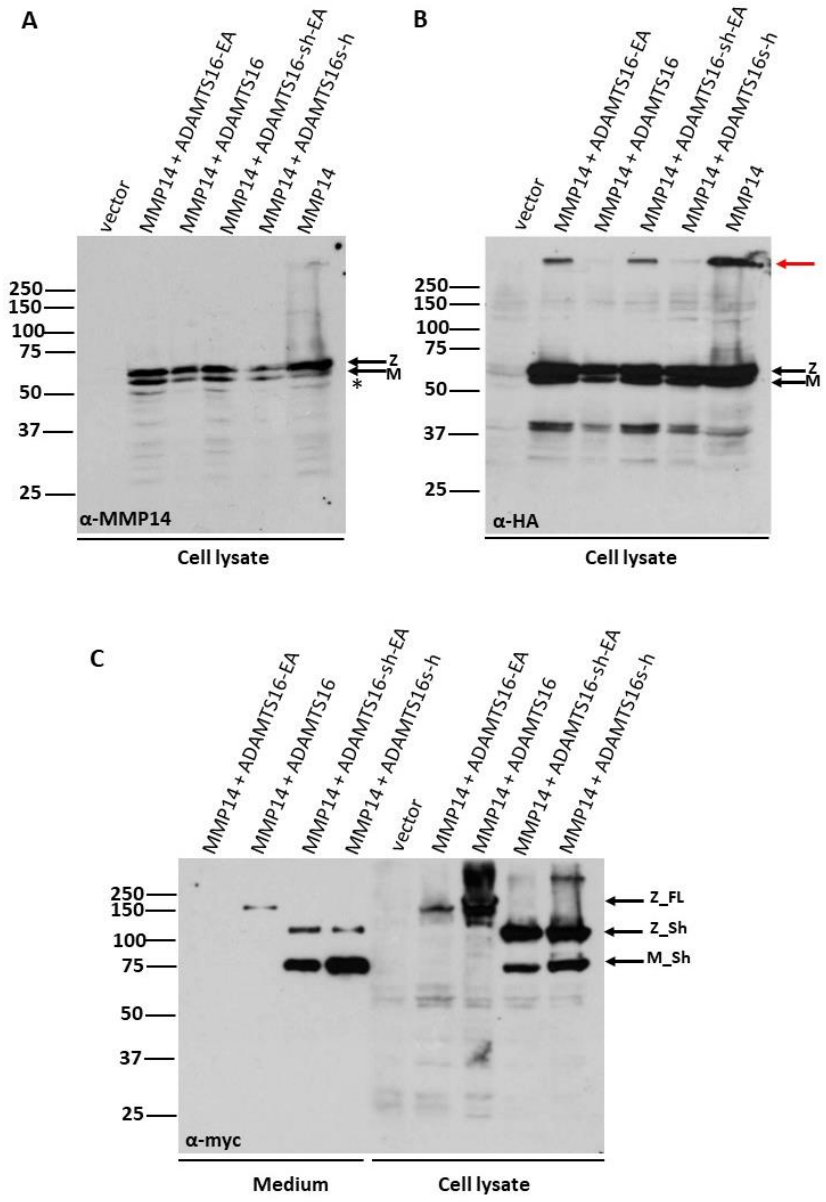

Figure 5: Cell lysate of COS-7 cells co-expressing MMP14 with wtADAMTS16 or ADAMTS16-sh and their corresponding active site mutants analyzed by western blot shows potential cleavage of MMP14 by ADAMTS16. **A.** Cell lysate was analyzed for N-terminal MMP14 cleavage products using an anti-MMP14 antibody against the N-terminus of MMP14. The black arrows indicate the zymogen (Z) and the mature (M) form of MMP14. The asterisk indicates a potential degradation of MMP14 by wtADAMTS16 and ADAMTS16-sh. **B.** Cell lysate was analyzed for C-terminal MMP14 cleavage products using an anti-HA antibody against the C-terminus of MMP14. The black arrows indicate the zymogen (Z) and the mature (M) form of MMP14. Red arrow indicates a high molecular weight band observed only if MMP14 is expressed alone or in combination with the inactive mutants ADAMTS16-EA and ADAMTS16-sh-EA. **C.** Western blot analysis of conditioned medium and cell lysate for C-terminal ADAMTS16 cleavage products. The black arrows indicate the zymogen of wtADAMTS16 and its corresponding mutant ADAMTS16-EA (Z_FL) and the zymogen of the truncated ADAMTS16-sh and its inactive mutant (Z_Sh) as well as the mature form of ADAMTS16-sh (M_Sh).

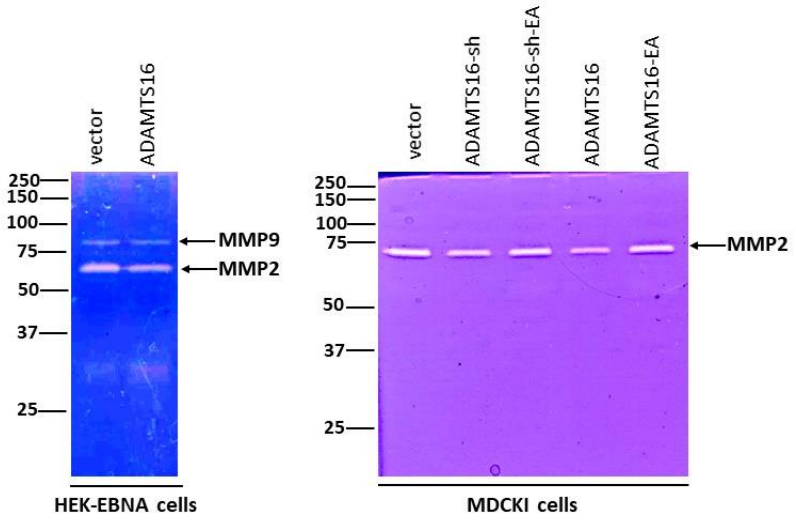

Figure 6: Gelatin zymogram of HEK-EBNA cells and the epithelial cell line MDCKI stably expressing various ADAMTS16 constructs. The black arrows indicate the bands corresponding to MMP2 and MMP9 respectively. The cells were incubated for 48 h under serum free conditions, the conditioned medium was concentrated and 10 µg overall protein was loaded on the gel.

Because we previously showed that N-terminal FN cleavage and the so released 30 kDa N-terminal heparin binding domain of FN can increase *MMP3* expression in MDCKI cells and because of indications of MMP14 processing by ADAMTS16, we aimed to see whether ADAMTS16 can influence MMP3 activity on a protein level in addition to increased expression. Therefore we co-expressed ADAMTS16 with MMP3 in HEK-EBNA cells and analyzed the conditioned medium for potential MMP3 cleavage. However, it was not possible to see any cleavage products of MMP3 by western blot, neither under reducing nor under non-reducing conditions. Interestingly we could however, observe a reduction of MMP3 protein levels in the conditioned medium of cells co-expressing MMP3 with wtADAMTS16 (Fig. 7A). To further investigate whether ADAMTS16 is processing MMP3, we incubated purified ADAMTS16-sh with conditioned medium of MMP3 expressing HEK-EBNA cells in the presence or absence of EDTA. Although we observed a second MMP3 band in the sample incubated with active ADAMTS16-sh it remains unclear whether this is really a cleavage product of MMP3 (Fig. 7B). As a last attempt to investigate whether ADAMTS16 influences enzyme activity of MMP3 we performed a casein zymogram using MDCKI cells stably expressing ADAMTS16. We could see an increase in MMP3 protein levels in the conditioned medium of wtADAMTS16 expressing cells. Moreover we observed an increase in pro-MMP3 in the conditioned medium of cells expressing the inactive mutant ADAMTS16-EA. This indicates that ADAMTS16-EA binds to MMP3 but does

not enzymatically process it. Additionally ADAMTS16-EA binding may prevent MMP3 from being processed by other proteinases (Fig. 7C).

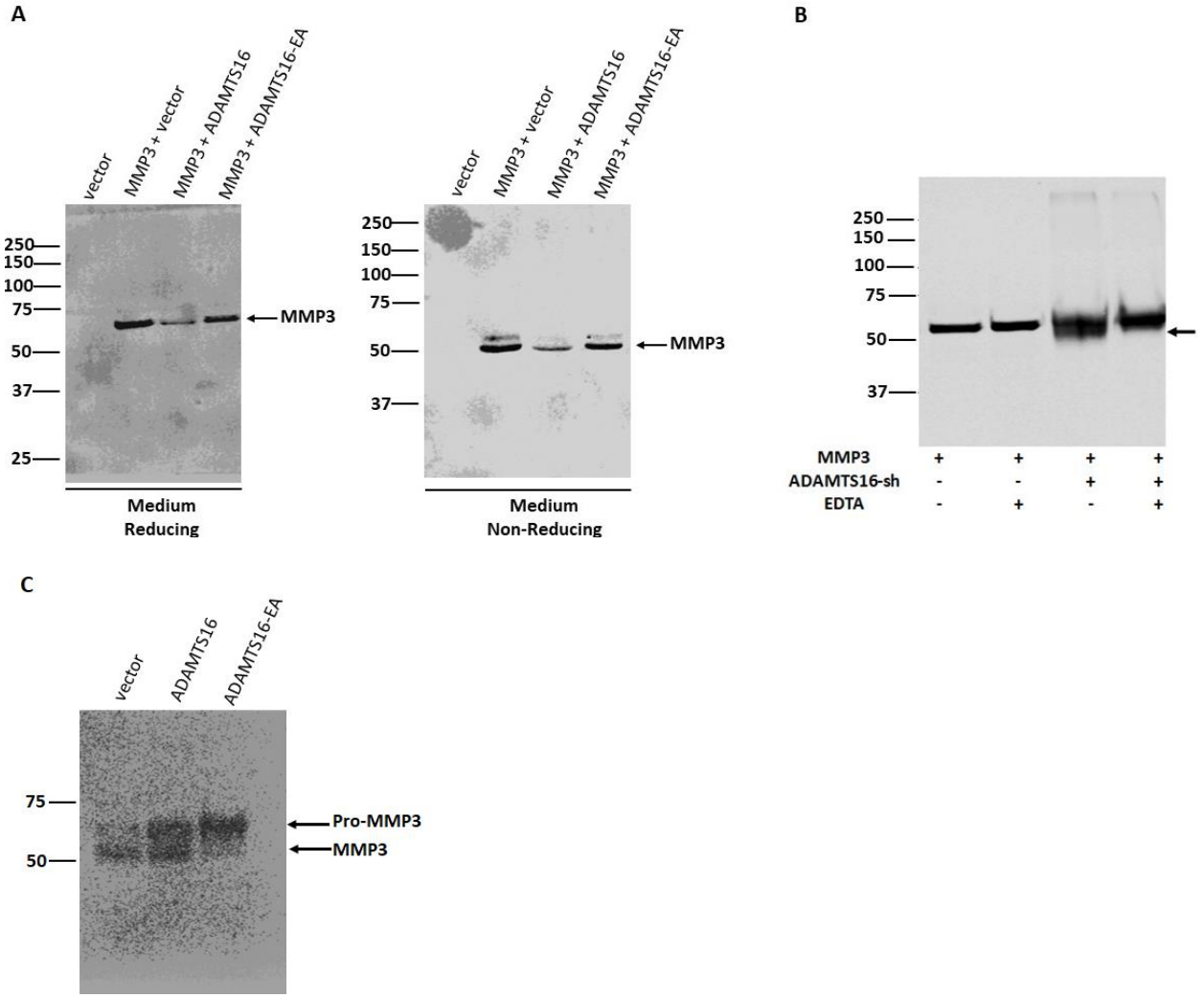

Figure 7: Western blot analysis and casein zymogram showed that ADAMTS16 is processing and influencing the activity of MMP3. **A.** Conditioned medium of HEK-EBNA cells co-transfected with MMP3 and ADAMTS16 was analyzed by western blot under reducing and non-reducing conditions. The blot was probed with anti-MMP3 antibody to stain for MMP3 cleavage products. Strong reduction of MMP3 levels were observed in conditioned medium of cells co-expressing MMP3 with wtADAMTS16 (black arrow). **B.** Incubation of purified recombinant ADAMTS16-sh with conditioned medium of MMP3 expressing cells in presence or absence of EDTA. A second MMP3 band could be observed in conditioned medium in presence of active ADAMTS16-sh (black arrow). **C.** Casein zymogram using conditioned medium of MDCKI cells stably expressing ADAMTS16 showed increase in MMP3 levels in cells expressing wtADATMS16. Additionally increase in pro-MMP3 could be observed in the medium of cells expressing ADAMTS16-EA. The cells were maintained under serum free conditions for 48 h, the medium was concentrated and 5 µg of protein was loaded on the gel.

5.2.4 ADAMTS16 is expressed in various cancer cell lines and during development

Various cancer cell lines were tested for endogenous *ADAMTS16* expression by RT-PCR. Not surprisingly *ADAMTS16* was not expressed in the non-tumorigenic HEK-EBNA cells. As already published *ADAMTS16* is endogenously expressed in human brain tissue [215], therefore we also analyzed mRNA from human brain tissue and found relatively strong expression of *ADAMTS16*. Compared to the relative *ADAMTS16* mRNA expression in human brain tissue the glioblastoma cell lines U343 and LN229 showed increased expression, where most other brain tumor cell lines showed reduced *ADAMTS16* expression. Additionally various other cancer cell lines of different origin showed endogenous expression of *ADAMTS16* (Fig.8).

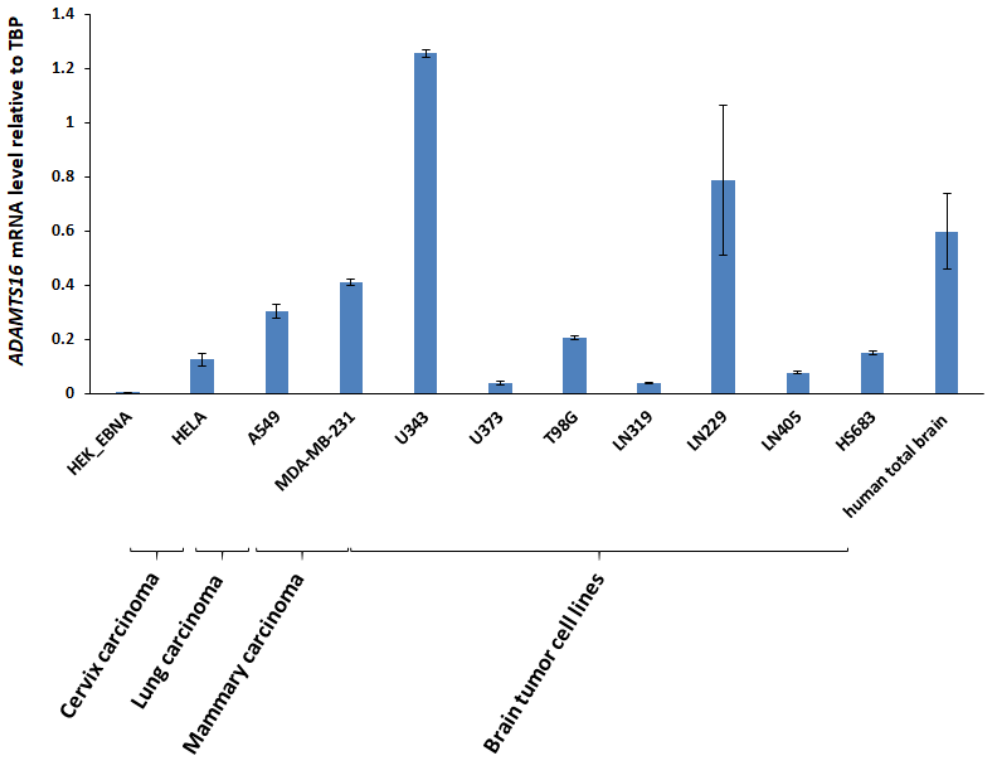

Figure 8: RT-PCR analysis of various cancer cell lines for endogenous *ADAMTS16* mRNA expression. The data was normalized to the housekeeping gene *TBP*. Additionally the endogenous *ADAMTS16* mRNA levels of the non-tumorigenic HEK-EBNA cell line and of total human brain tissue was analyzed in addition to the cancer cell lines. Each bar represents the mean ± S.E.M from technical replicas.

In addition to cancer cell lines we analyzed the expression of *Adamts16* during development by in situ hybridization. Therefore we analyzed the tissue of 16.5 day (E16.5) old mouse embryos. We found *Adamts16* expression in the glomeruli and the tubular epithelial cells of the kidney, around the larger blood vessels of the liver, in the epithelial cells of the pancreas and the testis, in brain tissue, in the cells of the peritoneum and in stromal cells within the connective tissue around the intestine and colon. Further we found *Adamts16* to be expressed during cranio facial development, most likely within structures further developing into teeth. We also found *Adamts16* expression within the developing limbs, however, we could not clearly elucidate by the images whether *Adamts16* is expressed by cells of the tendons, or nerve cells. To determine more precisely which cell linage exactly expresses *Adamts16* would require further investigations (Fig. 9).

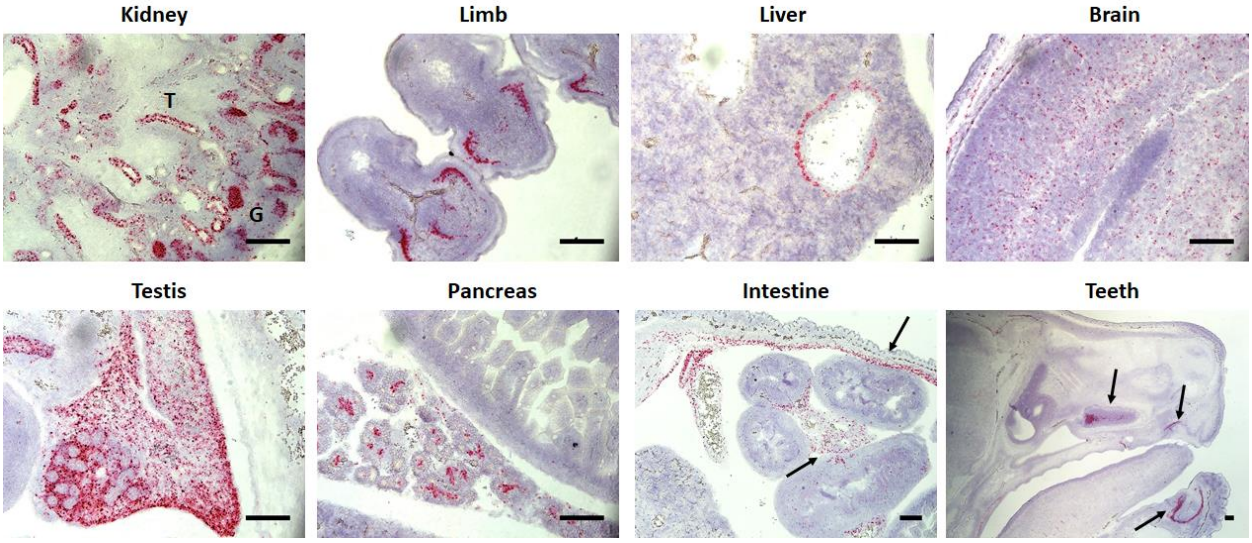

Figure 9: In situ hybridization of embryonal tissue at time point E16.5 shows strong expression of *Adamts16* mRNA (red) within the kidney glomeruli (G) and tubular epithelial cells (T). Further *Adamts16* expression was observed in the limbs, around the large blood vessels of the liver, the testis and the pancreas. Additionally we found expression of *Adamts16* within the peritoneum and by stromal cells within the connective tissue around the intestine and colon (black arrows). *Adamts16* is further expressed by structures most likely developing into teeth (black arrows). Scale bars 100 µm.

Because previous studies showed a possible involvement of ADAMTS16 during kidney development and branching [219, 221] we had a closer look at *Adamts16* expression in the kidney at different stages of development. We found that *Adamts16* is already expressed at E10.5, which is an early stage of kidney development, where the kidney can be seen as an S shaped body. *Adamts16* expression remains constantly high during embryogenesis until birth (Fig. 10A). We also analyzed postnatal kidney tissue of mice. We could observe a very strong *Adamts16* expression directly after birth within the glomeruli and

the renal tubular epithelial cells, similar to the kidney at time point E16.5. When the mice reach the age of 10 days the expression of *Adamts16* is still very high. However, the expression is reduced when the mice reach adulthood. After 4 and 8 weeks the expression is already relatively low and strongly localized within and in close proximity to the cells of the glomeruli (Fig. 10B). *Adamts16* expression therefore strongly decreases upon aging. This indicates that ADAMTS16 may play a major role during kidney development and is required for tissue remodeling during organ development and growth, but most likely does not have a major function in tissue maintenance in adult kidneys.

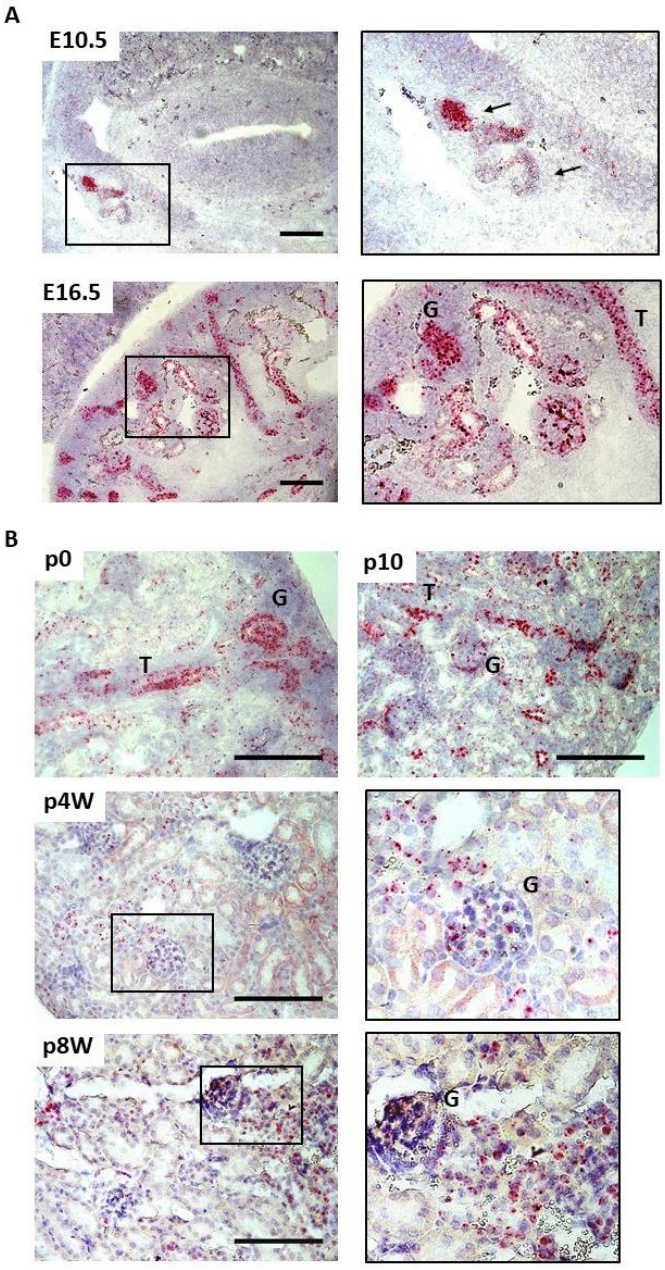

Figure 10: In situ hybridization for *Adamts16* expression during kidney development and maturation. **A.** Tissues of mouse embryos at time point E10.5 and E16.5 were analyzed for *Adamts16* mRNA expression (red). At time point E10.5 *Adamts16* expression can be seen in the S-shaped body of the developing kidney (black arrows). At time point E16.5 *Adamts16* is expressed in the glomeruli (G) and the renal tubular epithelial cells (T). Scale bars 100 µm. The boxed areas are 2X magnifications of the left picture. **B.** Tissue of new born and adult mice was analyzed for *Adamts16* mRNA expression (red). After birth (p0) and at the age of 10 days (p10) high *Adamts16* expression can be observed in the kidney tissue, especially in cell of the glomeruli (G) and the tubular epithelial cell (T). After 4 and 8 weeks the expression is very low and can only be seen within the glomeruli (G) and in cells close to it. Scale bars 100 µm. The boxed areas are 2X magnifications of the left image.

5.2.5 ADAMTS16 affects cell migration and proliferation

To analyze the influence of ADAMTS16 on cell migration and proliferation we used a variety of different cell types either stably or transiently expressing ADAMTS16. In the first assay, we coated glass chamber slides with FN and seeded HEK-EBNA cells stably expressing wtADAMTS16, ADAMTS16-EA or vector only on top of the FN. After 24 h the cells were fixed and the actin skeleton was stained with phalloidin. Cells expressing wtADAMTS16 have markedly reduced amounts of filopodia compared to cells either expressing the inactive ADAMTS16-EA or vector only (Fig. 11A). Additionally, we used a Boyden chamber assay to evaluate the migration potential of ADAMTS16 expressing cells. For this we let the cells migrate towards 10% FCS on either untreated filters, or on filters where the lower filter side was FN coated. HEK-EBNA cells showed no migration on untreated filters. However, HEK-EBNA cells stably expressing wtADAMTS16 showed a very strong migration on filters where the lower side was coated with FN. Cells expressing the truncated ADAMTS16-sh also showed increased migration, however, less strong than the wtADAMTS16 cells. Nevertheless, cells expressing the inactive full length ADAMTS16-EA showed a similar migration rate than cells expressing ADAMTS16-sh, indicating a contribution of the C-terminus of ADAMTS16 to cell migration in HEK-EBNA cells. In addition to HEK cells we also analyzed MDCKI cells stably expressing ADAMTS16 for their migration behavior on untreated and FN coated filters. MDCKI cells showed a stronger overall migration compared to HEK-EBNA cells towards FCS. However, no differences could be observed between untreated und FN coated filters with respect to MDCKI cell migration. Under both conditions a stronger migration of wtADAMTS16 and ADAMTS16-sh expressing cells could be observed, although the differences were not as dramatic as in HEK cells. Additionally the cells expressing inactive ADAMTS16-EA did not show an increased migratory behavior, as is the case for HEK cells (Fig. 11B). In addition to cell migration we had a look at cell proliferation of ADAMTS16 expressing cells. For this we used the glioblastoma cell line LN229 and the epithelial MDCKI cells. LN229 cells transiently expressing wtADAMTS16 showed a massively reduced proliferation after 7 days in culture. However, no difference in cell proliferation could be observed for ADAMTS16 expressing MDCKI cells (Fig. 11C). These findings indicate that the effects of ADAMTS16 expression on cell proliferation and migration strongly depend on the cell type and not only on the ADAMTS16 expression itself.

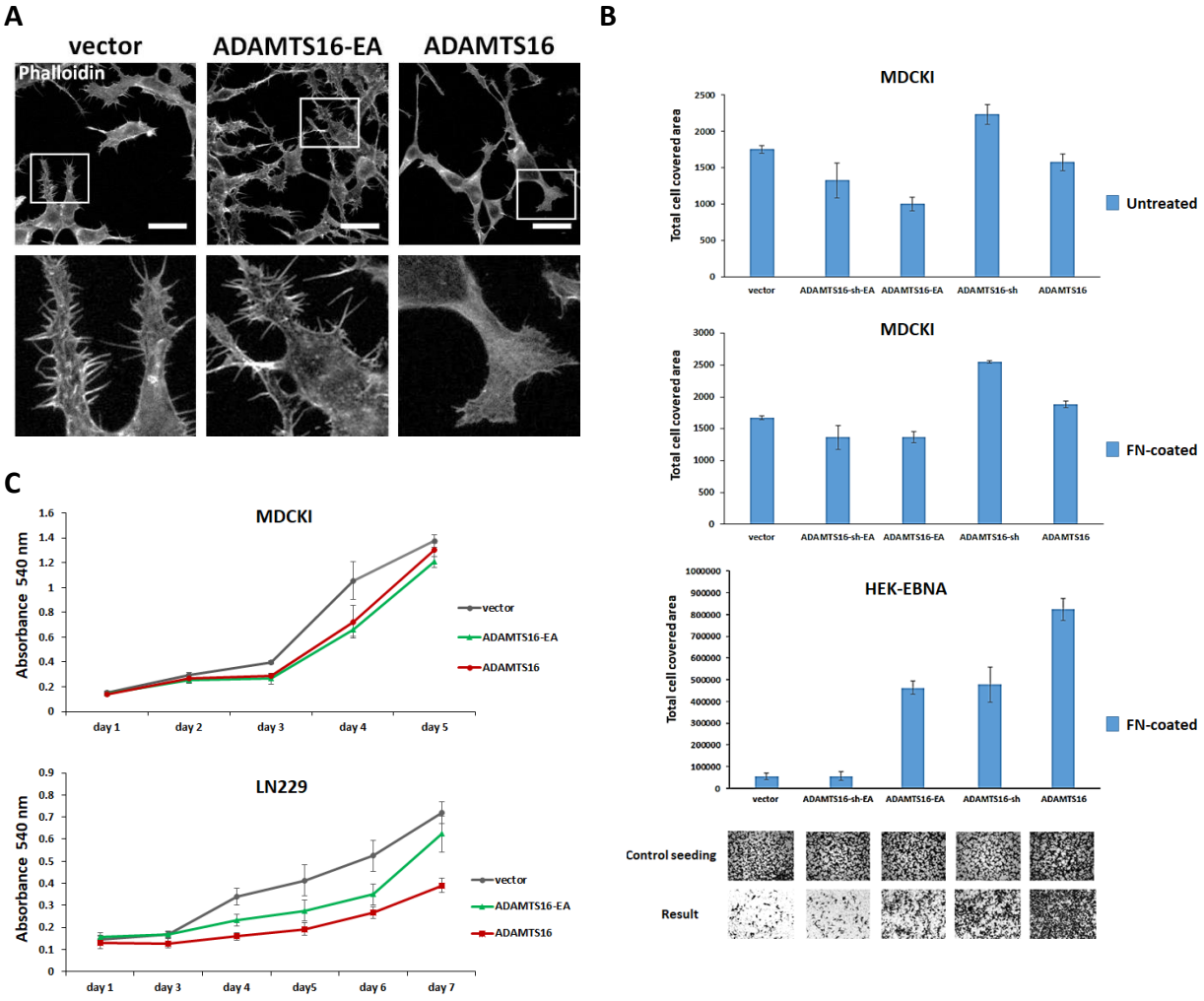

Figure 11: MDCKI, HEK-EBNA and LN229 cells overexpressing wtADAMTS16 and ADAMTS16-sh showed distinct proliferation rates and migration behaviors. **A.** HEK-EBNA cells stably expressing wtADAMTS16, ADAMTS16-EA and vector control were seeded on FN coated glass chamber slides. The actin cytoskeleton was stained with phalloidin. Large amounts of long filopodia in vector control and cells expressing the inactive ADAMTS16-EA could be observed, where cells expressing wtADAMTS16 showed reduced filopodia formation. Scale bar 50 µm. Boxed areas are 4X magnifications of the upper pictures. **B.** MDCKI and HEK-EBNA cell were allowed to migration towards 10% FCS for 24 h. The lower filter side was either left untreated or coated with 100 µg/ml FN. Migration was quantified measuring the cell covered area of the lower filter side. Stronger overall migration of MDCKI cells expressing wtADAMTS16 and ADAMTS16-sh was observed. Additionally strong migration of HEK-EBNA cells expressing wtADAMTS16 and ADAMTS16-sh on FN coated filters could be observed. Each bar represents the mean area ± S.E.M from technical replicates. Representative photos of fixed and stained cells that have migrated to the lower side of the filter are shown below the bar graph. **C.** Stably expressing MDCKI cells or transiently transfected LN229 cells were seeded into 96 well chambers and cell proliferation was assessed by using a MTT cell proliferation assay. Strong reduction in cell proliferation in wtADAMTS16 expressing cells after 7 days in culture could be observed. Each bar represents the mean area ± S.E.M from technical triplicates.

6. Discussion and Future Directions

ADAMTS16 is an orphan member of the ADAMTS family. Although its physiological role during development and diseases has been addressed in a variety of different studies, its substrates and underlying mechanism of action remained so far unknown.

Therefore we aimed to characterize ADAMTS16, identify possible substrates and its mechanism of action. In the present work we discovered that ADAMTS16 cleaves FN and that the released 30 kDa N-terminal heparin binding domain of FN can increase *MMP3* expression in MDCKI cells. Moreover we observed strong C-terminal processing of ADAMTS16 in vitro. Analyzing the cell-free ECM of HEK-EBNA cells stably expressing ADAMTS16 showed that ADAMTS16 is, at least to some extent, secreted and processed extracellularly with the C-terminus remaining bound to the ECM. However, we could not conclusively assess whether ADAMTS16 is exclusively C-terminally truncated extracellularly, or if it is also processed intracellularly within the secretory pathway. Treatment with protease inhibitors showed an accumulation of full length ADAMTS16 in the *trans*-Golgi network. Moreover in the absence of protease inhibitors ADAMTS16 is barely detectable within the cell lysate. This findings indicate that ADAMTS16 is very efficiently C-terminally truncated directly after translation. Additionally we showed that ADAMTS16 has autocatalytic abilities and is able to C-terminally truncate itself. Because we observed C-terminal fragments in the cell lysate of cells expressing inactive ADAMTS16-EA, we have strong proof that at least one other proteinase is involved in the C-terminal processing of ADAMTS16. Nevertheless, we were neither able to identify the responsible proteinase nor the exact cleavage site. This would require further investigations. Further we observed differences in C-terminal processing between different cell lines. We could not detect any full length ADAMTS16 in the medium of LN229 cells, MDCKI cells or HEK-EBNA cells. However we detected very low amounts of full length ADAMTS16 in conditioned medium of COS-7 cells. Interestingly the band size corresponded rather to the zymogen form of ADAMTS16 and not the furin-processed mature form of ADAMTS16. This observation, which seems to be very cell type specific, in this case COS-7 cells, might have several reasons. Due to the fact that we only observed the zymogen form in the medium but not the mature form of ADAMTS16, might mean that furin activation is not as efficient as it is in other cell lines and, as a consequence, ADAMTS16 lacks activity and can no longer effectively C-terminally process itself. Another explanation could be the absence of the proteinase responsible for C-terminal truncation of ADAMTS16 in COS-7 cells. This theory is plausible because ADAMTS4 has been shown to be C-terminally processed by MMP17 [171] and it is therefore likely that either MMP17 or another membrane bound MMP also processes ADAMTS16. It is possible that COS-7 cells do not express the

proteinase responsible for C-terminal ADAMTS16 processing. Due to the fact that co-expression of ADAMTS16 and MMP14 in COS-7 cells did not lead to an increase in C-terminal truncation of ADAMTS16, as observed by western blot analysis, we can conclude that at least MMP14 is not responsible for ADAMTS16 processing. Additionally the binding partner for ADAMTS16 on the cell surface or within the ECM could be missing in COS-7 cells so that ADAMTS16 is secreted, but cannot bind in close proximity to the cell surface and is therefore not efficiently C-terminally processed.

Our first attempt to find substrates for ADAMTS16 was by phage display. Therefore we used a commercially available phage library. The variety of potential substrates was rather limited and also the overall coverage of the consensus sequence with the target sequence of the potential ADAMTS16 binders was rather low. A reason for this can be that the peptides presented by the phages are only 7 amino acids long and do not contain any secondary structural elements. This can of course decrease the chance of finding any potential substrates, because substrate binding may require certain structural elements such as helixes and more than 7 amino acids in length. It is worth mentioning that especially the extracellular proteoglycans and glycoproteins identified in the phage display as potential binders share the same overlapping sequence with the consensus sequence. A lot of ECM glycoproteins and proteoglycans share common structural features, which allow them to interact with each other or bind to cell surface receptors. Thus it could be a coincidence that these binders were found in the screen and they might not be real substrates or binders of ADAMTS16. This is further supported by the fact that only 3 amino acids of the overall consensus sequence do overlap with the target sequence. On the other hand, we found ADAMTS16 to be co-localized with laminin and FN within the ECM. Additionally we even identified FN as a substrate of ADAMTS16. It is therefore possible that ADAMTS16 binds to FN and laminin via the identified target sequence. Additionally previous work showed that a truncated version of ADAMTS16 only containing its protease domains, can bind and cleave aggrecan in vitro [154]. Also neurocan is a likely target of ADAMTS16 because of its strong localization within the brain matrix, similar to ADAMTS16. Summarizing those findings, ADAMTS16 was shown to bind at least three of the glycoproteins and proteoglycans identified in the phage display screen and it is therefore possible that these proteins share this common structural feature to bind ADAMTS16 and or other members of the ADAMTS family.

We decided to analyze MMP14 further since it showed strong coverage with the consensus sequence identified and literature indicates that it is often expressed during processes also involving ADAMTS16, such as osteoarthritis (OA), esophageal squamous cell carcinoma and during kidney and testis development [221, 222, 227, 228, 233-235]. By analyzing the cell lysate of co-expressing cells, using an antibody

against the N-terminus of MMP14, the reduction of a lower molecular size band could be observed. However, no real reduction in full length MMP14 was observed. Additionally we observed a high molecular size band when analyzing the cell lysate with an antibody against the C-terminal HA-tag of MMP14 in combination with inactive ADAMTS16-EA and ADAMTS16-EA-sh. Because we could not observe the same effect using an antibody against ADAMTS16, we can conclude that it is not a complex of ADAMTS16-EA and MMP14. Especially because the band is also observed when MMP14 is expressed alone. It is however, likely that MMP14 forms a complex with another protein and upon cleavage by ADAMTS16 this complex formation is no longer possible. It would require further investigations, mainly using mass spectrometry, to decide whether it is a MMP14-protein complex, or an oligomerization of MMP14 alone. Analysis of MMP14 activity did not show any changes in the presence or absence of ADAMTS16. This indicates that cleavage of MMP14 by ADAMTS16 has no influence on its activity. Another reason for this observation might be that ADAMTS16 can indeed activate MMP14 but due to the fact that MMP14 is also activated by other proprotein convertases such as furin, MMP14 is already efficiently activated in the used cell systems and the presence of ADAMTS16 does not add to this process in a closed cellular in vitro system. However, studies on MMP14 activity showed that the kidneys of MMP14 null mice had increased deposition of collagen IV, laminin, perlecan, and nidogen and this phenotype was independent of MMP14 mediated MMP2 activation [233].

Activation of proteinases in vivo is usually much more complex compared to a single cell in vitro system. Although the processing of the propetide is one of the key steps in regulating proteinase activity, C-terminal processing can also severely influence protease activity. Moreover, it strongly affects the specificity of a proteinase towards its substrates, as observed in a variety of ADAMTS family members. Therefore it is likely that MMP14 processing by ADAMTS16 still influences the activity and or substrate specificity of MMP14 without affecting MMP2 activity.

We also investigated whether ADAMTS16 can influence MMP3 activity directly and not only upregulate its expression. Unlike MMP14 which is a transmembrane proteinase, MMP3 is fully secreted. Therefore we analyzed the conditioned medium of HEK-EBNA cells co-expressing MMP3 and ADAMTS16. In the presence of active ADAMTS16 a reduction in the band corresponding to MMP3 is visible. However, no cleavage products were identified. A possible explanation for this is that the cleavage products are too small or their concentration is too low to be detected. Another explanation could be that MMP3 is activated and binds to the ECM, which leads to a clearance of soluble MMP3 from the conditioned medium. It would be necessary to analyze the cell free ECM of those cells to see whether there is an accumulation of MMP3 in the ECM of cells co-expressing MMP3 with active ADAMTS16. It is also likely

that the expression level of MMP3 in the presence of active ADAMTS16 is simply lower, because the cells are forced to overexpress two fully active proteinases.

In a further attempt, purified ADAMTS16-sh was incubated with the conditioned medium containing MMP3. Although we observed a second band in the presence of active ADAMTS16-sh the bands were not clearly separated, but appeared as smeared double bands. This effect could also be observed in the presence of the metalloproteinase inhibitor EDTA. However, this effect is not correlated to the presence of EDTA but to ADAMTS16-sh. Because the experiment was repeated several times, yielding the same result, a technical mistake is unlikely. Nevertheless there is a possibility that EDTA does not completely inhibit ADAMTS16-sh and that even in its presence, there is a slight degradation of MMP3.

We further analyzed the concentrated medium of MDCKI cells stably expressing ADAMTS16 for MMP3 activity by casein zymography. Casein zymography, although extensively used in various publications, is not the ideal way to determine MMP3 activity. We found that in the presence of active ADAMTS16 the overall amount of MMP3 is increased. This is not surprising because analysis of the mRNA in this cells showed an increase in *MMP3* expression in the presence of active ADAMTS16. However, we observed an accumulation of inactive MMP3 in the conditioned medium of cells expressing inactive ADAMTS16-EA. ADAMTS16-EA most likely binds to MMP3 but is not capable to further process it. Moreover, due to its binding, ADAMTS16-EA prevents MMP3 from being processed by other proteinases as well. Thus keeping it in its zymogen form.

Because ADAMTS16 was already described to have a role in various diseases and during development, we analyzed a variety of cancer cell lines as well as embryonal tissue for *ADAMTS16* expression. We found *ADAMTS16* to be expressed in various cancer cell lines. It has to be noted that we analyzed cultured cell lines and no standard control could be used in this work. Therefore one cannot conclude whether the expression of *ADAMTS16* is abnormal in those cell lines. We also analyzed the RNA of total human brain cell extract. There we found relative high levels of endogenous *ADAMTS16* expression, which is not surprising because previous studies already reported endogenous *ADAMTS16* expression in human adult brain [236]. However, also this is not an ideal base level to access whether the expression levels of *ADAMTS16* in the investigated brain tumor cell lines are down respectively upregulated. For this it would be necessary to figure out the exact cell types of the brain that are expressing *ADAMTS16*. To gain a better understanding whether *ADAMTS16* is upregulated during tumor progression a bigger collection of samples would be needed and these would need to be compared to healthy tissue.

We further analyzed the expression of *ADAMTS16* during development. Because previous publications reported a correlation of ADAMTS16 and kidney development and branching [219, 220] we had a closer look at *Adamts16* expression in mouse embryonal as well as adult kidney tissue. We observed that *Adamts16* expression starts at very early developmental time points (E10.5) and remains high until birth. Although the expression of *Adamts16* remains high shortly after birth and during the adolescence of the mice, expression levels of *Adamts16* are massively reduced in adult tissue of fully grown mice. This suggests that ADAMTS16 is required during organ development and might participates in ECM remodeling during organ growth. However, after the organ is fully grown the expression of *Adamts16* is significantly reduced and strongly localized around and within cells of the glomeruli, where it is most likely involved in the maintenance of its basement membrane.

To gain further insight into the cellular function of ADAMTS16 and its potential effects on cell behavior, we performed a couple of functional assays, such as cell proliferation and migration assays and also had a closer look at filopodia formation in ADAMTS16 expressing cells. Filopodia are actin-rich plasma membrane protrusions that allow cells to probe their environment. Therefore filopodia have an important role in cell migration, wound healing and neurite outgrowth. Additionally filopodia are involved in cell adhesion to the ECM [237]. The ECM plays a major role during filopodia development mainly via the activation of small GTPases of the Rho superfamily [238]. Studies showed that cell signaling via the ECM can activate CDC42, which subsequently leads to increased filopodia formation [239]. Interestingly integrins accumulate in filopodia. Via the integrin receptors, filopodia can probe the matrix along the leading edge that promotes cell adhesion and migration [237]. During cell spreading, integrin-containing filopodia form the initial adhesion sites. Subsequently other focal adhesion complex proteins, such as talin, paxillin and FAK, are recruited to these sites to form mature focal adhesions [240]. This is interesting because ADAMTS16 was shown in our studies to degrade FN and therefore most likely subsequently prevents FN-integrin binding and filopodia development. In the presence of active ADAMTS16 the surrounding FN is digested, something that potentially influences filopodia formation. In the absence of FN, integrin mediated filopodia-FN interactions can no longer occur and the formation of mature focal adhesions might be inhibited. Indeed we observed a reduction of filopodia formation in HEK-EBNA cells expressing wtADAMTS16 when seeded on a FN coated surface. Cells expressing inactive ADAMTS16-EA, however, showed strong filopodia development when seeded on a FN coated surface. Because FN-integrin interactions and consequently filopodia formation are the first steps in the development of mature focal

adhesion, it would be necessary to further investigate the effect of ADAMTS16 on focal adhesions and subsequently on the regulation of FAK and Rho mediated pathways.

The expression of proteinases especially members of the MMP family often lead to an increased migratory behavior of cancer cells, but also of epithelial cells during development. Additionally a variety of ADAMTS family members have been associated with an increased migratory behavior during development and disease [241, 242]. Therefore we aimed at testing whether ADAMTS16 expression can increase cell migration. Thus we used HEK-EBNA cells and the epithelial cell line MDCKI. MDCKI cells stably expressing active ADAMTS16 and ADAMTS16-sh showed stronger migration compared to cells expressing vector or inactive mutant controls. However, on untreated filters HEK-EBNA cells did not show any migration at all. Several publications stated that coating the underside or both sides of the Boyden chamber filter membrane with FN can facilitate and increase cell migration in a variety of cell types [243]. Therefore the lower filter side of the Boyden chamber was coated with FN and the migration of MDCKI and HEK-EBNA cells stably expressing ADAMTS16 was analyzed again. The epithelial cell line MDCKI showed no significant differences between the migration on coated and untreated filters could be observed. However, HEK-EBNA cells migrated significantly more on FN coated filters. Moreover, cells expressing wtADAMTS16 showed a massively increased migration. Interestingly, also cells expressing the inactive full length mutant ADAMTS16-EA showed an increased migration compared to vector control or cells expressing the truncated inactive mutant ADATMS16-sh-EA. This leads to the conclusion that the C-terminus can influence the migratory potential independent of catalytic activity, at least in HEK-EBNA cells. Why these cells migrate more on coated filters remains unclear. FN however can act as a chemoattractant and/or adhesive molecule. Cells might migrate towards FN, which allows them a better adhesion. Due to the fact that cells expressing an active ECM proteinase most likely already have a lower overall adhesion due to the proteolytic decrease of adhesive proteins, this might be a possible explanation why HEK cells stably expressing wtADAMTS16 migrate stronger towards FN. However, there is the possibility that upon FN coating a lot of ECM bound chemoattractants can bind to FN and the cells migrate along this gradient. Again due to the ECM remodeling capacities of ADAMTS16, cells expressing wtADAMTS16 migrate faster. Whether FN is a chemoattractant itself or binds chemoattractants would need further investigations.
In a last assay we investigated the effect of ADAMTS16 on cell proliferation. ADAMTS16 did not influence cell proliferation in MDCKI cells, however, the proliferation of wtADAMTS16-expressing LN229 cells was massively reduced compared to vector control or cells expressing the inactive mutant. The reduced proliferation of LN229 cells expressing wtADAMTS16 is most likely due to the reduction of FN within their

matrix. Increased FN expression has been previously linked to increased cell proliferation during tumor growth as well as in developmental processes [244-246]. Consequently it was shown that the knockdown of FN in the colorectal cancer cell line SW480 led to reduced cell proliferation [241]. Therfore we can conclude that excessive expression of ADAMTS16 in LN229 cells and the correlated decrease in matrix FN through ADAMTS16 mediated digestion, results in decreased cell proliferation. MDCKI cells however do produce FN in 2D cell layers, but they do not assamble FN into large fibres as observed for LN229 cells or fibroblasts. This could be an explanation for the fact that no differences in cell proliferation of MDCKI cells expressing wtADAMTS16 or ADAMTS16-EA could be observed.

Interestingly in 3D spheroid morphogenesis assays using MDCKI cells, the inactive ADAMTS16-EA led to a strong accumulation of FN in their matrix. This is most likely due to the binding and protection of ADAMTS16 to fibronectin. The binding of ADAMTS16-EA can therefore prevent either other proteinases from binding to FN and/or protect the proteolytcaly sensitve linker domain of FN from proteolytic cleavage. The resulting increase in FN in the matrix can have other effects, such as increased matrix stiffness and activation of FN-integrin dependent pathways, such as the phosphorylation of FAK and the consequent activation of the Rho/Rock pathway. Further investigations addressing these pathways would be needed.

The observed effect of inactive ADAMTS16-EA is especially interesting because a variety of papers report not only that mutations in the *ADAMTS16* gene have severe influences on blood pressure regulation [227], but also lead to reduced metastasis and cell growth in ovarien cancer [229]. Altough *ADAMTS16* knockouts were done to investiate the effect of ADAMTS16 on blood pressure regulation, it is most likely not enough to fully understand the complexity of ADAMTS16 in regard of blood pressure regulation and cancer metastasis. As shown by our studies, it would be worthwhile having a closer look at the mutations themselves and address the question whether or not these mutations influence the activity and cellular localization of ADAMTS16. Subsequently a study addressing the composition and stiffness of the tissue, especially in regard to FN accumulation and the resulting downstream signalling cascades would be needed. As our results showed a simple knockout is not enough to address the complex function of ADAMTSs in regulating cellular functions, especially with respect to ADAMTS16. Many ADAMTS, as well as MMP or ADAM knockout animals do not show a specific phenotype. This is not surprising considering the complexity and importance of ECM remodelling during development. Morover, the lack of a certain proteinase can easely be compensated for by the activity of a closely related family member with similar substrate specificity. However, overexpression of a variety of proteinases has severe consequences and leads to the development of a variety of diseasees such as OA, cancer or tissue fibrosis. Interestingly the

study of Yasukawa et al. regarding therapeutic outcome and overall survival of ovarien cancer patients showed that it is not so much a matter of ADAMTS16 expression itself, but whether certain missense mutations occur within the *ADAMTS16* gene. Cancer cells expressing wtADAMTS16 showed a stronger migration and invasive behaviour compared to tumor cells expressing mutant ADAMTS16. Mutant ADAMTS16 expressing cells even showed a reduced migration and invasion compared to vector control tumor cells. Indicating that the mutations are not simply loss of function mutations, but that the protein can, although mutated, still inflence cell signalling and cancer progression. Interestingly none of the identified mutations were in the catalytic domain, but rather within the C-terminal TSR1 domains or the PLAC domain. Our studies clearly showed that these domains have functional roles in ECM binding and most likely substrate recognition. Further ADAMTS16 is strongly C-terminally processed, which is most likely a form of activity regulation. Mutations in these domains therefore can have severe consequences in regard to substrate specificity or activity. The sudy of these mutations and their functional effects could open a variety of possibiliies with respect to personalized therapy. Moreover, studying them would also give a better understanding of the biochemical and biological function of single domains within the protein.

The identification of FN as a substrate of ADAMTS16 opens a variety of possibilities on how to further progress with the research in this area. Especially the fact that ADAMTS16 can influence tissue stiffness thereby having important regulatory influences on several pathways such as FAK phosphorylation and activation of the Rho/Rock pathway provides a variety of new interesting insights into proteinase function. Additionally the potential of ADAMTS16 in influencing the activety of several members of the MMP family should be further investigated. This would give further insights into the protease web and would increase our understanding of the complex regulation of protease activity and function. A better understanding of the close interplay of proteinases and the resulting changes in activity can lead to a better understanding of diseases such as cancer and OA and can lead to the development of better and more efficient therapeutic agents.

Extracellular proteinases have long been simply reduced to their function on ECM degradation, but studies addressing the changes in cell signaling upon protein cleavage remain limited. The ECM itself has long been neglected and thought of as a simple scaffold for cell adhesion and or as barrier for cell migration without further influence on cell signaling and behavior. However recent work focusing on tissue mechanics and engineering, showed that the composition of the ECM and its stiffness tremendously influences cell signaling. The tissue composition guides stem cell differentiation as well as cancer relapse

after radiation therapy [247, 248]. The ECM also acts as barrier and absorbent of a variety of chemo-therapeutic agents and antibodies, which makes cancer treatment so challenging. Therefore a better understanding of the function of extracellular proteinases and how they influence tissue mechanics can lead to a better understanding of disease mechanisms and lead to the development of more efficient therapies.

7. References

1. Frantz, C., Stewart, K.M. & Weaver, V.M. The extracellular matrix at a glance. *J. Cell. Sci.* **123**, 4195-4200 (2010).
2. Hynes, R.O. The extracellular matrix: not just pretty fibrils. *Science (New York, N.Y.)* **326**, 1216-1219 (2009).
3. Rozario, T. & DeSimone, D.W. The extracellular matrix in development and morphogenesis: a dynamic view. *Developmental biology* **341**, 126-140 (2010).
4. Gordon, M.K. & Hahn, R.A. Collagens. *Cell and tissue research* **339**, 247-257 (2010).
5. Mouw, J.K., Ou, G. & Weaver, V.M. Extracellular matrix assembly: a multiscale deconstruction. *Nature reviews. Molecular cell biology* **15**, 771-785 (2014).
6. Ricard-Blum, S. The collagen family. *Cold Spring Harbor perspectives in biology* **3**, a004978 (2011).
7. Fan, D., Takawale, A., Lee, J. & Kassiri, Z. Cardiac fibroblasts, fibrosis and extracellular matrix remodeling in heart disease. *Fibrogenesis & tissue repair* **5**, 15 (2012).
8. Alberts, B. Molecular Biology of the Cell. **4th edition** (Garland Science, 2002).
9. Van Obberghen-Schilling, E. *et al.* Fibronectin and tenascin-C: accomplices in vascular morphogenesis during development and tumor growth. *The International journal of developmental biology* **55**, 511-525 (2011).
10. Hsia, H.C. & Schwarzbauer, J.E. Meet the tenascins: multifunctional and mysterious. *The Journal of biological chemistry* **280**, 26641-26644 (2005).
11. Chiquet-Ehrismann, R. & Tucker, R.P. Tenascins and the importance of adhesion modulation. *Cold Spring Harbor perspectives in biology* **3** (2011).
12. Karp, G. Cell and Molecular Biology: Concepts and Experiments. **7th edition** (John Wiley and Sons, 1999).
13. Campbell, N.A. & Mathieu, R. Biology. (E.R.P.I. 1995).
14. Tanaka, H. *et al.* Circulating level of large splice variants of tenascin-C is a marker of piecemeal necrosis activity in patients with chronic hepatitis C. *Liver international : official journal of the International Association for the Study of the Liver* **26**, 311-318 (2006).
15. Spring, J., Beck, K. & Chiquet-Ehrismann, R. Two contrary functions of tenascin: dissection of the active sites by recombinant tenascin fragments. *Cell* **59**, 325-334 (1989).
16. Schaefer, L. & Schaefer, R.M. Proteoglycans: from structural compounds to signaling molecules. *Cell and tissue research* **339**, 237-246 (2010).
17. Schmidt, T.A., Gastelum, N.S., Nguyen, Q.T., Schumacher, B.L. & Sah, R.L. Boundary lubrication of articular cartilage: role of synovial fluid constituents. *Arthritis and rheumatism* **56**, 882-891 (2007).
18. Kresse, H. & Schonherr, E. Proteoglycans of the extracellular matrix and growth control. *Journal of cellular physiology* **189**, 266-274 (2001).
19. Abdel-Wahab, N., Wicks, S.J., Mason, R.M. & Chantry, A. Decorin suppresses transforming growth factor-beta-induced expression of plasminogen activator inhibitor-1 in human mesangial cells through a mechanism that involves Ca2+-dependent phosphorylation of Smad2 at serine-240. *The Biochemical journal* **362**, 643-649 (2002).
20. Brandan, E., Cabello-Verrugio, C. & Vial, C. Novel regulatory mechanisms for the proteoglycans decorin and biglycan during muscle formation and muscular dystrophy. *Matrix biology : journal of the International Society for Matrix Biology* **27**, 700-708 (2008).
21. Hildebrand, A. *et al.* Interaction of the small interstitial proteoglycans biglycan, decorin and fibromodulin with transforming growth factor beta. *The Biochemical journal* **302 (Pt 2)**, 527-534 (1994).

22. Schaefer, L. *et al.* Decorin-mediated regulation of fibrillin-1 in the kidney involves the insulin-like growth factor-I receptor and Mammalian target of rapamycin. *The American journal of pathology* **170**, 301-315 (2007).
23. Hynes, R.O. & Naba, A. Overview of the matrisome--an inventory of extracellular matrix constituents and functions. *Cold Spring Harbor perspectives in biology* **4**, a004903 (2012).
24. Lu, P., Weaver, V.M. & Werb, Z. The extracellular matrix: a dynamic niche in cancer progression. *The Journal of cell biology* **196**, 395-406 (2012).
25. Klingberg, F. *et al.* Prestress in the extracellular matrix sensitizes latent TGF-beta1 for activation. *The Journal of cell biology* **207**, 283-297 (2014).
26. Kim, J.H. *et al.* Matrix cross-linking-mediated mechanotransduction promotes posttraumatic osteoarthritis. *Proceedings of the National Academy of Sciences of the United States of America* **112**, 9424-9429 (2015).
27. Kalluri, R. Basement membranes: structure, assembly and role in tumour angiogenesis. *Nature reviews. Cancer* **3**, 422-433 (2003).
28. Aumailley, M. & Timpl, R. Attachment of cells to basement membrane collagen type IV. *The Journal of cell biology* **103**, 1569-1575 (1986).
29. Yurchenco, P.D., Tsilibary, E.C., Charonis, A.S. & Furthmayr, H. Models for the self-assembly of basement membrane. *The journal of histochemistry and cytochemistry : official journal of the Histochemistry Society* **34**, 93-102 (1986).
30. Yurchenco, P.D., Smirnov, S. & Mathus, T. Analysis of basement membrane self-assembly and cellular interactions with native and recombinant glycoproteins. *Methods in cell biology* **69**, 111-144 (2002).
31. Yurchenco, P.D. & Schittny, J.C. Molecular architecture of basement membranes. *FASEB journal : official publication of the Federation of American Societies for Experimental Biology* **4**, 1577-1590 (1990).
32. Domogatskaya, A., Rodin, S. & Tryggvason, K. Functional diversity of laminins. *Annual review of cell and developmental biology* **28**, 523-553 (2012).
33. Xu, R. *et al.* Sustained activation of STAT5 is essential for chromatin remodeling and maintenance of mammary-specific function. *The Journal of cell biology* **184**, 57-66 (2009).
34. Tanjore, H. & Kalluri, R. The role of type IV collagen and basement membranes in cancer progression and metastasis. *The American journal of pathology* **168**, 715-717 (2006).
35. Barnard, K., Burgess, S.A., Carter, D.A. & Woolley, D.M. Three-dimensional structure of type IV collagen in the mammalian lens capsule. *Journal of structural biology* **108**, 6-13 (1992).
36. Yurchenco, P.D. & Furthmayr, H. Self-assembly of basement membrane collagen. *Biochemistry* **23**, 1839-1850 (1984).
37. Timpl, R., Wiedemann, H., van Delden, V., Furthmayr, H. & Kuhn, K. A network model for the organization of type IV collagen molecules in basement membranes. *European journal of biochemistry* **120**, 203-211 (1981).
38. Kuhn, K. *et al.* Macromolecular structure of basement membrane collagens. *FEBS letters* **125**, 123-128 (1981).
39. Hudson, B.G. *et al.* The pathogenesis of Alport syndrome involves type IV collagen molecules containing the alpha 3(IV) chain: evidence from anti-GBM nephritis after renal transplantation. *Kidney international* **42**, 179-187 (1992).
40. Barker, D.F. *et al.* Identification of mutations in the COL4A5 collagen gene in Alport syndrome. *Science (New York, N.Y.)* **248**, 1224-1227 (1990).
41. Kalluri, R., Gattone, V.H., 2nd, Noelken, M.E. & Hudson, B.G. The alpha 3 chain of type IV collagen induces autoimmune Goodpasture syndrome. *Proceedings of the National Academy of Sciences of the United States of America* **91**, 6201-6205 (1994).

42. Butkowski, R.J., Langeveld, J.P., Wieslander, J., Hamilton, J. & Hudson, B.G. Localization of the Goodpasture epitope to a novel chain of basement membrane collagen. *The Journal of biological chemistry* **262**, 7874-7877 (1987).
43. Schwarzbauer, J.E. & DeSimone, D.W. Fibronectins, their fibrillogenesis, and in vivo functions. *Cold Spring Harbor perspectives in biology* **3** (2011).
44. Sabatier, L. *et al.* Fibrillin assembly requires fibronectin. *Molecular biology of the cell* **20**, 846-858 (2009).
45. Chiquet-Ehrismann, R. *et al.* Tenascin variants: differential binding to fibronectin and distinct distribution in cell cultures and tissues. *Cell regulation* **2**, 927-938 (1991).
46. Kubow, K.E. *et al.* Mechanical forces regulate the interactions of fibronectin and collagen I in extracellular matrix. *Nature communications* **6**, 8026 (2015).
47. Dallas, S.L. *et al.* Fibronectin regulates latent transforming growth factor-beta (TGF beta) by controlling matrix assembly of latent TGF beta-binding protein-1. *The Journal of biological chemistry* **280**, 18871-18880 (2005).
48. Pankov, R. & Yamada, K.M. Fibronectin at a glance. *J. Cell. Sci.* **115**, 3861-3863 (2002).
49. George, E.L., Georges-Labouesse, E.N., Patel-King, R.S., Rayburn, H. & Hynes, R.O. Defects in mesoderm, neural tube and vascular development in mouse embryos lacking fibronectin. *Development (Cambridge, England)* **119**, 1079-1091 (1993).
50. Mosher, D.F. Fibronectin. *Academic Press. Inc.* (1989).
51. Hynes, R.O. Fibronectins. *Springer- Verlag, New York* (1990).
52. Main, A.L., Harvey, T.S., Baron, M., Boyd, J. & Campbell, I.D. The three-dimensional structure of the tenth type III module of fibronectin: an insight into RGD-mediated interactions. *Cell* **71**, 671-678 (1992).
53. Leahy, D.J., Aukhil, I. & Erickson, H.P. 2.0 A crystal structure of a four-domain segment of human fibronectin encompassing the RGD loop and synergy region. *Cell* **84**, 155-164 (1996).
54. Mao, Y. & Schwarzbauer, J.E. Fibronectin fibrillogenesis, a cell-mediated matrix assembly process. *Matrix biology : journal of the International Society for Matrix Biology* **24**, 389-399 (2005).
55. Wayner, E.A., Garcia-Pardo, A., Humphries, M.J., McDonald, J.A. & Carter, W.G. Identification and characterization of the T lymphocyte adhesion receptor for an alternative cell attachment domain (CS-1) in plasma fibronectin. *The Journal of cell biology* **109**, 1321-1330 (1989).
56. Liao, Y.F., Gotwals, P.J., Koteliansky, V.E., Sheppard, D. & Van De Water, L. The EIIIA segment of fibronectin is a ligand for integrins alpha 9beta 1 and alpha 4beta 1 providing a novel mechanism for regulating cell adhesion by alternative splicing. *The Journal of biological chemistry* **277**, 14467-14474 (2002).
57. Schwarzbauer, J.E. Alternative splicing of fibronectin: three variants, three functions. *BioEssays : news and reviews in molecular, cellular and developmental biology* **13**, 527-533 (1991).
58. Fogerty, F.J., Akiyama, S.K., Yamada, K.M. & Mosher, D.F. Inhibition of binding of fibronectin to matrix assembly sites by anti-integrin (alpha 5 beta 1) antibodies. *The Journal of cell biology* **111**, 699-708 (1990).
59. Sechler, J.L., Cumiskey, A.M., Gazzola, D.M. & Schwarzbauer, J.E. A novel RGD-independent fibronectin assembly pathway initiated by alpha4beta1 integrin binding to the alternatively spliced V region. *Journal of cell science* **113 (Pt 8)**, 1491-1498 (2000).
60. Sechler, J.L. & Schwarzbauer, J.E. Coordinated regulation of fibronectin fibril assembly and actin stress fiber formation. *Cell adhesion and communication* **4**, 413-424 (1997).
61. Zhong, C. *et al.* Rho-mediated contractility exposes a cryptic site in fibronectin and induces fibronectin matrix assembly. *The Journal of cell biology* **141**, 539-551 (1998).
62. Bonnans, C., Chou, J. & Werb, Z. Remodelling the extracellular matrix in development and disease. *Nature reviews. Molecular cell biology* **15**, 786-801 (2014).

63. Zhang, Q., Magnusson, M.K. & Mosher, D.F. Lysophosphatidic acid and microtubule-destabilizing agents stimulate fibronectin matrix assembly through Rho-dependent actin stress fiber formation and cell contraction. *Molecular biology of the cell* **8**, 1415-1425 (1997).
64. Elosegui-Artola, A. *et al.* Mechanical regulation of a molecular clutch defines force transmission and transduction in response to matrix rigidity. *Nature cell biology* **18**, 540-548 (2016).
65. McKeown-Longo, P.J. & Mosher, D.F. Binding of plasma fibronectin to cell layers of human skin fibroblasts. *The Journal of cell biology* **97**, 466-472 (1983).
66. Singer, II The fibronexus: a transmembrane association of fibronectin-containing fibers and bundles of 5 nm microfilaments in hamster and human fibroblasts. *Cell* **16**, 675-685 (1979).
67. McKeown-Longo, P.J. & Mosher, D.F. Interaction of the 70,000-mol-wt amino-terminal fragment of fibronectin with the matrix-assembly receptor of fibroblasts. *The Journal of cell biology* **100**, 364-374 (1985).
68. Schwarzbauer, J.E. Identification of the fibronectin sequences required for assembly of a fibrillar matrix. *The Journal of cell biology* **113**, 1463-1473 (1991).
69. McDonald, J.A. *et al.* Fibronectin's cell-adhesive domain and an amino-terminal matrix assembly domain participate in its assembly into fibroblast pericellular matrix. *The Journal of biological chemistry* **262**, 2957-2967 (1987).
70. Ingham, K.C., Brew, S.A. & Erickson, H.P. Localization of a cryptic binding site for tenascin on fibronectin. *The Journal of biological chemistry* **279**, 28132-28135 (2004).
71. Kozaki, T. *et al.* Recombinant expression and characterization of a novel fibronectin isoform expressed in cartilaginous tissues. *The Journal of biological chemistry* **278**, 50546-50553 (2003).
72. Kim, N.G. & Gumbiner, B.M. Adhesion to fibronectin regulates Hippo signaling via the FAK-Src-PI3K pathway. *The Journal of cell biology* **210**, 503-515 (2015).
73. Sechler, J.L. *et al.* A novel fibronectin binding site required for fibronectin fibril growth during matrix assembly. *The Journal of cell biology* **154**, 1081-1088 (2001).
74. Johnson, K.J., Sage, H., Briscoe, G. & Erickson, H.P. The compact conformation of fibronectin is determined by intramolecular ionic interactions. *The Journal of biological chemistry* **274**, 15473-15479 (1999).
75. Bultmann, H., Santas, A.J. & Peters, D.M. Fibronectin fibrillogenesis involves the heparin II binding domain of fibronectin. *The Journal of biological chemistry* **273**, 2601-2609 (1998).
76. Sechler, J.L., Takada, Y. & Schwarzbauer, J.E. Altered rate of fibronectin matrix assembly by deletion of the first type III repeats. *The Journal of cell biology* **134**, 573-583 (1996).
77. Pankov, R. *et al.* Integrin dynamics and matrix assembly: tensin-dependent translocation of alpha(5)beta(1) integrins promotes early fibronectin fibrillogenesis. *The Journal of cell biology* **148**, 1075-1090 (2000).
78. Dzamba, B.J. & Peters, D.M. Arrangement of cellular fibronectin in noncollagenous fibrils in human fibroblast cultures. *Journal of cell science* **100 (Pt 3)**, 605-612 (1991).
79. Chen, H. & Mosher, D.F. Formation of sodium dodecyl sulfate-stable fibronectin multimers. Failure to detect products of thiol-disulfide exchange in cyanogen bromide or limited acid digests of stabilized matrix fibronectin. *The Journal of biological chemistry* **271**, 9084-9089 (1996).
80. Litvinovich, S.V. *et al.* Formation of amyloid-like fibrils by self-association of a partially unfolded fibronectin type III module. *Journal of molecular biology* **280**, 245-258 (1998).
81. Briknarova, K., Akerman, M.E., Hoyt, D.W., Ruoslahti, E. & Ely, K.R. Anastellin, an FN3 fragment with fibronectin polymerization activity, resembles amyloid fibril precursors. *Journal of molecular biology* **332**, 205-215 (2003).
82. Ohashi, T., Kiehart, D.P. & Erickson, H.P. Dynamics and elasticity of the fibronectin matrix in living cell culture visualized by fibronectin-green fluorescent protein. *Proceedings of the National Academy of Sciences of the United States of America* **96**, 2153-2158 (1999).

83. Sakai, T., Larsen, M. & Yamada, K.M. Fibronectin requirement in branching morphogenesis. *Nature* **423**, 876-881 (2003).
84. Onodera, T. *et al.* Btbd7 regulates epithelial cell dynamics and branching morphogenesis. *Science (New York, N.Y.)* **329**, 562-565 (2010).
85. Kinsey, R. *et al.* Fibrillin-1 microfibril deposition is dependent on fibronectin assembly. *Journal of cell science* **121**, 2696-2704 (2008).
86. Stocker, W. *et al.* The metzincins--topological and sequential relations between the astacins, adamalysins, serralysins, and matrixins (collagenases) define a superfamily of zinc-peptidases. *Protein science : a publication of the Protein Society* **4**, 823-840 (1995).
87. Egeblad, M. & Werb, Z. New functions for the matrix metalloproteinases in cancer progression. *Nature reviews. Cancer* **2**, 161-174 (2002).
88. Brooks, P.C. *et al.* Localization of matrix metalloproteinase MMP-2 to the surface of invasive cells by interaction with integrin alpha v beta 3. *Cell* **85**, 683-693 (1996).
89. Yu, Q. & Stamenkovic, I. Localization of matrix metalloproteinase 9 to the cell surface provides a mechanism for CD44-mediated tumor invasion. *Genes & development* **13**, 35-48 (1999).
90. Yu, W.H., Woessner, J.F., Jr., McNeish, J.D. & Stamenkovic, I. CD44 anchors the assembly of matrilysin/MMP-7 with heparin-binding epidermal growth factor precursor and ErbB4 and regulates female reproductive organ remodeling. *Genes & development* **16**, 307-323 (2002).
91. Sternlicht, M.D. & Werb, Z. How matrix metalloproteinases regulate cell behavior. *Annual review of cell and developmental biology* **17**, 463-516 (2001).
92. Van Wart, H.E. & Birkedal-Hansen, H. The cysteine switch: a principle of regulation of metalloproteinase activity with potential applicability to the entire matrix metalloproteinase gene family. *Proceedings of the National Academy of Sciences of the United States of America* **87**, 5578-5582 (1990).
93. Pei, D. & Weiss, S.J. Furin-dependent intracellular activation of the human stromelysin-3 zymogen. *Nature* **375**, 244-247 (1995).
94. Strongin, A.Y. *et al.* Mechanism of cell surface activation of 72-kDa type IV collagenase. Isolation of the activated form of the membrane metalloprotease. *The Journal of biological chemistry* **270**, 5331-5338 (1995).
95. Kashiwagi, M., Tortorella, M., Nagase, H. & Brew, K. TIMP-3 is a potent inhibitor of aggrecanase 1 (ADAM-TS4) and aggrecanase 2 (ADAM-TS5). *The Journal of biological chemistry* **276**, 12501-12504 (2001).
96. Tortorella, M.D. *et al.* Purification and cloning of aggrecanase-1: a member of the ADAMTS family of proteins. *Science (New York, N.Y.)* **284**, 1664-1666 (1999).
97. Sottrup-Jensen, L. & Birkedal-Hansen, H. Human fibroblast collagenase-alpha-macroglobulin interactions. Localization of cleavage sites in the bait regions of five mammalian alpha-macroglobulins. *The Journal of biological chemistry* **264**, 393-401 (1989).
98. Yang, Z., Strickland, D.K. & Bornstein, P. Extracellular matrix metalloproteinase 2 levels are regulated by the low density lipoprotein-related scavenger receptor and thrombospondin 2. *The Journal of biological chemistry* **276**, 8403-8408 (2001).
99. Giannelli, G., Falk-Marzillier, J., Schiraldi, O., Stetler-Stevenson, W.G. & Quaranta, V. Induction of cell migration by matrix metalloprotease-2 cleavage of laminin-5. *Science (New York, N.Y.)* **277**, 225-228 (1997).
100. Shi, F. & Sottile, J. MT1-MMP regulates the turnover and endocytosis of extracellular matrix fibronectin. *Journal of cell science* **124**, 4039-4050 (2011).
101. Manka, S.W. *et al.* Structural insights into triple-helical collagen cleavage by matrix metalloproteinase 1. *Proceedings of the National Academy of Sciences of the United States of America* **109**, 12461-12466 (2012).

102. Ferreras, M., Felbor, U., Lenhard, T., Olsen, B.R. & Delaisse, J. Generation and degradation of human endostatin proteins by various proteinases. *FEBS letters* **486**, 247-251 (2000).
103. Dong, Z., Kumar, R., Yang, X. & Fidler, I.J. Macrophage-derived metalloelastase is responsible for the generation of angiostatin in Lewis lung carcinoma. *Cell* **88**, 801-810 (1997).
104. Manes, S. *et al.* Identification of insulin-like growth factor-binding protein-1 as a potential physiological substrate for human stromelysin-3. *The Journal of biological chemistry* **272**, 25706-25712 (1997).
105. Whitelock, J.M., Murdoch, A.D., Iozzo, R.V. & Underwood, P.A. The degradation of human endothelial cell-derived perlecan and release of bound basic fibroblast growth factor by stromelysin, collagenase, plasmin, and heparanases. *The Journal of biological chemistry* **271**, 10079-10086 (1996).
106. Levi, E. *et al.* Matrix metalloproteinase 2 releases active soluble ectodomain of fibroblast growth factor receptor 1. *Proceedings of the National Academy of Sciences of the United States of America* **93**, 7069-7074 (1996).
107. Sheu, B.C. *et al.* A novel role of metalloproteinase in cancer-mediated immunosuppression. *Cancer research* **61**, 237-242 (2001).
108. Noe, V. *et al.* Release of an invasion promoter E-cadherin fragment by matrilysin and stromelysin-1. *Journal of cell science* **114**, 111-118 (2001).
109. Kajita, M. *et al.* Membrane-type 1 matrix metalloproteinase cleaves CD44 and promotes cell migration. *The Journal of cell biology* **153**, 893-904 (2001).
110. Deryugina, E.I., Ratnikov, B.I., Postnova, T.I., Rozanov, D.V. & Strongin, A.Y. Processing of integrin alpha(v) subunit by membrane type 1 matrix metalloproteinase stimulates migration of breast carcinoma cells on vitronectin and enhances tyrosine phosphorylation of focal adhesion kinase. *The Journal of biological chemistry* **277**, 9749-9756 (2002).
111. Kessenbrock, K., Plaks, V. & Werb, Z. Matrix metalloproteinases: regulators of the tumor microenvironment. *Cell* **141**, 52-67 (2010).
112. Liotta, L.A. *et al.* Metastatic potential correlates with enzymatic degradation of basement membrane collagen. *Nature* **284**, 67-68 (1980).
113. Szarvas, T., vom Dorp, F., Ergun, S. & Rubben, H. Matrix metalloproteinases and their clinical relevance in urinary bladder cancer. *Nature reviews. Urology* **8**, 241-254 (2011).
114. McKerrow, J.H. *et al.* A functional proteomics screen of proteases in colorectal carcinoma. *Molecular medicine (Cambridge, Mass.)* **6**, 450-460 (2000).
115. Lochter, A. *et al.* Matrix metalloproteinase stromelysin-1 triggers a cascade of molecular alterations that leads to stable epithelial-to-mesenchymal conversion and a premalignant phenotype in mammary epithelial cells. *The Journal of cell biology* **139**, 1861-1872 (1997).
116. English, W.R. *et al.* Membrane type 4 matrix metalloproteinase (MMP17) has tumor necrosis factor-alpha convertase activity but does not activate pro-MMP2. *The Journal of biological chemistry* **275**, 14046-14055 (2000).
117. Seals, D.F. & Courtneidge, S.A. The ADAMs family of metalloproteases: multidomain proteins with multiple functions. *Genes & development* **17**, 7-30 (2003).
118. Nakayama, K. Furin: a mammalian subtilisin/Kex2p-like endoprotease involved in processing of a wide variety of precursor proteins. *The Biochemical journal* **327 (Pt 3)**, 625-635 (1997).
119. Howard, L., Maciewicz, R.A. & Blobel, C.P. Cloning and characterization of ADAM28: evidence for autocatalytic pro-domain removal and for cell surface localization of mature ADAM28. *The Biochemical journal* **348 Pt 1**, 21-27 (2000).
120. Schlomann, U. *et al.* The metalloprotease disintegrin ADAM8. Processing by autocatalysis is required for proteolytic activity and cell adhesion. *The Journal of biological chemistry* **277**, 48210-48219 (2002).

121. Anders, A., Gilbert, S., Garten, W., Postina, R. & Fahrenholz, F. Regulation of the alpha-secretase ADAM10 by its prodomain and proprotein convertases. *FASEB journal : official publication of the Federation of American Societies for Experimental Biology* **15**, 1837-1839 (2001).
122. Nath, D. *et al.* Interaction of metargidin (ADAM-15) with alphavbeta3 and alpha5beta1 integrins on different haemopoietic cells. *Journal of cell science* **112 (Pt 4)**, 579-587 (1999).
123. Zhu, X. & Evans, J.P. Analysis of the roles of RGD-binding integrins, alpha(4)/alpha(9) integrins, alpha(6) integrins, and CD9 in the interaction of the fertilin beta (ADAM2) disintegrin domain with the mouse egg membrane. *Biology of reproduction* **66**, 1193-1202 (2002).
124. Howard, L., Nelson, K.K., Maciewicz, R.A. & Blobel, C.P. Interaction of the metalloprotease disintegrins MDC9 and MDC15 with two SH3 domain-containing proteins, endophilin I and SH3PX1. *The Journal of biological chemistry* **274**, 31693-31699 (1999).
125. Rocks, N. *et al.* Emerging roles of ADAM and ADAMTS metalloproteinases in cancer. *Biochimie* **90**, 369-379 (2008).
126. Black, R.A. *et al.* A metalloproteinase disintegrin that releases tumour-necrosis factor-alpha from cells. *Nature* **385**, 729-733 (1997).
127. Solomon, K.A., Pesti, N., Wu, G. & Newton, R.C. Cutting edge: a dominant negative form of TNF-alpha converting enzyme inhibits proTNF and TNFRII secretion. *Journal of immunology (Baltimore, Md. : 1950)* **163**, 4105-4108 (1999).
128. Sahin, U. *et al.* Distinct roles for ADAM10 and ADAM17 in ectodomain shedding of six EGFR ligands. *The Journal of cell biology* **164**, 769-779 (2004).
129. Blobel, C.P. ADAMs: key components in EGFR signalling and development. *Nature reviews. Molecular cell biology* **6**, 32-43 (2005).
130. Koike, H. *et al.* Membrane-anchored metalloprotease MDC9 has an alpha-secretase activity responsible for processing the amyloid precursor protein. *The Biochemical journal* **343 Pt 2**, 371-375 (1999).
131. Maretzky, T. *et al.* ADAM10 mediates E-cadherin shedding and regulates epithelial cell-cell adhesion, migration, and beta-catenin translocation. *Proceedings of the National Academy of Sciences of the United States of America* **102**, 9182-9187 (2005).
132. Alfandari, D. *et al.* Xenopus ADAM 13 is a metalloprotease required for cranial neural crest-cell migration. *Current biology : CB* **11**, 918-930 (2001).
133. Martin, J., Eynstone, L.V., Davies, M., Williams, J.D. & Steadman, R. The role of ADAM 15 in glomerular mesangial cell migration. *The Journal of biological chemistry* **277**, 33683-33689 (2002).
134. Blobel, C.P. *et al.* A potential fusion peptide and an integrin ligand domain in a protein active in sperm-egg fusion. *Nature* **356**, 248-252 (1992).
135. Zhu, X., Bansal, N.P. & Evans, J.P. Identification of key functional amino acids of the mouse fertilin beta (ADAM2) disintegrin loop for cell-cell adhesion during fertilization. *The Journal of biological chemistry* **275**, 7677-7683 (2000).
136. Lammich, S. *et al.* Constitutive and regulated alpha-secretase cleavage of Alzheimer's amyloid precursor protein by a disintegrin metalloprotease. *Proceedings of the National Academy of Sciences of the United States of America* **96**, 3922-3927 (1999).
137. Buxbaum, J.D. *et al.* Evidence that tumor necrosis factor alpha converting enzyme is involved in regulated alpha-secretase cleavage of the Alzheimer amyloid protein precursor. *The Journal of biological chemistry* **273**, 27765-27767 (1998).
138. Yamada, D. *et al.* Increased expression of ADAM 9 and ADAM 15 mRNA in pancreatic cancer. *Anticancer research* **27**, 793-799 (2007).
139. Mitsui, Y. *et al.* ADAM28 is overexpressed in human breast carcinomas: implications for carcinoma cell proliferation through cleavage of insulin-like growth factor binding protein-3. *Cancer research* **66**, 9913-9920 (2006).

140. Kelwick, R., Desanlis, I., Wheeler, G.N. & Edwards, D.R. The ADAMTS (A Disintegrin and Metalloproteinase with Thrombospondin motifs) family. *Genome biology* **16**, 113 (2015).
141. Stanton, H., Melrose, J., Little, C.B. & Fosang, A.J. Proteoglycan degradation by the ADAMTS family of proteinases. *Biochimica et biophysica acta* **1812**, 1616-1629 (2011).
142. Wang, P. *et al.* Proprotein convertase furin interacts with and cleaves pro-ADAMTS4 (Aggrecanase-1) in the trans-Golgi network. *The Journal of biological chemistry* **279**, 15434-15440 (2004).
143. Longpre, J.M. *et al.* Characterization of proADAMTS5 processing by proprotein convertases. *The international journal of biochemistry & cell biology* **41**, 1116-1126 (2009).
144. Majerus, E.M., Zheng, X., Tuley, E.A. & Sadler, J.E. Cleavage of the ADAMTS13 propeptide is not required for protease activity. *The Journal of biological chemistry* **278**, 46643-46648 (2003).
145. Koo, B.H. *et al.* Regulation of ADAMTS9 secretion and enzymatic activity by its propeptide. *The Journal of biological chemistry* **282**, 16146-16154 (2007).
146. Gomis-Ruth, F.X. Catalytic domain architecture of metzincin metalloproteases. *The Journal of biological chemistry* **284**, 15353-15357 (2009).
147. Crawley, J.T., de Groot, R., Xiang, Y., Luken, B.M. & Lane, D.A. Unraveling the scissile bond: how ADAMTS13 recognizes and cleaves von Willebrand factor. *Blood* **118**, 3212-3221 (2011).
148. Gerhardt, S. *et al.* Crystal structures of human ADAMTS-1 reveal a conserved catalytic domain and a disintegrin-like domain with a fold homologous to cysteine-rich domains. *Journal of molecular biology* **373**, 891-902 (2007).
149. Mosyak, L. *et al.* Crystal structures of the two major aggrecan degrading enzymes, ADAMTS4 and ADAMTS5. *Protein science : a publication of the Protein Society* **17**, 16-21 (2008).
150. Fushimi, K., Troeberg, L., Nakamura, H., Lim, N.H. & Nagase, H. Functional differences of the catalytic and non-catalytic domains in human ADAMTS-4 and ADAMTS-5 in aggrecanolytic activity. *The Journal of biological chemistry* **283**, 6706-6716 (2008).
151. Kuno, K. & Matsushima, K. ADAMTS-1 protein anchors at the extracellular matrix through the thrombospondin type I motifs and its spacing region. *The Journal of biological chemistry* **273**, 13912-13917 (1998).
152. Somerville, R.P. *et al.* Characterization of ADAMTS-9 and ADAMTS-20 as a distinct ADAMTS subfamily related to Caenorhabditis elegans GON-1. *The Journal of biological chemistry* **278**, 9503-9513 (2003).
153. Kashiwagi, M. *et al.* Altered proteolytic activities of ADAMTS-4 expressed by C-terminal processing. *The Journal of biological chemistry* **279**, 10109-10119 (2004).
154. Zeng, W. *et al.* Glycosaminoglycan-binding properties and aggrecanase activities of truncated ADAMTSs: comparative analyses with ADAMTS-5, -9, -16 and -18. *Biochimica et biophysica acta* **1760**, 517-524 (2006).
155. Murphy, G. Tissue inhibitors of metalloproteinases. *Genome biology* **12**, 233 (2011).
156. Yamamoto, K. *et al.* LRP-1-mediated endocytosis regulates extracellular activity of ADAMTS-5 in articular cartilage. *FASEB journal : official publication of the Federation of American Societies for Experimental Biology* **27**, 511-521 (2013).
157. Yamamoto, K. *et al.* Low density lipoprotein receptor-related protein 1 (LRP1)-mediated endocytic clearance of a disintegrin and metalloproteinase with thrombospondin motifs-4 (ADAMTS-4): functional differences of non-catalytic domains of ADAMTS-4 and ADAMTS-5 in LRP1 binding. *The Journal of biological chemistry* **289**, 6462-6474 (2014).
158. Fernandes, R.J. *et al.* Procollagen II amino propeptide processing by ADAMTS-3. Insights on dermatosparaxis. *The Journal of biological chemistry* **276**, 31502-31509 (2001).

159. Colige, A. *et al.* Cloning and characterization of ADAMTS-14, a novel ADAMTS displaying high homology with ADAMTS-2 and ADAMTS-3. *The Journal of biological chemistry* **277**, 5756-5766 (2002).
160. Colige, A. *et al.* Characterization and partial amino acid sequencing of a 107-kDa procollagen I N-proteinase purified by affinity chromatography on immobilized type XIV collagen. *The Journal of biological chemistry* **270**, 16724-16730 (1995).
161. Colige, A. *et al.* Novel types of mutation responsible for the dermatosparactic type of Ehlers-Danlos syndrome (Type VIIC) and common polymorphisms in the ADAMTS2 gene. *The Journal of investigative dermatology* **123**, 656-663 (2004).
162. Verma, P. & Dalal, K. ADAMTS-4 and ADAMTS-5: key enzymes in osteoarthritis. *Journal of cellular biochemistry* **112**, 3507-3514 (2011).
163. Stanton, H. *et al.* ADAMTS5 is the major aggrecanase in mouse cartilage in vivo and in vitro. *Nature* **434**, 648-652 (2005).
164. Song, R.H. *et al.* Aggrecan degradation in human articular cartilage explants is mediated by both ADAMTS-4 and ADAMTS-5. *Arthritis and rheumatism* **56**, 575-585 (2007).
165. Hughes, C.E., Caterson, B., Fosang, A.J., Roughley, P.J. & Mort, J.S. Monoclonal antibodies that specifically recognize neoepitope sequences generated by 'aggrecanase' and matrix metalloproteinase cleavage of aggrecan: application to catabolism in situ and in vitro. *The Biochemical journal* **305 (Pt 3)**, 799-804 (1995).
166. Abbaszade, I. *et al.* Cloning and characterization of ADAMTS11, an aggrecanase from the ADAMTS family. *The Journal of biological chemistry* **274**, 23443-23450 (1999).
167. Gendron, C. *et al.* Proteolytic activities of human ADAMTS-5: comparative studies with ADAMTS-4. *The Journal of biological chemistry* **282**, 18294-18306 (2007).
168. Larkin, J. *et al.* Translational development of an ADAMTS-5 antibody for osteoarthritis disease modification. *Osteoarthritis and cartilage* **23**, 1254-1266 (2015).
169. Chiusaroli, R. *et al.* Targeting of ADAMTS5's ancillary domain with the recombinant mAb CRB0017 ameliorates disease progression in a spontaneous murine model of osteoarthritis. *Osteoarthritis and cartilage* **21**, 1807-1810 (2013).
170. Lee, N.V. *et al.* Fibulin-1 acts as a cofactor for the matrix metalloprotease ADAMTS-1. *The Journal of biological chemistry* **280**, 34796-34804 (2005).
171. Gao, G. *et al.* ADAMTS4 (aggrecanase-1) activation on the cell surface involves C-terminal cleavage by glycosylphosphatidyl inositol-anchored membrane type 4-matrix metalloproteinase and binding of the activated proteinase to chondroitin sulfate and heparan sulfate on syndecan-1. *The Journal of biological chemistry* **279**, 10042-10051 (2004).
172. Sadler, J.E. Pathophysiology of thrombotic thrombocytopenic purpura. *Blood* **130**, 1181-1188 (2017).
173. Levy, G.G. *et al.* Mutations in a member of the ADAMTS gene family cause thrombotic thrombocytopenic purpura. *Nature* **413**, 488-494 (2001).
174. Moake, J.L. *et al.* Unusually large plasma factor VIII:von Willebrand factor multimers in chronic relapsing thrombotic thrombocytopenic purpura. *The New England journal of medicine* **307**, 1432-1435 (1982).
175. Zheng, X.L. Structure-function and regulation of ADAMTS-13 protease. *Journal of thrombosis and haemostasis : JTH* **11 Suppl 1**, 11-23 (2013).
176. Schneider, S.W. *et al.* Shear-induced unfolding triggers adhesion of von Willebrand factor fibers. *Proceedings of the National Academy of Sciences of the United States of America* **104**, 7899-7903 (2007).
177. Shim, K., Anderson, P.J., Tuley, E.A., Wiswall, E. & Sadler, J.E. Platelet-VWF complexes are preferred substrates of ADAMTS13 under fluid shear stress. *Blood* **111**, 651-657 (2008).

178. Mariotte, E. *et al.* Epidemiology and pathophysiology of adulthood-onset thrombotic microangiopathy with severe ADAMTS13 deficiency (thrombotic thrombocytopenic purpura): a cross-sectional analysis of the French national registry for thrombotic microangiopathy. *The Lancet. Haematology* **3**, e237-245 (2016).
179. Lotta, L.A., Garagiola, I., Palla, R., Cairo, A. & Peyvandi, F. ADAMTS13 mutations and polymorphisms in congenital thrombotic thrombocytopenic purpura. *Human mutation* **31**, 11-19 (2010).
180. Li, Z. *et al.* C-terminal ADAMTS-18 fragment induces oxidative platelet fragmentation, dissolves platelet aggregates, and protects against carotid artery occlusion and cerebral stroke. *Blood* **113**, 6051-6060 (2009).
181. Luque, A., Carpizo, D.R. & Iruela-Arispe, M.L. ADAMTS1/METH1 inhibits endothelial cell proliferation by direct binding and sequestration of VEGF165. *The Journal of biological chemistry* **278**, 23656-23665 (2003).
182. Molokwu, C.N., Adeniji, O.O., Chandrasekharan, S., Hamdy, F.C. & Buttle, D.J. Androgen regulates ADAMTS15 gene expression in prostate cancer cells. *Cancer investigation* **28**, 698-710 (2010).
183. Dubail, J. *et al.* ADAMTS-2 functions as anti-angiogenic and anti-tumoral molecule independently of its catalytic activity. *Cellular and molecular life sciences : CMLS* **67**, 4213-4232 (2010).
184. El Hour, M. *et al.* Higher sensitivity of Adamts12-deficient mice to tumor growth and angiogenesis. *Oncogene* **29**, 3025-3032 (2010).
185. Rodriguez-Manzaneque, J.C., Fernandez-Rodriguez, R., Rodriguez-Baena, F.J. & Iruela-Arispe, M.L. ADAMTS proteases in vascular biology. *Matrix biology : journal of the International Society for Matrix Biology* **44-46**, 38-45 (2015).
186. Lee, N.V. *et al.* ADAMTS1 mediates the release of antiangiogenic polypeptides from TSP1 and 2. *The EMBO journal* **25**, 5270-5283 (2006).
187. Martino-Echarri, E. *et al.* Contribution of ADAMTS1 as a tumor suppressor gene in human breast carcinoma. Linking its tumor inhibitory properties to its proteolytic activity on nidogen-1 and nidogen-2. *International journal of cancer* **133**, 2315-2324 (2013).
188. Cal, S. & Lopez-Otin, C. ADAMTS proteases and cancer. *Matrix biology : journal of the International Society for Matrix Biology* **44-46**, 77-85 (2015).
189. Hsu, Y.P., Staton, C.A., Cross, N. & Buttle, D.J. Anti-angiogenic properties of ADAMTS-4 in vitro. *International journal of experimental pathology* **93**, 70-77 (2012).
190. Llamazares, M. *et al.* The ADAMTS12 metalloproteinase exhibits anti-tumorigenic properties through modulation of the Ras-dependent ERK signalling pathway. *Journal of cell science* **120**, 3544-3552 (2007).
191. Viloria, C.G. *et al.* Genetic inactivation of ADAMTS15 metalloprotease in human colorectal cancer. *Cancer research* **69**, 4926-4934 (2009).
192. Choi, G.C. *et al.* The metalloprotease ADAMTS8 displays antitumor properties through antagonizing EGFR-MEK-ERK signaling and is silenced in carcinomas by CpG methylation. *Molecular cancer research : MCR* **12**, 228-238 (2014).
193. Du, W. *et al.* ADAMTS9 is a functional tumor suppressor through inhibiting AKT/mTOR pathway and associated with poor survival in gastric cancer. *Oncogene* **32**, 3319-3328 (2013).
194. Moncada-Pazos, A. *et al.* The ADAMTS12 metalloprotease gene is epigenetically silenced in tumor cells and transcriptionally activated in the stroma during progression of colon cancer. *Journal of cell science* **122**, 2906-2913 (2009).
195. Liu, Y.J., Xu, Y. & Yu, Q. Full-length ADAMTS-1 and the ADAMTS-1 fragments display pro- and antimetastatic activity, respectively. *Oncogene* **25**, 2452-2467 (2006).
196. Ricciardelli, C. *et al.* The ADAMTS1 protease gene is required for mammary tumor growth and metastasis. *The American journal of pathology* **179**, 3075-3085 (2011).

197. Viapiano, M.S., Hockfield, S. & Matthews, R.T. BEHAB/brevican requires ADAMTS-mediated proteolytic cleavage to promote glioma invasion. *Journal of neuro-oncology* **88**, 261-272 (2008).
198. Beristain, A.G., Zhu, H. & Leung, P.C. Regulated expression of ADAMTS-12 in human trophoblastic cells: a role for ADAMTS-12 in epithelial cell invasion? *PloS one* **6**, e18473 (2011).
199. Rao, N. *et al.* ADAMTS4 and its proteolytic fragments differentially affect melanoma growth and angiogenesis in mice. *International journal of cancer* **133**, 294-306 (2013).
200. Fontanil, T. *et al.* Interaction between the ADAMTS-12 metalloprotease and fibulin-2 induces tumor-suppressive effects in breast cancer cells. *Oncotarget* **5**, 1253-1264 (2014).
201. Obaya, A.J., Rua, S., Moncada-Pazos, A. & Cal, S. The dual role of fibulins in tumorigenesis. *Cancer letters* **325**, 132-138 (2012).
202. Baird, B.N. *et al.* Fibulin-2 is a driver of malignant progression in lung adenocarcinoma. *PloS one* **8**, e67054 (2013).
203. Yi, C.H., Smith, D.J., West, W.W. & Hollingsworth, M.A. Loss of fibulin-2 expression is associated with breast cancer progression. *The American journal of pathology* **170**, 1535-1545 (2007).
204. Mjaatvedt, C.H., Yamamura, H., Capehart, A.A., Turner, D. & Markwald, R.R. The Cspg2 gene, disrupted in the hdf mutant, is required for right cardiac chamber and endocardial cushion formation. *Developmental biology* **202**, 56-66 (1998).
205. Kern, C.B. *et al.* Reduced versican cleavage due to Adamts9 haploinsufficiency is associated with cardiac and aortic anomalies. *Matrix biology : journal of the International Society for Matrix Biology* **29**, 304-316 (2010).
206. McCulloch, D.R. *et al.* ADAMTS metalloproteases generate active versican fragments that regulate interdigital web regression. *Developmental cell* **17**, 687-698 (2009).
207. Enomoto, H. *et al.* Cooperation of two ADAMTS metalloproteases in closure of the mouse palate identifies a requirement for versican proteolysis in regulating palatal mesenchyme proliferation. *Development (Cambridge, England)* **137**, 4029-4038 (2010).
208. Silver, D.L. *et al.* The secreted metalloprotease ADAMTS20 is required for melanoblast survival. *PLoS genetics* **4**, e1000003 (2008).
209. Stupka, N. *et al.* Versican processing by a disintegrin-like and metalloproteinase domain with thrombospondin-1 repeats proteinases-5 and -15 facilitates myoblast fusion. *The Journal of biological chemistry* **288**, 1907-1917 (2013).
210. Dubail, J. & Apte, S.S. Insights on ADAMTS proteases and ADAMTS-like proteins from mammalian genetics. *Matrix biology : journal of the International Society for Matrix Biology* **44-46**, 24-37 (2015).
211. Apte, S.S. A disintegrin-like and metalloprotease (reprolysin-type) with thrombospondin type 1 motif (ADAMTS) superfamily: functions and mechanisms. *The Journal of biological chemistry* **284**, 31493-31497 (2009).
212. Le Goff, C. *et al.* ADAMTSL2 mutations in geleophysic dysplasia demonstrate a role for ADAMTS-like proteins in TGF-beta bioavailability regulation. *Nature genetics* **40**, 1119-1123 (2008).
213. Ahram, D. *et al.* A homozygous mutation in ADAMTSL4 causes autosomal-recessive isolated ectopia lentis. *American journal of human genetics* **84**, 274-278 (2009).
214. Robinson, P.N. & Godfrey, M. The molecular genetics of Marfan syndrome and related microfibrillopathies. *Journal of medical genetics* **37**, 9-25 (2000).
215. Cal, S. *et al.* Cloning, expression analysis, and structural characterization of seven novel human ADAMTSs, a family of metalloproteinases with disintegrin and thrombospondin-1 domains. *Gene* **283**, 49-62 (2002).
216. Gao, S., De Geyter, C., Kossowska, K. & Zhang, H. FSH stimulates the expression of the ADAMTS-16 protease in mature human ovarian follicles. *Molecular human reproduction* **13**, 465-471 (2007).

217. Pyun, J.A., Kim, S. & Kwack, K. Interaction between thyroglobulin and ADAMTS16 in premature ovarian failure. *Clinical and experimental reproductive medicine* **41**, 120-124 (2014).
218. Pyun, J.A., Kim, S., Cha, D.H. & Kwack, K. Epistasis between polymorphisms in TSHB and ADAMTS16 is associated with premature ovarian failure. *Menopause (New York, N.Y.)* **21**, 890-895 (2014).
219. Jacobi, C.L., Rudigier, L.J., Scholz, H. & Kirschner, K.M. Transcriptional regulation by the Wilms tumor protein, Wt1, suggests a role of the metalloproteinase Adamts16 in murine genitourinary development. *The Journal of biological chemistry* **288**, 18811-18824 (2013).
220. Gopalakrishnan, K. *et al.* Targeted disruption of Adamts16 gene in a rat genetic model of hypertension. *Proceedings of the National Academy of Sciences of the United States of America* **109**, 20555-20559 (2012).
221. Abdul-Majeed, S., Mell, B., Nauli, S.M. & Joe, B. Cryptorchidism and infertility in rats with targeted disruption of the Adamts16 locus. *PloS one* **9**, e100967 (2014).
222. Kevorkian, L. *et al.* Expression profiling of metalloproteinases and their inhibitors in cartilage. *Arthritis and rheumatism* **50**, 131-141 (2004).
223. Davidson, R.K. *et al.* Expression profiling of metalloproteinases and their inhibitors in synovium and cartilage. *Arthritis research & therapy* **8**, R124 (2006).
224. Surridge, A.K. *et al.* Characterization and regulation of ADAMTS-16. *Matrix biology : journal of the International Society for Matrix Biology* **28**, 416-424 (2009).
225. Chen, S.J. *et al.* The early-immediate gene EGR-1 is induced by transforming growth factor-beta and mediates stimulation of collagen gene expression. *The Journal of biological chemistry* **281**, 21183-21197 (2006).
226. Zhang, W., Ou, J., Inagaki, Y., Greenwel, P. & Ramirez, F. Synergistic cooperation between Sp1 and Smad3/Smad4 mediates transforming growth factor beta1 stimulation of alpha 2(I)-collagen (COL1A2) transcription. *The Journal of biological chemistry* **275**, 39237-39245 (2000).
227. Joe, B. *et al.* Positional identification of variants of Adamts16 linked to inherited hypertension. *Human molecular genetics* **18**, 2825-2838 (2009).
228. Sakamoto, N. *et al.* Serial analysis of gene expression of esophageal squamous cell carcinoma: ADAMTS16 is upregulated in esophageal squamous cell carcinoma. *Cancer science* **101**, 1038-1044 (2010).
229. Yasukawa, M. *et al.* ADAMTS16 mutations sensitize ovarian cancer cells to platinum-based chemotherapy. *Oncotarget* (2016).
230. Schmittgen, T.D. & Livak, K.J. Analyzing real-time PCR data by the comparative C(T) method. *Nature protocols* **3**, 1101-1108 (2008).
231. Kosasih, H.J. *et al.* A Disintegrin and Metalloproteinase with Thrombospondin Motifs-5 (ADAMTS-5) Forms Catalytically Active Oligomers. *The Journal of biological chemistry* **291**, 3197-3208 (2016).
232. Evans, B.R. *et al.* Mutation of membrane type-1 metalloproteinase, MT1-MMP, causes the multicentric osteolysis and arthritis disease Winchester syndrome. *American journal of human genetics* **91**, 572-576 (2012).
233. Riggins, K.S. *et al.* MT1-MMP-mediated basement membrane remodeling modulates renal development. *Experimental cell research* **316**, 2993-3005 (2010).
234. Rose, B.J. & Kooyman, D.L. A Tale of Two Joints: The Role of Matrix Metalloproteases in Cartilage Biology. *Disease markers* **2016**, 4895050 (2016).
235. Pang, L. *et al.* Membrane type 1-matrix metalloproteinase induces epithelial-to-mesenchymal transition in esophageal squamous cell carcinoma: Observations from clinical and in vitro analyses. *Scientific reports* **6**, 22179 (2016).

236. Cal, S. *et al.* Cloning, expression analysis, and structural characterization of seven novel human ADAMTSs, a family of metalloproteinases with disintegrin and thrombospondin-1 domains. *Gene* **283**, 49-62 (2002).
237. Mattila, P.K. & Lappalainen, P. Filopodia: molecular architecture and cellular functions. *Nature reviews. Molecular cell biology* **9**, 446-454 (2008).
238. Nobes, C.D. & Hall, A. Rho, rac, and cdc42 GTPases regulate the assembly of multimolecular focal complexes associated with actin stress fibers, lamellipodia, and filopodia. *Cell* **81**, 53-62 (1995).
239. Fantin, A. *et al.* NRP1 Regulates CDC42 Activation to Promote Filopodia Formation in Endothelial Tip Cells. *Cell reports* **11**, 1577-1590 (2015).
240. Partridge, M.A. & Marcantonio, E.E. Initiation of attachment and generation of mature focal adhesions by integrin-containing filopodia in cell spreading. *Molecular biology of the cell* **17**, 4237-4248 (2006).
241. Ismat, A., Cheshire, A.M. & Andrew, D.J. The secreted AdamTS-A metalloprotease is required for collective cell migration. *Development (Cambridge, England)* **140**, 1981-1993 (2013).
242. Kelwick, R. *et al.* Metalloproteinase-dependent and -independent processes contribute to inhibition of breast cancer cell migration, angiogenesis and liver metastasis by a disintegrin and metalloproteinase with thrombospondin motifs-15. *International journal of cancer* **136**, E14-26 (2015).
243. Somersalo, K. & Saksela, E. Fibronectin facilitates the migration of human natural killer cells. *European journal of immunology* **21**, 35-42 (1991).
244. Han, S.W. & Roman, J. Fibronectin induces cell proliferation and inhibits apoptosis in human bronchial epithelial cells: pro-oncogenic effects mediated by PI3-kinase and NF-kappa B. *Oncogene* **25**, 4341-4349 (2006).
245. Yi, W., Xiao, E., Ding, R., Luo, P. & Yang, Y. High expression of fibronectin is associated with poor prognosis, cell proliferation and malignancy via the NF-kappaB/p53-apoptosis signaling pathway in colorectal cancer. *Oncology reports* **36**, 3145-3153 (2016).
246. Williams, C.M., Engler, A.J., Slone, R.D., Galante, L.L. & Schwarzbauer, J.E. Fibronectin expression modulates mammary epithelial cell proliferation during acinar differentiation. *Cancer research* **68**, 3185-3192 (2008).
247. Miroshnikova, Y.A. *et al.* Tissue mechanics promote IDH1-dependent HIF1alpha-tenascin C feedback to regulate glioblastoma aggression. *Nature cell biology* **18**, 1336-1345 (2016).
248. Beachley, V.Z. *et al.* Tissue matrix arrays for high-throughput screening and systems analysis of cell function. *Nature methods* **12**, 1197-1204 (2015).

8. Appendix

8.1 Supplementary Figures

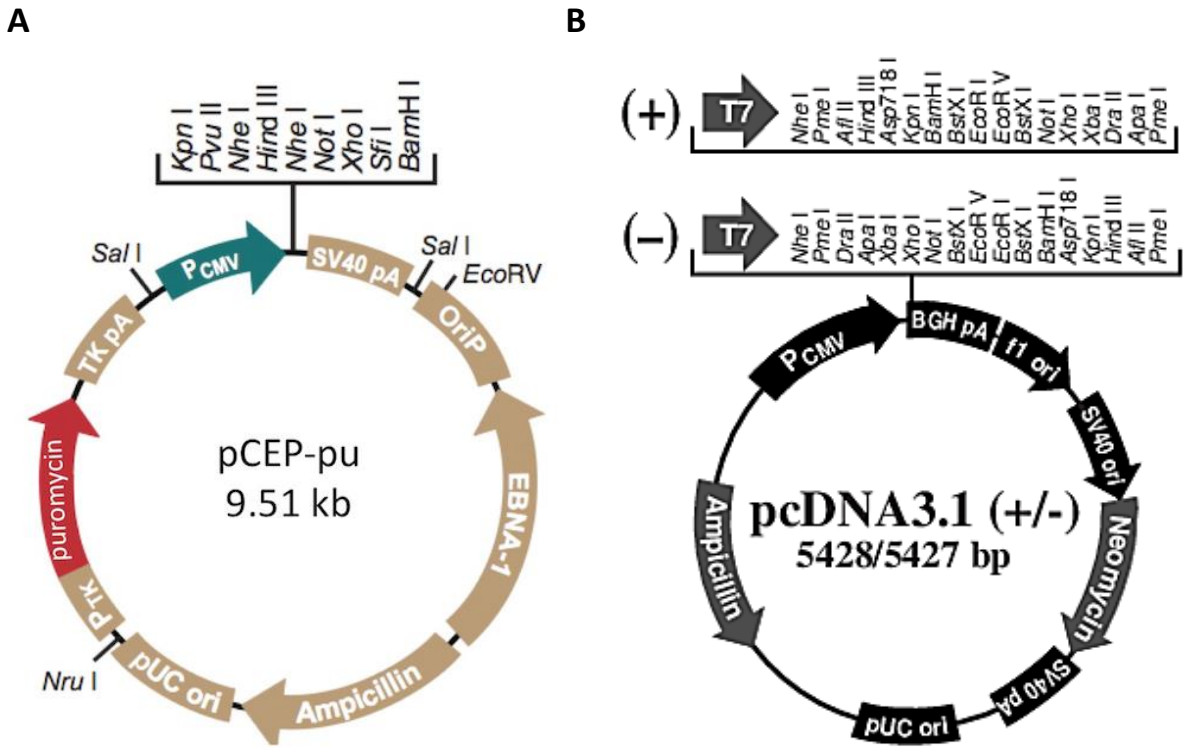

Supplementary Figure 1: Vectors used for ADAMTS16 and MMP14 gene transfer. **A.** pCEP-pu expression vector. Myc_His_6-tag was added to ADAMTS16 genes and ADAMTS16-Myc_His_6 was cloned into the pCEP-pu vector. pCEP-pu_ ADAMTS16-Myc_His_6 was used for stable transfection of HEK-EBNA cells and MDCKI cells and transient transfection of COS-7 and LN229 cells. **B.** pcDNA3.1 expression vector. HA-tag was added to the C-terminus of MMP14 and MMP14-HA was cloned into pcDNA3.1vector. pcDNA3.1_MMP14-HA was used to transiently transfect COS-7 cells.

```
Mouse_ADAMTS16          1    MESRGCAALWVLLLAQVSEQQTPACALGLAAAASGSPEDPQPPPFSGSSWLETGEYDLVS  60
Mouse_ADAMTS16-EA       1    MESRGCAALWVLLLAQVSEQQTPACALGLAAAASGSPEDPQPPPFSGSSWLETGEYDLVS  60
Mouse_ADAMTS16-sh       1    MESRGCAALWVLLLAQVSEQQTPACALGLAAAASGSPEDPQPPPFSGSSWLETGEYDLVS  60
Mouse_ADAMTS16-sh-EA    1    MESRGCAALWVLLLAQVSEQQTPACALGLAAAASGSPEDPQPPPFSGSSWLETGEYDLVS  60

Mouse_ADAMTS16         61    AYEVDHRGDYVSHDIMHYQRRRRRRAVTQPGGDALHLRLKGPRHDLHLDLKAASNLMAPG  120
Mouse_ADAMTS16-EA      61    AYEVDHRGDYVSHDIMHYQRRRRRRAVTQPGGDALHLRLKGPRHDLHLDLKAASNLMAPG  120
Mouse_ADAMTS16-sh      61    AYEVDHRGDYVSHDIMHYQRRRRRRAVTQPGGDALHLRLKGPRHDLHLDLKAASNLMAPG  120
Mouse_ADAMTS16-sh-EA   61    AYEVDHRGDYVSHDIMHYQRRRRRRAVTQPGGDALHLRLKGPRHDLHLDLKAASNLMAPG  120

Mouse_ADAMTS16        121    FMVQTLGKGGTKSVQMFPPEENCFYQGSLRSQGNSSVALSTCQGLLGMIRTKDTDYFLKP  180
Mouse_ADAMTS16-EA     121    FMVQTLGKGGTKSVQMFPPEENCFYQGSLRSQGNSSVALSTCQGLLGMIRTKDTDYFLKP  180
Mouse_ADAMTS16-sh     121    FMVQTLGKGGTKSVQMFPPEENCFYQGSLRSQGNSSVALSTCQGLLGMIRTKDTDYFLKP  180
Mouse_ADAMTS16-sh-EA  121    FMVQTLGKGGTKSVQMFPPEENCFYQGSLRSQGNSSVALSTCQGLLGMIRTKDTDYFLKP  180

Mouse_ADAMTS16        181    LPPHLTSKLNRSAQGDSPSHVLYKRSTERQAPRENEVLMITRKRDLARPHLHHDNFHLGP  240
Mouse_ADAMTS16-EA     181    LPPHLTSKLNRSAQGDSPSHVLYKRSTERQAPRENEVLMITRKRDLARPHLHHDNFHLGP  240
Mouse_ADAMTS16-sh     181    LPPHLTSKLNRSAQGDSPSHVLYKRSTERQAPRENEVLMITRKRDLARPHLHHDNFHLGP  240
Mouse_ADAMTS16-sh-EA  181    LPPHLTSKLNRSAQGDSPSHVLYKRSTERQAPRENEVLMITRKRDLARPHLHHDNFHLGP  240

Mouse_ADAMTS16        241    SQKQHFCGRRKKYMPQPPNDDLYILPDEYKPSSRHKRSLLKSHRNEELNVETLVVVDRKM  300
Mouse_ADAMTS16-EA     241    SQKQHFCGRRKKYMPQPPNDDLYILPDEYKPSSRHKRSLLKSHRNEELNVETLVVVDRKM  300
Mouse_ADAMTS16-sh     241    SQKQHFCGRRKKYMPQPPNDDLYILPDEYKPSSRHKRSLLKSHRNEELNVETLVVVDRKM  300
Mouse_ADAMTS16-sh-EA  241    SQKQHFCGRRKKYMPQPPNDDLYILPDEYKPSSRHKRSLLKSHRNEELNVETLVVVDRKM  300

Mouse_ADAMTS16        301    MQSHGHENITTYVLTILNMVSALFKDGTIGGNINIVIVGLILLEDEQPGLAISHHADHTL  360
Mouse_ADAMTS16-EA     301    MQSHGHENITTYVLTILNMVSALFKDGTIGGNINIVIVGLILLEDEQPGLAISHHADHTL  360
Mouse_ADAMTS16-sh     301    MQSHGHENITTYVLTILNMVSALFKDGTIGGNINIVIVGLILLEDEQPGLAISHHADHTL  360
Mouse_ADAMTS16-sh-EA  301    MQSHGHENITTYVLTILNMVSALFKDGTIGGNINIVIVGLILLEDEQPGLAISHHADHTL  360

Mouse_ADAMTS16        361    TSFCQWQSGLMGKDGTRHDHAILLTGLDICSWKNEPCDTLGFAPISGMCSKYRSCTVNED  420
Mouse_ADAMTS16-EA     361    TSFCQWQSGLMGKDGTRHDHAILLTGLDICSWKNEPCDTLGFAPISGMCSKYRSCTVNED  420
Mouse_ADAMTS16-sh     361    TSFCQWQSGLMGKDGTRHDHAILLTGLDICSWKNEPCDTLGFAPISGMCSKYRSCTVNED  420
Mouse_ADAMTS16-sh-EA  361    TSFCQWQSGLMGKDGTRHDHAILLTGLDICSWKNEPCDTLGFAPISGMCSKYRSCTVNED  420

Mouse_ADAMTS16        421    SGLGLAFTIAHESGHNFGMVHDGEGNMCKKSEGNIMSPTLAGRNGVFSWSSCSRQYLHKF  480
Mouse_ADAMTS16-EA     421    SGLGLAFTIAHASGHNFGMVHDGEGNMCKKSEGNIMSPTLAGRNGVFSWSSCSRQYLHKF  480
Mouse_ADAMTS16-sh     421    SGLGLAFTIAHESGHNFGMVHDGEGNMCKKSEGNIMSPTLAGRNGVFSWSSCSRQYLHKF  480
Mouse_ADAMTS16-sh-EA  421    SGLGLAFTIAHASGHNFGMVHDGEGNMCKKSEGNIMSPTLAGRNGVFSWSSCSRQYLHKF  480

Mouse_ADAMTS16        481    LSTAQAICLADQPKPVKEYKYPEKLPGQLYDANTQCKWQFGEKAKLCMLDFRKDICKALW  540
Mouse_ADAMTS16-EA     481    LSTAQAICLADQPKPVKEYKYPEKLPGQLYDANTQCKWQFGEKAKLCMLDFRKDICKALW  540
Mouse_ADAMTS16-sh     481    LSTAQAICLADQPKPVKEYKYPEKLPGQLYDANTQCKWQFGEKAKLCMLDFRKDICKALW  540
Mouse_ADAMTS16-sh-EA  481    LSTAQAICLADQPKPVKEYKYPEKLPGQLYDANTQCKWQFGEKAKLCMLDFRKDICKALW  540

Mouse_ADAMTS16        541    CHRIGRKCETKFMPAAEGTLCGQDMWCRGGQCVKYGDEGPKPTHGHWSDWSPWSPCSRTC  600
Mouse_ADAMTS16-EA     541    CHRIGRKCETKFMPAAEGTLCGQDMWCRGGQCVKYGDEGPKPTHGHWSDWSPWSPCSRTC  600
Mouse_ADAMTS16-sh     541    CHRIGRKCETKFMPAAEGTLCGQDMWCRGGQCVKYGDEGPKPTHGHWSDWSPWSPCSRTC  600
Mouse_ADAMTS16-sh-EA  541    CHRIGRKCETKFMPAAEGTLCGQDMWCRGGQCVKYGDEGPKPTHGHWSDWSPWSPCSRTC  600

Mouse_ADAMTS16        601    GGGISHRDRLCTNPRPSHGGKFCQGSTRTLKLCNSQRCPLDSVDFRAAQCAEYNSKRFRG  660
Mouse_ADAMTS16-EA     601    GGGISHRDRLCTNPRPSHGGKFCQGSTRTLKLCNSQRCPLDSVDFRAAQCAEYNSKRFRG  660
Mouse_ADAMTS16-sh     601    GGGISHRDRLCTNPRPSHGGKFCQGSTRTLKLCNSQRCPLDSVDFRAAQCAEYNSKRFRG  660
Mouse_ADAMTS16-sh-EA  601    GGGISHRDRLCTNPRPSHGGKFCQGSTRTLKLCNSQRCPLDSVDFRAAQCAEYNSKRFRG  660

Mouse_ADAMTS16        661    WLYKWKPYTQLEDQDLCKLYCIAEGFDFFFSLSNKVKDGTPCSEDSRNVCIDGMCERVGC  720
Mouse_ADAMTS16-EA     661    WLYKWKPYTQLEDQDLCKLYCIAEGFDFFFSLSNKVKDGTPCSEDSRNVCIDGMCERVGC  720
Mouse_ADAMTS16-sh     661    WLYKWKPYTQLEDQDLCKLYCIAEGFDFFFSLSNKVKDGTPCSEDSRNVCIDGMCERVGC  720
Mouse_ADAMTS16-sh-EA  661    WLYKWKPYTQLEDQDLCKLYCIAEGFDFFFSLSNKVKDGTPCSEDSRNVCIDGMCERVGC  720

Mouse_ADAMTS16        721    DNVLGSDATEDSCGVCKGNNSDCVTHRGLYSKHHSTNQYYHMVTIPSGARSIHIYETNIS  780
Mouse_ADAMTS16-EA     721    DNVLGSDATEDSCGVCKGNNSDCVTHRGLYSKHHSTNQYYHMVTIPSGARSIHIYETNIS  780
Mouse_ADAMTS16-sh     721    DNVLGSDATEDSCGVCKGNNSDCVTHRGLYSKHHSTNQYYHMVTIPSGARSIHIYETNIS  780
Mouse_ADAMTS16-sh-EA  721    DNVLGSDATEDSCGVCKGNNSDCVTHRGLYSKHHSTNQYYHMVTIPSGARSIHIYETNIS  780

Mouse_ADAMTS16        781    TSYISVRNSLKRYYLNGHWSVDWPGRYKFSGATFNYKRSYKEPENLTSPGPTNETLIVEL  840
Mouse_ADAMTS16-EA     781    TSYISVRNSLKRYYLNGHWSVDWPGRYKFSGATFNYKRSYKEPENLTSPGPTNETLIVEL  840
Mouse_ADAMTS16-sh     781    TSYISVRNSLKRYYLNGHWSVDWPGRYKFSGATFNYKRSYKEPENLTSPGPTNETLIVEL  840
Mouse_ADAMTS16-sh-EA  781    TSYISVRNSLKRYYLNGHWSVDWPGRYKFSGATFNYKRSYKEPENLTSPGPTNETLIVEL  840
```

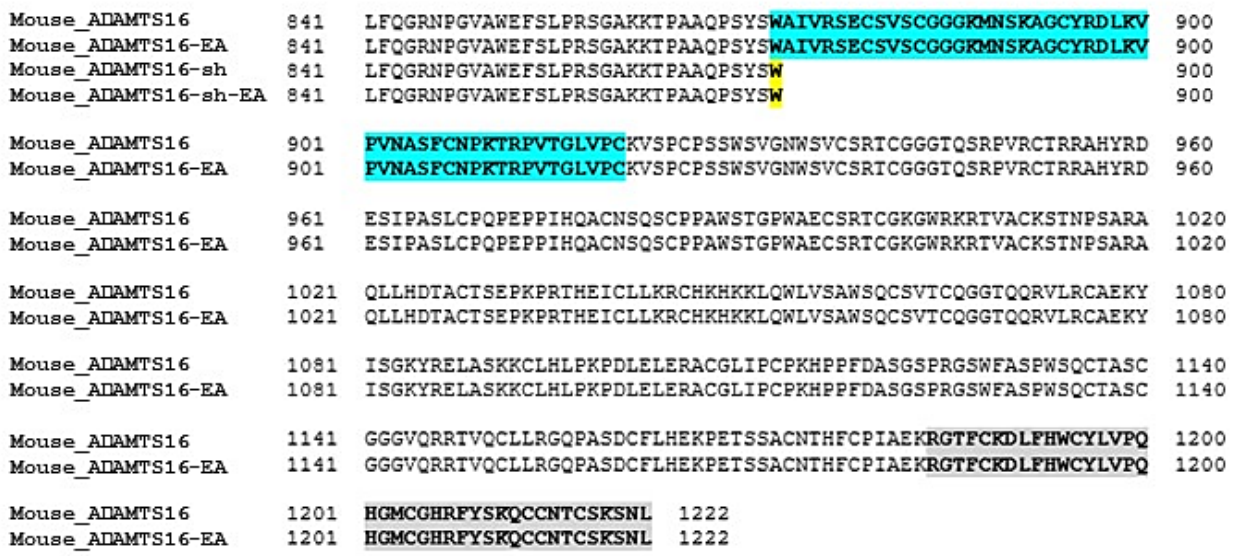

Supplementary Figure 2: Protein alignment of the used mouse ADAMTS16 constructs. The mouse_ADAMTS16 sequence corresponds to the wild type ADAMTS16 sequence (UniProt accession number Q69Z28). The active site mutant E432/A432 is marked in red. The last amino acid of the C-terminally truncated ADAMTS16-sh is marked in yellow. Additionally the furin cleavage site, the first C-terminal TSR1 motif (TSR type-1 2) and the PLAC domain are annotated.

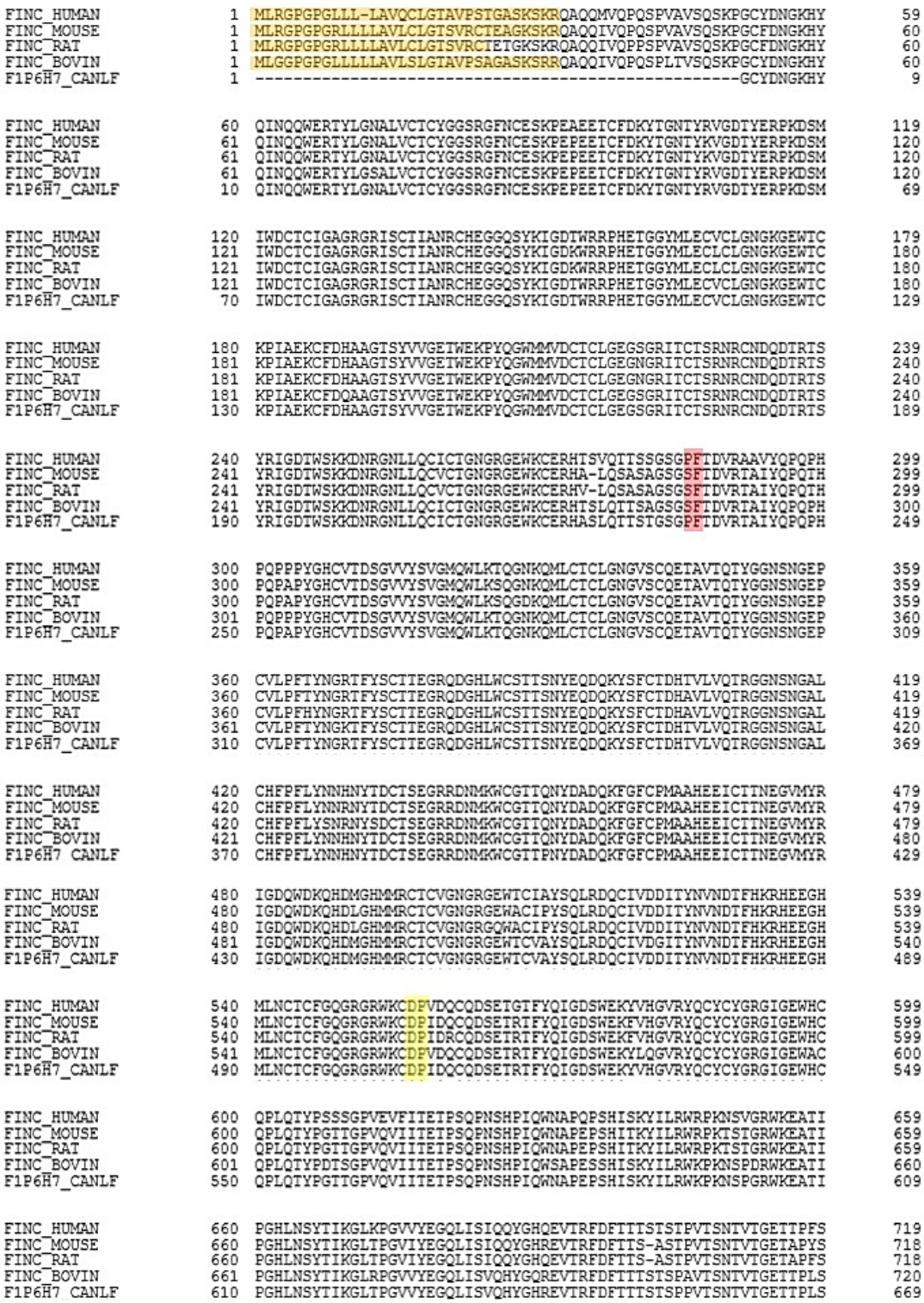

Supplementary Figure 3: The Universal Protein Resource (UniProt) protein alignment of FN. Alignment starts at the N-terminal signal peptide until fibronectin type-III 1 domain. Signal peptides at the N-terminus (orange), the N-terminal ADAMTS16 cleavage site leading to the release of the 30 kDa N-terminal heparin binding domain of FN (P1/P1', red) and the second potential ADAMTS16 cleavage site identified by MS (P1/P1', yellow) are annotated.

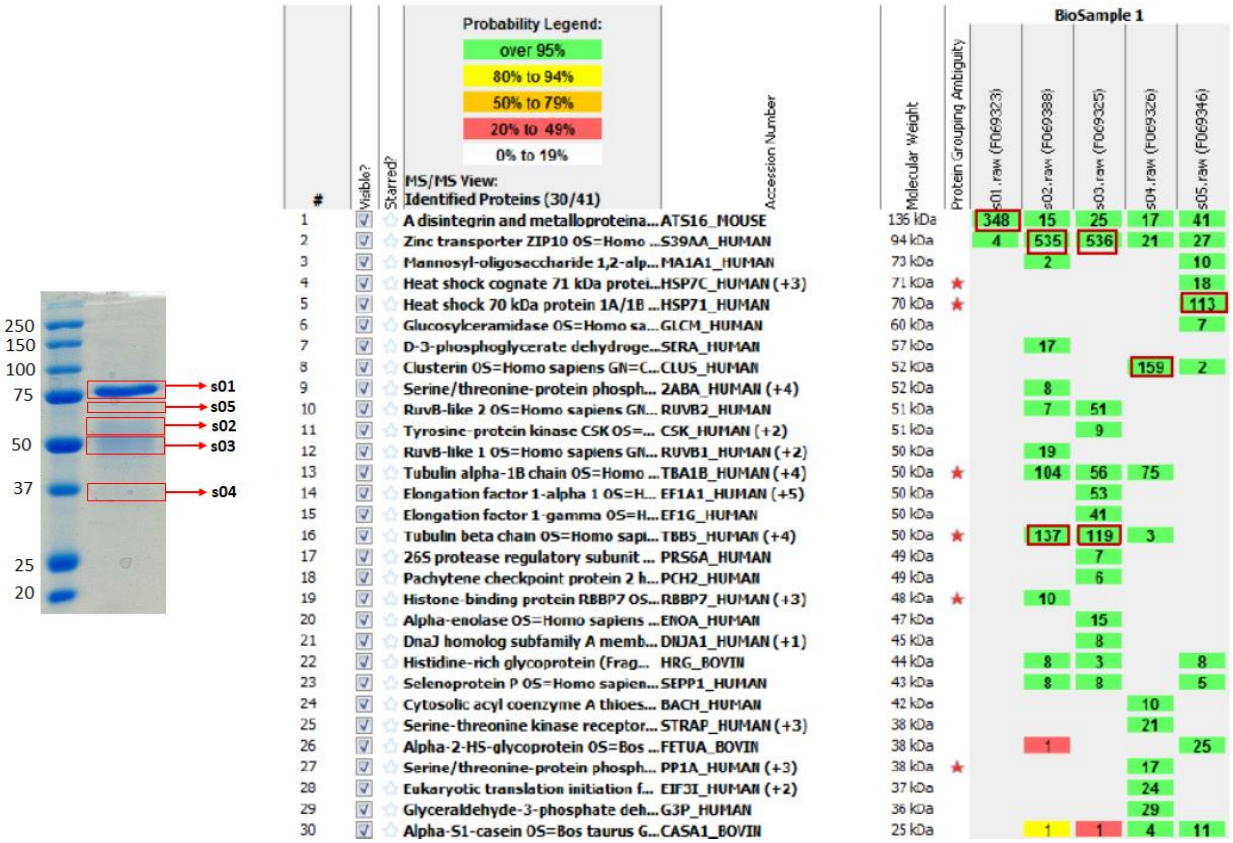

Supplementary Figure 4: In-gel digest and protein identification of co-purified proteins during ADAMTS16-sh purification. Scaffold data supplementing the discussed results in chapter 5.2.1 “ADAMTS16 is C-terminally processed and forms high order oligomers”.

8.2 Abbreviations

- ADAM A Disintegrin and Metalloproteinase
- ADAMTS A Disintegrin and Metalloproteinase with Thrombospondin motifs
- ADAMTSL ADAMTS-like protein
- APP Amyloid precursor protein
- BM Basement membrane
- C-terminus Carboxy-terminus
- Col Collagen
- CLUS Clusterin
- DOC Deoxycholate
- ECM Extracellular matrix
- EGF Epidermal growth factor
- EGFR Epidermal growth factor receptor
- EMMPRIN Extracellular matrix metalloproteinase inducer
- FAK Focal adhesion kinase
- FBN Fibrillin
- FGF Fibroblast growth factors
- FN Fibronectin
- GAG Glycosaminoglycan
- HA Hyaluronan
- HB-EGF Heparin-binding epidermal growth factor
- HSP71 Heat shock 70 kDa protein 1A/1B
- IGF Insulin-like growth factor
- IEL Isolated ectopia lentis
- LRP Low-density lipoprotein-related protein
- MMP Matrix metalloproteinase
- MS Mass spectrometry
- N-terminus Amino-terminus

- OA Osteoarthritis
- PG Proteoglycan
- PLAC Protease and lacunin
- SH3 domain Src-homology 3 domain
- SLRP Small leucine-rich proteoglycans
- TGF-β Transforming growth factor-β
-TIMP Tissue Inhibitors of Metalloproteinases
- TN Tenascin
- TNF-α Tumor necrosis factor-α
- TGN *Trans*-Golgi network
- TSR Thrombospondin type 1 motif
- TTP Thrombotic thrombocytopenic purpura
-VEGF Vascular endothelial growth factor
- vWF Von Willebrand Factor
-Wt1 Wilms tumor protein